# Speciation of trace metals and their uptake by rice in paddy soils

**Yunyu Pan**

**Thesis committee**

**Promotor**
Prof. Dr R.N.J. Comans
Professor of Soil Chemistry and Chemical Soil Quality
Wageningen University

**Co-promotors**
Dr G.F. Koopmans
Researcher, Soil Chemistry and Chemical Soil Quality Group
Wageningen University

Dr J. Song
Researcher, Key Laboratory of Soil Environment and Pollution Remediation,
Institute of Soil Science, Chinese Academy of Sciences, Nanjing, China

**Other members**
Prof. Dr W. de Vries, Wageningen University
Prof. Dr E. Smolders, KU Leuven, Belgium
Dr J.P.M. Vink, Deltares, Utrecht
Prof. Dr A.J. Hendriks, Radboud University, Nijmegen

This research was conducted under the auspices of the Graduate School of Socio-Economic and Natural Sciences of the Environment (SENSE).

# Speciation of trace metals and their uptake by rice in paddy soils

**Yunyu Pan**

**Thesis**
submitted in fulfilment of the requirements for the degree of doctor
at Wageningen University
by the authority of the Rector Magnificus
Prof. Dr M.J. Kropff,
in the presence of the
Thesis Committee appointed by the Academic Board
to be defended in public
on Tuesday 12 May 2015
at 4 p.m. in the Aula.

Yunyu Pan

Speciation of trace metals and their uptake by rice in paddy soils

193 pages

PhD thesis, Wageningen University, Wageningen, NL (2015)

With references, with summaries in Chinese, Dutch, and English

ISBN: 978-94-6257-274-4

# Table of Contents

# Chapter 1

# General introduction

*Yunyu Pan*

## *1.1 General introduction*

### *1.1.1 Background*

Toxic compounds such as persistent organic pollutants and trace metals have placed an increasing pressure on the quality of soils over the past decades, because of intensive human activities resulting in an elevated discharge of these compounds from various anthropogenic sources including industrial and domestic sewage discharges, mining, fertilization, smelting, e-waste recycling, and wastewater irrigation (Kuo et al., 2006; Römkens et al., 2009a; Zeng et al., 2011; Luo et al., 2012; Fu et al., 2013). Organic pollutants can be degraded to less harmful components in soil by biological or chemical processes, whereas trace metals are non-degradable contaminants (Pan and Wang, 2012). Consequently, trace metals can accumulate in soils and can be taken up by the edible parts of food crops, which can eventually lead to adverse effects on human beings via food consumption (Brus et al., 2009; Römkens et al., 2009b). Since the cadmium (Cd) poisoning tragedy of the “itai-itai” disease, which was caused via the consumption of Cd contaminated rice (*Oryza sativa* L.), was reported in Japan in the late 1960s (Nordberg, 2004), there has been a worldwide increase in the concern about the risks of trace metal contamination in soils. Nowadays, with the fast urbanization and industrialization and rapid economic growth in China, China is facing the threats of trace metal contamination of soils as well. According to the results of a monitoring program as reported in the Communique of the Chinese National Soil Contamination Survey (2005-2013), soil levels of a range of contaminants exceeded the Chinese Environmental Quality Standard for Soils (GB 15618-1995) in 16% of the total number of soils sampled across China. In 83% of the soil samples in which this standard was exceeded, the contamination was due to the presence of trace metals, particularly Cd, Hg, As, and Pb. The most heavily trace metal contaminated areas in China are located in regions such as the Northeastern Industrial Base, Yangtze River Delta, and Pearl River Delta (Fig. 1). The widespread contamination of soils with trace metals in these Chinese regions has raised public and governmental concerns, especially in relation to food safety.

Contamination of paddy soils with trace metals and the accumulation of trace metals in rice grains is a worldwide concern. Rice is one of the most important crops grown for human consumption in the world (Meharg et al., 2013). Rice is the staple food for more than 65% of the Chinese people (Zhang et al., 2005) and, therefore, it plays a very important role in food security for the Chinese people. In these aforementioned most heavily contaminated areas of China, rice is intensively cropped (Fig. 1) and the rice production in these parts of China contribute greatly to the total annual rice yield in China (Peng et al., 2009). However, the presence of elevated trace metal levels in paddy soils can result in phytotoxic symptoms of the rice plants including a yield reduction of the rice grains and sometimes even the absence of any detectable yield (Arunakumara et al., 2013). Also, trace metal contamination of paddy soils can lead to a decline in the nutritional value of the rice grains and an accumulation of trace metals in the rice grains (Arunakumara et al., 2013). The consumption of rice with high levels of trace metals can lead to unacceptable human health risks. For typical rice-eating populations, the dietary intake of Cd is known to be the major Cd exposure pathway for human beings (Brus et al., 2009; Römkens et al., 2009b). Chronic human exposure to Cd may cause bone disease, lung edema, renal dysfunction, liver damage, anemia, hypertension, and genotoxic damage (Agency for Toxic Substances and Disease Registry, 2012). Human health risks associated with the long-term consumption of Cd contaminated rice grains can even be increased when Zn, Fe, and Ca contents in diets are insufficient for human needs, because low dietary levels of these minerals enhance intestinal absorption and organ retention of Cd (Reeves and Chaney, 2002, 2004; de Livera et al., 2011). For minimizing uptake of trace metals by rice and to safeguard food security and human health, it is important to understand the processes controlling the uptake of trace metals by rice plants in paddy soils.

The uptake of trace metals by rice plants is largely determined by the bioavailability of trace metals in paddy soils (Simmons et al., 2008; Römkens et al., 2009b). In addition to this, rice plant-specific factors play a role in the uptake of trace metals (Yu et al., 2006; Römkens et al., 2009b). The bioavailability of trace metals in paddy soils is determined by complex (competition) interactions between trace metals and major cations and reactive surfaces of soil constituents like soil organic matter (SOM), Fe-, Al-, and Mn-(hydr)oxides, and clay (Weng et al., 2002). These interactions are affected by soil properties such as the pH and redox potential (Eh). However, only very little is known on how the Eh affects these interactions and, in turn, the bioavailability of trace metals for uptake by rice plants. For rice, this is particularly important, because rice is mostly

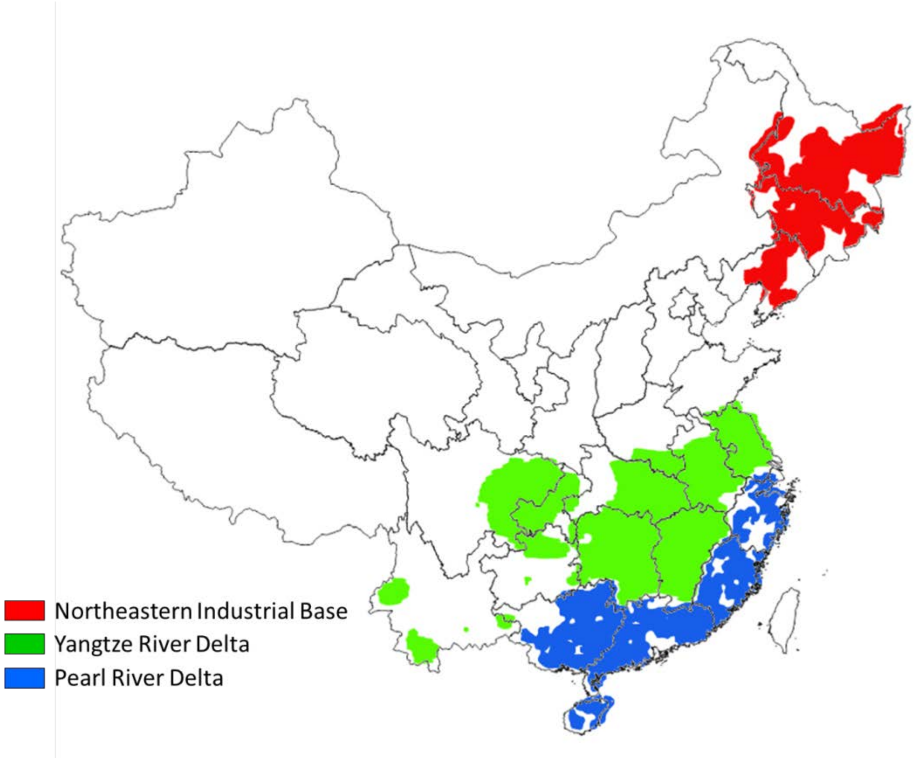

**Fig. 1.** Regions in China with intensive rice production (Ministry of Agriculture of the People’s Republic of China, 2014).

grown in paddy fields where alternating flooding and draining of the fields lead to a continuously fluctuating Eh (Kögel-Knabner et al., 2010). A complicating factor in predicting the effects of redox processes on the bioavailability of trace metals and their uptake by rice plants is the relatively slow kinetics of many of the chemical reactions involved in redox processes, leading to non-equilibrium conditions in flooded soils. Consequently, it is uncertain whether commonly used multi-surface models, which assume thermodynamic equilibrium, can be applied to predict the bioavailability of trace metals in flooded paddy soils where anaerobic conditions prevail. A further complicating factor when quantifying the relationship between the bioavailability of trace metals and their uptake by rice plants is the temporal variation in the latter, which changes according to the different growth stages of the rice plants. For example, rice has a critical grain filling stage, and the Eh and the resulting bioavailability of the trace metals during this stage will greatly determine the levels of trace metals in the rice grains (Chaney et al., 1996; Kashem and Singh, 2001; Simmons et al., 2005, 2008). Therefore, attention should be paid to investigate the bioavailability of trace metals in paddy soils exposed to alternating flooding and drainage periods and to link this to the uptake of trace metals by rice plants over time.

### *1.1.2. Traditional water management for lowland rice growing period*

Rice is usually cropped in lowland paddy fields. Rice undergoes three growth phases: the vegetative phase (i.e., he seedling and tillering stages), the reproductive phase (i.e., the booting stage), and the ripening phase (i.e., the filling stage and final harvest) (Fig. 2). During the cultivation of lowland rice, flooding conditions prevail during almost the entire cropping period, because lowland rice is extremely sensitive to water shortage (Kögel-Knabner et al., 2010). Nevertheless, according to the traditional water management for the cultivation of lowland rice, flooded paddy soils are usually drained

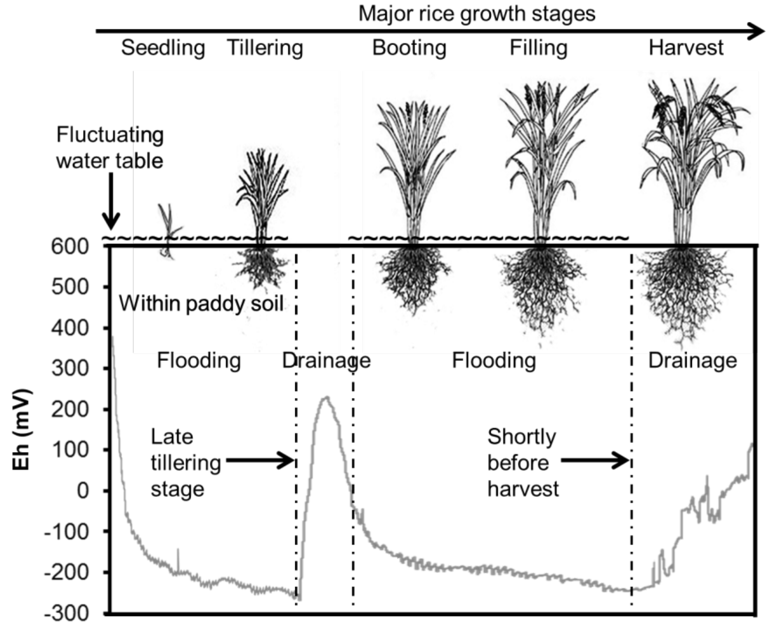

**Fig. 2.** Traditional water management for the cultivation of lowland rice in paddy soils (the gray Eh line is based on the in-situ measurement of Eh in the bottom soil layer of the pot experiment described in Chapter 5 of this Ph.D. thesis).

during two stages of rice growth, i.e., the late tillering stage in order to control ineffective tillering and shortly before the harvest to enable faster rice ripening and to facilitate access to the paddy field and to ease harvesting (Fig. 2; Kögel-Knabner et al., 2010). In other words, the late tillering stage and the late grain filling stage shortly before harvesting coincide with the drainage periods (Fig. 2). Hence, paddy soils undergo at least two successive flooding and drainage periods resulting in a continuously fluctuating Eh (Fig. 2). These flooding and draining periods can considerably affect the redox chemistry of paddy soils by either reduction or oxidation processes.

### *1.1.3. Redox chemistry in lowland paddy soils*

One of the unique features of lowland paddy soils is the continuously fluctuating Eh due to alternating flooding and drainage conditions, as discussed above. During the flooding periods, the Eh decreases after the depletion of oxygen and the following reduction processes will take place, either sequentially or simultaneously: denitrification, reductive dissolution of Mn(III/IV) and Fe(III) oxides, reduction of $SO_4^{2-}$ to $S^{2-}$, and methanogenesis (Fig. 3; Yu et al., 2007; Kögel-Knabner et al., 2010). These reduction processes lead to large changes in the chemical composition of the soil solution. For example, reductive dissolution of Mn (III/IV)- and Fe (III)-(hydr)oxides present within the soil solid phase can cause elevated concentrations of $Mn^{2+}$ and $Fe^{2+}$ in the soil solution (Fig. 3; Tack et al., 2006; Grybos et al., 2007; Shaheen et al., 2014). When further reduced, the reduction of $SO_4^{2-}$ can lead to the formation of poorly soluble metal sulfides (Fig. 3; de Livera et al., 2011; Khaokaew et al., 2011; Fulda et al., 2013). The above mentioned reduction processes occur in parallel with the oxidation of SOM (Fig. 3). Subsequently, dissolved organic matter (DOM) will concomitantly be released into the soil solution after flooding (Kalbitz et al., 2000; Vink et al., 2010; Shaheen et al., 2014). Also, the pH can change markedly during flooding. The pH of acid soils increases after flooding because reduction processes consume protons, while the pH of alkaline soils decreases because the increased gaseous carbon dioxide ($CO_2$) concentration resulting from the mineralization of organic matter causes acidification (Du Laing et al., 2009; Kögel-Knabner et al., 2010). After draining, however, the oxidation of paddy soils can (partially) reverse these reduction processes, leading to the precipitation of fresh Mn (III/IV)- and Fe (III)-(hydr)oxides, the dissolution of metal sulfides, and a change of the pH to its antecedent value (Murase and Kimura, 1997; Du Laing et al., 2009; de Livera et al., 2011). In either reduction or oxidation processes, soil and soil solution chemistry change markedly, especially with regard to metal-(hydr)oxides and organic matter. The magnitude of the redox processes is determined by soil properties, especially pH. However, the current knowledge of the effects of pH on the redox chemistry of metal-(hydr)oxides and organic matter in soil systems with alternating flooding and drainage conditions is still limited. To our knowledge, , there is little information on the effects of Eh on the redox chemistry of metal-hydroxides and organic matter in soils with a contrasting pH.

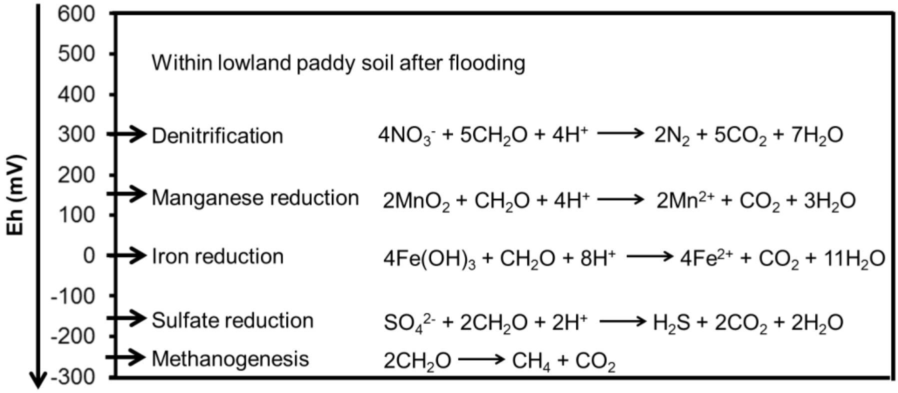

**Fig. 3.** Redox reactions in lowland paddy soils during flooding (adapted from Stumm and Morgan [1981]). $CH_2O$ represents organic matter.

### *1.1.4. Solubility of trace metals in lowland paddy soils*

In the previous section, the most important redox reactions have been described for lowland paddy soils during flooding. Alternating flooding and drainage of lowland paddy soils will lead to changes in the Eh, which will, in turn, affect the pH and the reactive surface area of SOM and short-rang ordered Mn- and Fe-(hydr)oxides. The changes in these soil properties will influence the solubility of trace metals. The pH and soil constituents including SOM and metal- (hydr)oxides play an important role in the adsorption of trace metals in soils (Weng et al., 2001). Consequently, a decrease in the reactive surface area of these soil constituents during flooding might lead to an increase in the solubility of trace metals. The mobilization of trace metals might be even further amplified by the release of DOM after flooding, because trace metals including Cu and Pb can bind strongly to DOM (Amery et al., 2007; Koopmans and Groenenberg, 2011). On the other hand, the presence of $S^{2-}$ from the reduction of $SO_4^{2-}$ might lead to the precipitation of trace metals in the form of poorly soluble minerals (de Livera et al., 2011; Khaokaew et al., 2011; Fulda et al., 2013). In addition to this, an increase in the pH of acidic soils can elevate the adsorption of trace metals to the reactive surfaces of SOM and metal-(hydr)oxides while a decrease in the pH of alkaline soils can lead to desorption of trace metals from these surfaces (Weng et al., 2001). During drainage and subsequent oxidation of paddy soils, the (partial) reversal of the above mentioned reduction processes can either immobilize trace metals via their precipitation with freshly formed Mn (III/IV)- and Fe(III)-(hydr)oxides or mobilize trace metals via the dissolution of trace metal sulfide precipitates. Also, the change of the pH back to its antecedent value will influence the adsorption of trace metals by SOM and metal-(hydr)oxides. These complex and dynamic effects of flooding and drainage on the Eh and the redox chemistry of paddy soils will have a large influence on the solubility of trace metals, which will, in turn, affect the bioavailability of trace metals for uptake by rice plants. However, the current knowledge of the effects of changes in Eh and redox chemistry on the solubility of trace metals in contaminated paddy soil systems exposed to alternating flooding and drainage conditions is still limited.

### *1.1.5. In-situ measurement of free trace metal concentrations in the soil solution of lowland paddy soils*

The speciation of trace metals in paddy soils is of great importance in determining their bioavailability for uptake by rice plants. Free trace metal ions in soil solution are usually considered to be the most bioavailable trace metal species for plant uptake (Bell et al., 1991; Parker and Pedler, 1997). To measure free trace metal concentrations in solution systems, various analytical techniques can be used including Ion-Selective Electrodes (Otto and Thomas, 1985), Cathodic Stripping Voltammetry (Xue and Sunda, 1997), Gellyfish (Senn et al., 2004), Absence of Gradients and Nernstian Equilibrium Stripping (Chito et al., 2012), Permeation Liquid Membranes (Parthasarathy et al., 1997), and the Donnan Membrane Technique (DMT; Temminghoff et al., 2000). In this Ph.D. thesis, I focus on the use of the DMT, because this technique does not perturb the equilibrium between free trace metal ions and other forms of trace metals in solution and it allows for measuring the free ion concentrations of multiple elements at the same time (Temminghoff et al., 2000).

The lab DMT developed by Temminghoff et al. (2000) has been successfully used to measure the free metal concentrations in synthetic multicomponent systems (Osté et al., 2002) and soil solution extracts (Weng et al., 2001; Koopmans et al., 2008; Koopmans and Groenenberg, 2011). However, the use of the lab DMT to measure free metal concentrations in the soil solution of flooded paddy soils is difficult because it is a complicated task to sample flooded paddy soils without perturbing the Eh and maintaining anaerobic conditions during the DMT experiment in the laboratory. Therefore, it would be preferable to measure free trace metal concentrations in-situ without significantly disturbing the system. The so-called field DMT (Fig. 4), which is a modified version of the lab DMT, has been developed for in-situ measurements of free trace metal concentrations. In this field DMT cell, only one chamber containing the acceptor solution with two cation exchange membranes on both sides is used, without any pumping (Fig. 4; van der Stelt et al., 2005). The use of an additional membrane in the field DMT cell is expected to facilitate a faster exchange of cations between the surrounding donor solution and the acceptor solution (Fig. 4; Kalis et al., 2006). The field DMT has been successfully used in-situ to measure free nutrient concentrations in slurries of animal manure (van der Stelt et al., 2005) and free metal concentrations in

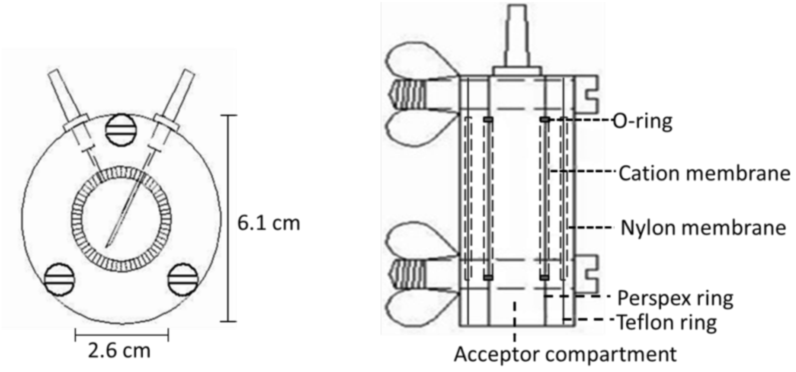

**Front view of field DMT** **Side view of field DMT**

**Fig. 4.** Front view and side view of the field DMT cell, modified from the field DMT cell developed by van der Stelt et al. (2005). The modified field DMT cell was tested in a flooded paddy soil in a column experiment in Chapter 4 of this Ph.D. thesis.

waters (Kalis et al., 2006; Sigg et al., 2006; Unsworth et al., 2006; Chito et al., 2012; Vega and Weng, 2013). Before the field DMT can be used in paddy fields, this analytical technique first needs to be tested since it has not been used previously to measure free trace metal concentrations in-situ in flooded soils.

### *1.1.6. Geochemical speciation modeling of trace metals solubility in lowland paddy soils*

Multi-surface models can be a useful tool to investigate the partitioning of trace metals between the soil solution and the soil solid phase and the speciation of trace metals within these soil compartments. In the next two sections, first an approach will be described which can be used to predict the speciation of trace metals only in solution, followed by a description of the multi-surface modeling approach which can be used to predict solid-solution partitioning of trace metals.

#### *1.1.6.1. Soil solution speciation modeling*

In soil solution, trace metals can be present as free metal ions or they can be complexed by inorganic ligands or DOM (Fig. 5; Weng et al., 2002; Koopmans et al., 2008; Groenenberg et al., 2010). Trace metal binding with inorganic ligands can be predicted based on known stability constants for the formation of trace metal complexes with such ligands (Fig. 5). Trace metal binding with DOM can be predicted by advanced multi-surface models including Model VI (Tipping, 1998) and the Non-Ideal Competitive Adsorption Donnan (NICA-Donnan) model (Fig. 5; Kinniburgh et al., 1999). The NICA-Donnan model is a combination of the NICA model for predicting specific competitive binding of ions to humic substances (HS) including fulvic acids (FA) and humic acids (HA) and a Donnan model for non-specific electrostatic binding of ions (Kinniburgh et al., 1999; Groenenberg et al., 2010). This model has successfully been applied to describe the binding of protons and metal ions to purified FA and HA (Kinniburgh et al., 1999; Milne et al., 2001, 2003). For the application of the NICA-Donnan model to predict trace metal binding to DOM in soil solution, information is required on the fractions of HA and FA in DOM. According to a recent overview of Groenenberg et al. (2010), FA dominated the composition of DOM for a range of different soils, with an average contribution of FA to the total dissolved organic carbon (DOC) concentration amounting to 35%. The average contribution of hydrophilic compounds to the DOC concentration in the overview of Groenenberg et al. (2010) was 61% whereas the average HA contribution was low (4%). However, the nature and reactivity of DOM can be different when the Eh of paddy soils changes from aerobic conditions to anaerobic conditions during flooding. Under anaerobic conditions, Hanke et al. (2014) found a decrease in the affinity of DOM to bind to short-range ordered Fe-(hydr)oxides. They attributed these findings to compositional changes in the DOM due to anaerobic processes. Furthermore, compositional changes of DOM including the formation of reduced sulfur-containing ligands can take place (Qian et al., 2002). Trace metals have a higher affinity to bind to reduced sulfur-containing ligands of HA than to oxygen-containing ligands such as carboxylic groups (Smith et al., 2002; Maurer et al., 2012). Consequently, model predictions for trace metals such as Cu and Pb with a high affinity to bind to DOM might be biased under anaerobic conditions. Therefore, it is important to validate the NICA-Donnan model with regard to its ability to predict trace metal speciation under a wide variety of geochemical conditions including anaerobic conditions. Also, it is important to measure the speciation of DOM in paddy soils during alternating flooding and draining conditions.

#### *1.1.6.2. Partitioning of trace metals between soil solution and the soil solid phase*

For the solid-solution partitioning of trace metals, multi-surface modeling approach can be used to predict trace metal complexation by different reactive surfaces, including SOM and DOM, short-range ordered and crystalline Fe-(hydr)oxides, and clay (Weng et al., 2001; Bonten et al., 2008), and precipitation as minerals (Meima and Comans, 1997). For predicting the interactions of trace metals with these reactive surfaces and trace metal precipitation, different multi-surface models can be used (Fig. 5). Specifically, adsorption of trace metals to both SOM and DOM can be described by the NICA-Donnan model (Kinniburgh et al., 1999; Koopal et al., 2005), to clay minerals by a non-specific cation exchange model using a Donnan approach, and to amorphous Fe- and Al-(hydr)oxides by the two site diffusive double layer model for HFO from Dzombak and Morel (1990). These different models can be combined into the so-called multi-surface modeling approach whereby the total adsorption of trace metals is calculated from the prediction of trace metal complexation by the individual reactive surfaces of the aforementioned soil constituents (Weng et al., 2002). In this modeling approach, no interactions between the various reactive surfaces are assumed other than competition for ion binding. This multi-surface approach where different models are assembled into was recently reviewed by Groenenberg and Lofts (2014). The application of the multi-surface approach has been shown to adequately predict the solubility of most trace metals for aerobic soils (e.g., Weng et al., 2001; Cancès et al., 2003; Bonten et al., 2008). However, it is unclear on whether this approach can be applied to predict the partitioning of trace metals for paddy soils exposed to alternating flooding and drainage conditions. With the change from aerobic to anaerobic conditions, formation of minerals such as metal sulfides in flooded soils or sediments can take place (Morse and Luther, 1999; Weber et al., 2009). Since there is still little experimental evidence on the chemical identity of such metal (particularly Cu) sulfides formed under anaerobic conditions (Weber et al., 2009), it is difficult to include this process in multi-surface models. Also, the size of reactive surfaces of adsorbents including SOM and Fe-(hydr)oxides can decrease upon flooding while compositional changes can take place within the SOM and DOM including the formation of reduced sulfur-containing ligands (Qian et al., 2002) which influence the reactivity of these surfaces for binding trace metals. These processes are not necessarily incorporated within multi-surface models.

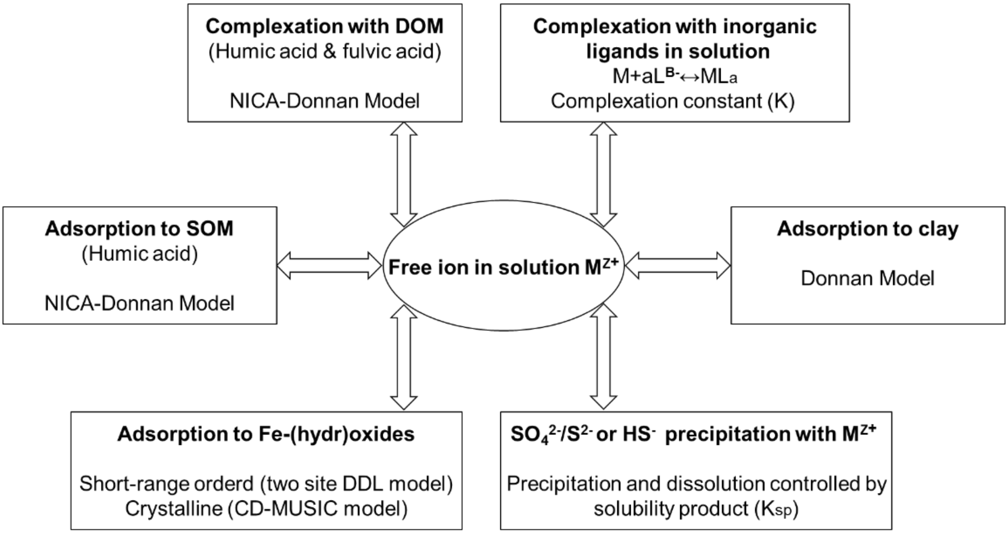

**Fig. 5.** Conceptual structure of the reactions and multi-surface models used in the multi-surface approach to predict trace metal partitioning and speciation (adapted from Weng et al. [2002]).

Moreover, chemical processes such as precipitation and dissolution of Fe-(hydr)oxides and trace metal minerals under alternating flooding and drainage conditions can be kinetically-limited (Pan et al., 2014), which might restrict the applicability of multi-surface models for such systems due to their chemical equilibrium nature. This warrants specific research into the extent to which existing multi-surface models can be applied to dynamic systems including lowland paddy soils to predict the solubility of trace metals under changing redox conditions.

### *1.1.7. Uptake of trace metals by rice plants cultivated on lowland paddy soils*

Uptake of trace metals by rice plants is closely related to the bioavailability of trace metals in paddy soils (Simmons et al., 2008; Römkens et al., 2009b). For trace metals in paddy soils, three operationally defined pools can be distinguished, which exhibit a different bioavailability: the total, reactive, and directly available trace metal pools (Römkens et al., 2009a). Among these trace metal pools, the reactive pool represents trace metals adsorbed to reactive surfaces of SOM, short-range ordered metal-(hydr)oxides, and clay and controls the trace metal concentration in soil solution (Weng et al., 2001), while the directly available pool represents the free or total dissolved trace metal concentration in soil solution which can be directly related to the uptake of trace metals by plants (Lofts et al., 2004; Pejnenburg et al., 2007). The equilibrium between the reactive pool and the directly available pool can be described with empirical regression models (e.g., Römkens et al., 2009a) or multi-surface models (e.g., Groenenberg and Lofts, 2014), as discussed in the previous section. Reactive pool can be determined by extraction of soil with 0.43 M $HNO_3$, 0.1 M HCl, or 0.05 M EDTA, whereas the readily available pool can be determined by extraction of soil with 0.01 M $CaCl_2$ (Römkens et al., 2009a). The total trace metal pool is usually larger than the reactive trace metal pool and includes non-reactive and fixed trace metals forms (Römkens et al., 2009a). For paddy soils with a wide range in soil properties such as pH, DOC, and CEC, regression-based log-log linear relationships have been used to link the directly available Cd pool as determined by the 0.01 M $CaCl_2$ extraction of soil to the Cd content of rice grains (Simmons et al., 2008; Römkens et al., 2009b). In some studies, this directly available trace metal pool was replaced by the reactive Cd pool based on the 0.43 M $HNO_3$ extraction of soil in combination with pH, SOM, and clay (Brus et al., 2009; Römkens et al., 2009b). However, most of the relationships in these aforementioned studies were determined for a specific growth stage of the rice plants, i.e., the rice grain filling stages. The solubility of trace metals in soil solution under alternating flooding and drainage conditions and how this sequence of processes is linked with metal uptake by rice plants over time has received less attention.

Uptake of trace metals by rice plants does not only depend on the bioavailability of trace metals in soils but the uptake characteristics of trace metals by various rice cultivars and genotypes are important as well (Yu et al., 2006; Römkens et al., 2009b). The uptake of trace metals in rice grains is controlled by two processes: uptake by the roots and translocation from roots to the shoots, followed by accumulation in the rice grains (Liu et al., 2007; Uraguchi et al., 2009). Römkens et al. (2009b) calculated the rice-root ratios for Indica and Japonica cultivars and they found higher Cd ratios for the Indica cultivars than for the Japonica cultivars. Uptake of trace metals by rice does not only differ for rice cultivars and genotypes but differs during the different rice growth stages as well (Chaney et al., 1996; Kashem and Singh, 2001; Simmons et al., 2005, 2008). Particularly, the rice grain filling stage has been frequently studied, which might increase the concentrations of trace metals in soil solution due to the dissolution of metal sufides and potentially might increase the uptake of trace metals by rice grains (Chaney et al., 1996; Kashem and Singh, 2001; Simmons et al., 2005, 2008). Nevertheless, the knowledge about the uptake of trace metals in different rice tissues during whole rice growing period has received little attention too, and as a consequence, the linkage between the uptake of trace metals by different rice tissues and the solubility of trace metals during the major rice growth stages is still limited.

## *1.2. Objectives*

Given the above research needs, the main objective of my Ph.D. thesis is to increase the understanding with regard to solubility of trace metals in paddy soils as affected by changes in the Eh due to alternating flooding and drainage conditions and how this is related to the uptake of trace metals by rice plants. The specific objectives are:

(i) To determine how flooding and draining cycles affect the redox chemistry of metal-(hydr)oxides and organic matter in paddy soils and how the pH influences these processes. Also, to determine to what extent a multi-surface modeling approach can be used to predict the solubility of Mn and Fe during flooding and draining cycles in paddy soils.

(ii) To determine how two flooding and drainage events affect the solubility of trace metals in field-contaminated paddy soils and, moreover, to examine to what extent the multi-surface modeling approach can be used to predict solubility of trace metals under changing redox conditions.

(iii) To test the potential of the field DMT to measure free trace metal concentrations in-situ in soil solution of a flooded paddy soil under anaerobic conditions and to validate NICA-Donnan model with regard to their ability to predict trace metal speciation under anaerobic conditions.

(iv) To study the relationship between solubility of trace metals during alternating flooding and drainage periods and their uptake by rice plants during the major rice growth stages.

### *1.3. Outline*

This Ph.D. thesis consists of six chapters including the General Introduction. The specific objectives stated above are corresponding with the following four chapters:

In Chapter 2, we performed a carefully-designed column experiment with two paddy soils with similar soil properties but contrasting pH. We monitored the Eh continuously and measured the chemical composition of soil solution samples taken regularly at four depths along the soil profile during two successive flooding and drainage cycles. To determine the dominant mineral phases of Mn and Fe under equilibrium conditions, stability diagrams of Mn and Fe were constructed as a function of Eh and pH. Geochemical equilibrium model calculations were performed to identify Mn and Fe solubility-controlling minerals and to compare the predicted total dissolved concentrations with their measured values.

In Chapter 3, we used the same column experiment as described in Chapter 2. We measured the total dissolved trace metal concentrations in soil solution samples taken along the soil profile during two successive flooding and drainage cycles. Furthermore, we modeled the partitioning of trace metals between the soil solution and the soil solid phase under both aerobic and anaerobic conditions and examined to what extent the multi-surface modeling approach can be used to predict trace metal solubility under changing redox conditions.

In Chapter 4, we tested the potential application of the field DMT to measure the free trace metal concentrations in-situ in soil solution of a flooded field-contaminated paddy soil in a soil column experiment. The Eh and pH and the concentrations of DOC, Fe, Mn, S, total dissolved and free trace metals were monitored at three depths as a function of flooding time. Further, we used the measured free trace metal concentrations by the field DMT to validate the NICA-Donnan model by comparing the field DMT measurements of free trace metal concentrations in both the aerobic and anaerobic layers of the soil column experiment with predictions of the free trace metal concentrations.

In Chapter 5, we designed a pot experiment with a field-contaminated paddy soil to grow two rice cultivars exhibiting either a low or a high ability to accumulate Cd in brown rice. The Eh and pH and the concentrations of DOC, Fe, Mn, S, and trace metals in soil solution were monitored at five depths during the major rice growth stages including tillering, booting, filling, and final harvest. Rice plants were harvested at these different stages and the corresponding trace metal contents in the different rice tissues were determined. Finally, we studied the relationship between the solubility of trace metals over time and their uptake by different rice tissues during major rice growth stages.

My Ph.D. thesis finishes with the General Discussion in Chapter 6 in which the results of the different chapters are synthesized and the recommendations for future research are provided.

## References

Agency for Toxic Substances and Disease Registry, 2012. Toxicological profile for cadmium. Available at www.atsdr.cdc.gov/toxprofiles/tp5.pdf (verified Nov. 2014).

Amery, F., Degryse, F., Degeling, W., Smolders, E., Merckx, R., 2007. The copper-mobilizing-potential of dissolved organic matter in soils varies 10-fold depending on soil incubation and extraction procedures. Environ Sci Technol 41, 2277–2281.

Arunakumara, K.K.I.U., Walpola, B.C., Yoon, M.H., 2013. Current status of heavy metal contamination in Asia's rice lands. Rev Environ Sci Bio 12, 355-377.

Bell, P.F., Chaney, R.L., Angle, J.S., 1991. Free metal activity and total metal concentrations as indexes of micronutrient availability to barley [Hordeum vulgare (L.) ‘Klages’]. Plant Soil 130, 51–62.

Bonten, L.T.C., Groenenberg, J.E., Weng, L., van Riemsdijk, W.H., 2008. Use of speciation and complexation models to estimate heavy metal sorption in soils. Geoderma 146, 303–310.

Brus, D.J., Li, Z.B., Song, J., Koopmans, G.F., Temminghoff, E.J.M., Yin, X.B., Yao, C.X., Zhang, H.B., Luo, Y.M., Japenga, J., 2009. Predictions of spatially averaged cadmium contents in rice grains in the Fuyang Valley, P.R. China. J Environ Qual 38, 1126–1136.

Cancès, B., Ponthieu, M., Castrec-Rouelle, M., Aubry, E., Benedetti, M.F., 2003. Metal ions speciation in a soil and its solution: Experimental data and model results. Geoderma 113, 341–355.

Chaney, R.L, J.A. Ryan,Y.M. Li, R.M. Welch, P.G. Reeves, S.L. Brown, Green, C.E., 1996. Phyto-availability and bio-availability in risk assessment for cadmium in agricultural environments. In: Sources of Cadmium in the Environment, OECD, Paris, France, pp. 49–78.

Chito, D., Weng, L.P., Galceran, J., Companys, E., Puy, J., van Riemsdijk, W.H., van Leeuwen, H.P., 2012. Determination of free $Zn^{2+}$ concentration in synthetic and natural samples with AGNES (Absence of Gradients and Nernstian Equilibrium Stripping) and DMT (Donnan Membrane Technique). Sci Total Environ 421, 238–244.

de Livera, J., McLaughlin, M.J., Hettiarachchi, G.M., Kirby, J.K., Beak, D.G., 2011. Cadmium solubility in paddy soils: Effects of soil oxidation, metal sulfides and competitive ions. Sci Total Environ 409, 1489–1497.

Du Laing, G., Rinklebe, J., Vandecasteele, B., Meers, E., Tack, F.M.G., 2009. Trace metal behaviour in estuarine and riverine floodplain soils and sediments: A review. Sci Total Environ 407, 3972–3985.

Dzombak, D.A., Morel, F.M.M., 1990. Surface complexation modeling: Hydrous ferric oxide. Wiley, New York, pp. 393.

Fu, S., Wei, C.Y., 2013. Multivariate and spatial analysis of heavy metal sources and variations in a large old antimony mine, China. J Soil Sediment 13, 106–116.

Fulda, B., Voegelin, A., Kretzschmar, R., 2013. Redox-controlled changes in cadmium solubility and solid-phase speciation in a paddy soil as affected by reducible sulfate and copper. Environ Sci Technol 47, 12775–12783.

Gao, R., Temminghoff, E.J.M., van Leeuwen, H.P., van Valenberg, H.J.F., Eisner, M.D., van Boekel, M.A.J.S., 2009. Simultaneous determination of free calcium, magnesium, sodium and potassium ion concentrations in simulated milk ultrafiltrate and reconstituted skim milk using the Donnan Membrane Technique. Int Dairy J 19, 431–436.

Groenenberg, J.E., Koopmans, G.F., Comans, R.N.J., 2010. Uncertainty analysis of the nonideal competitive adsorption-donnan model: Effects of dissolved organic matter variability on predicted metal speciation in soil solution. Environ Sci Technol 44, 1340–1346.

Groenenberg, J.E., Lofts, S., 2014. The use of assemblage models to describe trace element partitioning, speciation, and fate: A review. Environ Toxicol Chem 33, 2181–2196.

Grybos, M., Davranche, M., Gruau, G., Petitjean, P., 2007. Is trace metal release in wetland soils controlled by organic matter mobility or Fe-oxyhydroxides reduction? J Colloid Interf Sci 314, 490–501.

Hanke, A., Sauervvein, M., Kaiser, K., Kalbitz, K., 2014. Does anoxic processing of dissolved organic matter affect organic-mineral interactions in paddy soils? Geoderma 228, 62–66.

Kalbitz, K., Solinger, S., Park, J.H., Michalzik, B., Matzner, E., 2000. Controls on the dynamics of dissolved organic matter in soils: A review. Soil Sci 165, 277–304.

Kalis, E.J.J., Weng, L.P., Dousma, F., Temminghoff, E.J.M., van Riemsdijk, W.H., 2006. Measuring free metal ion concentrations in situ in natural waters using the Donnan Membrane Technique. Environ Sci Technol 40, 955–961.

Kashem, M.A., Singh, B.R., 2001. Metal availability in contaminated soils: I. Effects of flooding and organic matter on changes in Eh, pH and solubility of Cd, Ni and Zn. Nutr Cycl Agroecosys 61, 247–255.

Khaokaew, S., Chaney, R.L., Landrot, G., Ginder-Vogel, M., Sparks, D.L., 2011. Speciation and release kinetics of cadmium in an alkaline paddy soil under various flooding periods and draining conditions. Environ Sci Technol 45, 4249–4255.

Kinniburgh, D.G., van Riemsdijk, W.H., Koopal, L.K., Borkovec, M., Benedetti, M.F., Avena, M.J., 1999. Ion binding to natural organic matter: competition, heterogeneity, stoichiometry and thermodynamic consistency. Colloid Surface A 151, 147–166.

Kögel-Knabner, I., Amelung, W., Cao, Z.H., Fiedler, S., Frenzel, P., Jahn, R., Kalbitz, K., Kolbl, A., Schloter, M., 2010. Biogeochemistry of paddy soils. Geoderma 157, 1–14.

Koopal, L.K., Saito, T., Pinheiro, J.P., van Riemsdijk, W.H., 2005. Ion binding to natural organic matter: General considerations and the NICA-Donnan model. Colloid Surface A 265, 40–54.

Koopmans, G.F., Groenenberg, J.E., 2011. Effects of soil oven-drying on concentrations and speciation of trace metals and dissolved organic matter in soil solution extracts of sandy soils. Geoderma 161, 147–158.

Koopmans, G.F., Schenkeveld, W.D.C., Song, J., Luo, Y.M., Japenga, J., Temminghoff, E.J.M., 2008. Influence of EDDS on metal speciation in soil extracts: Measurement and mechanistic multicomponent modeling. Environ Sci Technol 42, 1123–1130.

Kuo, S., Lai, M.S., Lin, C.W., 2006. Influence of solution acidity and $CaCl_2$ concentration on the removal of heavy metals from metal-contaminated rice soils. Environ Pollut 144, 918–925.

Liu, J.G., Qian, M., Cai, G.L., Yang, J.C., Zhu, Q.S., 2007. Uptake and translocation of Cd in different rice cultivars and the relation with Cd accumulation in rice grain. J Hazard Mater 143, 443–447.

Liu, Z.H., Li, Z.G., Tang, P.Q., Li, Z.P., Wu, W.B., Yang, P., You, L.Z., Tang, H.J., 2013. Change analysis of rice area and production in China during the past three decades. J Geogr Sci 23, 1005–1018.

Lofts, S., Spurgeon, D.J., Svendsen, C., Tipping, E., 2004. Deriving soil critical limits for Cu, Zn, Cd, and Pb: A method based on free ion concentrations. Environ Sci Technol 38, 3623–3631.

Luo, X.S., Yu, S., Zhu, Y.G., Li, X.D., 2012. Trace metal contamination in urban soils of China. Sci Total Environ 421, 17–30.

Maurer, F., Christl, I., Hoffmann, M., Kretzschmar, R., 2012. Reduction and reoxidation of humic acid: Influence on speciation of cadmium and silver. Environ Sci Technol 46, 8808–8816.

Meharg, A.A., Norton, G., Deacon, C., Williams, P., Adomako, E.E., Price, A., Zhu, Y.G., Li, G., Zhao, F.J., McGrath, S., Villada, A., Sommella, A., De Silva, P.M.C.S., Brammer, H., Dasgupta, T., Islam, M.R., 2013. Variation in rice cadmium related to human exposure. Environ Sci Technol 47, 5613–5618.

Meima, J.A., Comans, R.N.J., 1998. Application of surface complexation precipitation modeling to contaminant leaching from weathered municipal solid waste incinerator bottom ash. Environ Sci Technol 32, 688–693.

Milne, C.J., Kinniburgh, D.G., van Riemsdijk, W.H., Tipping, E., 2003. Generic NICA-Donnan model parameters for metal-ion binding by humic substances. Environ Sci Technol 37, 958–971.

Ministry of Agriculture of the People’s Republic of China, 2014. Advantageous areas for rice growth and production in China. Available at http://www.moa.gov.cn/zwllm/zwdt/200809/t20080912_1132619.htm (verified Nov. 2014).

Ministry of Environmental Protection of the People’s Republic of China, Ministry of Land and Resources of the People’s Republic of China, 2014. The Communique of the Chinese National Soil Contamination Survey (2005-2013). Available at http://www.mep.gov.cn/gkml/hbb/qt/201404/W020140417558995804588.pdf (verified Nov. 2014).

Morse, J.W., Luther, G.W., 1999. Chemical influences on trace metal-sulfide interactions in anoxic sediments. Geochim Cosmochim Ac 63, 3373–3378.

Murase, J., Kimura, M., 1997. Anaerobic reoxidation of $Mn^{2+}$, $Fe^{2+}$, $S^0$ and $S^{2-}$ in submerged paddy soils. Biol Fert Soils 25, 302–306.

Nordberg, G.F., 2004. Cadmium and health in the 21st century – historical remarks and trends for the future. Biometals 17, 485–489.

Osté, L.A., Temminghoff, E.J.M., Lexmond, T.M., van Riemsdijk, W.H., 2002. Measuring and modeling zinc and cadmium binding by humic acid. Anal Chem 74, 856–862.

Otto, M., Thomas, J.D.R., 1985. Model studies on multiple channel analysis of free magnesium, calcium, sodium, and potassium at physiological concentration levels with ion-selective electrodes. Anal Chem 57, 2647–2651.

Pan, K., Wang, W.X., 2012. Trace metal contamination in estuarine and coastal environments in China. Sci Total Environ 421, 3–16.

Pan, Y.Y., Koopmans, G.F., Bonten, L.T.C., Song, J., Luo, Y.M., Temminghoff, E.J.M., Comans, R.N.J., 2014. Influence of pH on the redox chemistry of metal (hydr)oxides and organic matter in paddy soils. J Soil Sediment 14, 1713–

1726.

Parker, D.R., Pedler, J.F., 1997. Reevaluating the free-ion activity model of trace metal availability to higher plants. Plant Soil 196, 223–228.

Parthasarathy, N., Pelletier, M., Buffle, J., 1997. Hollow fiber based supported liquid membrane: A novel analytical system for trace metal analysis. Anal Chim Acta 350, 183–195.

Peijnenburg, W.J.G.M., Zablotskaja, M., Vijver, M.G., 2007. Monitoring metals in terrestrial environments within a bioavailability framework and a focus on soil extraction. Ecotox Environ Safe 67, 163–179.

Peng, S.B., Tang, Q.Y., Zou, Y.B., 2009. Current status and challenges of rice production in China. Plant Prod Sci 12, 3–8.

Qian, J., Skyllberg, U., Frech, W., Bleam, W.F., Bloom, P.R., Petit, P.E., 2002. Bonding of methyl mercury to reduced sulfur groups in soil and stream organic matter as determined by X-ray absorption spectroscopy and binding affinity studies. Geochim Cosmochim Ac 66, 3873–3885.

Reeves, P.G., Chaney, R.L., 2002. Nutritional status affects the absorption and whole-body and organ retention of cadmium in rats fed rice-based diets. Environ Sci Technol 36, 2684–2692.

Reeves, P.G., Chaney, R.L., 2004. Marginal nutritional status of zinc, iron, and calcium increases cadmium retention in the duodenum and other organs of rats fed rice-based. Environ Res 96, 311–322.

Römkens, P.F.A.M., Guo, H.Y., Chu, C.L., Liu, T.S., Chiang, C.F., Koopmans, G.F., 2009a. Characterization of soil heavy metal pools in paddy fields in Taiwan: Chemical extraction and solid-solution partitioning. J Soil Sediment 9, 216–228.

Römkens, P.F.A.M., Guo, H.Y., Chu, C.L., Liu, T.S., Chiang, C.F., Koopmans, G.F., 2009b. Prediction of cadmium uptake by brown rice and derivation of soil-plant transfer models to improve soil protection guidelines. Environ Pollut 157, 2435–2444.

Shaheen, S.M., Rinklebe, J., Rupp, H., Meissner, R., 2014. Lysimeter trials to assess the impact of different flood-dry-cycles on the dynamics of pore water concentrations of As, Cr, Mo and V in a contaminated floodplain soil. Geoderma 228–229, 5–13.

Sigg, L., Black, F., Buffle, J., Cao, J., Cleven, R., Davison, W., Galceran, J., Gunkel, P., Kalis, E., Kistler, D., Martin, M., Noel, S., Nur, Y., Odzak, N., Puy, J., van Riemsdijk, W., Temminghoff, E., Tercier-Waeber, M.L., Toepperwien, S., Town, R.M., Unsworth, E., Warnken, K.W., Weng, L.P., Xue, H.B., Zhang, H., 2006. Comparison of analytical techniques for dynamic trace metal speciation in natural freshwaters. Environ Sci Technol 40, 1934–1941.

Simmons, R.W., Noble, A.D., Pongsakul, P., Sukreeyapongse, O., Chinabut, N., 2008. Analysis of field-moist Cd contaminated paddy soils during rice grain fill allows reliable prediction of grain Cd levels. Plant Soil 302, 125–137.

Simmons, R.W., Pongsakul, P., Saiyasitpanich, D., Klinphoklap, S., 2005. Elevated levels of cadmium and zinc in paddy soils and elevated levels of cadmium in rice grain downstream of a zinc mineralized area in Thailand: Implications for public health. Environ Geochem Hlth 27, 501–511.

Smith, D.S., Bell, R.A., Kramer, J.R., 2002. Metal speciation in natural waters with emphasis on reduced sulfur groups as strong metal binding sites. Comp Biochem Phys C 133, 65–74.

Stumm, W.J., Morgan, J.J., 1981. Aquatic chemsitry. An introduction to emphasizing chemical equlibria in natural waters. John Wiley & Sons, USA.

Tack, F.M.G., van Ranst, E., Lievens, C., Vandenberghe, R.E., 2006. Soil solution Cd, Cu and Zn concentrations as affected by short-time drying or wetting: The role of hydrous oxides of Fe and Mn. Geoderma 137, 83–89.

Temminghoff, E.J.M., Plette, A.C.C., van Eck, R., van Riemsdijk, W.H., 2000. Determination of the chemical speciation of trace metals in aqueous systems by the Wageningen Donnan Membrane Technique. Anal Chim Acta 417, 149–157.

Tipping, E., 1998. Humic ion-binding model VI: An improved description of the interactions of protons and metal ions with humic substances. Aquat Geochem 4, 3–48.

Unsworth, E.R., Warnken, K.W., Zhang, H., Davison, W., Black, F., Buffle, J., Cao, J., Cleven, R., Galceran, J., Gunkel, P., Kalis, E., Kistler, D., van Leeuwen, H.P., Martin, M., Noel, S., Nur, Y., Odzak, N., Puy, J., van Riemsdijk, W., Sigg, L., Temminghoff, E., Tercier-Waeber, M.L., Toepperwien, S., Town, R.M., Weng, L.P., Xue, H.B., 2006. Model predictions of metal speciation in freshwaters compared to measurements by in situ techniques. Environ Sci Technol 40, 1942–1949.

Uraguchi, S., Mori, S., Kuramata, M., Kawasaki, A., Arao, T., Ishikawa, S., 2009. Root-to-shoot Cd translocation via the xylem is the major process determining shoot and grain cadmium accumulation in rice. J Exp Bot 60, 2677–2688.

van der Stelt, B., Temminghoff, E.J.M., van Riemsdijk, W.H., 2005. Measurement of ion speciation in animal slurries using the Donnan Membrane Technique. Anal Chim Acta 552, 135–140.

Vega, F.A., Weng, L.P., 2013. Speciation of heavy metals in River Rhine. Water Res 47, 363–372.

Vink, J.P.M., Harmsen, J., Rijnaarts, H., 2010. Delayed immobilization of heavy metals in soils and sediments under reducing and anaerobic conditions; consequences for flooding and storage. J Soil Sediment 10, 1633-1645.

Weber, F.A., Voegelin, A., Kretzschmar, R., 2009. Multi-metal contaminant dynamics in temporarily flooded soil under sulfate limitation. Geochim Cosmochim Ac 73, 5513–5527.

Weng, L.P., Temminghoff, E.J.M., Lofts, S., Tipping, E., van Riemsdijk, W.H., 2002. Complexation with dissolved organic matter and solubility control of heavy metals in a sandy soil. Environ Sci Technol 36, 4804-4810.

Weng, L.P., Temminghoff, E.J.M., van Riemsdijk, W.H., 2001. Contribution of individual sorhents to the control of heavy metal activity in sandy soil. Environ Sci Technol 35, 4436–4443.

Xue, H.B., Sunda, W.G., 1997. Comparison of [$Cu^{2+}$] measurements in lake water determined by ligand exchange and cathodic stripping voltammetry and by ion-selective electrode. Environ Sci Technol 31, 1902–1909.

Yu, H., Wang, J.L., Fang, W., Yuan, J.G., Yang, Z.Y., 2006. Cadmium accumulation in different rice cultivars and screening for pollution-safe cultivars of rice. Sci Total Environ 370, 302–309.

Yu, K.W., Bohme, F., Rinklebe, J., Neue, H.U., DeLaune, R.D., 2007. Major biogeochemical processes in soils – A microcosm incubation from reducing to oxidizing conditions. Soil Sci Soc Am J 71, 1406–1417.

Zeng, F.R., Ali, S., Zhang, H.T., Ouyang, Y.B., Qiu, B.Y., Wu, F.B., Zhang, G.P., 2011. The influence of pH and organic matter content in paddy soil on heavy metal availability and their uptake by rice plants. Environ Pollut 159, 84–91.

Zhang, X., Wang, D., Fang, F., Zhen, Y., Liao, X., 2005. Food safety and rice production in China. Res. Agric. Modernization 26, 85–88. (in Chinese)

# Chapter 2

# Influence of pH on the redox chemistry of metal (hydr)oxides and organic matter in paddy soils

*Yunyu Pan, Gerwin F. Koopmans, Luc T.C. Bonten, Jing Song, Yongming Luo, Erwin J.M. Temminghoff, Rob N.J. Comans*

Published in Journal of Soils and Sediments, **2014**

## Abstract

*Purpose* The primary purpose of this study was to determine how flooding and draining cycles affect the redox chemistry of metal (hydr)oxides and organic matter in paddy soils and how the pH influences these processes. Our secondary purpose was to determine to what extent a geochemical thermodynamic equilibrium model can be used to predict the solubility of Mn and Fe during flooding and draining cycles in paddy soils.

*Material and methods* We performed a carefully-designed column experiment with two paddy soils with similar soil properties but contrasting pH. We monitored the redox potential (Eh) continuously and took soil solution samples regularly at four depths along the soil profile during two successive flooding and drainage cycles. To determine dominant mineral phases of Mn and Fe under equilibrium conditions, stability diagrams of Mn and Fe were constructed as a function of Eh and pH. Geochemical equilibrium model calculations were performed to identify Mn and Fe solubility-controlling minerals and to compare predicted total dissolved concentrations with their measured values.

*Results and discussion* Flooding led to strong Eh gradients in the columns of both soils. In the acidic soil, pH increased with decreasing Eh and vice versa, whereas pH in the alkaline soil was buffered by $CaCO_3$. In the acidic soil, Mn and Fe solubility increased during flooding due to reductive dissolution of their (hydr)oxides and decreased during drainage because of re-oxidation. In the alkaline soil, Mn and Fe solubility did not increase during flooding due to Mn(II) and Fe(II) precipitation as $MnCO_3$, $FeCO_3$, and FeS. The predicted levels of soluble Mn and Fe in the acidic soil were much higher than their measured values, but predictions and measurements were rather similar in the alkaline soil. This difference is likely due to kinetically-limited reductive dissolution of Mn and Fe (hydr)oxides in the acidic soil. During flooding, the solubility of dissolved organic matter increased in both soils, probably because of reductive dissolution of Fe (hydr)oxides and the observed increase in pH.

*Conclusions* Under alternating flooding and draining conditions, the pH greatly affected Mn and Fe solubility via influencing either reductive dissolution or carbonate formation. Comparison between measurements and geochemical equilibrium model predictions revealed that reductive dissolution of Mn and Fe (hydr)oxides was kinetically-limited in the acidic soil. Therefore, when applying such models to systems with changing redox conditions, such rate-limiting reactions should be parameterized and implemented to enable more accurate predictions of Mn and Fe solubility.

*Keywords:* DOC, geochemical modeling, metal (hydr)oxides, paddy soils, redox

## *2.1. Introduction*

Rice feeds more than 2 billion people worldwide and it is the most important staple food for people in Southeast Asia (Meharg et al., 2013). About 90 % of the world rice production is cropped and consumed in Southeast Asia. Rice is usually cropped in lowland paddy soils. During cultivation of lowland rice, flooding conditions prevail during almost the entire cropping period, because lowland rice is extremely sensitive to water shortage (Kögel-Knabner et al., 2010). Nevertheless, flooded paddy soils need to be drained during two stages of rice growth: the late tillering stage in order to control ineffective tillering and shortly before the harvest to enable faster rice ripening and easier harvesting (Kögel-Knabner et al., 2010). Therefore, paddy soils undergo at least two successive flooding and drainage periods. These flooding and draining periods can considerably affect the redox chemistry of paddy soils by either reduction or oxidation processes.

During flooding of paddy soils, the redox potential (Eh) decreases after $O_2$ depletion. With a decreasing Eh, the following reduction processes can take place either sequentially or simultaneously: $NO_3^-$, Mn (III/IV), Fe (III), and $SO_4^{2-}$ can be used as alternative terminal electron acceptors (Ponnamperuma, 1972; Yu et al., 2007; Kögel-Knabner et al., 2010). These processes lead to large changes in the chemical composition of the soil solution. After flooding and $O_2$ depletion, $NO_3^-$ reduction controls the Eh in the soil solution, leading to atmospheric losses of $N_2$ (Yu et al., 2007; Kögel-Knabner et al., 2010). Subsequently, Mn (III/IV) and Fe (III) (hydr)oxides will reductively dissolve, causing elevated concentrations of $Mn^{2+}$ and $Fe^{2+}$ in the soil solution (Gotoh and Patrick, 1972; Ponnamperuma, 1972; Tack et al., 2006; Grybos et al., 2007; Yu et al., 2007; Frohne et al., 2011; Shaheen et al., 2014). When further reduced, $SO_4^{2-}$ will transform into sulfide, eventually precipitating with metals including Fe and Mn as solid sulfides (Lindsay and Sadiq, 1983; Du Laing et al., 2009; de Livera et al., 2011; Frohne et al., 2011; Khaokaew et al., 2011; Fulda et al., 2013). The above mentioned reduction processes occur in parallel with the oxidation of organic matter. Subsequently, dissolved organic matter (DOM) will concomitantly be released into the soil solution after flooding (Hagedorn et al., 2000; Kalbitz et al., 2000; Fiedler and Kalbitz, 2003; Sahrawat, 2004; Tack et al., 2006; Grybos et al., 2007; Yu et al., 2007; Vink et al., 2010; Shaheen et al., 2014). In addition to DOM, the pH can also change markedly after flooding. The pH of acid soils increases after flooding because reduction processes consume protons, while the pH of alkaline soils decreases because the increased gaseous carbon dioxide ($CO_2$) concentration resulting from the mineralization of organic matter causes acidification (Ponnamperuma, 1972; Sahrawat, 2005; Yu et al., 2007; Du Laing et al., 2009; Kögel-Knabner et al., 2010). After draining, however, oxidation of paddy soils can reverse these reduction processes, leading to the precipitation of fresh Mn (III/IV) and Fe (III) (hydr)oxides, the dissolution of metal sulfides, and a change of the pH to its antecedent value (Murase and Kimura, 1997; Du Laing et al., 2009; de Livera et al., 2011). In either reduction or oxidation processes, soil and soil solution chemistry change markedly, especially with regard to metal (hydr)oxides and organic matter. The magnitude of the redox processes is determined by soil properties, especially pH. However, the current knowledge of the effects of pH and buffering compounds on the redox chemistry of metal (hydr)oxides and organic matter in soil systems with alternating flooding and drainage conditions is still limited.

The effects of flooding on soil and soil solution chemistry have been quantified in many studies and at different scales, each having specific advantages (Rupp et al., 2010). In some studies, a batch approach with a closed slurry system was used (Patrick and Henderson, 1981; Lindsay and Sadiq, 1983; Patrick and Jugsujinda, 1992; Murase and Kimura, 1997; Yu et al., 2007; Rupp et al., 2010; Frohne et al., 2011). This approach, however, does not represent the field situation because it does not allow for the development of Eh gradients along the flooded soil column. In some studies, soil cores with an intact soil profile were used, but these studies lack continuous Eh monitoring (Ritvo et al., 2004; Loeb et al., 2008a; Loeb et al., 2008b). This lack of continuous Eh monitoring limits the insight into temporal changes in redox processes after flooding. In some studies, a continuous Eh measurement device was used to monitor Eh dynamics in submerged sediments and wetlands (Song et al., 2004; van der Geest and Paumen, 2008; Unger et al., 2008; Rupp et al., 2010; Vorenhout et al., 2011; de Jonge et al., 2012; Shaheen et al., 2014). To our knowledge, however, there is no report in the literature about applying continuous Eh measurements to study redox processes in lowland paddy soils with a fluctuating water table. In addition, only few studies report on the application of geochemical equilibrium models to interpret the effects of Eh changes on the solubility of soil metal (hydr)oxides in such systems (Gao et al., 2010). While the application of such models can potentially provide valuable insight into the effect of redox changes on the solubility of metal (hydr)oxides, their chemical equilibrium nature warrants specific research into the extent to which such models can be applied to dynamic systems including paddy soils, undergoing alternating flooding and drainage.

In this study, our primary purpose is to determine how flooding and draining cycles affect the redox chemistry and occurrence of metal (hydr)oxides and organic matter in paddy soils. Since these reactive mineral and organic surfaces play an important role in regulating the retention and availability of trace metals in soils, it is prerequisite to understand the stability of these surfaces in soil systems with fluctuating redox conditions. We focus particularly on how the pH influences these processes, because pH is known to strongly affect the solubility of Mn and Fe and organic carbon and microbial activity. To fulfill this primary purpose, we have carefully designed and performed a column experiment with two paddy soils with similar soil properties but contrasting pH. The Eh was monitored continuously at four depths along the soil profile during two successive flooding and drainage periods. Soil solution samples were taken regularly at the same four depths to determine their chemical composition, such as pH, dissolved organic carbon (DOC), and total dissolved Mn and Fe concentrations. Moreover, our secondary purpose is to use geochemical equilibrium modelling to identify the Mn and Fe solubility-controlling minerals and to compare predicted total dissolved concentrations with their measured values. To fulfill this secondary purpose, we have constructed stability diagrams to identify the dominant mineral phases of Fe and Mn under different Eh and pH conditions. Subsequently, the total dissolved concentrations of Mn and Fe in the soil solution were calculated on the basis of assumed equilibrium with the identified most likely controlling mineral phases using the Objects Representing CHEmical Speciation and TRAnsport (ORCHESTRA) framework, which includes a chemical speciation model and models for ion sorption to three reactive surfaces: organic matter, clay minerals, and amorphous metal (hydr)oxides (Meeussen, 2003; Bonten et al., 2008). Finally, we compared the measured Mn and Fe concentrations with the predicted concentrations to identify potential rate limiting reactions during the flooding and drainage periods. Since this study was performed in a wider context in which the processes that govern the retention and availability of trace metals in paddy soils are investigated, two field-contaminated soils have been selected for the column experiment.

## 2.2. Materials and methods

### 2.2.1. Site description and soil collection

In May 2010, two soils with a clay loam texture were sampled from the 0-20 cm layer of two paddy fields in Zhejiang Province, southeast of China. One soil (TZ soil) was collected from a site nearby a former transformer and electronic waste stripping and recycling factory in the vicinity of Taizhou city. The other soil (FY soil) was collected from a site nearby a galvanizing plant in the vicinity of Fuyang city. This site has been described before by Wang et al. (2007) and Brus et al. (2009). The soils were air-dried at 40 °C, passed through a 2 mm sieve, and stored until further use for physical-chemical analysis and the column experiment.

### 2.2.2. Experimental set-up of the column experiment

For the column experiment, transparent plastic columns made of acrylic glass with a height of 18 cm and a diameter of 10 cm were used (Fig. 1). Two pieces of filter paper (Schleicher & Schuell 589$^3$) on glass wool were positioned at the bottom of each column. Soils were then placed in the columns in a 6.6 cm layer. The column experiment was performed in duplicate for each of the two soils. The four columns were kept in a temperature-controlled room at 20 °C and subjected to two successive flooding and drainage periods. The Eh monitoring data were used to determine the length of the flooding period. When the Eh stabilized, the soil columns were either drained or flooded. The first flooding period lasted for 46 days, and was followed by a drainage period of 12 days. The second flooding period, which was shorter than the first flooding period, lasted for 28 days, and was followed by a drainage period of 14 days. For flooding of the columns, a 2 mM $CaCl_2$ solution was used. The solution was pumped by a peristaltic pump from the bottom of the column in an upward direction to remove entrapped air bubbles. The solution was pumped at a rate of 0.25 ml min$^{-1}$ for about 18-20 hours to reach a final solution level of 3 cm above the soil-water interface. Additional background solution was regularly added from the top of the column to compensate for water evaporation, because the columns were open at the top and in contact with the atmosphere. For drainage, the soil solution was removed from the bottom of the column by a peristaltic pump at a rate of 0.5 ml min$^{-1}$ for about 10 hours. For Eh monitoring, glass fiber probes (Paleoterra Products, Amsterdam, The Netherlands) were inserted vertically in the soil columns after the packing of the columns. Four Eh measuring points made of platinum rings were distributed along the probes at positions enabling Eh measurement at 1 cm above the soil-water interface (+1 cm), at the interface (0 cm), 2 cm below the interface (-2 cm), and 5 cm below the interface (-5 cm). The Ag-AgCl reference electrodes were positioned in the water layer. The Eh was automatically measured every 15 min and stored in a data logger (Vorenhout et al., 2004). The Eh relative to the standard hydrogen electrode was calculated from the measured potential with a temperature-dependent correction for the potential of the Ag-AgCl reference electrode. The temperature was measured by platinum electrodes at two positions within the soil column: +1 cm and -2 cm. For collection of soil solution samples, four soil moisture samplers (SMS) (Rhizonsphere Research Products, Wageningen, The Netherlands) with a diameter of 2.5 mm, a mean pore size of 0.15 μm, and a 5 cm porous section were placed at the same depths (+1 cm, 0 cm, -2 cm, and -5 cm) in the soil columns at which the Eh was measured. The connector of the SMS was made of silicone and closed the holes in the plastic column very tightly preventing air penetration into the soil column. At certain time intervals based on the Eh dynamics, about 5 mL of soil solution were sampled from the soil columns with a vacuumed syringe. This syringe was connected to the female luer lock of the SMS, which was closed again immediately after sampling. During the first flooding period, soil solution was sampled on seven occasions for the TZ soil and on six occasions for the FY soil. During the first drainage and the second flooding period, soil solution was sampled on two occasions for each period. During the second drainage period, soil solution was sampled on one occasion for the TZ soil and on two occasions for the FY soil. After sampling on each occasion, around 20 ml background solution was added from the top of the column to compensate for the loss of the sampled soil solution. The soil solution samples were split in two subsamples. One subsample was used to measure the concentrations of metals and sulfur after acidification by adding concentrated $HNO_3$ to a level of 1.2% (v:v). The other subsample was used to measure the pH and the concentrations of DOC and different dissolved N species, i.e., $NH_4^+$ and N-($NO_3^-$+$NO_2^-$). The samples were stored in polypropylene tubes at 4 °C until chemical analysis as further detailed below.

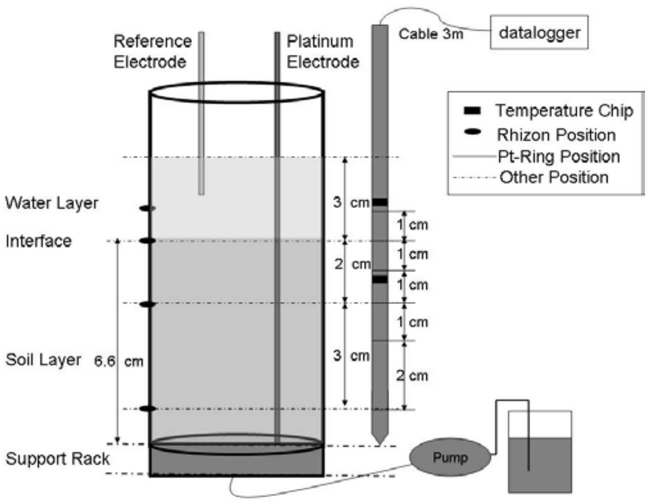

**Fig. 1.** Experimental set-up of the soil columns used in the experiment with alternating flooding and drainage conditions

*2.2.3. Soil analyses*

The pH, $CaCO_3$, soil organic matter (SOM), and clay (< 2µm) content were determined using standard analytical procedures: the pH was determined by measuring in a settling 1:10 (w:v) suspension of soil in 0.01 M $CaCl_2$, $CaCO_3$ by measuring the volume of carbon dioxide produced after addition of hydrochloric acid (HCl), SOM by loss-on-ignition (550 °C), and clay by the sieve and pipette method (Houba et al., 1997; Houba et al., 2000). Dissolved organic carbon and sulfur were measured in the same $CaCl_2$ extracts as those used for the measurement of pH after filtration over a 0.45-µm filter (Schleicher & Schuell 602H). Dissolved organic carbon was measured by using a fully automated segmented flow analyzer (SFA; Skalar San$^{++}$) by persulfate and tetraborate oxidation under UV light and infrared detection. Sulfur was measured by inductively coupled plasma atomic emission spectrometry (ICP-AES; Varian Vista Pro). In the geochemical modelling (see below), total sulphur was interpreted as $SO_4^{2-}$ (in the original unsaturated soils), which was validated by direct measurement of $SO_4^{2-}$ with Ion Chromatography (DIONEX, ICS-2100; results not shown) (Dick and Tabatabai, 1979). Amorphous (short-ranged ordered) Mn and Fe (hydr)oxides and phosphorus (P) were determined by using the acid ammonium oxalate extraction method (Novozamsky et al., 1986). Concentrations of Al, Fe, Mn, and P in the extracts (i.e., Al-ox, Fe-ox, Mn-ox, and P-ox) were measured by ICP-AES. The total soil content of metal (hydr)oxides, which includes both amorphous and crystalline forms, was determined by using the dithionite citrate bicarbonate (DCB) extraction method (Hiemstra et al., 2010). Concentrations of Al, Fe, and Mn in the extracts (i.e., Al-DCB, Fe-DCB, and Mn-DCB) were measured by ICP-AES. Total soil N content was measured after soil digestion using hydrogenperoxide ($H_2O_2$; 30%) and sulphuric acid ($H_2SO_4$; 95-97%) mixed in a ratio of 1.6:1 (v:v) under the influence of Se as a catalyst; salicylic acid ($C_7H_6O_3$) was added to prevent loss of nitrate (Novozamsky et al., 1984).

### *2.2.4. Soil solution analyses*

The pH in soil solution samples was directly measured after sampling with a combined glass electrode. The DOC concentrations were measured by an SFA. The $NH_4^+$ and N-($NO_3^-$+$NO_2^-$) concentrations were measured colorimetrically. In the acidified subsamples, Fe, Mn, Ca, and S were measured with the ICP-AES. When Fe, Mn, and S concentrations were below detection limit of the ICP-AES, a high resolution-inductively coupled plasma-mass spectrometer (HR-ICP-MS; Thermo Element 2) was used.

### *2.2.5. Data analysis and interpretation*

#### *2.2.5.1. Stability diagrams*

Stability diagrams, assuming thermodynamic equilibrium, show the dominant mineral phases controlling metal solubility as a function of Eh and pH in the soil systems. To determine the solubility-controlling minerals for Mn and Fe, we constructed stability diagrams by using the ORCHESTRA framework (version: 15 December 2013) (Meeussen, 2003). To construct the stability diagrams, we assumed the following conditions: the $CO_2$ pressure was defined as 10 times the ambient atmospheric $p\mathrm{CO}_2$ (316 Pa) (Lindsay, 1979; Du Laing et al., 2007), $SO_4^{2-}$ was taken as the amount of S measured in the 0.01 M $CaCl_2$ extracts, and the soil contents of amorphous Fe, Mn, and Al (hydr)oxides were taken from the results of the acid ammonium oxalate extraction method. The minerals with their formation constants include: $MnO_2$ (log K = -41.38), $MnCO_3$ (log K = -7.567), $Fe(OH)_3$ (log K = -3.191), $FeCO_3$ (log K = 5.125), FeS (log K =49.642), and $Al(OH)_3$ (log K= -8.291) (Allison et al., 1991). The constructed stability diagrams not only show the dominant minerals of Mn and Fe in the soil system, but also show the measured Eh-pH values for each sample occasion during the two successive flooding and drainage periods of the column experiment. The dominant minerals of Mn and Fe were further used in the geochemical equilibrium model for predicting the total dissolved Mn and Fe concentrations in the soil solution.

#### *2.2.5.2. Geochemical modeling of the total dissolved Mn and Fe*

To determine to what extent the identified dominant phases of Mn and Fe control the total dissolved concentrations of Fe and Mn in the soil solution, we performed geochemical model calculations with the ORCHESTRA framework (version: 15 December 2013) (Meeussen, 2003). A comparison between model results and experimental observations can help to identify whether non-equilibrium conditions are present. Shortly, the model we used included full speciation in the soil solution and ion sorption to three reactive surfaces: organic matter, clay minerals, and amorphous metal (hydr)oxides. This "multi-surface" geochemical modelling approach was largely based on Bonten et al. (2008) and Dijkstra et al. (2009). Metal sorption to both SOM and DOM is described by the NICA-Donnan model (Kinniburgh et al., 1999; Koopal et al., 2005), to clay minerals by a non-specific cation exchange model using a Donnan approach, and to amorphous Fe and Al (hydr)oxides by the two site diffusive double layer model for HFO from Dzombak and Morel (1990). For the reactivity of the sorption surfaces, we used the same assumptions as in Bonten et al. (2008). In our model calculations, we included the measured pH and Eh values, a moisture content of 0.24 (L $kg^{-1}$) for the TZ soil and 0.20 (L $kg^{-1}$) for the FY soil, $CO_2$ defined as 10 times ambient $pCO_2$ (316 Pa) (Lindsay, 1979; Du Laing et al., 2007), the amorphous Mn, Fe, and Al (hydr)oxides from the acid ammonium oxalate extraction, $SO_4^{2-}$ from the 0.01 M $CaCl_2$ extracts, Ca and DOC from the soil solution samples, and Cl at the background concentration (4 mM). During the model calculations, Mn and Fe were allowed to precipitate in the form of all solubility-controlling minerals as identified on the basis of the Eh-pH diagrams.

## ***2.3. Results and discussion***

### *2.3.1. Physical-chemical soil properties*

Selected physical-chemical soil properties of the two paddy soils used in this study are summarized in Table 1.

**Table 1**

Selected physical and chemical properties of the two paddy soils used in the column experiment

| Soil property | Unit | TZ soil | FY soil |
|---|---|---|---|
| Clay (< 2 µm) | % | 33 | 25 |
| SOM[b] | % | 7.0 | 9.2 |
| $CaCO_3$ | % | ND[a] | 21 |
| pH ($CaCl_2$)[c] | | 4.9 | 7.5 |
| DOC ($CaCl_2$)[c] | mg C $L^{-1}$ | 124 | 189 |
| S-$SO_4^{2-}$ ($CaCl_2$) | mmol $kg^{-1}$ | 4.7 | 7.0 |
| Al-ox[d] | mmol $kg^{-1}$ | 43±0.05 | 36±0.1 |
| Fe-ox[d] | mmol $kg^{-1}$ | 107±2 | 52±0.3 |
| Fe-DCB[e] | mmol $kg^{-1}$ | 209±4 | 168±2 |
| Mn-ox[d] | mmol $kg^{-1}$ | 2.4±0.03 | 3±0.02 |
| Mn-DCB[e] | mmol $kg^{-1}$ | 4±0.5 | 7±0.03 |
| P-ox[d] | mmol $kg^{-1}$ | 4±0.03 | 11±0.1 |
| Total N | mmol $kg^{-1}$ | 193 | 207 |

[a] Not detected

[b] Soil organic matter by loss on ignition (550 °C) (Houba et al. 1997)

[c] 1:10 (w:v) 0.01 M $CaCl_2$ (Houba et al. 2000)

[d] Extraction with acid ammonium oxalate (Novozamsky et al. 1986); this soil property was determined in duplicate and average ± standard deviation is presented

[e] Extraction with dithionite citrate bicarbonate (Hiemstra et al. 2010); this soil property was determined in duplicate and average ± standard deviation is presented

Most soil properties of the two soils were reasonably similar. However, the pH and the soil contents of $CaCO_3$ and Fe (hydr)oxides differed markedly between the two soils.

The pH of the FY soil was much higher than the pH of the TZ soil, which can be explained by the presence of $CaCO_3$ in the FY soil (Table 1). The presence of $CaCO_3$ can be attributed to the application of lime by farmers to control pathogens and to reduce phyto-toxicity of heavy metals. The deposition of alkaline dust from local industrial activities may also contribute to the $CaCO_3$ content of this soil (Wang et al., 2007; Brus et al., 2009). The Fe-ox content, which represents the pool of amorphous Fe (hydr)oxides in soil, was about 2 times higher in the TZ soil than in the FY soil. The contribution of amorphous Fe (hydr)oxides to the total soil content of Fe (hydr)oxides (i.e., Fe-DCB), which includes both amorphous and crystalline Fe (hydr)oxides, was about 51 % in the TZ soil and 31 % in the FY soil.

### *2.3.2. Dynamics of Eh and pH during two successive flooding and drainage periods*

Fig. 2 shows the Eh as a function of time in the TZ and FY soils. During the first flooding period, the Eh of the two soils responded differently to flooding of the soil columns. In the two bottom layers of the TZ soil, the Eh decreased gradually to a level of around -200 mV, while the Eh in the water layer remained constant at a level of 400 mV. At the soil-water interface, the Eh first decreased to around 250 mV but increased again to around 400 mV from 20 days onwards. In the FY soil, however, the Eh decreased rapidly to around -250 mV in all layers, although the Eh decrease was slower in the two top layers than in the two bottom layers. This rapid Eh decrease might be due to the higher pH (Table 1) and a higher DOC concentration or more easily degradable hydrophilic DOC in the FY soil than in the TZ soil (Table 1), because these two parameters favor a more rapid mineralization (Jandl and Sollins, 1997; Sahrawat, 2004) and depletion of $O_2$. During the first drainage period, the Eh increased rapidly in almost all layers of both soils, except for the bottom layer of the TZ soil. This Eh increase during drainage was due to re-aeration of the soil columns. During the second flooding period, the Eh of the two soils responded similarly. The Eh remained at a level of around 300 to 500 mV in the two top layers, while the Eh decreased rapidly to a level of around -200 mV in the two bottom layers. During the second drainage period, the Eh increased rapidly again to a level of around 400 to 600 mV in all layers of the two soils due to the re-aeration of the soil columns.

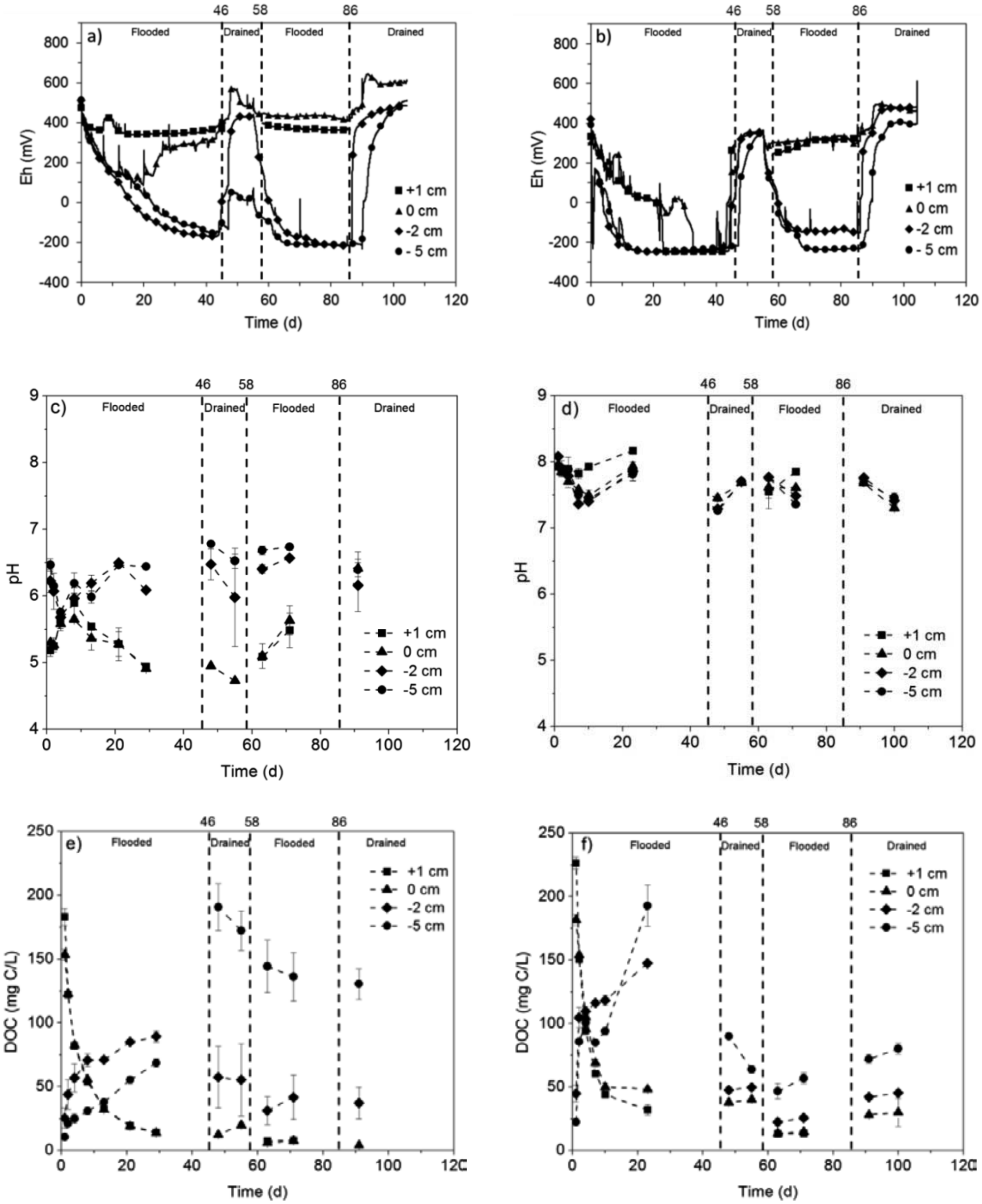

**Fig. 2.** Eh, and pH and DOC concentrations in the soil solution as a function of time in the TZ soil (a, c, and e) and the FY soil (b, d, and f) (+1 cm refers to 1 cm above the interface, 0 cm equals the interface between the soil surface and the water layer, and -2 cm and -5 cm refer to 2 and 5 cm below the interface, respectively)

In the different layers of the FY soil, the pH remained relatively constant and varied between 7.5 and 8.0 (Fig. 2d), consistent with the presence of $CaCO_3$ in this soil (Table 1), which buffers the pH at this level. In contrast, the pH differed greatly between the top layers and the two bottom layers in the more acidic TZ soil (Fig. 2c). During the first flooding period, the pH decreased by about 0.4 pH unit in the two top layers, whereas the pH increased by about 1 pH unit in the two bottom layers. These pH changes were negatively correlated to the Eh changes in the TZ soil (Fig. 2a). In the two top layers, the aerobic conditions led to proton production causing a pH decrease, whereas in the two bottom layers, the anaerobic conditions led to proton consumption causing a pH increase. Similar flooding effects of acidic soils on pH have been found before (Ponnamperuma, 1972; Sahrawat, 2005; Yu et al., 2007; Kögel-Knabner et al., 2010; Frohne et al., 2011; Shaheen et al., 2014). During the first drainage and the second flooding period of the TZ soil, the pH differences between the top layers and the two bottom layers remained present. During the second drainage period, however, the pH differences between the top layer and the two bottom layers disappeared, consistent with all layers returning to aerobic conditions.

### *2.3.3. Effects of flooding and drainage conditions on DOC and dissolved N species*

A large difference in the DOC concentration was found at the initial sampling occasion between the two top and the two bottom layers during the first flooding period for both soils (Fig. 2e and 2f). At this initial sampling occasion, the DOC concentrations were about 4-5 times higher in the two top layers than in the bottom layers. The reason for this difference might be attributed to the leaching and displacement of DOC via upward transport during the saturation of the columns from the bottom with the 2 mM $CaCl_2$ solution. In addition to displacement, mineralization of labile DOC in the period until the first sampling occasion might have proceeded for a relatively longer time in the bottom part of the soil column than in the top part during the column filling process, because the filling of the column took 18 to 20 hours. Yet, the higher DOC concentrations in the two top layers decreased rapidly from around 180-230 mg C $L^{-1}$ to around 25-50 mg C $L^{-1}$ in both soils. Apparently, a large part of the DOC was rapidly mineralized. The soils used in our column experiment had been dried at 40 °C. Soil drying at this temperature has been demonstrated to greatly increase the concentration of easily degradable hydrophilic DOC compounds in soil solution extracts, which was attributed to lysis of microbial biomass (Koopmans and Groenenberg, 2011) or disruption of soil aggregates (Chepkwony et al., 2001). Also, this occurrence of labile DOC would explain why the rapid decrease is not observed in the second flooding period, because this DOC pool may have been largely depleted during the first flooding period. During the first flooding period, however, the DOC concentrations in the two bottom layers increased gradually in both soils. This increase might be related to reduction processes affecting both the pH and the solubility of amorphous Mn and Fe (hydr)oxides, because the Eh in these layers was strongly lowered during the first flooding period (Fig. 2a and 2b). A release of DOC has been found before when exposing soils or sediments to flooding (Mulholland et al., 1990; Sedell and Dahm, 1990; Fiedler and Kalbitz, 2003; Sahrawat, 2004; Vink et al., 2010; Frohne et al., 2011; Shaheen et al., 2014). The possible mechanisms underlying the increase in DOC concentrations during the first flooding period will be further discussed in section 2.3.7. During the remaining part of the column experiment, the DOC concentrations remained at a higher level in the bottom layers than in the top layers, especially for the TZ soil.

Similar to DOC, a large difference in the $NO_3^-$ concentration was found at the initial sampling occasion between the two top and the two bottom layers in both soils during the first flooding period (Fig. A.1a and A.1b). At this initial sampling occasion, $NO_3^-$ was present in the two top layers, whereas the $NO_3^-$ concentrations were near the detection limit in the two bottom layers. The absence of $NO_3^-$ in the two bottom layers can be explained by vertical displacement during the initial saturation of the columns and by microbial mineralization of DOC in combination with denitrification of $NO_3^-$. After depletion of $O_2$ in the soil, $NO_3^-$ is successively used as an alternative terminal electron acceptor for the microbial mineralization of organic matter. During the remaining part of the column experiment, the $NO_3^-$ concentrations were near the detection limit in the TZ soil. In the FY soil, however, the $NO_3^-$ concentrations increased in all layers after the first flooding period, especially in the two top layers. This increase of the $NO_3^-$ concentrations was consistent with the higher Eh in the top layers of the FY soil (Fig. 2b), which might have enabled nitrification of $NH_4^+$ to $NO_3^-$ with $O_2$ as an electron acceptor. In parallel with the $NO_3^-$ change, $NH_4^+$ concentrations also differed in the two soils. During the first flooding period, the $NH_4^+$ concentrations increased gradually in all soil layers for both soils (Fig. A.1c and A.1d). Moreover, a higher rate of $NH_4^+$ production was found in the FY soil than in the TZ soil, because microbial activity is favored at neutral to alkaline conditions (Sahrawat, 2004). In the remaining part of the column experiment, the $NH_4^+$ concentrations remained at an elevated level in all layers in both soils except in the two top layers in the FY soil. This exception is consistent with the increase of the $NO_3^-$ concentrations in the top layers of the FY soil after the first flooding period because $NH_4^+$ was probably converted to $NO_3^-$ under aerobic conditions (Yu et al., 2007).

### *2.3.4. Species of Mn and Fe in the soil systems under different Eh-pH conditions*

The equilibrium speciation of Mn and Fe in the soil system is controlled by Eh and pH conditions, which can be shown in a so-called stability diagram. This stability diagram, assuming thermodynamic equilibrium, shows the dominant minerals that control metal solubility as a function of Eh and pH in the soil system. Although such a stability diagram does not provide conclusive evidence for the presence of specific minerals, an indication of the likeliness of specific solubility-controlling minerals as a function of Eh and pH can be obtained. For example, under aerobic conditions, Mn is mainly present as solid Mn (IV) in the form of $MnO_2$ according to the stability diagram of Mn (Fig. 3a and 3b). Under anaerobic conditions, however, the stability diagram indicates that Mn (IV) is reduced to Mn (II), and either precipitates as solid $MnCO_3$ at pH values above 6 or remains in solution mainly as $Mn^{2+}$ at lower pH values. When Mn is precipitated as $MnCO_3$, the concentration of Mn in the soil solution is controlled by the solubility of that mineral.

Besides the Eh and pH, soil constituents, such as carbonate, sulfur, and amorphous Mn and Fe (hydr)oxides in the soil system, determine the speciation of Mn and Fe. Carbonate and sulfur are important, because Mn and Fe can precipitate with these components either as $MnCO_3$ (rhodochrosite) and $FeCO_3$ (siderite) or as FeS (troilite) and $FeS_2$ (pyrite). The parameters used for the stability diagrams of Mn (Fig. 3a and 3b) and Fe (Fig. 3c and 3d) are summarized in section 2.2.5.1.

Besides the stability fields of the dominant Mn and Fe species, the stability diagrams also show the measured Eh and pH values of each sampling occasion, indicating the most likely species of Mn and Fe in the soil system during the column experiment.

For Mn, the dominant minerals that may control Mn solubility differed greatly between the two soils. In the acidic TZ soil, Mn is expected to be mainly present as dissolved $Mn^{2+}$ but at a few sampling occasions as solid $MnCO_3$ during the soil column

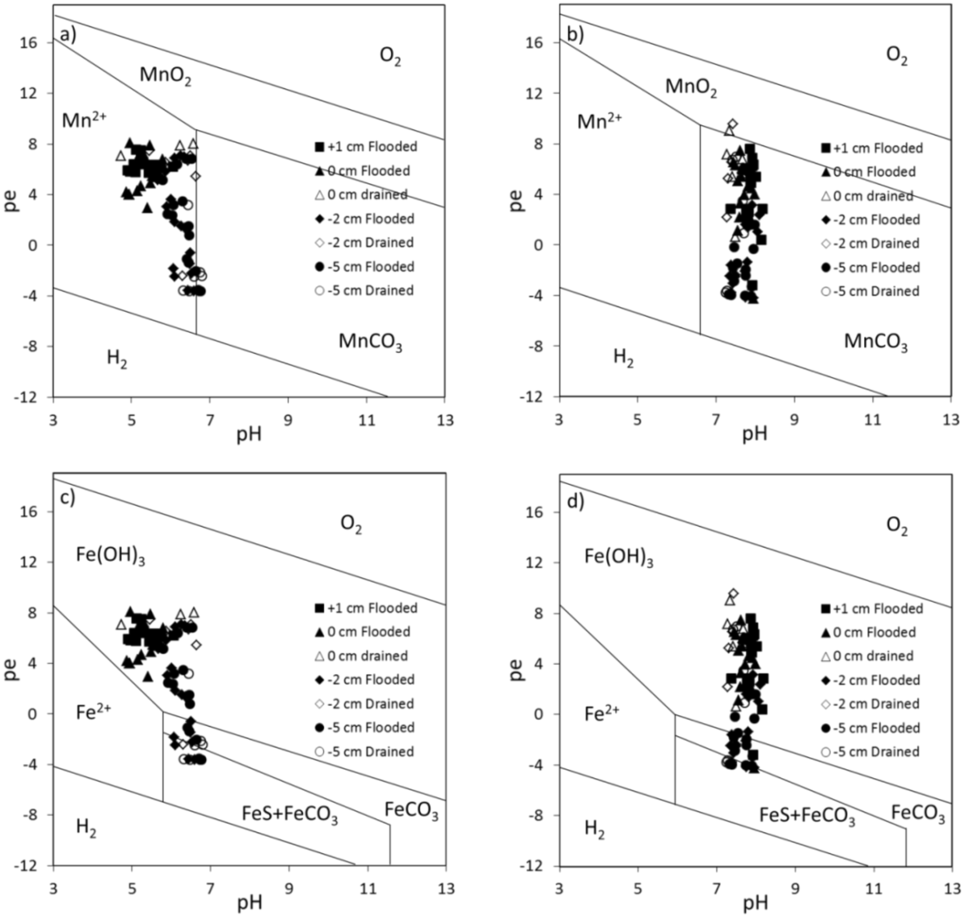

**Fig. 3.** Stability diagrams of Mn and Fe in the TZ soil (a and c) and the FY soil (b and d). pe in the diagrams is calculated by pe=Eh·F/cRT, where pe is the electron activity, Eh is the measured redox potential in volts, F is the Faraday constant (96485 J/V/mole), R is the gas constant (8.314 J/mole), T is the temperature in degrees Kelvin (298.15°K=25°C ), and c is the constant (2.303).

whereas solid $MnCO_3$ can be formed in the calcareous FY soil (Fig. 3a and 3b). Therefore, $Mn^{2+}$ concentrations are expected to be higher in the TZ soil than in the FY soil. For Fe, the dominant minerals that may control Fe solubility follow the same pattern in both soils (Fig. 3c and 3d), despite the large pH difference between the two soils (Table 1). With decreasing Eh, the dominant mineral phase shifts from amorphous $Fe(OH)_3$ to solid $FeCO_3$ and finally to formation of FeS together with $FeCO_3$. For most sampling occasions, Fe is expected to be in the form of $Fe(OH)_3$, while $FeCO_3$ and FeS may have formed at much fewer sampling occasions. The minerals $FeCO_3$ and FeS may mostly have formed at 2 cm and 5 cm below the interface in both soils. Although the mineral phases controlling Fe solubility are expected to be the same for both soils, $Fe^{2+}$ concentrations are still expected to be higher in the TZ soil than in the FY soil because of the lower pH of the TZ soil (Table 1).

### *2.3.5. Effects of flooding and drainage on the solubility of Mn*

During the first flooding period, the trend in the measured Mn concentrations in the TZ soil (Fig. 4a; closed symbols) was similar to the trend in the concentrations of DOC (Fig. 2e) and $NO_3^-$ (Fig. A.1a) for this soil: the initial concentrations of Mn were higher in the two top layers than in the two bottom layers and slowly decreased and reached equilibrium with time. The initially high Mn concentrations might be due to the difference in exposure time to anaerobic conditions between the lower part and the upper part of the soil column and subsequent upward leaching of Mn. Since the soil columns were saturated from the bottom, the two bottom layers became anaerobic at an earlier stage, leading to reductive dissolution of Mn (III/IV) (hydr)oxides and upward transport of dissolved Mn to the upper part of the column. In the two bottom layers, however, the Mn concentrations slowly increased with time. This increase was probably the result of reductive dissolution of Mn, i.e., Mn (IV) which is mainly present as solid $MnO_2$ being reduced to $Mn^{2+}$, as has been found before (Yu et al., 2007; Rupp et al., 2010; Shaheen et al., 2014). In the FY soil, however, the Mn concentrations showed a different pattern (Fig. 4b). The Mn concentrations were generally low and increased slightly over the entire monitoring period. This observation is consistent with the stability diagram for Mn for this soil (Fig. 3b). In the calcareous FY soil, Mn (II) formed upon reductive dissolution of Mn (III/IV) (hydr)oxides is most likely present as solid $MnCO_3$. Consequently, the Mn concentrations are lower in equilibrium with this mineral in the FY soil than in the TZ soil, where Mn is mainly present as dissolved $Mn^{2+}$ (Fig. 3a). During the first drainage period, the measured Mn concentrations decreased in most layers in both soils. This Mn decrease was attributed to the re-aeration and re-oxidation of the columns, and subsequent precipitation of Mn, most likely as $MnO_2$. During the second flooding period, the measured Mn concentrations increased in all layers in both soils, and the measured Mn concentrations were again

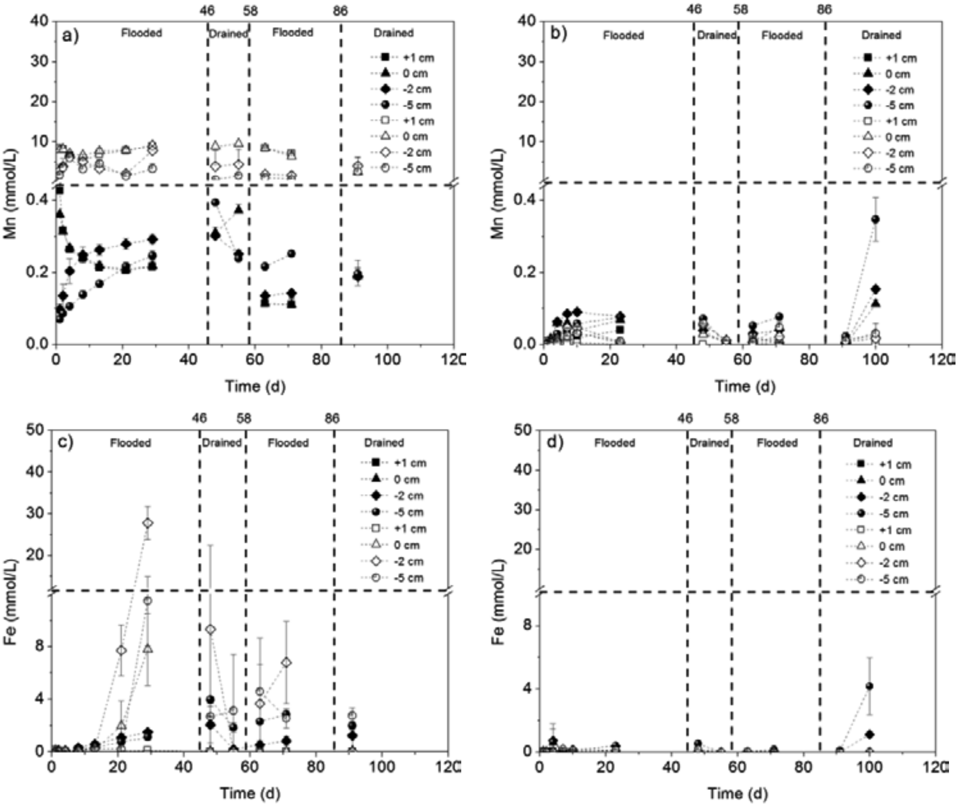

**Fig. 4.** Measured (closed symbols) and predicted (open symbols) Mn and Fe concentrations in the soil solution as a function of time in the TZ soil (a and c) and the FY soil (b and d) (+1 cm refers to 1 cm above the interface, 0 cm equals the interface between the soil surface and the water layer, and -2 cm and -5 cm refer to 2 and 5 cm below the interface, respectively)

higher in the TZ soil than in the FY soil, as discussed above. During the second drainage period, the Mn concentrations increased unexpectedly at the last sampling occasion in the FY soil, in parallel with a decrease in pH, which is in contrast with the pH development during the first drainage period (Fig. 2d).

In addition to the measured concentrations of total dissolved Mn, Fig. 4 (open symbols) shows the predicted Mn concentrations of the individual sampling occasions, as obtained by geochemical equilibrium modeling. For the TZ soil, the predicted Mn concentrations (Fig. 4a) are much higher than the measured Mn concentrations. This large difference between predicted and measured Mn concentrations might be due to kinetically-limited reduction of $MnO_2$ in the soil system resulting in a non-equilibrium state, meaning a large fraction of Mn might remain as solid $MnO_2$ despite of sufficiently reducing conditions. Although Mn was released slowly from the soil solid phase, the measured Mn concentrations are consistently higher than the predicted Mn concentration under fully aerobic conditions, i.e., $2.52\times10^{-6}$ mmol Mn $L^{-1}$, which supports our idea that reductive dissolution of Mn for the TZ soil is indeed kinetically limited. For the FY soil, however, the predicted Mn concentrations agree reasonably well with the measured concentrations (Fig. 4b). This agreement is consistent with the likely formation of solid $MnCO_3$ in this calcareous soil of which the predicted equilibrium concentrations of Mn do indeed match fairly well with the measurements. Consequently, for this alkaline soil, it is difficult to assess whether reductive dissolution of $MnO_2$ was kinetically limited during flooding, because of the rather low solubility of Mn maintained by $MnCO_3$ during the soil column experiment.

### *2.3.6. Effects of flooding and drainage on the solubility of Fe*

During the whole monitoring period, the measured Fe concentrations remained low in the two top layers for both soils (Fig. 4; closed symbols). For both soils, the aerobic conditions in these layers (Fig. 2a and 2b) probably caused Fe to remain present in the form of hardly soluble Fe (III) (hydr)oxides, as is shown in the stability diagram of Fe (Fig. 3c and 3d). In the two bottom layers of both soils, the measured Fe concentrations increased during the two flooding periods, whereas they decreased during the two drainage periods. This increase in the Fe concentration during the two flooding periods is probably the result of reductive dissolution of Fe (III) (hydr)oxides (Yu et al., 2007; Rupp et al., 2010; Frohne et al., 2011; Shaheen et al., 2014), whereas the decrease during the two drainage periods is probably caused by re-oxidation and subsequent precipitation of Fe (Yu et al., 2007; Rupp et al., 2010; Frohne et al., 2011; Shaheen et al., 2014) in the form of $Fe(OH)_3$, as shown in the stability diagrams (Fig. 3c and 3d). Similar to Mn, the Fe concentrations were lower in the calcareous FY soil (Fig. 4d) than in the acidic TZ soil (Fig. 4c). In the FY soil, the solubility of Fe, similar to that of Mn, might be controlled at such a lower level by the solid $FeCO_3$, as is suggested by the stability diagram of Fe (Fig. 3d). Like Mn (Fig. 4b), an unexpected increase of measured Fe concentrations was observed at the last sampling occasion in the second drainage period in the FY soil, possibly also related to the decreasing pH (Fig. 2d). Similar to Mn, we also predicted what the Fe concentrations would have been under fully aerobic conditions: 0.19 mmol Fe $L^{-1}$ for the TZ soil and 0.09 mmol Fe $L^{-1}$ for the FY soil. For both soils, the measured Fe concentrations were near or below these concentrations for all sampling occasions in the two top layers and for some of the occasions in the two bottom layers, suggesting that Fe (hydr)oxides indeed controlled the solubility of Fe. For the other sampling occasions in the two bottom layers, Eh was strongly reduced and the measured Fe concentrations were higher than the aerobic equilibrium concentrations, which is thus likely due to reductive dissolution of Fe (hydr)oxides.

In addition to the measured concentrations of total dissolved Fe, Fig. 4 (open symbols) shows the predicted Fe concentrations of the individual sampling occasions, as obtained by geochemical equilibrium modeling. Although the predicted Fe concentrations vary with time in the TZ soil (Fig. 4c), the trends of these predicted Fe concentrations generally agree with the trends of the measured Fe concentrations, suggesting that the solubility of Fe tends towards equilibrium with Fe (III) (hydr)oxides for most sampling occasions and towards reductive dissolution for strongly reduced conditions as mentioned before. However, as exceptions, the predicted Fe concentrations were much higher at the last two sampling occasions of the first flooding period and at the two sampling occasions of the second flooding period. These exceptions might be due to a kinetically-limited reduction of Fe (III) (hydr)oxides resulting in a non-equilibrium state, meaning that a large fraction of Fe (III) (hydr)oxides might remain despite of sufficiently reducing conditions. This idea, similar to kinetically-limited reduction of Mn (hydr)oxides in the TZ soil, is supported by comparing the measured Fe concentrations at these sampling occasions with the aerobic equilibrium Fe concentrations in the two bottom layers as discussed before. In the FY soil, in general, the predicted Fe concentrations agree reasonably well with the measured concentrations (Fig. 4d). Also, both predicted and measured Fe concentrations are lower in the calcareous FY soil than in the acidic TZ soil. For most sampling occasions, such lower Fe concentrations in the FY soil are due to the lower solubility of Fe (hydr)oxides at the much higher pH of this soil (Table 1). For sampling occasions with strongly reduced conditions, such low Fe concentrations in the FY soil might also be due to the formation of solid $Fe(II)CO_3$, because this mineral exhibits a low solubility at a high pH. Therefore, $FeCO_3$ might then control the Fe solubility in the FY soil instead of Fe (hydr)oxides. Indeed, the model predicts the formation of $FeCO_3$ in the two bottom layers during the first flooding period from the fourth to the seventh sampling occasion and during the second flooding period.

In addition to the formation of $FeCO_3$, the model predicts simultaneous FeS formation for five sample occasions of the TZ soil and for four sample occasions of the FY soil both in two bottom layers predominantly during flooding periods (Fig. 3c and 3d). According to Postma and Jakobsen (1996), the simultaneous reduction of Fe (III) (hydr)oxides and $SO_4^{2-}$ is rather common in sediments with a wide range of environment conditions including the stability of Fe (hydr)oxides and pH. In our study, the Eh values in the two bottom layers were low enough (Fig. 2) to induce reduction of both Fe (III) (hydr)oxides and $SO_4^{2-}$ so as to facilitate subsequent FeS formation. The formation of sulfide and FeS is supported by the low measured S concentrations on many sample occasions (Fig. A.1e and A.1f). However, the solid FeS is not expected to control the Fe solubility in both soils, because the total amount of Fe (i.e., Fe-oxalate) that would be available for forming a precipitate with sulfur is much higher than the amount of $SO_4^{2-}$ in the soil (Table 1).

### *2.3.7. Mobilization of DOC during flooding and drainage periods*

Fig. 5 shows the relationship between the DOC and total dissolved Fe concentrations in the soil solution at the two bottom layers in the TZ and the FY soils during the two flooding and drainage periods. We have presented the results only from the two bottom layers because in these layers anaerobic conditions were present during the two flooding periods of both soils (Fig. 2a and 2b). In the TZ soil, the DOC concentrations were highly correlated to the Fe concentrations ($R^2$=0.75). This high correlation can be attributed to the reductive dissolution of Fe (III) (hydr)oxides. Since SOM can bind to Fe (hydr)oxides (Kaiser et al., 1997; Weng et al., 2008) and is often at least partly associated with these metal (hydr)oxides in soils (Regelink et al., 2013), it is mobilized as DOC to the soil solution upon a decrease in the reactive surface area of Fe (III) (hydr)oxides due to reductive dissolution. In addition, the increase in pH in the two bottom layers of the TZ soil (Fig. 2c) might have contributed to the mobilization of DOC, since the affinity of organic matter for binding to Fe (III) (hydr)oxides is reduced towards a higher pH. At an elevated pH, the surface charge of metal (hydr)oxides becomes less positive, leading to an increase in DOC solubility (Weng et al., 2008). In addition to DOC mobilization by reductive dissolution of Fe (III) (hydr)oxides, as suggested by Fig. 5a, release of fermentation products might also have contributed to the elevated DOC concentrations because mineralization is incomplete under anaerobic conditions (Vink et al., 2010).

No correlation was found between DOC and Fe concentrations for the FY soil. Although flooding conditions are likely to have also affected the reactive surface area of Fe (hydr)oxides via reductive dissolution, no increase was found in Fe solubility (Fig. 4d), whereas DOC clearly increased in the two bottom layers during flooding of the FY soil (Fig. 2f). After reduction of Fe (III) (hydr)oxides, dissolved Fe (II) probably precipitated as $FeCO_3$ or FeS, as discussed above on the basis of the stability diagrams (Fig. 3d) and model predictions (Fig. 4d). Hence, the formation of Fe (II) precipitates might explain the absence of a relationship between Fe and DOC for this soil. Similar to the TZ soil, the presence of fermentation products might also have contributed to the increase in DOC (Vink et al., 2010).

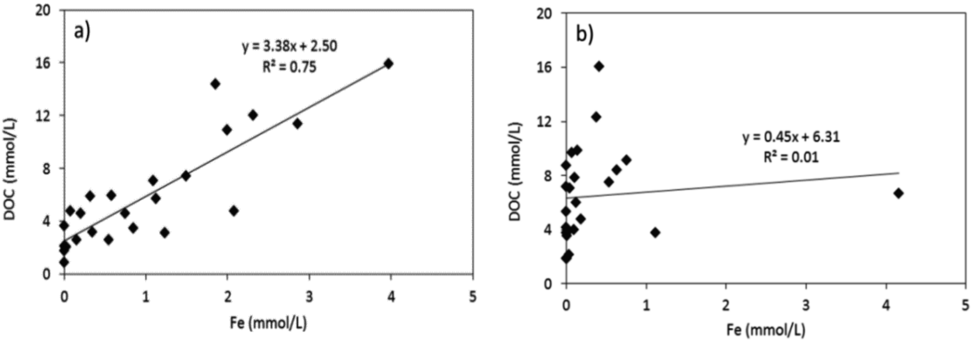

**Fig. 5.** Relationship between measured DOC and Fe concentrations in the soil solution sampled from the two bottom layers of the TZ soil (a) and the FY soil (b) during two successive flooding and drainage periods

### *2.4. Conclusions*

During successive flooding and drainage periods of two paddy soils, reduction and oxidation processes greatly affected Mn and Fe solubility. However, the extent of these solubility changes was greatly determined by pH. In the acidic soil, reductive dissolution of Mn and Fe (hydr)oxides increased the solubility of Mn and Fe. However, in the alkaline soil, the solubility of Mn and Fe was limited by the precipitation of Mn

(II) and Fe (II) in the form of solid carbonates. The Eh and pH also strongly affected the DOC solubility in both soils. In the acidic soil, the DOC solubility probably increased as a result of reductive dissolution of Fe(III) (hydr)oxides and an increased pH during flooding. In the alkaline soil, the DOC solubility also increased but could not be correlated to reductive dissolution of Fe (hydr)oxides, probably because of dissolved Fe (II) precipitating as solid $FeCO_3$ or FeS. The dynamics in Eh and pH also greatly affected the concentrations of $NO_3^-$ and $NH_4^+$ during flooding and drainage periods. Besides the observed marked effects of Eh and pH on the behavior of Mn and Fe (hydr)oxides and organic matter upon flooding and draining of the two soils, the comparison between measurements and equilibrium model predictions suggest rate limiting reactions, i.e., kinetically limited reduction of Mn and Fe (hydr)oxides. Therefore, for a more accurate application of equilibrium speciation models to systems with changing redox conditions, implementation of these kinetically limited reactions should be considered.

## References

Allison, J.D., Brown, D.S., Novo-Gradac, K.J., 1991. MINTEQA2/PRODEFA2, A geochemical assessment model for environmental systems: version 3.0 user's manual. US EPA, Athens, GA. EPA/600/3-91/021

Bonten, L.T.C., Groenenberg, J.E., Weng, L.P., van Riemsdijk, W.H., 2008. Use of speciation and complexation models to estimate heavy metal sorption in soils. Geoderma 146, 303–310.

Brus, D.J., Li, Z.B., Song, J., Koopmans, G.F., Temminghoff, E.J.M., Yin, X.B., Yao, C.X., Zhang, H.B., Luo, Y.M., Japenga, J., 2009. Predictions of spatially sveraged cadmium contents in rice grains in the Fuyang Valley, PR China. J Environ Qual 38, 1126–1136.

Chepkwony, C.K., Haynes, R.J., Swift, R.S., Harrison, R., 2001. Mineralization of soil organic P induced by drying and rewetting as a source of plant-available P in limed and unlimed samples of an acid soil. Plant Soil 234, 83–90.

de Jonge, M., Teuchies, J., Meire, P., Blust, R., Bervoets, L., 2012. The impact of increased oxygen conditions on metal-contaminated sediments part I: Effects on redox status, sediment geochemistry and metal bioavailability. Water Res 46, 2205–2214.

de Livera, J., McLaughlin, M.J., Hettiarachchi, G.M., Kirby, J.K., Beak, D.G., 2011. Cadmium solubility in paddy soils: Effects of soil oxidation, metal sulfides and competitive ions. Sci Total Environ 409, 1489–1497.

Dick, W.A., Tabatabai, M.A., 1979. Ion chromatographic determination of sulfate and nitrate in soils. Soil Sci Soc Am J 43, 899–904.

Dijkstra, J.J., Meeussen, J.C.L., Comans, R.N.J., 2009. Evaluation of a generic multisurface sorption model for inorganic soil contaminants. Environ Sci Technol 43, 6196–6201.

Du Laing, G., Rinklebe, J., Vandecasteele, B., Meers, E., Tack, F.M.G., 2009. Trace metal behaviour in estuarine and riverine floodplain soils and sediments: A review. Sci Total Environ 407, 3972–3985.

Du Laing, G., Vanthuyne, D.R.J., Vandecasteele, B., Tack, F.M.G., Verloo, M.G., 2007. Influence of hydrological regime on pore water metal concentrations in a contaminated sediment-derived soil. Environ Pollut 147, 615–625.

Dzombak, D.A., Morel, F.M.M., 1990. Surface complexation modeling: Hydrous Ferric Oxide. Wiley, New York, pp 393.

Fiedler, S., Kalbitz, K., 2003. Concentrations and properties of dissolved organic matter in forest soils as affected by the redox regime. Soil Sci 168, 793–801.

Frohne, T., Rinklebe, J., Diaz-Bone, R.A., Du Laing, G., 2011. Controlled variation of redox conditions in a floodplain soil: Impact on metal mobilization and biomethylation of arsenic and antimony. Geoderma 160, 414–424.

Fulda, B., Voegelin, A., Kretzchmar, R., 2013. Redox-controlled changes in cadmium solubility and solid-phase speciation in a paddy soil as affected by reducible sulfate and copper. Environ Sci Technol 47, 12775–12783.

Gao, X.P., Schroeder, T.J., Hoffland, E., Zou, C.Q., Zhang, F.S., van der Zee, S.E.A.T.M., 2010. Geochemical modeling of zinc bioavailability for rice. Soil Sci Soc Am J 74, 301–309.

Gotoh, S., Patrick, W.H., 1972. Transformation of manganese in a waterlogged soil as affected by redox potential and pH. Soil Sci Soc Am Pro 36, 738–742

Grybos, M., Davranche, M., Gruau, G., Petitjean, P., 2007. Is trace metal release in wetland soils controlled by organic matter mobility or Fe-oxyhydroxides reduction? J Colloid Interf Sci 314, 490–501.

Hagedorn, F., Kaiser, K., Feyen, H., Schleppi, P., 2000. Effects of redox conditions and flow processes on the mobility of dissolved organic carbon and nitrogen in a forest soil. J Environ Qual 29, 288–297.

Hiemstra, T., Antelo, J., Rahnemaie, R., van Riemsdijk, W.H., 2010. Nanoparticles in natural systems I: The effective reactive surface area of the natural oxide fraction in field samples. Geochim Cosmochim Ac 74, 41–58.

Houba, V.J.G., Temminghoff, E.J.M., Gaikhorst, G.A., van Vark, W., 2000. Soil analysis procedures using 0.01 M calcium chloride as extraction reagent. Commun Soil Sci Plant Anal 31, 1299–1396.

Houba, V.J.G., van der Lee, J.J.G., Novozamsky, I., 1997. Soil and plant analysis. Part 1:soil analysis procedures. Wageningen University, Wageningen, The Netherlands.

Jandl, R., Sollins, P., 1997. Water extractable soil carbon in relation to the belowground carbon cycle. Biol Fert Soils 25, 196–201.

Kaiser, K., Guggenberger, G., Haumaier, L., Zech, W., 1997. Dissolved organic matter sorption on subsoils and minerals studied by C-13-NMR and DRIFT spectroscopy. Eur J Soil Sci 48, 301–310.

Kalbitz, K., Solinger, S., Park, J.H., Michalzik, B., Matzner, E., 2000. Controls on the dynamics of dissolved organic matter in soils: A review. Soil Sci 165, 277–304.

Khaokaew, S., Chaney, R.L., Landrot, G., Ginder-Vogel, M., Sparks, D.L., 2011. Speciation and release kinetics of cadmium in an alkaline paddy soil under various flooding periods and draining conditions. Environ Sci Technol 45, 4249–4255

Kinniburgh, D.G., van Riemsdijk, W.H., Koopal, L.K., Borkovec, M., Benedetti, M.F., Avena, M.J., 1999. Ion binding to natural organic matter: competition, heterogeneity, stoichiometry and thermodynamic consistency. Colloid Surface A 151, 147–166.

Kögel-Knabner, I., Amelung, W., Cao, Z.H., Fiedler, S., Frenzel, P., Jahn, R., Kalbitz, K., Kolbl, A., Schloter, M., 2010. Biogeochemistry of paddy soils. Geoderma 157, 1–14.

Koopal, L.K., Saito, T., Pinheiro, J.P., van Riemsdijk, W.H., 2005. Ion binding to natural organic matter: General considerations and the NICA-Donnan model. Colloid Surface A 265, 40–54.

Koopmans, G.F., Groenenberg, J.E., 2011. Effects of soil oven-drying on concentrations and speciation of trace metals and dissolved organic matter in soil solution extracts of sandy soils. Geoderma 161, 47–158.

Lindsay, W.L., 1979. Chemical equilibria in soils. John Wiley & Sons, New York, pp 449.

Lindsay, W.L., Sadiq, M., 1983. Use of pe + pH to predict and interpret metal solubility relationships in soils. Sci Total Environ 28, 169–178.

Loeb, R., Lamers, L.P.M., Roelofs, J.G.M., 2008a. Effects of winter versus summer flooding and subsequent desiccation on soil chemistry in a riverine hay meadow. Geoderma 145, 84–90.

Loeb, R., Lamers, L.P.M., Roelofs, J.G.M., 2008b. Prediction of phosphorus mobilisation in inundated floodplain soils. Environ Pollut 156, 325–331.

Meeussen, J.C.L., 2003. ORCHESTRA: An object-oriented framework for implementing chemical equilibrium models. Environ Sci Technol 37, 1175–1182.

Meharg, A.A., Norton, G., Deacon, C., Williams, P., Adomako, E.E., Price, A., Zhu, Y.G., Li, G., Zhao, F.J., McGrath, S., Villada, A., Sommella, A., De Silva, P.M.C.S., Brammer, H., Dasgupta, T., Islam, M.R., 2013. Variation in rice cadmium related to human exposure. Environ Sci Technol 47, 5613–5618.

Mulholland, P.J., Dahm, C.N., David, M.B., Ditoro, D.M., Fisher, T.R., Hemond, H.F., Kögel-Knabner, I., Meybeck, M.H., Meyer, J.L., Sedell, J.R., 1990. What are the temporal and spatial variations of organic-acids at the ecosystems level. Life Sci R 48, 315–329

Murase, J., Kimura, M., 1997. Anaerobic reoxidation of $Mn^{2+}$, $Fe^{2+}$, $S^0$ and $S^{2-}$ in submerged paddy soils. Biol Fert Soils 25, 302–306.

Novozamsky, I., Houba, V.J.G., Temminghoff, E.J.M., van der Lee, J.J., 1984. Determination of 'total' N and 'total' P in a single soil digest. Neth J Agric Sci 32, 322–324.

Novozamsky, I., van Eck, R., Houba, V.J.G., van der Lee, J.J., 1986. Use of ICP-AES for determination of iron, aluminium and phosphorus in Tamm's soil extracts. Neth J Agric Sci 34, 185–191.

Patrick, W.H., Henderson, R.E., 1981. Reduction and reoxidation cycles of manganese and iron in flooded soil and in water solution. Soil Sci Soc Am J 45, 855–859.

Patrick, W.H., Jugsujinda, A., 1992. Sequential reduction and oxidation of inorganic nitrogen, manganese, and iron in flooded soil. Soil Sci Soc Am J 56, 1071–1073.

Ponnamperuma, F.N., 1972. The chemistry of submerged soils. Adv Agron 24, 29–96.

Postma, D., Jakobsen, R., 1996. Redox zonation: Equilibrium constraints on the Fe(III)/$SO_4$-reduction interface. Geochim Cosmochim Ac 60, 3169–3175.

Regelink, I.C., Weng, L., Koopmans, G.F., van Riemsdijk, W.H., 2013. Asymmetric flow field-flow fractionation as a new approach to analyse iron-(hydr)oxide nanoparticles in soil extracts. Geoderma 202, 134–141.

Ritvo, G., Shitumbanuma, V., Dixon, J.B., 2004. Soil solution sulfide control by two iron-oxide minerals in a submerged microcosm. Aquaculture 239, 217–235.

Rupp, H., Rinklebe, J., Bolze, S., Meissner, R., 2010. A scale-dependent approach to study pollution control processes in wetland soils using three different techniques. Ecol Eng 36, 1439–1447.

Sahrawat, K.L., 2004. Organic matter accumulation in submerged soils. Adv Agron 81, 169–201.

Sahrawat, K.L., 2005. Fertility and organic matter in submerged rice soils. Curr Sci India 88, 735–739.

Sedell, J.R., Dahm, C.N., 1990. Spatial and temporal scales of dissolved organic-carbon in streams and rivers. Life Sci R 48, 261–279.

Shaheen, S.M., Rinklebe, J., Rupp, H., Meissner, R., 2014. Lysimeter trials to assess the impact of different flood-dry-cycles on the dynamics of pore water concentrations of As, Cr, Mo and V in a contaminated floodplain soil. Geoderma 228–229, 5–13.

Song, J., Luo, Y.M., Zhao, Q.G., Christie, P., 2004. Microcosm studies on anaerobic phosphate flux and mineralization of lake sediment organic carbon. J Environ Qual 33, 2353–2356.

Tack, F.M.G., van Ranst., E., Lievens, C., Vandenberghe, R.E., 2006. Soil solution Cd, Cu and Zn concentrations as affected by short-time drying or wetting: The role of hydrous oxides of Fe and Mn. Geoderma 137, 83–89.

Unger, I.M., Muzika, R.M., Motavalli, P.P., Kabrick, J., 2008. Evaluation of continuous in situ monitoring of soil changes with varying flooding regimes. Commun Soil Sci Plan 39, 1600–1619.

van der Geest, H.G., Paumen, M.L., 2008. Dynamics of metal availability and toxicity in historically polluted floodplain sediments. Sci Total Environ 406, 419–425.

Vink, J.P.M., Harmsen, J., Rijnaarts, H., 2010. Delayed immobilization of heavy metals in soils and sediments under reducing and anaerobic conditions; consequences for flooding and storage. J Soils Sediments 10, 1633–1645.

Vorenhout, M., van der Geest, H.G., Hunting, E.R., 2011. An improved datalogger and novel probes for continuous redox measurements in wetlands. Int J Environ an Ch 91, 801–810.

Vorenhout, M., van der Geest, H.G., van Marum, D., Wattel, K., Eijsackers, H.J.P., 2004. Automated and continuous redox potential measurements in soil. J Environ Qual 33, 1562–1567.

Wang, G.Q., Koopmans, G.F., Song, J., Temminghoff, E.J.M., Luo, Y.M., Zhao, Q.G., Japenga, J., 2007. Mobilization of heavy metals from contaminated paddy soil by EDDS, EDTA, and elemental sulfur. Environ Geochem Hlth 29, 221–235.

Weng, L.P., van Riemsdijk, W.H., Hiemstra, T., 2008. $Cu^{2+}$ and $Ca^{2+}$ adsorption to goethite in the presence of fulvic acids. Geochim Cosmochim Ac 72, 5857–5870.

Yu, K.W., Bohme, F., Rinklebe, J., Neue, H.U., DeLaune, R.D., 2007. Major biogeochemical processes in soils - A microcosm incubation from reducing to oxidizing conditions. Soil Sci Soc Am J 71, 1406–1417.

## Appendix

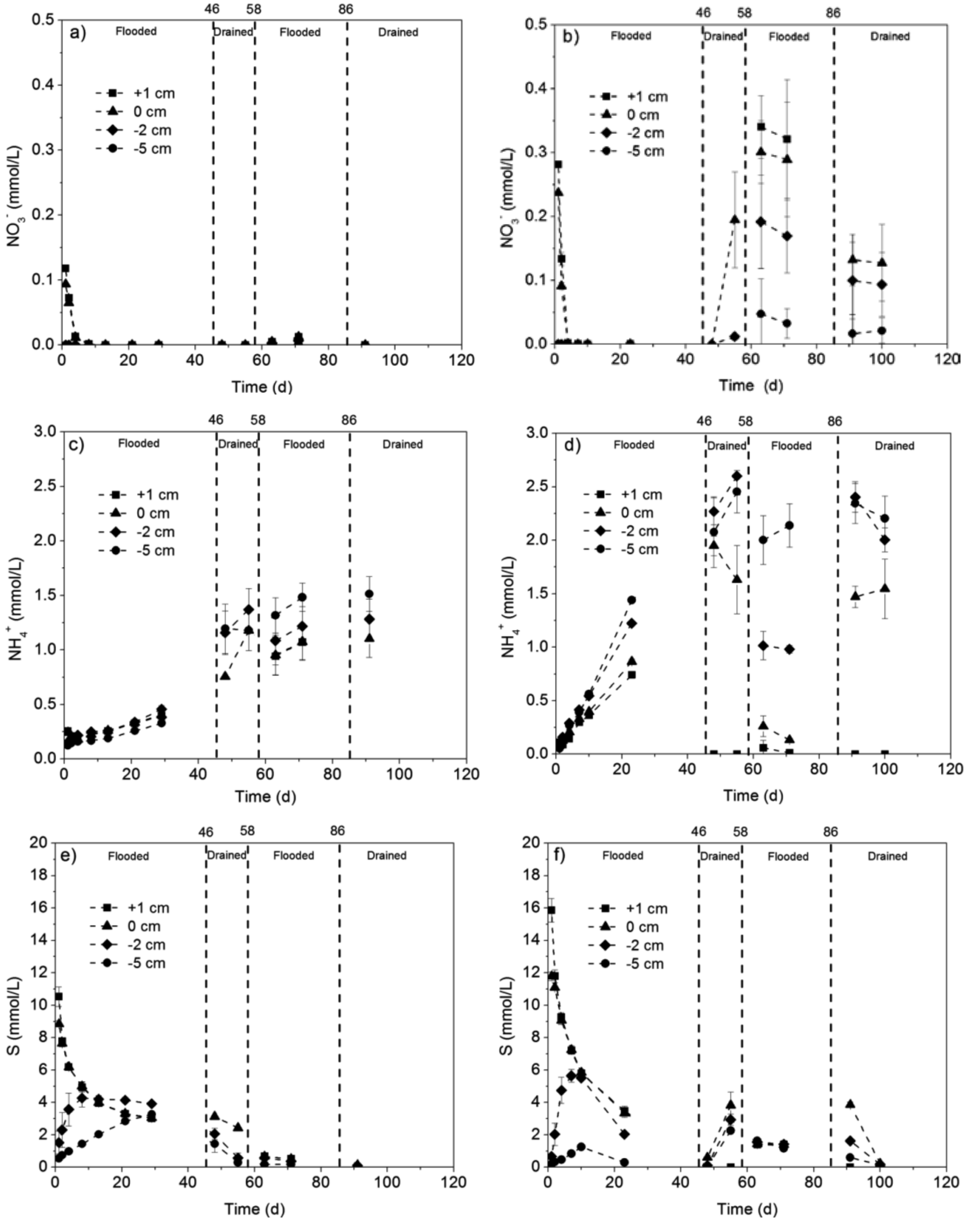

**Fig. A.1.** $NO_3^-$, $NH_4^+$ and S concentrations in the soil solution as a function of time in the TZ soil (a, c and e) and the FY soil (b, d and f) (+1 cm refers to 1 cm above interface; 0 cm equals the depth of interface; -2 cm and -5 cm refer to 2 and 5 cm below the interface, respectively).

When soil is further reduced, $SO_4^{2-}$ follows as an electron acceptor. Figure S1e and S1f shows total dissolved S concentration in soil solution, which is the sum of $SO_4^{2-}$ and other S species. Because the solubility of sulfide is very low, most of the S in solution will have been $SO_4^{2-}$.

During the first flooding period, the trend of measured S concentrations in both soils was similar to the trend of DOC (Fig. 2e and 2f), nitrate (Fig. A.1a and A.1b) and Mn concentrations (Fig. 4a): the initial concentrations of S in the two top layers were higher than in the two bottom layers; additionally, S concentrations decreased in the two top layers, while S concentrations increased in the two bottom layers except the sampling occasion at day 23 in the FY soil. Here also, the initial higher S concentration in the top layers might be caused by the upward displacement of $SO_4^{2-}$ during the flooding of the columns from the bottom to the top. And the first sampling occasion was only after the whole column was flooded. The followed decrease of S concentrations at two top layers during the flooding period might be because of re-adsorption on Fe (III) (hydr)oxides under aerobic conditions (Fig. 2a). The increase of S concentrations at two bottom layers during the flooding period might be attributed to the reductive Fe dissolution (Fig. 4c and 4d) releasing $SO_4^{2-}$ that was complex by Fe (III) (hydr)oxides.

After the first flooding period, S concentrations continuously decreased to around the detection limit in the TZ soil. In the FY soil, S concentrations in the bottom two layers peaked at approximately 10 days and then decreased. In the first drainage period, S concentrations again increased, then slowly decreased in the second flooding period and steeply decreased in the second drainage period. The decrease of S concentrations could be due to re-adsorption on newly-formed Fe (III) (hydr)oxides during the drainage periods and the formation of FeS and other metal sulfides during the flooding periods as the model predicted. The model predicts, in the TZ soil, that FeS is present at the last sampling occasion at 2 cm below interface during the first flooding period, and it remains at the first sampling occasion at this layer in the first drainage period, and later on FeS is present at two bottom layers during the second flooding period, and remains at 5 cm below interface during the second drainage period. These model predictions are consistent with the measured low S concentrations in the TZ soil. The model predicts, in the FY soil, that FeS is formed during second flooding period, which is consistent with the observed low S concentrations at same period. The observed increase of S concentrations during the first drainage period might be due to oxidation of FeS as model predicted, and less complexed $SO_4^{2-}$ with Fe (III) (hydr)oxides in the FY soil than in TZ soil because of the higher pH in the FY soil.

# Chapter 3

# Solubility of trace metals in two contaminated paddy soils exposed to alternating flooding and drainage

*Yunyu Pan, Luc T.C. Bonten, Gerwin F. Koopmans, Jing Song,*

*Yongming Luo, Erwin J.M. Temminghoff, Rob N.J. Comans*

Submitted to Geoderma, **2015**

## Abstract

Uptake of trace metals by crops is determined by the solubility of trace metals. In paddy soils, flooding and drainage influence redox chemistry and consequently trace metal solubility and thus uptake by rice plants. Current knowledge on how the changes in redox chemistry affect the solubility of trace metals in contaminated paddy soils is still limited. The objectives of our study were to investigate (i) the effects of flooding and drainage on trace metal solubility in paddy soils and (ii) to what extent a multi-surface modeling approach can predict trace metal solubility under changing redox conditions. We performed a column experiment with two contaminated paddy soils with similar soil properties but contrasting pH. During two successive flooding and drainage cycles, dynamics in Eh, pH and dissolved organic matter concentrations greatly affected trace metal solubility for both soils. Multi-surface model predictions indicate that under aerobic conditions, the higher pH of the alkaline soil leads to a stronger complexation of trace metals by reactive surfaces of the soil and, consequently, to lower dissolved concentrations than in the acidic soil. Under anaerobic conditions, results shows that sulfide precipitates control trace metal solubility in both soils, but still the higher pH of the alkaline soil leads to lower trace metal concentrations in soil solution at equilibrium. Furthermore, model calculations showed that stoichiometry and solubility of copper sulfide minerals can substantially affect solubility of other trace metals and that these should be considered when predicting the solubility of trace metals under anaerobic conditions.

*Keywords:* redox potential, trace metal concentration, soil solution, paddy soil, multi-surface models

### *3.1. Introduction*

Rice is the most important staple food for a large part of the human population, especially in South and Southeast Asia (Laborte et al., 2012; Meharg et al., 2013). Contamination of paddy soils with trace metals in industrialized regions in South and Southeast Asia (Wang et al., 2007; Römkens et al., 2009a; Fu et al., 2013) can lead to an increase in their uptake by rice plants and their accumulation in rice grains (Römkens et al., 2009b; Zeng et al., 2011). Consequently, the consumption of rice with high levels of trace metals can lead to unacceptable human health risks (Simmons et al., 2005; Brus et al., 2009; Meharg et al., 2013). For example, the Cd content of rice grains cropped in paddy fields across the western plains of Taiwan has been demonstrated to frequently exceed the food quality standard of the World Health Organization, even at low levels of Cd contamination (Römkens et al., 2009b). This finding illustrates the need for a thorough understanding of the processes controlling the uptake of trace metals by rice plants.

Apart from rice plant-specific factors (Yu et al., 2006; Römkens et al., 2009b), the uptake of trace metals by rice plants is largely determined by the bioavailability of trace metals in the soil (Simmons et al., 2008; Römkens et al., 2009b), which, in turn, is determined by the solubility of trace metals. The solubility of trace metals has been intensively studied in aerobic soils (Sauve et al., 2000; Tye et al., 2004; Rieuwerts, 2007) but has received less attention in paddy soils. Rice is usually cropped in lowland paddy soils. Flooding conditions prevail during almost the entire cropping period, because lowland rice is extremely sensitive to water shortage (Kögel-Knabner et al., 2010). Flooded paddy soils undergo at least two drainage periods, which include the late tillering stage to control ineffective tillering and the period shortly before the harvest to enable faster rice ripening and easier harvesting (Kögel-Knabner et al., 2010). During flooding of paddy soils, the redox potential (Eh) will decrease after the depletion of $O_2$ and subsequently the following reduction reactions will either sequentially or simultaneously take place: denitrification and transformation of Mn(III/IV) to Mn(II), of Fe(III) to Fe(II), and of $SO_4^{2-}$ to $S^{2-}$ (Murase and Kimura, 1997; Yu et al., 2007). These reduction reactions will occur in parallel with the oxidation of organic matter. Reductive dissolution of Mn(III/IV)- and Fe(III)-(hydr)oxides during flooding will lead to an increase in the $Mn^{2+}$ and $Fe^{2+}$ concentrations in soil solution while organic matter will be released, resulting in an elevated level of dissolved organic matter (DOM) (Tack et al., 2006; Grybos et al., 2007; Pan et al., 2015). Soil organic matter (SOM) and metal-(hydr)oxides play an important role in the adsorption of trace metals in soils (Weng et al., 2001). Consequently, a decrease in the reactive surface of these soil constituents, particularly Fe-(hydr)oxides, during flooding might lead to an increase in the solubility of trace metals. The mobilization of trace metals might be even further amplified by the release of DOM, because trace metals, especially Cu and Pb, can bind strongly to DOM (Amery et al., 2007; Koopmans and Groenenberg, 2011). On the other hand, the presence of $S^{2-}$ from the reduction of $SO_4^{2-}$ might lead to the precipitation of trace metals in the form of poorly soluble sulfide minerals (de Livera et al., 2011; Khaokaew et al., 2011; Fulda et al., 2013). In addition to this, the pH of acid soils can increase after flooding, because reduction processes consume protons (Kögel-Knabner et al., 2010), causing an increase in the adsorption of trace metals to reactive surfaces of SOM, DOM, and metal-(hydr)oxides (Weng et al., 2001). During drainage and subsequent oxidation of paddy soils, the above mentioned reduction reactions will be (partially) reversed, leading to the precipitation of fresh Mn (III/IV)- and Fe(III)-(hydr)oxides, dissolution of trace metal sulfide precipitates, and a change of the pH back to its antecedent value. These complex and dynamic effects of flooding and drainage on the Eh and the redox chemistry of paddy soils will have a large influence on the solubility of trace metals, which will, in turn, affect the bioavailability of trace metals for uptake by rice plants. However, the current knowledge of the effects of changes in Eh and redox chemistry on the solubility of trace metals in contaminated soil systems exposed to alternating flooding and drainage conditions is still limited.

The multi-surface modeling approach can be a useful tool to investigate the partitioning of trace metals between soil solution and the solid phase. Specifically, multi-surface models can be used to predict trace metal complexation by different reactive surfaces, including SOM and DOM, short-range ordered and crystalline Fe-(hydr)oxides, and clay minerals (Weng et al., 2001; Bonten et al., 2008), and precipitation of trace metals as minerals (Meima and Comans, 1997). Multi-surface models have been shown to adequately predict the solubility of most trace metals for aerobic soils (e.g., Weng et al., 2001; Cancès et al., 2003; Dijkstra et al., 2009). However, it is unclear to what extent the multi-surface modeling approach is applicable to predict the partitioning of trace metals in paddy soils exposed to alternating flooding and drainage conditions. With the change from aerobic to anaerobic conditions, formation of sulfide minerals in flooded soils or sediments can take place (Morse and Luther, 1999; Weber et al., 2009). Since there is still little experimental evidence on the chemical identity of such (particularly Cu) sulfides formed under anaerobic conditions (Weber et al., 2009), it is difficult to include this process in multi-surface models. Also, the reactive surfaces of adsorbents including SOM and Fe-(hydr)oxides can decrease upon flooding while compositional changes can take place within the SOM and DOM including the formation of reduced sulfur-containing ligands (Qian et al., 2002) which influence the reactivity of these surfaces for binding trace metals. These processes are not necessarily incorporated within multi-surface models. Moreover, chemical processes such as precipitation and dissolution of Fe-(hydr)oxides and trace metal minerals under alternating flooding and drainage conditions can be kinetically-limited (Pan et al., 2014), which might restrict the applicability of multi-surface models for such systems due to their chemical equilibrium nature. This warrants specific research into the extent to which existing multi-surface models can be applied to dynamic systems such as paddy soils to predict the solubility of trace metals under changing redox conditions.

In this study, we determined how two flooding and drainage events affect the solubility of trace metals in a carefully designed column experiment with two field-contaminated paddy soils exhibiting similar soil properties but contrasting pH. The effects of alternating flooding and drainage of these columns on the Eh, pH, and the occurrence of metal-(hydr)oxides and organic matter have been reported previously by Pan et al. (2014). In the current study, we investigate the effects of flooding and drainage on the solubility of trace metals. Additionally, we examine to what extent multi-surface modeling approach can be used to predict trace metal solubility under these changing redox conditions.

## *3.2. Materials and methods*

### *3.2.1. Site description and soil collection*

In Zhejiang Province, P.R. China, two soil samples (0-20 cm) with a clay loam texture were sampled from a site nearby a former transformer and electronic waste stripping and recycling factory in the vicinity of Taizhou city (TZ soil) and from a site nearby a galvanizing plant in the vicinity of Fuyang city (FY soil), respectively (Pan et al., 2014).

The two soils were severely contaminated with trace metals because of industrial activities in the proximity of the sampling sites (Wang et al., 2007; Brus et al., 2009; Sun et al., 2013). The two soils were dried at 40 °C, passed through a 2 mm sieve, and stored at room temperature before analyzing the soil characteristics and preparing the column experiment.

### *3.2.2. Experimental setup of the column experiment*

A detailed experimental setup of the column experiment has been described in Pan et al. (2014). Briefly, the column experiment was performed in duplicate for each of the two paddy soils. For flooding of the soil columns, a 2 mM $CaCl_2$ solution was used. The solution was pumped by a peristaltic pump from the bottom of the column in an upward direction to remove entrapped air bubbles. Along the profile of the columns, the Eh was monitored continuously at 1 cm above the soil-water interface (+1 cm), at the interface (0 cm), 2 cm below the interface (-2 cm), and 5 cm below the interface (-5 cm) during two successive flooding-draining cycles. Besides Eh monitoring at these four depths, soil solution was sampled regularly at the same depths to determine its chemical composition including pH and the concentrations of total dissolved trace metals, Fe, Mn, and dissolved organic carbon (DOC).

### *3.2.3. Soil characteristics*

Data on pH and soil contents of $CaCO_3$, SOM, clay (< 2μm), DOC, and short-range ordered metal-(hydr)oxides were taken from Pan et al. (2014). The available S-$SO_4^{2-}$ content was determined by extraction of soil with 0.01 M $CaCl_2$ at a soil to solution ratio of 1:10 (w:v), followed by the measurement of $SO_4^{2-}$ with ion chromatography (DIONEX, ICS-2100) (Dick and Tabatabai, 1979). In the current study, the size of the reactive trace metal pools was determined by 0.43 M $HNO_3$ extraction while the total soil contents of trace metals were determined by digestion with Aqua Regia (Houba et al., 1997). The Cd, Cu, Ni, Zn, and Pb concentrations in the $HNO_3$ extracts and the Aqua Regia digests were measured by inductively coupled plasma atomic emission spectroscopy (ICP-AES; Varian Vista Pro).

### *3.2.4. Soil solution analyses*

Data on the pH and DOC concentrations of the soil solution samples were taken from Pan et al. (2014). In the current study, total dissolved concentrations of Cd, Cu, Ni, Zn, and Pb were measured in acidified solution subsamples by ICP-AES. When trace metal concentrations were below the detection limit of the ICP-AES, they were measured by high resolution inductively coupled plasma mass spectrometry (HR-ICP-MS; Thermo Element 2).

### *3.2.5. Geochemical modeling of the total dissolved trace metals*

We used multi-surface modeling approach to predict the total dissolved trace metal concentrations in soil solution. Briefly, this approach used here was set up as multi-surface models similar to that of Bonten et al. (2008) and Dijkstra et al. (2009), and included ion adsorption to three reactive surfaces within the soil solid phase, i.e., SOM, clay minerals, and short-range ordered metal-(hydr)oxides, and accounted for the full speciation of trace metals in soil solution, i.e., trace metals complexed by DOC and inorganic ligands and their free form. Trace metal adsorption to both SOM and DOM is described by the NICA-Donnan model (e.g., Kinniburgh et al. 1999; Koopal et al. 2005), to clay minerals by a non-specific cation exchange model using a Donnan approach, and to short-range ordered Fe- and Al-(hydr)oxides by the two site diffusive double layer model for hydrous ferric oxide (HFO) of Dzombak and Morel (1990). For the reactivity of these adsorption surfaces, we used the same assumptions as in Bonten et al. (2008) and Pan et al. (2014) except for DOM. The DOM was assumed to consist of 40% generic fulvic acid (FA) while 60% was taken to be inert with respect to proton and metal binding (Groenenberg et al., 2010; Pan et al., 2015). For proton and metal binding to FA, we used the generic NICA-Donnan parameters (Milne et al., 2003). For trace metal complexation with inorganic ligands, we used the stability constants from the MINTEQ database (US-EPA, 1999). Different from most other multi-surface modeling studies, we included several redox couples in our model calculations, i.e., $NO_3^-/N_2$, Mn(IV)/Mn(II), Fe(III)/Fe(II), $SO_4^{2-}/S^{2-}$, and Cu(II)/Cu(I). The distribution of the elements between these redox forms was calculated from the measured Eh values. For Cu(I), we neglected complexation with SOM and DOM, which may be justified as it is a monovalent cation which generally shows very little complexation with organic matter (Maurer et al., 2013). Input for our model calculations included: the measured pH and Eh values, a moisture content of 0.24 L $kg^{-1}$ for the TZ soil and 0.20 L $kg^{-1}$ for the FY soil, a $CO_2$ pressure defined as 10 times ambient $pCO_2$ (316 Pa) (Du Laing et al., 2007), the soil content of short-range ordered Mn-, Fe-, and Al-(hydr)oxides (from soil extraction with acid ammonium oxalate), the available S-$SO_4^{2-}$ content (from soil extraction with 0.01 M $CaCl_2$), the Ca and DOC concentrations as measured in the soil solution samples, and $Cl^{-1}$ at the background concentration of the 2 mM $CaCl_2$ solution (all taken from Pan et al., 2014), as well as the size of the reactive trace metal pools (from soil extraction with 0.43 M $HNO_3$). Finally, we included several minerals in our model calculations (see Table 1). To examine to what extent our multi-surface models can be applied under anaerobic conditions, we performed two types of model calculations: one including the formation of metal sulfides and cuprite ($Cu_2O$) and one without these minerals. Model calculations were done within the Objects Representing CHEmical Speciation and TRAnsport (ORCHESTRA) framework (Meeussen, 2003).

**Table 1**

Selected solubility products of minerals in this study

| Mineral | Metal | Mineral[a] | log $K_{sp}^{0a}$ | Reaction[a] |
|---|---|---|---|---|
| Metal sulfides | Cu | Chalcocite ($Cu_2S$) | –34.9 | $Cu_2S+H^+\leftrightarrow 2Cu^++HS^-$ |
| | Cd | Greenockite (CdS) | –14.4 | $CdS+H^+\leftrightarrow Cd^{2+}+HS^-$ |
| | Pb | Galena (PbS) | –14.0 | $PbS+H^+\leftrightarrow Pb^{2+}+HS^-$ |
| | Zn | ZnS | –9.1 | $ZnS+H^+\leftrightarrow Zn^{2+}+HS^-$ |
| | Ni | Millerite (NiS) | –5.6 | $NiS+H^+\leftrightarrow Ni^{2+}+HS^-$ |
| | Fe | FeS | –2.9 | $FeS+H^+\leftrightarrow Fe^{2+}+HS^-$ |
| Oxide | Cu | Cuprite ($Cu_2O$) | –1.4 | $Cu_2O+2H^+\leftrightarrow 2Cu^++H_2O$ |
| Carbonates | Zn | $ZnCO_3\cdot H_2O$ | –10.26 | $ZnCO_3\cdot H_2O\leftrightarrow Zn^{2+}+CO_3^{2-}+H_2O$ |
| | Fe | Siderite ($FeCO_3$) | –10.24 | $FeCO_3\leftrightarrow Fe^{2+}+CO_3^{2-}$ |
| | Mn | Rhodochrosite ($MnCO_3$) | –10.58 | $MnCO_3\leftrightarrow Mn^{2+}+CO_3^{2-}$ |
| Hydroxides | Fe | Ferrihydrite ($Fe(OH)_3$) | 3.2 | $Fe(OH)_3+3H^+\leftrightarrow Fe^{3+}+3H_2O$ |
| | Al | Gibbsite ($Al(OH)_3$) | 8.3 | $Al(OH)_3+3H^+\leftrightarrow Al^{3+}+3H_2O$ |

[a] Solubility products are from the MINTEQ.v4 database (US-EPA, 1999).

## *3.3. Results and discussion*

### *3.3.1. Physical-chemical soil properties*

Selected physical-chemical soil properties of the two paddy soils used in the column experiment in this study are summarized in Table 2. The total and reactive trace metal contents were measured in the current study, whereas the other data was taken from Pan et al. (2014). The total Cd, Cu, Ni, and Zn contents in the TZ soil exceed the Chinese environmental quality standard for soils (GB 15618-1995; Grade II for soil pH<6.5) about 28 (Cd), 9 (Cu), and 1.3 (Ni) times, respectively, while total contents of these trace metals in the FY soil exceed this standard (GB 15618-1995; Grade II for soil pH between 6.5 and 7.5) about 36 (Cd), 1.4 (Cu), 2.4 (Ni), and 9 (Zn) times, respectively. Apparently, the TZ soil is heavily contaminated with Cd and Cu whereas this is the case with respect to Cd and Zn for the FY soil. The ratio between the reactive Cd content as determined by soil extraction with 0.43 M $HNO_3$ and the total Cd content as based on soil digestion with Aqua Regia was 87% for the TZ soil and 78% for the FY soil, indicating Cd is highly reactive, which is in agreement with other studies (McBride et al., 2006; Meers et al., 2007; Römkens et al., 2009a). This ratio for Pb is about two times higher in the TZ soil (61%) than in the FY soil (34%). The ratios between the reactive Zn and Ni contents and their total contents were 27% and 22% for the TZ soil, respectively. For the FY soil, this ratio was 71% for Zn and it was 34% for Ni. The available S-$SO_4^{2-}$ contents in the two paddy soils (Table 2) were in the upper range of the available S-$SO_4^{2-}$ contents (0.06 to 6.6 mmol $kg^{-1}$) reported for other paddy soils in different regions (Lefroy et al., 1992; Fulda et al., 2013). The availability of $SO_4$ is relevant because, under anaerobic conditions, $SO_4$ may be reduced to sulfide and limit the solubility of trace metals present in soil by precipitation of sulfide minerals (Weber et al., 2009; Fulda et al., 2013; Hofacker et al., 2013).

**Table 2**

Selected physical and chemical properties of the two paddy soils used in the column experiment in this study. The total and reactive trace metal contents were measured in the current study whereas the other data were taken from Pan et al. (2014).

| Soil property | Unit | TZ soil | FY soil | Standard (pH<6.5)[g] | Standard (6.5≤pH≤7.5)[g] |
|---|---|---|---|---|---|
| Clay (<2 μm) | % | 33 | 25 | - | - |
| SOM[b] | % | 7.0 | 9.2 | - | - |
| $CaCO_3$ | % | ND[a] | 21 | - | - |
| pH[c] | | 4.9 | 7.5 | - | - |
| DOC[c] | mg C $L^{-1}$ | 124 | 189 | - | - |
| S-$SO_4^{2-}$[c] | mmol $kg^{-1}$ | 4.7 | 7.0 | - | - |
| Al-ox[d] | mmol $kg^{-1}$ | 43±0.05 | 36±0.1 | - | - |
| Fe-ox[d] | mmol $kg^{-1}$ | 107±2 | 52±0.3 | - | - |
| Mn-ox[d] | mmol $kg^{-1}$ | 2.4±0.03 | 3±0.02 | - | - |
| Reactive Cu[e] | μmol $kg^{-1}$ | 4634±11 | 1031±25 | - | - |
| Total Cu[f] | μmol $kg^{-1}$ | 7271 | 2172 | 787 | 1574 |
| Reactive Cd[e] | μmol $kg^{-1}$ | 65±0.7 | 75±1 | - | - |
| Total Cd[f] | μmol $kg^{-1}$ | 75 | 96 | 2.7 | 2.7 |
| Reactive Pb[e] | μmol $kg^{-1}$ | 152±2 | 61±2 | - | - |
| Total Pb[f] | μmol $kg^{-1}$ | 251 | 179 | 1207 | 1448 |
| Reactive Zn[e] | μmol $kg^{-1}$ | 697±8 | 24546±108 | - | - |
| Total Zn[f] | μmol $kg^{-1}$ | 2600 | 34735 | 3059 | 3823 |
| Reactive Ni[e] | μmol $kg^{-1}$ | 192±2 | 704±4 | - | - |
| Total Ni[f] | μmol $kg^{-1}$ | 893 | 2062 | 682 | 852 |

[a] Not detected;

[b] Soil organic matter by loss on ignition (550 °C) (Houba et al. 1997);

[c] 1:10 (w/v) 0.01 M $CaCl_2$ (Houba et al. 2000); determined in duplicate and presented as average ± standard deviation;

[d] Extraction with acid ammonium oxalate (Novozamsky et al. 1986); determined in duplicate and presented as average ± standard deviation;

[e] 1:10 (w/v) 0.43 M $HNO_3$ (Houba et al., 1997); determined in duplicate and presented as average ± standard deviation;

[f] Aqua Regia (Houba et al., 1997);

[g] Grade II of Chinese environmental quality standard for soils (GB 15618-1995).

### *3.3.2. Impact of two flooding-draining cycles on dynamics of Eh, pH, Mn, Fe, and DOC*

The impact of two flooding-draining cycles on the dynamics of Eh and pH and the concentrations of total dissolved Mn and Fe and DOC in the two paddy soils has previously been presented and discussed in Pan et al. (2014). Since these characteristics are known to be important in determining the solubility of trace metals in floodplain soils and sediments (Du Laing et al. 2009; Schulz-Zunkel and Krueger, 2009; Shaheen et al., 2014), the effects of alternating flooding and drainage conditions on these characteristics are briefly summarized here so as to facilitate the interpretation of the dynamics in trace metal solubility in the same two paddy soils (see Section 3.3.4). During the two successive flooding-draining cycles, vertical gradients in the Eh developed in both paddy soils (Fig. 1). Based on the measured Eh range for both paddy soils, redox reactions including denitrification and reduction of Mn(III/IV) to Mn(II), of Fe(III) to Fe(II), and of $SO_4^{2-}$ to $S^{2-}$ can occur (Fig. 1). Besides Eh, the pH changed during the column experiment. In general, the pH of the acidic TZ soil increased with decreasing

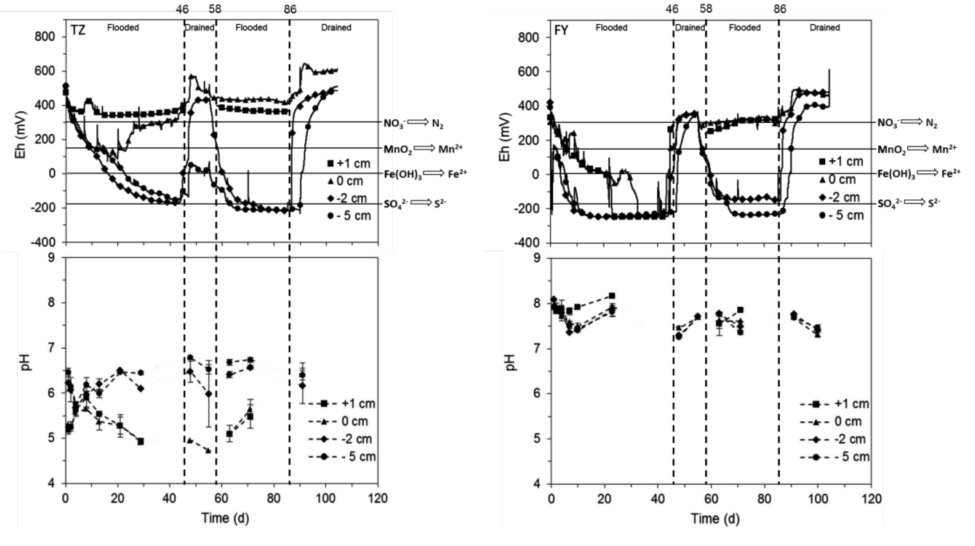

**Fig. 1.** Measured Eh (top) and pH (bottom) as a function of time in the TZ soil (left) and the FY soil (right) and Eh values (horizontal solid lines) for successive reduction reactions (Murase and Kimura, 1997). The figures of Eh and pH are modified from Pan et al. (2014) (+1 cm refers to 1 cm above the interface, 0 cm refers to the interface

between the soil surface and the water layer, and -2 cm and -5 cm refer to 2 and 5 cm below the interface, respectively).

Eh and vice versa, whereas the pH of the alkaline FY soil was buffered by $CaCO_3$ (Fig. 1). The decrease in Eh upon flooding led to a different response in the solubility of Mn- and Fe-(hydr)oxides between the acidic TZ soil and the alkaline FY soil. In the acidic TZ soil, the solubility of Mn and Fe increased during flooding due to reductive dissolution of their (hydr)oxides and decreased during drainage because of re-oxidation (Pan et al., 2014). In the alkaline FY soil, Mn and Fe solubility did not increase during flooding, because Mn(II) and Fe(II) immediately precipitated as $MnCO_3$, $FeCO_3$, and/or FeS (Pan et al., 2014). Both reductive dissolution of Fe-(hydr)oxides and the increase in pH led to an elevated level of DOC in soil solution (Pan et al., 2014).

### *3.3.3. Trace metal distribution between the solution and solid phase under aerobic and anaerobic conditions*

To understand the dynamics in the solubility of trace metals, we first predicted the speciation of Cu, Cd, Pb, Zn, and Ni under aerobic and anaerobic conditions using the multi-surface model described in Section 3.2.5. Figure 2 shows the distribution of these trace metals between the soil solution and different reactive surfaces (i.e., SOM, clay minerals, and short-range ordered Fe- and Al-(hydr)oxides) and trace metal minerals within the solid phase of the TZ and FY soils under both aerobic and anaerobic conditions. For the Eh and pH, typical values representing aerobic and anaerobic conditions for both paddy soils were chosen from Figure 1. For both paddy soils, the contribution of total dissolved trace metals to the total trace metal content is very low and less than 5% under both aerobic and anaerobic conditions. Under aerobic conditions, the predicted adsorption of trace metals to different reactive surfaces within the solid phase differs in both paddy soils. Soil organic matter is the most important adsorption surface for the five trace metals considered in this study, except for Zn in the FY soil, which largely occurs in the form of a $ZnCO_3$ mineral. The high importance of SOM in the complexation of trace metals has been found before in many other studies in which trace metal speciation was predicted for aerobic soils (e.g., Weng et al., 2001; Cancès et al., 2003; Bonten et al., 2008; Dijkstra et al., 2009). Adsorption of trace metals to clay minerals plays a minor role and does only contribute substantially to Cd, Ni, and Zn binding in the TZ soil. Besides adsorption to SOM and clay minerals, about 40% of Pb in the TZ soil and about 20% of Ni and Pb in the FY soil are bound to Fe- and Al-(hydr)oxides. Similar results have been found by Weng et al. (2001) and Grybos et al. (2007).

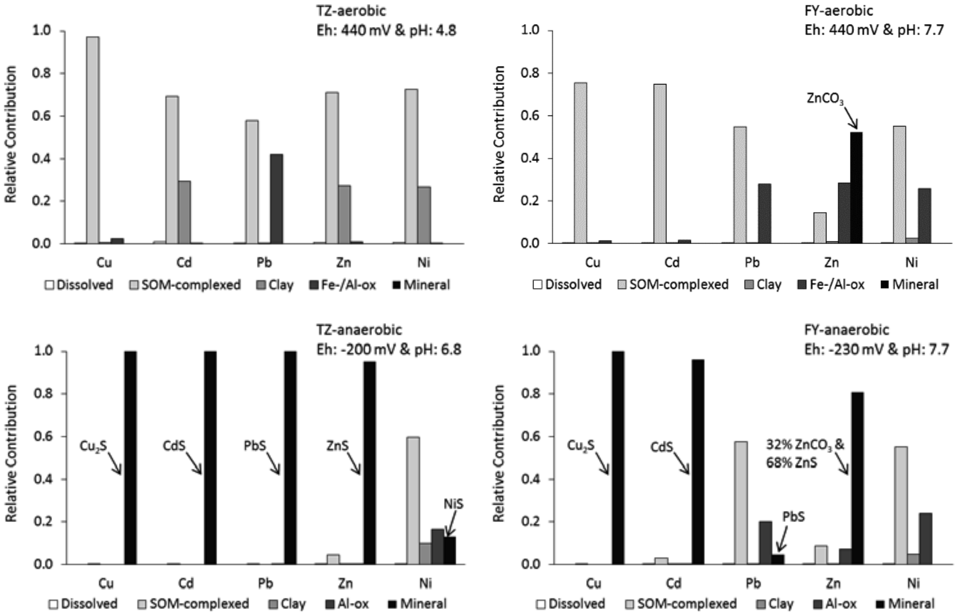

**Fig. 2.** Predicted distribution of trace metals between the soil solution and different reactive surfaces (i.e., SOM, clay minerals, and short-range ordered Fe- and Al-(hydr)oxides) and trace metal minerals within the solid phase of the TZ soil (left) and FY soil (right) under aerobic (top) and anaerobic conditions (bottom). For the Eh and pH, typical values representing aerobic and anaerobic conditions for both paddy soils were chosen from Fig. 1.

Under anaerobic conditions, the predicted speciation of the five trace metals changes markedly for the two paddy soils (Fig. 2). The most striking change is the formation of sulfide precipitates, which becomes the dominant species of trace metals except for Ni in the TZ soil and for Pb and Ni in the FY soil. In the two paddy soils, the formation of sulfide precipitates generally follows the sequence of the thermodynamical “sulfide ladder” (Weber et al., 2009). According to this “sulfide ladder”, trace metals will precipitate in the form of sulfide minerals in the following order: Cu, Cd, Pb, Zn, and Ni, as follows from the increase in the solubility products of their sulfide minerals (Table 1).

The relative contribution of NiS in the TZ soil is only 13%, because Ni forms the least stable sulfide minerals of all the five trace metals considered here and the amount of sulphur in this paddy soil is clearly insufficient to precipitate all trace metals in the form of sulfides when all available S-$SO_4^{2-}$ is reduced to $S^{2-}$ (Table 2). For the FY soil, 32% of the Zn was predicted to be present in the form of ZnS whereas 68% was present as $ZnCO_3$. The relative contribution of PbS in the FY soil is only 5% despite the fact of Pb having a higher position on the "sulfide ladder" than Zn (Weber et al., 2009). The formation of NiS is not predicted for the FY soil. This might be explained by the very high reactive Zn contents in the FY soil (Table 2) resulting in strong Zn competition with Pb and Ni for sulfide. Therefore, the role of SOM in the adsorption of Ni for the TZ soil and in the adsorption of Ni and Pb for the FY soils is more important than for the other trace metals. In summary, SOM is the dominant surface in the binding of trace metals under aerobic conditions whereas sulfide minerals largely control the solubility of trace metals under anaerobic conditions.

### *3.3.4. Impact of two flooding-draining cycles on the temporal dynamics of Cu, Cd, Pb, Zn and Ni solubility*

#### *3.3.4.1. Solubility of trace metals*

During the two successive flooding-draining cycles of the column experiment, the maximum total dissolved concentrations of Cu, Cd, Pb, Zn, and Ni in soil solution were clearly much lower in the FY soil than those in the TZ soil (Fig. 3). During aerobic conditions, the higher pH of the alkaline FY soil (Table 2) leads to a stronger binding of trace metals to the reactive surfaces within the soil solid phase than in the acidic TZ soil (Fig. 2), leading to lower trace metal concentrations in soil solution. The presence of $CaCO_3$ in the FY soil (Table 2) is predicted to lead to precipitation of Zn in the form of $ZnCO_3$, which maintains the Zn solubility at a lower level than in the TZ soil (Table 1 and Fig. 2). Under anaerobic conditions, the solubility of most trace metals in both soils is controlled by sulfide precipitates (Fig. 2), while the higher pH of the FY soil maintains lower trace metal concentrations in soil solution at equilibrium.

#### *3.3.4.2. Fuyang soil*

In the FY soil, the total dissolved Cu and Cd concentrations in all layers decreased sharply with time during the first flooding period. This can be explained by the low Eh

(Fig. 1), which allows for the reduction of $SO_4^{2-}$ to $S^{2-}$ and the precipitation of Cd and Cu in the form of sulfide minerals exhibiting a low solubility (Table 1 and Fig. 2). The Cd and Cu solubility increased in all layers during the first drainage period (Fig. 3), due to re-aeration of the soil columns and the development of aerobic conditions (Fig. 1) leading to the dissolution of Cd and Cu sulfide minerals. During the second flooding period, Cd and Cu solubility in the two bottom layers decreased again, followed by an increase in their solubility during the second drainage period. The solubility of Pb was low throughout the entire column experiment, except for the drainage period during the second sampling occasion. The low Pb solubility during the flooding periods can probably be attributed to the precipitation of this trace metal in the form of sulfide minerals (Fig. 2). In the second drainage period, when the Eh returned to higher levels than during the first drainage period (Fig. 1), the total dissolved Pb concentration increased again at the interface, probably due to the dissolution of Pb sulfide minerals. The total dissolved Zn concentration fluctuated around the same level throughout the entire column experiment, because $ZnCO_3$ probably controlled Zn solubility under both aerobic and anaerobic conditions (Fig. 2). The Ni solubility was clearly higher in the two bottom layers than in the two top layers during the first flooding period. This can be explained by the increase in the concentration of DOC in the two bottom layers (Pan et al., 2014) under anaerobic conditions (Fig. 1), leading to complexation of Ni by DOC (Grybos et al., 2007) and an increase in the solubility of Ni. We note that Ni is the only metal that is not predicted to form a sulfide mineral in this soil (Fig. 2), which probably explains why this effect of enhanced DOC complexation is not noticeable for the other metals. The total dissolved Ni concentrations in the two top layers decreased in the remainder of the column experiment to the same level as in the two bottom layers, while still closely following the DOC dynamics in the different soil layers (Pan et al., 2014).

### *3.3.4.3. Taizhou soil*

For the TZ soil, a large difference in the solubility of trace metals was found at the initial sampling occasion between the two upper and the two lower layers during the first flooding period. At this initial sampling occasion, the total dissolved trace metal concentrations were about 4 – 6 times higher in the two upper layers than those in the two lower layers. This initial difference in trace metal solubility might be due to the difference in pH at the first sampling occasion: the pH in the two upper layers was about

1 unit lower than the pH in the two lower layers (Fig. 1), leading to higher total dissolved trace metal concentrations in these upper layers (Fig. 1). In addition, vertical displacement of trace metals via upward transport during the saturation of the soil columns from the bottom with the 2 mM $CaCl_2$ solution might have contributed to the initial difference in the total dissolved trace metal concentrations. The solubility of Cd, Zn, and Ni in the two upper layers decreased gradually during the first flooding period, possibly in response to the decrease in the DOC concentrations in these layers (Pan et al., 2014), causing less of these trace metals to be present in soil solution by DOC-complexation. Surprisingly, the total dissolved Cu and Pb concentrations in the two upper layers first decreased and subsequently showed a gradual increase during the first flooding period whereas a decrease in these concentrations was expected due to the decreased DOC concentrations in the two upper layers (Pan et al., 2014). In the two lower layers, the total dissolved trace metal concentrations increased first and subsequently decreased during the first flooding period. The increase in trace metal solubility might be due to the temporary drop in pH in these layers (Fig. 1) and continuous release of DOC (Pan et al., 2014) whereas the decrease is consistent with the development of anaerobic conditions (Fig. 1) allowing for the reduction of $SO_4^{2-}$ to $S^{2-}$ and the precipitation of trace metals in the form of poorly-soluble sulfide minerals (Fig. 2). During the first drainage period of the TZ soil, the trace metal concentrations increased at the interface and a depth of -2 cm, but remained at a low level at a depth of -5 cm (Fig. 2), consistent with the Eh development (Fig. 1). The increase in trace metal solubility at the interface and a depth of -2 cm might be attributed to the oxidation of sulfide minerals, due to re-aeration of the soil columns and the development of aerobic conditions (Fig. 1). The low trace metal solubility at a depth of -5 cm can be explained by the Eh which remained low despite drainage of the soil columns and the high pH (Fig. 1) resulting in the probable persistence of sulfide minerals (Fig. 2). During the second flooding period, the trace metal concentrations decreased, but were higher in the two upper layers than in the two lower layers, consistent with the development of anaerobic conditions in the two lower layers (Fig. 1) allowing for the formation of trace metal sulfide minerals (Fig. 2). Contrary to the FY soil, the solubility of the trace metals remained low in all layers of the soil columns during the second drainage period. In the latter period, aerobic conditions developed in all layers upon re-aeration of the soil columns (Fig. 1) and, hence, oxidation of sulfide minerals and an increasing metal

solubility would be expected. The remaining relatively high pH in all layers (Fig. 1) might infer that metal sulfides in this relatively poorly-buffered soil might not yet have been fully oxidized, while the high pH might also have led to a stronger binding of the trace metals to SOM (Fig. 2). Both effects would be reflected in low remaining trace metal concentrations.

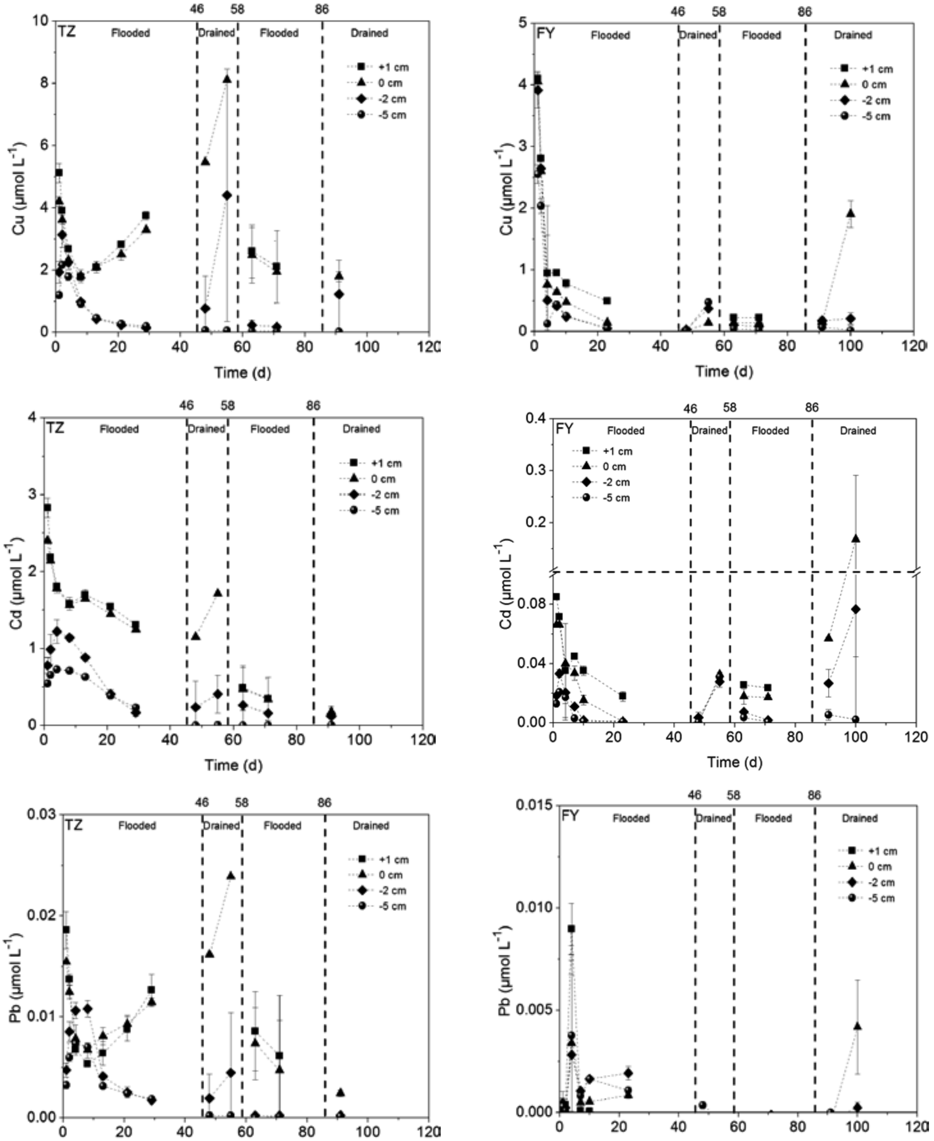

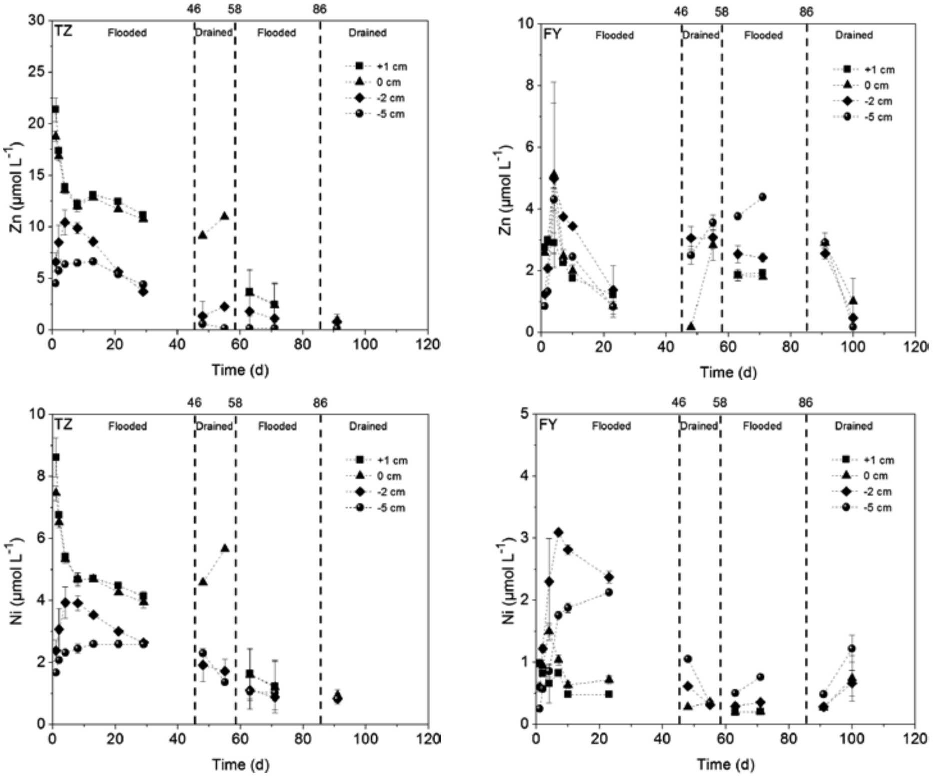

**Fig. 3.** Measured total dissolved Cu, Cd, Pb, Zn and Ni concentrations in soil solution as a function of time in the TZ soil (left) and the FY soil (right). The scale of Y-axis is different from the TZ to FY soil. (+1 cm refers to 1 cm above the interface, 0 cm equals the interface between the soil surface and the water layer, and -2 cm and -5 cm refer to 2 and 5 cm below the interface, respectively)

### *3.3.5. Modeling trace metal solubility*

To examine the applicability of the multi-surface model under anaerobic conditions, Figure 4 shows the ratios between the predicted and measured total dissolved concentrations of Cu, Cd, Pb, Zn, and Ni in soil solution as a function of Eh in the column experiment for both soils. We used two types of model calculations: one including the formation of sulfides and cuprite and one excluding these minerals.

### *3.3.5.1. Model calculations excluding the formation of sulfides and cuprite*

At Eh values above -100 mV, sulfur is present as $SO_4^{2-}$ and thus precipitation of trace metals in the form of sulfides will not take place. Therefore, our model predictions for samples with an Eh above -100 mV are expected to agree adequately (i.e., well within an order of magnitude) with the measurements, because several studies have frequently shown such an agreement for aerobic soils (e.g., Weng et al., 2001; Cancès et al., 2003; Dijkstra et al., 2004, 2009). For the TZ soil, this is indeed the case, because the ratios between the predicted and measured total dissolved concentrations for all trace metals except Pb are close to 1 when the Eh is above -100 mV. For Pb, however, this ratio is higher than 1. The overestimation of Pb solubility by multi-surface models has frequently been found before (e.g., Lofts and Tipping, 1998; Dijkstra et al., 2004; Heidman et al., 2005). Explanations for the discrepancy between predicted and measured Pb concentrations are discussed in detail in these studies and can be summarized as follows: uncertainties in adsorption parameters of Pb for complexation by Fe- and Al-(hydr)oxides and no incorporation of other potentially important adsorption processes in the model such as Pb complexation by manganese-(hydr)oxides. For the FY soil, however, the measured concentrations of Pb, Zn, Ni, and to a lesser extent those of Cd, are considerably overestimated at Eh values above -100 mV, whereas the Cu solubility is slightly underestimated. The overestimation of the solubility of Pb, Zn, Ni, and Cd is possibly due to the presence of 21% $CaCO_3$ in the alkaline FY soil (Table 2). Given the alkaline soil conditions and high trace metal loadings, specific retention processes of trace metals may take place, which are not generally included in multi-surface models based on generic adsorption models and stability constants. Such processes may include the formation of solid solutions of Ca and trace metal carbonates or of Fe and trace metal oxides (Davis et al., 1987; Karthikeyan et al., 1997), surface precipitates of trace metals on hydrous ferric oxides or calcite (Comans and Middelburg, 1987; Meima and Comans, 1998; Zhu, 2002), and other formation processes of solids such as Zn double layered hydroxides and Zn phyllosilicates (Zn-kerolite) (Khaokaew et al., 2012). Without specific data from mineralogical techniques on the speciation of trace metal minerals within the soil solid phase (Shenker and Bloom, 2005), it will be difficult to identify the possible role of such processes in controlling the solubility of trace metals in the alkaline FY soil and to predict the partitioning of trace metals more accurately with the current generic multi-surface models.

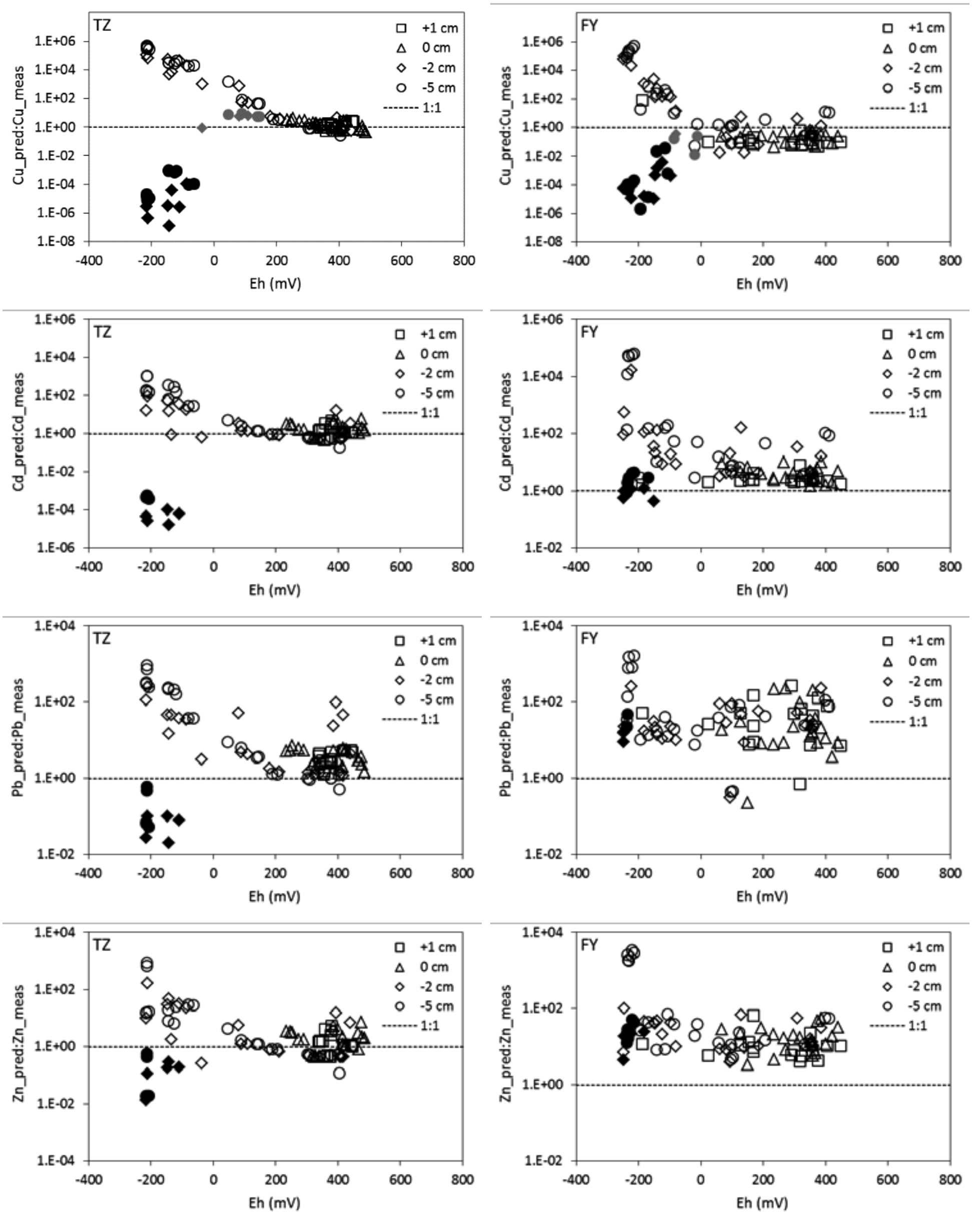
TZ
FY
Cu_pred:Cu_meas
Cd_pred:Cd_meas
Pb_pred:Pb_meas
Zn_pred:Zn_meas
Eh (mV)
+1 cm
0 cm
-2 cm
-5 cm
1:1
1.E+06
1.E+04
1.E+02
1.E+00
1.E-02
1.E-04
1.E-06
1.E-08
-400
-200
0
200
400
600
800

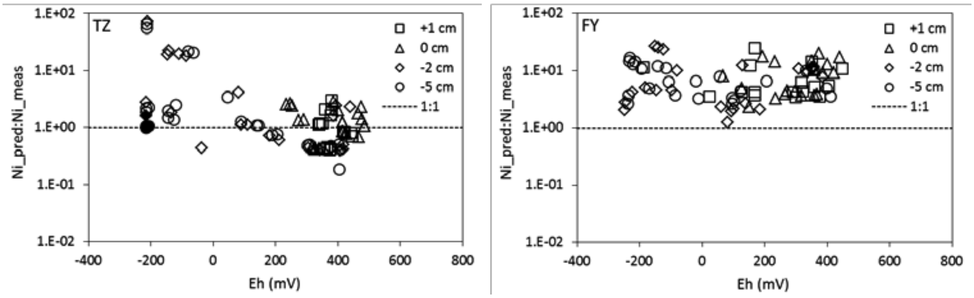

**Fig. 4.** Ratios between predicted and measured total dissolved concentrations of Cu, Cd, Pb, Zn, and Ni in soil solution as a function of Eh in the TZ soil (left) and the FY soil (right). The open symbols represent the model output without formation of sulfide minerals and $Cu_2O$ while the grey symbols are for $Cu_2O$ formation and the black symbols for sulfide formation. The dotted line (ratio=1) indicates no deviation between model predictions and measurements (+1 cm refers to 1 cm above the interface, 0 cm equals the interface between the soil surface and the water layer, and -2 cm and -5 cm refer to 2 and 5 cm below the interface, respectively)

### *3.3.5.2 Model calculations including the formation of sulfides and cuprite*

At Eh values below -100 mV, the formation of sulfide minerals can take place and differences between model predictions excluding or including such minerals will probably occur. Indeed, for the model calculations without sulfide precipitates, the predicted total dissolved trace metal concentrations increasingly overestimate the measured values with a decreasing Eh for both soils (Fig. 4; open symbols). When we incorporate the formation of trace metal sulfides (Table 1) in our model calculations, the quality of the predictions greatly improves for the FY soil, except for the solubility of Cu, which is increasingly underestimated with a decrease in Eh (Fig. 4; black symbols). For the TZ soil, the quality of the predictions improved for Pb, Zn, and Ni when incorporating the formation of trace metal sulfides in the model calculations. For Ni, we predict no (FY soil) or little (TZ soil) formation of NiS (Fig. 2), which is consistent with its high solubility product relative to the sulfide minerals of the other four trace metals considered here (Table 1), and the resulting position of Ni on the “sulfide ladder” (Weber et al., 2009). The large amount of reactive Zn in the FY soil (Table 2) might have consumed all sulfide via the precipitation of zinc sulfide minerals. This agrees with our observation of the Ni solubility in the FY soil being equally well predicted for both aerobic and anaerobic conditions, even when we neglect sulfide formation in our model calculations. Copper behaves differently from the other four trace metals considered in our study, because it can exist in both the +2 and +1 oxidation states under anaerobic conditions and Cu in both oxidation states can form copper sulfides (Morse and Luther, 1999; Weber et al., 2009). In our model calculations, we used $Cu_2S$ (chalcocite) (Table 1), which has a 2:1 Cu:S stoichiometry, whereas CuS would have a 1:1 stoichiometry. Several studies found that copper sulfides in anaerobic soil or sediment systems varied in stoichiometry, represented as $Cu_xS$ with x varying between 1 and 2 and with CuS and $Cu_2S$ as end members (Morse and Luther, 1999; Weber et al., 2009). For example, Pattrick et al. (1997) found a range in x varying between 1.12 and 1.39 for Cu sulfides in synthetic solutions under anaerobic conditions. Because the stoichiometry of $Cu_xS$ determines how much sulfide is available for other trace metals to form sulfide minerals, we can estimate the $Cu_xS$ stoichiometry in the TZ soil from quantitative comparison of the reactive trace metal contents with the available $S\text{-}SO_4^{2-}$ content (Table 2). Now, the measurements for TZ soil show that for sulfate reducing conditions during flooding, the concentrations of Cd, Pb, and Zn were very low (Fig. 3), most likely because these trace metals nearly completely precipitated as sulfide minerals. Probably also some part of the reactive Ni in the TZ soil precipitated as NiS. To fully precipitate these trace metals as sulfide minerals, this would require 0.91 (no NiS) to 1.11 (all Ni as NiS) mmol S $kg^{-1}$ soil. If we subtract these S contents from the available $S\text{-}SO_4^{2-}$ content, it shows that copper sulfide has consumed between 3.59 and 3.78 mmol S $kg^{-1}$ soil, resulting in a $Cu_xS$ stoichiometry between 1.22 and 1.29. These stoichiometries fit very well within the range found by Pattrick et al. (1997) for copper sulfides. Unfortunately, an improved estimate for the $Cu_xS$ stoichiometry itself is not sufficient to improve model predictions of the Cu solubility, because the solubility of the $Cu_xS$ precipitate is still unknown. The uncertainty in $Cu_xS$ stoichiometry and in the solubility product of $Cu_xS$ may contribute substantially to the differences between our model predictions and measurements of the dissolved trace metal concentrations in the TZ soil and also in the FY soil. For the FY soil, the $Cu_xS$ stoichiometry cannot be derived this way, because (an unknown) part of Zn is probably precipitated as carbonates and therefore not as sulfides (Fig. 2).

For both soils, Cu can form cuprite ($Cu_2O$) (Table 1) between an Eh of -100 and 100 mV (Fig. 4; grey symbols). The incorporation of this mineral in our model calculations slightly improves the quality of our model predictions of the Cu solubility for both soils in this Eh range (Fig. 4). When precipitation of copper sulfides is predicted (i.e. Eh<-100 mV) formation of CuO is no longer predicted.

In general, our multi-surface modeling has clearly shown the importance of including trace metal sulfide minerals in model calculations when predicting the solubility of trace metals under anaerobic conditions. Although this does not provide conclusive evidence for the presence of trace metal sulfide minerals in our paddy soils during flooding (Shenker and Bloom, 2005), our results provide a strong indication of the formation of such minerals under anaerobic conditions. However, for a confirmation of the formation of metal sulfides in these soils, mineralogical techniques such as x-ray diffraction, electron induced x-ray emission spectroscopy, and/or x-ray absorption near edge structure spectroscopy would be required (Shenker and Bloom, 2005).

### *3.4. Conclusions*

During two successive flooding-draining cycles of two paddy soils contaminated with trace metals, the dynamics in Eh and pH and the changes in DOM concentrations greatly affected the solubility of trace metals for both soils. The solubility of trace metals was generally much lower in the alkaline FY soil than in the acidic TZ soil, due to the higher pH level and the presence of $CaCO_3$ in the FY soil. Under aerobic conditions, the higher pH of the alkaline FY soil leads to a stronger binding of trace metals by reactive surfaces within the soil solid phase than for the acidic TZ soil. Under anaerobic conditions, the solubility of most trace metals in both soils is predicted to be controlled by sulfide precipitates, but the higher pH of the FY soil leads to lower trace metal concentrations in soil solution at equilibrium. Comparison between measured and predicted total dissolved trace metal concentrations by multi-surface modeling based on generic adsorption models and stability constants for the major reactive soil surfaces clearly showed the importance of including sulfide minerals in the model calculations when predicting the solubility of trace metals under anaerobic conditions. However, the presence and chemical identity of copper sulfide minerals formed during flooding, as well as their solubility products, should be established so as to allow their incorporation in multi-surface models and enable better model predictions of trace metal solubility under anaerobic conditions.

## References

Allison, J.D., Brown, D.S., Novo-Gradac, K.J., 1991. MINTEQA2/PRODEFA2, A geochemical assessment model for environmental systems: version 3.0 user's manual. US EPA, Athens, GA. EPA/600/3–91/021.

Amery, F., Degryse, F., Degeling, W., Smolders, E., Merckx, R., 2007. The copper-mobilizing-potential of dissolved organic matter in soils varies 10-fold depending on soil incubation and extraction procedures. Environ Sci Technol 41, 2277–2281.

Bonten, L.T.C., Groenenberg, J.E., Weng, L., van Riemsdijk, W.H., 2008. Use of speciation and complexation models to estimate heavy metal sorption in soils. Geoderma 146, 303–310.

Brus, D.J., Li, Z.B., Song, J., Koopmans, G.F., Temminghoff, E.J.M., Yin, X.B., Yao, C.X., Zhang, H.B., Luo, Y.M., Japenga, J., 2009. Predictions of spatially averaged cadmium contents in rice grains in the Fuyang Valley, P.R. China. J Environ Qual 38, 1126–1136.

Cancès, B., Ponthieu, M., Castrec-Rouelle, M., Aubry, E., Benedetti, M.F., 2003. Metal ions speciation in a soil and its solution: experimental data and model results. Geoderma 113, 341–355.

Comans, R.N.J., Middelburg, J.J., 1987. Sorption of trace metals on calcite: Applicability of the surface precipitation model. Geochim Cosmochim Ac 51, 2587–2591.

Davis, J.A., Fuller, C.C., Cook, A.D., 1987. A model for trace metal sorption processes at the calcite surface: Adsorption of $Cd^{2+}$ and subsequent solid solution formation. Geochim Cosmochim Ac 51, 1477–1490.

de Livera, J., McLaughlin, M.J., Hettiarachchi, G.M., Kirby, J.K., Beak, D.G., 2011. Cadmium solubility in paddy soils: Effects of soil oxidation, metal sulfides and competitive ions. Sci Total Environ 409, 1489–1497.

Dick, W.A., Tabatabai, M.A., 1979. Ion chromatographic determination of sulfate and nitrate in soils. Soil Sci Soc Am J 43, 899–904.

Dijkstra, J.J., Meeussen, J.C.L., Comans, R.N.J., 2009. Evaluation of a generic multisurface sorption model for inorganic soil contaminants. Environ Sci Technol 43, 6196–6201.

Du Laing, G., Rinklebe, J., Vandecasteele, B., Meers, E., Tack, F.M.G., 2009. Trace metal behaviour in estuarine and riverine floodplain soils and sediments: A review. Sci Total Environ 407, 3972–3985.

Du Laing, G., Vanthuyne, D.R.J., Vandecasteele, B., Tack, F.M.G., Verloo, M.G., 2007. Influence of hydrological regime on pore water metal concentrations in a contaminated sediment-derived soil. Environ Pollut 147, 615–625.

Dzombak, D.A., Morel, F.M.M., 1990. Surface complexation modeling: Hydrous ferric oxide. Wiley, New York, pp. 393.

Fu, S., Wei, C.Y., 2013. Multivariate and spatial analysis of heavy metal sources and variations in a large old antimony mine, China. J Soil Sediment 13, 106–116.

Fulda, B., Voegelin, A., Kretzschmar, R., 2013. Redox-controlled changes in cadmium solubility and solid-phase speciation in a paddy soil as affected by reducible sulfate and copper. Environ Sci Technol 47, 12775–12783.

Groenenberg, J.E., Koopmans, G.F., Comans, R.N.J., 2010. Uncertainty analysis of the nonideal competitive adsorption-donnan model: Effects of dissolved organic matter variability on predicted metal speciation in soil solution. Environ Sci Technol 44, 1340–1346.

Grybos, M., Davranche, M., Gruau, G., Petitjean, P., 2007. Is trace metal release in wetland soils controlled by organic matter mobility or Fe-oxyhydroxides reduction? J Colloid Interf Sci 314, 490–501.

Heidmann, I., Christl, I., Kretzschmar, R., 2005. Sorption of Cu and Pb to kaolinite-fulvic acid colloids: Assessment of sorbent interactions. Geochim Cosmochim Ac 69, 1675–1686.

Hofacker, A.F., Voegelin, A., Kaegi, R., Weber, F.A., Kretzschmar, R., 2013. Temperature-dependent formation of metallic copper and metal sulfide nanoparticles during flooding of a contaminated soil. Geochim Cosmochim Ac 103, 316–332.

Houba, V.J.G., Temminghoff, E.J.M., Gaikhorst, G.A., van Vark, W., 2000. Soil analysis procedures using 0.01 M calcium chloride as extraction reagent. Commun Soil Sci Plant Anal 31, 1299–1396.

Houba, V.J.G., van der Lee, J.J.G., Novozamsky, I., 1997. Soil and plant analysis. Part 1: soil analysis procedures. Wageningen University, Wageningen, The Netherlands.

Karthikeyan, K.G., Elliott, H.A., Cannon, F.S., 1997. Adsorption and coprecipitation of copper with the hydrous oxides of iron and aluminum. Environ Sci Technol 31, 2721–2725.

Khaokaew, S., Chaney, R.L., Landrot, G., Ginder-Vogel, M., Sparks, D.L., 2011. Speciation and release kinetics of cadmium in an alkaline paddy soil under various flooding periods and draining conditions. Environ Sci Technol 45, 4249–4255.

Khaokaew, S., Landrot, G., Chaney, R.L., Pandya, K., Sparks, D.L., 2012. Speciation and release kinetics of zinc in contaminated paddy soils. Environ Sci Technol 46, 3957–3963.

Kinniburgh, D.G., van Riemsdijk, W.H., Koopal, L.K., Borkovec, M., Benedetti, M.F., Avena, M.J., 1999. Ion binding to natural organic matter: competition, heterogeneity, stoichiometry and thermodynamic consistency. Colloid Surface A 151, 147–166.

Kögel-Knabner, I., Amelung, W., Cao, Z.H., Fiedler, S., Frenzel, P., Jahn, R., Kalbitz, K., Kolbl, A., Schloter, M., 2010. Biogeochemistry of paddy soils. Geoderma 157, 1–14.

Koopal, L.K., Saito, T., Pinheiro, J.P., van Riemsdijk, W.H., 2005. Ion binding to natural organic matter: General considerations and the NICA-Donnan model. Colloid Surface A 265, 40–54.

Koopmans, G.F., Groenenberg, J.E., 2011. Effects of soil oven-drying on concentrations and speciation of trace metals and dissolved organic matter in soil solution extracts of sandy soils. Geoderma 161, 147–158.

Laborte, A.G., de Bie, K., Smaling, E.M.A., Moya, P.F., Boling, A.A., van Ittersum, M.K., 2012. Rice yields and yield gaps in Southeast Asia: Past trends and future outlook. Eur J Agron 36, 9–20.

Lefroy, R.D.B., Mamaril, C.P., Blair, G.J., Gonzales, P. J., 1992. Sulphur cycling in rice wetlands. In sulphur cycling on the continents: wetlands, terrestrial ecosystems and associated water bodies. John Wiley & Sons Ltd:Chicherster, pp. 279−300.

Lofts, S., Tipping, E., 1998. An assemblage model for cation binding by natural particulate matter. Geochim Cosmochim Ac 62, 2609–2625.

Maurer, F., Christl, I., Fulda, B., Voegelin, A., Kretzschmar, R., 2013. Copper redox transformation and complexation by reduced and oxidized soil humic acid. 2. Potentiometric titrations and dialysis cell experiments. Environ Sci Technol 47, 10912–10921.

McBride, M.B., Barrett, K.A., Kim, B., Hale, B., 2006. Cadmium sorption in soils 25 years after amendment with sewage sludge. Soil Sci 171, 21–28.

Meers, E., Du Laing, G., Unamuno, V., Ruttens, A., Vangronsveld, J., Tack, F.M.G., Verloo, M.G., 2007. Comparison of cadmium extractability from soils by commonly used single extraction protocols. Geoderma 141, 247–259.

Meeussen, J.C.L., 2003. ORCHESTRA: An object-oriented framework for implementing chemical equilibrium models. Environ Sci Technol 37, 1175–1182.

Meharg, A.A., Norton, G., Deacon, C., Williams, P., Adomako, E.E., Price, A., Zhu, Y.G., Li, G., Zhao, F.J., McGrath, S., Villada, A., Sommella, A., De Silva, P.M.C.S., Brammer, H., Dasgupta, T., Islam, M.R., 2013. Variation in rice cadmium related to human exposure. Environ Sci Technol 47, 5613–5618.

Meima, J.A., Comans, R.N.J., 1998. Application of surface complexation precipitation modeling to contaminant leaching from weathered municipal solid waste incinerator bottom ash. Environ Sci Technol 32, 688–693.

Milne, C.J., Kinniburgh, D.G., van Riemsdijk, W.H., Tipping, E., 2003. Generic NICA-Donnan model parameters for metal-ion binding by humic substances. Environ Sci Technol 37, 958–971.

Morse, J.W., Luther, G.W., 1999. Chemical influences on trace metal-sulfide interactions in anoxic sediments. Geochim Cosmochim Ac 63, 3373–3378.

Murase, J., Kimura, M., 1997. Anaerobic reoxidation of $Mn^{2+}$, $Fe^{2+}$, $S^0$ and $S^{2-}$ in submerged paddy soils. Biol Fert Soils 25, 302–306.

Novozamsky, I., van Eck, R., Houba, V.J.G., van der Lee, J.J., 1986. Use of ICP-AES for determination of iron, aluminium and phosphorus in Tamm’s soil extracts. Neth J Agric Sci 34, 185–191.

Pan, Y.Y., Koopmans, G.F., Bonten, L.T.C., Song, J., Luo, Y.M., Temminghoff, E.J.M., Comans, R.N.J., 2014. Influence of pH on the redox chemistry of metal (hydr)oxides and organic matter in paddy soils. J Soil Sediment 14, 1713–1726.

Pan, Y.Y., Koopmans, G.F., Bonten, L.T.C., Song, J., Luo, Y.M., Temminghoff, E.J.M., Comans, R.N.J., 2015. In-situ measurement of free trace metal concentrations in a flooded paddy soil using the Donnan Membrane Technique. Geoderma 241–242, 59–67.

Pattrick, R.A.D., Mosselmans, J.F.W., Charnock, J.M., England, K.E.R., Helz, G.R., Garner, C.D., Vaughan, D.J., 1997. The structure of amorphous copper sulfide precipitates: An X-ray absorption study. Geochim Cosmochim Ac 61, 2023–2036.

Qian, J., Skyllberg, U., Frech, W., Bleam, W.F., Bloom, P.R., Petit, P.E., 2002. Bonding of methyl mercury to reduced sulfur groups in soil and stream organic matter as determined by X-ray absorption spectroscopy and binding affinity studies. Geochim Cosmochim Ac 66, 3873–3885.

Rieuwerts, J.S., 2007. The mobility and bioavailability of trace metals in tropical soils: A review. Chem Spec Bioavailab 19, 75–85.

Römkens, P.F.A.M., Guo, H.Y., Chu, C.L., Liu, T.S., Chiang, C.F., Koopmans, G.F., 2009a. Characterization of soil heavy metal pools in paddy fields in Taiwan:

Chemical extraction and solid-solution partitioning. J Soil Sediment 9, 216–228.

Römkens, P.F.A.M., Guo, H.Y., Chu, C.L., Liu, T.S., Chiang, C.F., Koopmans, G.F., 2009b. Prediction of cadmium uptake by brown rice and derivation of soil-plant transfer models to improve soil protection guidelines. Environ Pollut 157, 2435–2444.

Sauve, S., Hendershot, W., Allen, H.E., 2000. Solid-solution partitioning of metals in contaminated soils: Dependence on pH, total metal burden, and organic matter. Environ Sci Technol 34, 1125–1131.

Schulz-Zunkel, C., Krueger, F., 2009. Trace metal dynamics in floodplain soils of the River Elbe: A review. J Environ Qual 38, 1349–1362.

Shaheen, S.M., Rinklebe, J., Rupp, H., Meissner, R., 2014. Lysimeter trials to assess the impact of different flood-dry-cycles on the dynamics of pore water concentrations of As, Cr, Mo and V in a contaminated floodplain soil. Geoderma 228–229, 5–13.

Shenker, M., Bloom, P.R., 2005. Comments on "Amounts, forms, and solubility of phosphorus in soils receiving manure". Soil Sci Soc Am J 69, 1353–1354.

Simmons, R.W., Noble, A.D., Pongsakul, P., Sukreeyapongse, O., Chinabut, N., 2008. Analysis of field-moist Cd contaminated paddy soils during rice grain fill allows reliable prediction of grain Cd levels. Plant Soil 302, 125–137.

Simmons, R.W., Pongsakul, P., Saiyasitpanich, D., Klinphoklap, S., 2005. Elevated levels of cadmium and zinc in paddy soils and elevated levels of cadmium in rice grain downstream of a zinc mineralized area in Thailand: Implications for public health. Environ Geochem Hlth 27, 501–511.

Sun, M.M., Luo, Y.M., Teng, Y., Jia, Z.J., Li, Z.G., Deng, S.P., 2013. Remediation of polycyclic aromatic hydrocarbon and metal-contaminated soil by successive methyl-beta-cyclodextrin-enhanced soil washing-microbial augmentation: A laboratory evaluation. Environ Sci Pollut R 20, 976–986.

Tack, F.M.G., van Ranst, E., Lievens, C., Vandenberghe, R.E., 2006. Soil solution Cd, Cu and Zn concentrations as affected by short-time drying or wetting: The role of hydrous oxides of Fe and Mn. Geoderma 137, 83–89.

Tye, A.M., Young, S., Crout, N.M.J., Zhang, H., Preston, S., Zhao, F.J., McGrath, S.P., 2004. Speciation and solubility of Cu, Ni and Pb in contaminated soils. Eur J Soil Sci 55, 579–590.

US-EPA., 1999. MINTEQA2/PRODEFA2, A Geochemical assessment model for environmental systems: user manual supplement for version 4.0. National Exposure Research Laboratory, Ecosystems Research Division: Athens, GA.

Wang, G.Q., Koopmans, G.F., Song, J., Temminghoff, E.J.M., Luo, Y.M., Zhao, Q.G., Japenga, J., 2007. Mobilization of heavy metals from contaminated paddy soil by EDDS, EDTA, and elemental sulfur. Environ Geochem Hlth 29, 221–235.

Weber, F.A., Voegelin, A., Kretzschmar, R., 2009. Multi-metal contaminant dynamics in temporarily flooded soil under sulfate limitation. Geochim Cosmochim Ac 73, 5513–5527.

Weng, L.P., Temminghoff, E.J.M., van Riemsdijk, W.H., 2001. Contribution of individual sorhents to the control of heavy metal activity in sandy soil. Environ Sci Technol 35, 4436–4443.

Yu, H., Wang, J.L., Fang, W., Yuan, J.G., Yang, Z.Y., 2006. Cadmium accumulation in different rice cultivars and screening for pollution-safe cultivars of rice. Sci Total Environ 370, 302–309.

Yu, K.W., Bohme, F., Rinklebe, J., Neue, H.U., DeLaune, R.D., 2007. Major biogeochemical processes in soils – A microcosm incubation from reducing to oxidizing conditions. Soil Sci Soc Am J 71, 1406–1417.

Zeng, F.R., Ali, S., Zhang, H.T., Ouyang, Y.B., Qiu, B.Y., Wu, F.B., Zhang, G.P., 2011. The influence of pH and organic matter content in paddy soil on heavy metal availability and their uptake by rice plants. Environ Pollut 159, 84–91.

Zhu, C., 2002. Estimation of surface precipitation constants for sorption of divalent metals onto hydrous ferric oxide and calcite. Chem Geol 188, 23–32.

# Chapter 4

# In-situ measurement of free trace metal concentrations in a flooded paddy soil using the Donnan Membrane Technique

*Yunyu Pan, Gerwin F. Koopmans, Luc T.C. Bonten, Jing Song, Yongming Luo, Erwin J.M. Temminghoff, Rob N.J. Comans*

Published in Geoderma, **2015**

## Abstract

The field Donnan Membrane Technique (DMT) has been used successfully to measure in-situ free trace metal concentrations in surface waters. However, it has not been applied previously in submerged soil systems including flooded paddy rice fields. We tested this technique in a column experiment with a flooded paddy soil contaminated with trace metals and compared the DMT measurements with predictions from a geochemical speciation model. Flooding led to a strong gradient in the redox potential (Eh) along the soil column, and the pH and concentrations of Mn, Fe, and dissolved organic carbon increased with decreasing Eh. Total dissolved trace metal concentrations decreased from the overlying water layer to the soil layers, which might be ascribed to the elevated pH outweighing the effect of the increased DOC concentrations under anaerobic conditions. Also, free trace metal concentrations were lower in the soil solution of the upper and bottom soil layers than in the overlying water layer, largely due to the increased pH under anaerobic conditions. The DMT measurements and model predictions were similar in the aerobic water layer, except for Pb. In both anaerobic soil layers, however, Cu and Pb were poorly predicted. The applied geochemical modeling approach, which is frequently being used and performs well under aerobic conditions, does not fully capture all the chemical processes occurring under anaerobic conditions. Overall, the field DMT proved to be a useful tool for the in-situ measurement of free trace metal concentrations in flooded paddy soils.

*Keywords:* Donnan Membrane Technique, free trace metal concentration, redox potential, soil solution, paddy soil, speciation model

## *4.1. Introduction*

Rice is the most important staple food for human beings in Southeast Asia (Meharg et al. 2013) and around 90% of the annual rice production is cropped and consumed in this area (Laborte et al., 2012). In industrialized areas throughout Southeast Asia, paddy fields for rice production are often close to industrialized sites and trace metal contamination of paddy soils has become an increasing concern (Römkens et al., 2009a). Contamination of paddy soils with trace metals can lead to an increase in the uptake of trace metals by rice plants and an accumulation of trace metals in rice grains (Simmons et al., 2005; Römkens et al., 2009b). Dietary intake of Cd through rice consumption is one of the most important exposure pathways for human beings, especially for people in Asia (McLaughlin et al., 1999; Tsukahara et al., 2003).

Apart from differences in trace metal uptake characteristics among various rice cultivars and genotypes (Römkens et al., 2009b), trace metal uptake by rice largely depends on the bioavailability of trace metals in paddy soils. Speciation of trace metals in soils is of great importance for their bioavailability for uptake by plants. In soil solution, trace metals can be present as free metal ions or can be complexed by inorganic ligands or dissolved organic matter (DOM) (Weng et al., 2002; Koopmans et al., 2008; Koopmans and Groenenberg, 2011). The free trace metal ions in soil solution are usually considered to be the most bioavailable species for plant uptake (Bell et al., 1991; Smolders and McLaughlin, 1996; Parker and Pedler, 1997; Parker et al., 2001). To measure free trace metal concentrations in solution systems, several analytical techniques can be used including Ion-Selective Electrodes (Otto and Thomas, 1985), Cathodic Stripping Voltammetry (Xue and Sunda, 1997), Gellyfish (Senn et al., 2004), Absence of Gradients and Nernstian Equilibrium Stripping (Chito et al., 2012), Permeation Liquid Membranes (Parthasarathy et al., 1997), and the Donnan Membrane Technique (DMT; Temminghoff et al., 2000). These techniques all have their advantages and disadvantages (Batley et al., 2004; Sigg et al., 2006). In this study, we focus on the use of the DMT, because this technique does not perturb the equilibrium between free trace metal ions and other forms of trace metals in solution and it allows for measuring the free ion concentrations of multiple elements at the same time (Temminghoff et al., 2000).

For the so-called lab DMT developed by Temminghoff et al. (2000), the DMT cell consists of two chambers, i.e., the donor and the acceptor chamber. The donor solution, which is the solution of interest containing the free and complexed trace metals, is separated from the acceptor solution by a negatively charged semi-permeable cation exchange membrane. A peristaltic pump is used to continuously pump the donor and acceptor solutions across both chambers. Positively charged cations can pass the membrane while the transport of negatively charged ions and neutral complexes is restricted. When equilibrium is reached, the concentrations of free cations in the acceptor solution are either equal to the free cation concentrations in the donor solution or they can be calculated using a simple correction factor when a difference in ionic strength is present between the donor and acceptor solutions (Temminghoff et al., 2000). This lab DMT has been successfully used to measure the free metal concentrations in synthetic multicomponent systems (Osté et al., 2002) and in soil solution extracts (Weng et al., 2001; Koopmans et al., 2008; Koopmans and Groenenberg, 2011).

The use of the lab DMT to measure free metal concentrations in the soil solution of flooded paddy soils is difficult. For lowland rice production in paddy soils, flooding conditions prevail during almost the entire rice cropping period because lowland rice is extremely sensitive to water shortage (Kögel-Knabner et al., 2010). During the flooding of paddy soils, the redox potential (Eh) decreases and subsequently various reduction processes take place. For example, short-range ordered Mn- and Fe-(hydr)oxides will be reductively dissolved causing elevated $Mn^{2+}$ and $Fe^{2+}$ concentrations in soil solution (Tack et al., 2006; Grybos et al., 2007; Pan et al., 2014), while organic matter will be released leading to elevated DOM concentrations in soil solution (Kaiser et al., 1997; Vink et al., 2010; Pan et al., 2014). Therefore, a decrease in the reactive surface of these soil constituents might lead to an increase of the trace metal concentrations in soil solution (Ponnamperuma, 1972; Tack et al., 2006; Grybos et al., 2007). The presence of sulphide as a result of sulphate reduction, however, might lead to the formation of poorly soluble precipitates with trace metals exhibiting a low solubility (de Livera et al., 2011; Khaokaew et al., 2011; Fulda et al., 2013a). In addition, the pH of acid soils can increase after flooding, because reduction processes consume protons (Ponnamperuma, 1972; Kögel-Knabner et al., 2010), thereby increasing trace metal adsorption to reactive surfaces of soil organic matter (SOM) and short-range ordered metal-(hydr)oxides. Hence, changes in the Eh as induced by flooding of paddy soils can have a large influence on the free trace metal concentrations in soil solution. In such a complex and dynamic system, it is difficult to use the lab DMT to measure free trace metal concentrations, because it is a complicated task to sample flooded paddy soils without perturbing the Eh and maintaining anaerobic conditions during the DMT experiment in the laboratory. Therefore, it would be preferable to measure free trace metal concentrations in-situ without significantly disturbing the system. The so-called field DMT, which is a modified version of the lab DMT, has been developed for in-situ measurements. In this field DMT cell, only one chamber containing the acceptor solution with two cation exchange membranes on both sides is used, without any pumping (van der Stelt et al., 2005). The use of an additional membrane in the field DMT cell is expected to facilitate a faster cation exchange between the donor and the acceptor solutions (Kalis et al., 2006). The field DMT has been successfully used in-situ to measure free nutrient concentrations in slurries of animal manure (van der Stelt et al., 2005), free metal concentrations in simulated milk ultrafiltrate and reconstituted skim milk (Gao et al., 2009), and free trace metal concentrations in surface waters (Kalis et al., 2006; Sigg et al., 2006; Unsworth et al., 2006; Chito et al., 2012; Vega and Weng, 2013). Before the field DMT can be used in paddy fields, this analytical technique first needs to be tested since it has not been used previously to measure free trace metal concentrations in-situ in flooded soils.

The first objective of our study was to test the potential of the field DMT to measure the free trace metal concentrations in-situ in soil solution of a flooded paddy soil under anaerobic conditions. In our experimental approach, we carefully designed a soil column experiment with a field-contaminated paddy soil.

Speciation modeling can be a useful tool to investigate the underlying mechanisms of trace metal speciation in soil solution. Trace metal binding with inorganic ligands can be predicted based on known stability constants of metal complexes with such ligands and advanced models such as the Model VI (Tipping, 1998) and the Non-Ideal Competitive Adsorption Donnan (NICA-Donnan) model (Kinniburgh et al., 1999) can be used to predict complexation of trace metals with DOM (Weng et al., 2002; Koopmans et al., 2008; Koopmans and Groenenberg, 2011). Performing speciation calculations of trace metals for aqueous environmental systems is a complex task, due to the heterogeneity in the composition of DOM and the uncertainty and lack of model parameters (Groenenberg et al., 2010; Vega and Weng, 2013). Consequently, it is important to validate these models with regard to their ability to predict trace metal speciation under a wide variety of geochemical conditions, which can be done by comparing model results with independent DMT measurements of the free trace metal concentrations. Therefore, our second objective was to compare the field DMT measurements of free trace metal concentrations in both the aerobic and anaerobic layers of the soil column experiment with predictions of the free trace metal concentrations obtained by speciation modeling, using the Objects Representing CHEmical Speciation and TRAnsport (ORCHESTRA) framework (Meeussen, 2003), which includes the NICA-Donnan model.

## *4.2. Materials and methods*

### *4.2.1. Soil sampling and physical-chemical soil properties*

Soil with a clay loam texture was sampled from the 0-20 cm layer of a paddy field nearby a former transformer and electronic waste stripping and recycling factory in the vicinity of Taizhou city in Zhejiang Province in the southeast of China. This soil was air-dried, sieved through a 2 mm nylon sieve to remove stones and plant residues, and stored at room temperature of around 20°C until further use for physical-chemical analyses and the column experiment in which the field DMT was tested. The pH was measured in a settling 1:10 (w:v) suspension of soil in 0.01 M $CaCl_2$, SOM by loss-on-ignition (550°C), and clay by the sieve and pipette method (Houba et al., 1997; Houba et al., 2000). Short-range ordered (hydr)oxides of Al, Fe, and Mn were determined by using the acid ammonium oxalate extraction method (Novozamsky et al., 1986). Concentrations of Al, Fe, and Mn in the extracts (i.e., Al-ox, Fe-ox, and Mn-ox) were measured by inductively coupled plasma-atomic emission spectrometry (ICP-AES; IRIS Intrepid II). Total soil contents of trace metals were determined by digestion with Aqua Regia (Houba et al., 1997). Concentrations of Cd, Cu, Ni, Pb, and Zn in the digests were measured by ICP-AES. All these soil properties were determined in triplicate and average ± standard deviation is presented in Table 1.

### *4.2.2. Field DMT*

The field DMT was used to measure the free trace metal concentrations in-situ in the overlying water layer and soil solution of the flooded paddy soil in a soil column experiment. The design of the field DMT cell used in this study was slightly modified from the field DMT cell as used by van der Stelt et al. (2005) and Kalis et al. (2006). In our modified version of the field DMT cell (Fig. 1), we added a polytetrafluoroethylene (PTFE) ring to the outer shell of the Perspex ring on both sides of the cell so as to enable us to mount a nylon membrane with a pore size of 20 µm to both sides of the cell. This modification was done to prevent soil particles from blocking and damaging the cation exchange membrane, possibly affecting the transport of free trace metal ions over the membrane. Before assembling the field DMT cells, all cell parts were cleaned with 0.1 M $HNO_3$ and ultrapure water (UPW). The method of Kalis et al. (2006) was used to clean and saturate the cation exchange membranes (551652U, VWR International Ltd., Lutterworth, UK) with Ca and to adjust the pH of the membranes. The pH of the membranes was adjusted to the initial pH of the water layer and soil solution samples taken from the three different depths of the soil column where the DMT cells were installed before the start of the soil column experiment (see Section 4.2.3). PTFE tubes with Luer lock fittings were connected to the inlet and outlet of the field DMT cells (Fig. 1). Tubes with a length of either 3, 10, or 20 cm were used, because the field DMT cells were installed at three different depths along the soil column (see Section 4.2.3). The tubes were cleaned with 0.01 M $HNO_3$, UPW, and acceptor solution. The volume of the acceptor chamber is 12 mL. A background electrolyte of 2 mM $Ca(NO_3)_2$ was used in the acceptor solution. To accumulate trace metals to a concentration above the detection limit of our inductively coupled plasma-mass spectrometer (ICP-MS), we added 30 mg $L^{-1}$ of a well-characterized purified peat humic acid (PPHA) (Temminghoff et al., 1997) to the acceptor solution (Kalis et al., 2006; Koopmans et al., 2008). This PPHA was purified from forest floor material taken from the Tongbersven forest near Oisterwijk in The Netherlands using a recommended extraction procedure from the International Humic Substances Society (Temminghoff et al., 1997).

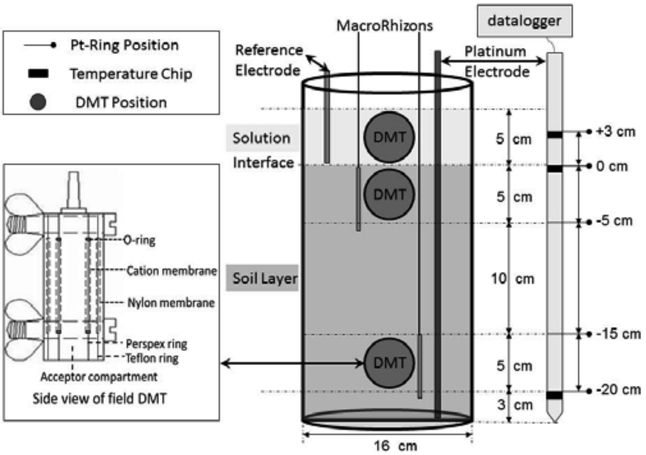

**Fig. 1.** Set-up of the soil column. The drawing of the field DMT cell was modified from van der Stelt et al. (2005). In our modified version of the field DMT cell, a PTFE ring was added to the outer shell of the Perspex ring on both sides of the cell so as to enable us to mount a nylon membrane with a pore size of 20 µm to both sides of the cell.

### *4.2.3. Set-up of the soil column experiment*

Six PVC columns with a diameter of 16 cm and a height of 35 cm were used in the soil column experiment (Fig. 1). Next, 3 kg air-dried soil and 2.25 L of 2 mM $Ca(NO_3)_2$ solution were mixed thoroughly in each column. With this soil:solution ratio, a water layer with a thickness of about 5 cm formed on top of the soil surface after the soil particles had settled down within one day. After assembling of the field DMT cells, one cell was installed in the water layer, one cell in the upper soil layer (0 cm to -5 cm), and one cell in the bottom soil layer (-15 cm to -20 cm) of each soil column (Fig. 1). The field DMT cells were empty when they were installed in the soil columns. The flooded columns were incubated for one week before we injected the acceptor solution (see Section 4.2.2) into the field DMT cells. During the entire soil column experiment, we monitored the Eh and the chemical composition of the overlying water layer and the soil solution from both soil layers. For Eh monitoring, a combined Eh-temperature glass fiber probe (Paleoterra Products, Amsterdam, The Netherlands) was inserted vertically in each of the six columns. The probes were tailor-made with five platinum Eh measurement points enabling us to monitor the Eh at 3 cm above the soil-water interface (+3 cm), at the interface (0 cm), and at 5 (-5 cm), 15 (-15 cm), and 20 cm (-20 cm) below the interface. The Eh values at +3 cm were used to characterize the Eh for the field DMT cell installed in the overlying water layer. Since the depths of 0 and -5 cm corresponded with the depth of the field DMT cell in the upper soil layer, the Eh values at 0 cm and -5 cm were averaged for this cell. The Eh values at -15 and -20 cm were averaged, because these depths corresponded with the depth of the field DMT cell in the bottom soil layer. The Ag-AgCl reference electrodes were positioned in the water layer. The Eh signal was automatically logged every 30 min. The Eh relative to the standard hydrogen electrode was calculated from the measured potential with a temperature-dependent correction for the potential of the Ag-AgCl reference electrode. The temperature was measured using the combined Eh-temperature probe by platinum electrodes at three positions within the soil columns: +3 cm, 0 cm, and -20 cm. The temperature within the soil columns over the entire course of the field DMT experiment was 25±1 °C. For collecting soil solution samples from the soil columns, two MacroRhizons (Rhizonsphere Research Products, Wageningen, The Netherlands) with a porous part of 9 cm, an outer diameter of 4.5 mm, and a mean pore size of 0.15 µm were installed between 0 and -5 cm and between -15 and -20 cm in each soil column. During the field DMT experiment, samples of the water layer and the soil solution, which represent the so-called donor solution, and the acceptor solution of the field DMT cell were taken after 2, 4, and 6 days for all three depths. At each sampling time, two soil columns were sampled. Soil solution from the MacroRhizons and acceptor solution from the field DMT cell were sampled with a vacuumed syringe. The water layer was sampled with a syringe and passed through a 0.2 µm filter (Minisart SRP15, Sartorius). The samples of the donor and acceptor solutions were split in two subsamples: one subsample was used to measure the concentrations of major cations and trace metals after acidification by adding concentrated $HNO_3$ to a final $HNO_3$ concentration of 0.14 M, whereas the other subsample was used to measure the pH. In addition to this, the dissolved organic carbon (DOC) concentration was measured in the donor solution samples. All samples were stored in polypropylene tubes at 4°C until further chemical analysis as given below.

### *4.2.4. Chemical analyses of the donor and acceptor solutions*

The pH of the donor and acceptor solution samples was measured directly after sampling with a combined glass electrode. The DOC concentrations in the donor solution samples were measured by a TOC analyzer (Multi C/N 3000). In the acidified subsamples taken from the donor and acceptor solution samples, K, Ca, Na, Mg, Fe, Mn, Al, and S were measured by ICP-AES and Cd, Cu, Ni, Pb, and Zn were measured by ICP-MS (Thermo Electron X7).

### *4.2.5. Modeling of trace metal speciation in donor and acceptor solutions using the ORCHESTRA framework*

The free trace metal concentrations in the donor (i.e., water and soil solution samples) and acceptor solutions were calculated from the measured total trace metal concentrations with the ORCHESTRA framework (version: 15 December 2013) (Meeussen, 2003), which includes the NICA-Donnan model (Kinniburgh et al., 1999). In this modeling approach, complexation of ions in solution by inorganic ligands and DOM is calculated and competition between protons and metals for binding with DOM is taken into account. For the acceptor solution, measured values of the total Al, Ca, Cd, Cu, Fe, K, Ni, Mg, Mn, Na, Pb, S, and Zn concentrations and pH were used as input. In our speciation model calculations, the inorganic ligands including carbonate and bicarbonate, hydroxide, and sulphate were taken into account. The concentrations of the inorganic carbon species were calculated from the chemical equilibrium with $pCO_2$ and the pH while the hydroxide concentrations were calculated from the pH. The measured total S concentrations were taken to represent the sulphate concentrations. The DOM concentration of the PPHA added to the acceptor solution was fixed at 30 mg $L^{-1}$. Specific NICA-Donnan parameters for binding of H, Cu(II), Ca, Cd, Ni, and Zn with PPHA were used in the model calculations (Kalis et al., 2006). However, no PPHA-specific NICA-Donnan parameters have been derived for Fe(III), Fe(II), Mn, Al, Mg, and Pb, and, therefore, generic parameters were used (Milne et al., 2003). For Cu(I), we neglected complexation with PPHA, which may be justified as it is a monovalent cation which generally shows very little complexation with organic matter. Also, Cu(I) complexation with DOM has been demonstrated to be much weaker than Cu(II) complexation (Maurer et al., 2013). In our model calculations for the acceptor solution, we included the redox couples Cu(II)/Cu(I) and Fe(III)/Fe(II). The distribution of Cu and Fe between their two redox forms was calculated based on measured Eh values. Since the Eh was only measured in the soil column, the Eh of the acceptor solution in the field DMT cell was assumed to be the same as for the water layer and the soil solution from the upper and bottom soil layers. Finally, the free metal concentrations were corrected for differences in ionic strength between the donor and acceptor solutions. For this correction, the concentrations of potassium were used because potassium exists almost entirely in the free form (Temminghoff et al., 2000):

$$\frac{(Me^{z+}{}_{don})}{(Me^{z+}{}_{acc})} = \left(\frac{(K^{+}{}_{don})}{(K^{+}{}_{acc})}\right)^{z} \qquad (1)$$

where ($Me^{z+}$) represents the free metal concentration of the metal ion of interest and ($K^{+}$) is the free concentration of potassium. The subscripts don and acc refer to the donor and acceptor solution, respectively. The superscript z represents the charge of the metal ion. For the donor solution, measured values of the total Al, Ca, Cd, Cu, Fe, K, Ni, Mg, Mn, Na, Pb, S, and Zn concentrations and pH were used as input. The same inorganic ligands as those for the acceptor solution were used in our model calculations for the donor solution. The DOM concentrations were calculated from the measured DOC concentrations assuming a carbon content of 50% (Weng et al., 2002). In our model calculations, 40% of DOM was assumed to consist of generic fulvic acid (FA) whereas 60% was taken to be inert with respect to proton and metal binding (Groenenberg et al., 2010). Generic NICA-Donnan parameters for metal binding with DOM were taken from Milne et al. (2003). Complexation of Cu(I) with DOM was neglected for the donor solution, as discussed above. Measured values of the Eh were included in the model calculations for the donor solution. Similar to the acceptor solution, the redox couples Cu(II)/Cu(I) and Fe(III)/Fe(II) were included in our model calculations for the donor solution. For both the donor and acceptor solutions, $pCO_2$ was defined as 10 times ambient $pCO_2$ (316 Pa) (Lindsay, 1979; Du Laing et al., 2007).

## *4.3. Results and discussion*

### *4.3.1. Soil properties*

Selected physical-chemical properties of the paddy soil used in this study are summarized in Table 1. This soil was most notably contaminated with Cd and Cu, because the total soil contents of these trace metals exceeded the Chinese environmental quality standard for soils (GB 15618-1995; Grade II for soil pH < 6.5) about 23 times for Cd and 9 times for Cu (Table 1). These elevated total soil contents of Cd and Cu were caused by irrigation with wastewater from a former transformer and electronic waste stripping and recycling factory.

**Table 1**

Selected physical and chemical properties of the paddy soil used in the soil column experiment. All soil properties were determined in triplicate and the average ± standard deviation is presented.

| Soil property | Unit | Value | Standard[f] |
|---|---|---|---|
| Clay (< 2 μm)[a] | % | 33.0±0.3 | - |
| SOM[b] | % | 7.2±0.1 | - |
| pH ($CaCl_2$)[c] | | 5.1±0.1 | - |
| Al-ox[d] | mmol $kg^{-1}$ | 38.0±0.3 | - |
| Fe-ox[d] | mmol $kg^{-1}$ | 95±4 | - |
| Mn-ox[d] | mmol $kg^{-1}$ | 1.2±0.1 | - |
| Total Ni[e] | mg $kg^{-1}$ | 45.0±0.1 | 40 |
| Total Zn[e] | mg $kg^{-1}$ | 151±1 | 200 |
| Total Cd[e] | mg $kg^{-1}$ | 7.0±0.0 | 0.3 |
| Total Cu[e] | mg $kg^{-1}$ | 469±1 | 50 |
| Total Pb[e] | mg $kg^{-1}$ | 46.0±0.1 | 250 |

[a] Clay by the sieve and pipette method (Houba et al., 1997);

[b] Soil organic matter (SOM) by loss on ignition (550 °C) (Houba et al., 1997);

[c] 1:10 (w:v) 0.01 M $CaCl_2$ extraction (Houba et al., 2000);

[d] Extraction with acid ammonium oxalate (Novozamsky et al., 1986);

[e] Aqua regia (Houba et al., 1997);

[f] Grade II (pH<6.5) of the Chinese environmental quality standard for soils (GB 15618-1995).

### *4.3.2. Monitoring results of the column experiment*

### *4.3.2.1. Eh, pH, Mn, Fe, and DOC*

The Eh, pH, and the concentrations of Mn, Fe, and DOC in the overlying water layer and the soil solution of the upper and bottom soil layers are presented in Fig. 2. After one week of flooding, the Eh showed a strong vertical gradient: aerobic conditions were maintained in the water layer with an Eh of around 400 mV, whereas slightly anaerobic conditions (Eh around 160 mV) to more strongly anaerobic conditions (Eh around 70

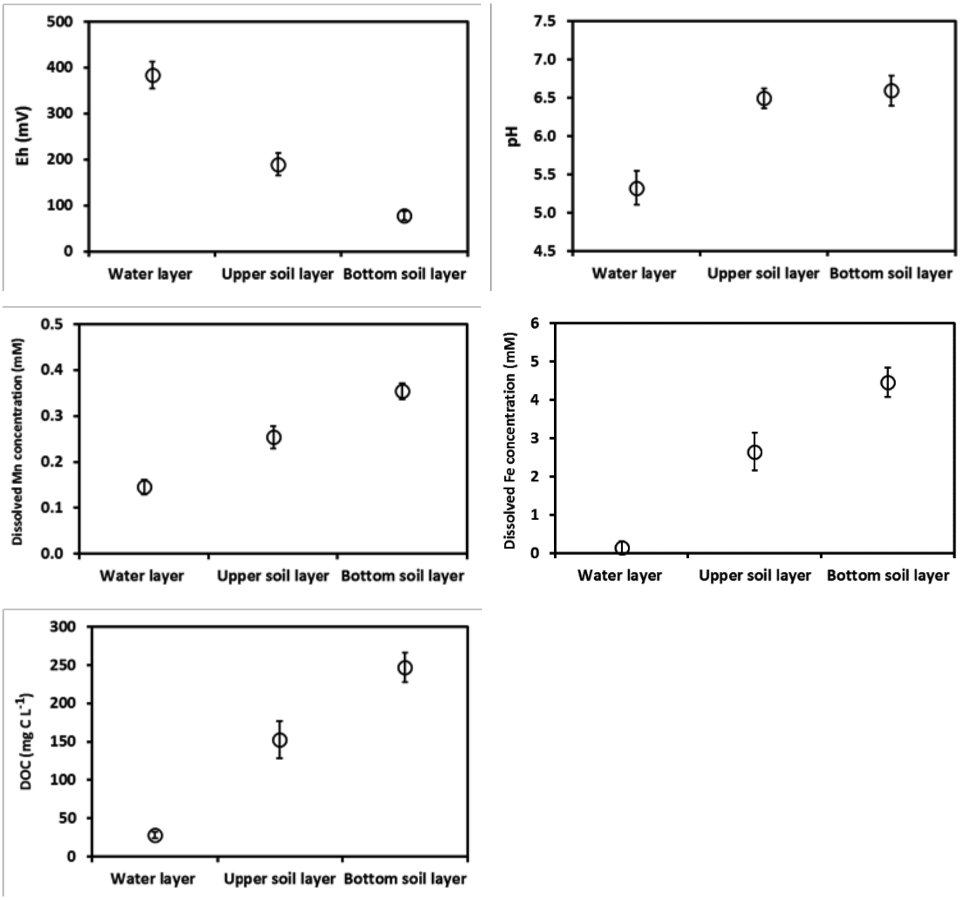

**Fig. 2.** The Eh, pH, and concentrations of Mn, Fe, and DOC in the water layer and the soil solution of the upper and bottom soil layers of the columns during the field DMT experiment. The presented average ± standard deviation was calculated over the sampling times at day 2, 4, and 6 of the field DMT experiment.

mV) were present in the upper and bottom soil layers, respectively. Under such anaerobic conditions, redox reactions including denitrification (Yu et al., 2007; Kögel-Knabner et al., 2010; Pan et al., 2014) and reductive dissolution of Mn- and Fe-(hydr)oxides can occur, with the latter reactions leading to elevated concentrations of $Mn^{2+}$ and $Fe^{2+}$ in soil solution (Tack et al., 2006; Grybos et al., 2007; Pan et al., 2014). In our soil column experiment, no sulphate reduction is expected, because this occurs only at Eh values of -200 mV and lower (Mansfeldt, 2004; Du Laing et al., 2009; Schulz-Zunkel and Krueger, 2009). Indeed, the total dissolved concentrations of Mn and Fe in the soil solution in the upper and bottom soil layers of the columns were clearly elevated as compared to those in the water layer (Fig. 2). Since redox reactions including denitrification and reductive dissolution of Mn- and Fe-(hydr)oxides lead to the consumption of protons, the pH increased to an almost neutral level in the upper and bottom soil layers, whereas the pH in the water layer remained acidic (Fig. 2). The DOC concentration clearly increased with depth (Fig. 2), which can be attributed to reductive dissolution of Fe-(hydr)oxides and the elevated pH, both leading to the release of adsorbed DOM (Kaiser et al., 1997; Pan et al., 2014). In addition to these explanations, the release of fermentation products might have contributed to the elevated DOC concentrations because mineralization can be incomplete under anaerobic conditions (Vink et al., 2010).

### *4.3.2.2. Total dissolved trace metal concentrations*

In Table 2, the total dissolved trace metal concentrations in the overlying water layer and the soil solution of the upper and bottom soil layers of the columns at day 6 of the field DMT experiment are presented. The total dissolved concentrations of all trace metals decreased from the water layer to the two soil layers of the soil profile (Table 2). These decreases were largest for Cd, Cu, and Pb and (much) smaller for Ni and Zn. Two different processes are expected to play a role in these changes in the total dissolved trace metal concentrations. First, the elevated pH in the soil solution in both soil layers of the soil profile will lead to a stronger binding of the trace metals to the soil solid phase, which is reflected in the decrease of both the free (see section 4.3.2.3) and total dissolved trace metal concentrations (Table 2). Secondly, an increased binding of trace metals to DOM resulting from the elevated pH and the increased DOC concentrations in the soil solution in both soil layers of the soil profile will lead to higher total dissolved trace metal concentrations. In our soil system, the net effect of these two opposing processes is a decrease in the total dissolved trace metal concentrations from the water layer to the two soil layers of the soil profile. However, the further decrease of the total dissolved Cu and Pb concentrations from the upper to the bottom soil layer is remarkable, because the DOC concentration in the soil solution in the bottom soil layer was higher than in the upper soil layer whereas the pH was nearly the same (Fig. 2). An increase in the total dissolved trace metal concentrations would have been expected, as has been shown by others when the DOM concentration in soil solution increased under aerobic conditions (Amery et al., 2007; Klitzke and Lang, 2007; Koopmans and Groenenberg, 2011). A possible explanation for this further decrease in the total dissolved Cu and Pb concentrations while their free concentrations remain the same is a decrease in the reactivity of DOM in the soil solution under anaerobic conditions relative to the DOM reactivity in the less anaerobic upper soil layer. This is in agreement with the findings of Hanke et al. (2014), who found a decrease in the affinity of DOM to bind to short-range ordered Fe-(hydr)oxides under anaerobic conditions. They attributed these findings to compositional changes in the DOM due to anaerobic processes. In parallel with a possible decrease in the reactivity of the DOM, reduction of humic acids present within SOM in the bottom soil layer, which was more strongly reduced than the upper soil layer (Fig. 2), might have led to compositional changes including the formation of reduced sulphur-containing ligands (Qian et al., 2002). Trace metals have a higher affinity to bind to reduced sulphur-containing ligands of humic acids than to oxygen-containing ligands such as carboxylic groups (Smith et al., 2002; Maurer et al., 2012). Consequently, reduction of humic acids present within SOM and formation of such reactive functional groups in the bottom soil layer might have contributed to the lower total dissolved Cu and Pb concentrations in this layer.

#### *4.3.2.3. Free trace metal concentrations*

In addition to the total dissolved trace metal concentrations, the free trace metal concentrations measured by the field DMT in the water layer and the soil solution of the upper and bottom soil layers of the columns are presented in Table 2. In this table, only data of day 6 of the field DMT experiment are presented, because the free trace metal concentrations at this sampling time were closest to Donnan equilibrium (results not shown). Since reduction of Cu(II) to Cu(I) can take place under the prevailing anaerobic conditions (Maurer et al., 2013; Fulda et al., 2013b), we included the free Cu(I) concentrations, which were derived from the field DMT experiment, in Table 2 as well. Additionally, the contribution of the measured free trace metal concentrations as a percentage of their measured total concentrations in the water layer and the soil solutions is presented.

The contribution of the free trace metal concentrations to their total dissolved concentrations ranged from 14 to 43% for Ni, 53 to 197% for Zn, 14 to 82% for Cd, 1 to 5% for Cu(II) and <0.1 to 12% for Cu(I), and 0.2 to 3% for Pb (Table 2). In some cases for Zn, the free concentration was higher than the total dissolved concentration. This might be due to external Zn contamination, which can be a complicating factor for the chemical analysis of Zn in solution at low Zn concentrations (Weng et al., 2002). Differences between the free trace metal concentrations and their total dissolved concentrations in solution are the result of the formation of trace metal complexes with inorganic ligands and DOM. According to our speciation model calculations (Fig. A.1), most of the Ni, Zn, and Cd were present in the free form, with small contributions of inorganically-complexed forms to their total dissolved concentrations in all layers of the soil columns. In contrast, Cu(II) and Pb were predicted to be mainly complexed by DOM, especially in the soil solution of the two soil layers of the soil columns (Fig. A.1). In the overlying water layer of the soil columns, Cd complexation by DOM was predicted to contribute only to a minor extent to its total dissolved concentration (Fig. A.1), due to the low DOC concentrations present in this layer (Fig. 2). In the soil solution of the two soil layers of the columns, the contribution of DOM-bound Cd increased considerably (Fig. A.1) because of the much higher DOC concentrations in these layers (Fig. 2). Our model predictions of the relative contribution of inorganic ligands and DOM to dissolved trace metal speciation are similar to those in previous studies (Temminghoff et al., 1997; Weng et al., 2002; Bonten et al., 2008; Koopmans et al., 2008). Reduction of Cu(II) to Cu(I), which was predominantly present in the free form (results not shown), occurred only in the two soil layers of the columns (Table 2; Fig. A.1). This is due to the presence of anaerobic conditions in these soil layers as compared to the water layer which remained aerobic (Fig. 2).

The measured free concentrations of all trace metals, except for Cu(I), in the soil solution in both soil layers of the columns were lower than those in the water layer (Table 2). This is caused by the higher pH of the two soil layers (Fig. 2), leading to a stronger trace metal binding to the soil solid phase (Weng et al., 2001). The free Cu(I) concentrations increased greatly in the soil solution in the bottom soil layer of the columns (Table 2), because this layer was more anaerobic than the other two layers (Fig. 2), as explained above, leading to an increased reduction of Cu(II) to Cu(I) (Maurer et al., 2013; Fulda et al., 2013b).

**Table 2**

Total dissolved and free trace metal concentrations ($-{}^{10}\log M$) in the water layer and the soil solution of the upper and bottom soil layers of the columns at day 6 of the field DMT experiment. The contribution of the free trace metal concentrations to the total dissolved concentrations is presented between brackets (%). Each value represents the average ± standard deviation of the two replicate soil columns (average ± standard deviation of the total dissolved and free trace metal concentrations based on ${}^{10}\log$-transformed values).

| | Ni | | Zn | | Cd | | Cu | | | Pb | |
|---|---|---|---|---|---|---|---|---|---|---|---|
| | Total[a] | Free | Total[a] | Free | Total[a] | Free | Total[a] | Free Cu (II) | Free Cu (I) | Total[a] | Free |
| Water layer | 5.37±0.08 | 5.98±0.40<br>(28±19%) | 4.98±0.12 | 5.06±0.41<br>(92±59%) | 5.29±0.13 | 6.18±0.44<br>(14±9%) | 5.25±0.16 | 6.61±0.48<br>(5±3%) | 11.10±0.25<br>(<0.1%) | 6.79±0.43 | 9.49±0.66<br>(0.2±0.1%) |
| Upper soil layer | 5.44±0.10 | 6.29±0.02<br>(14±3%) | 5.45±0.03 | 5.72±0.06<br>(53±4%) | 6.60±0.41 | 6.82±0.10<br>(82±79%) | 5.81±0.81 | 8.17±0.09<br>(1±1%) | 8.58±0.11<br>(0.3±0.3%) | 7.52±0.87 | 10.16±0.75<br>(2±2%) |
| Bottom soil layer | 5.36±0.02 | 5.77±0.28<br>(43±24%) | 5.52±0.04 | 5.22±0.02<br>(197±25%) | 6.41±0.03 | 6.69±0.16<br>(55±24%) | 6.84±0.09 | 8.68±0.29<br>(2±1%) | 7.83±0.22<br>(12±8%) | 8.67±0.13 | 10.34±0.26<br>(3±2%) |

[a] The detection limits of the ICP-MS for total dissolved trace metal concentrations in $-{}^{10}\log M$ are 8.59 for Ni, 7.78 for Zn, 9.80 for Cd, 8.72 for Cu, and 9.27 for Pb.

### *4.3.3. Comparison of DMT measurements with model predictions*

In Figure 3, the free trace metal concentrations in the water layer and the soil solution of the upper and bottom soil layers of the columns as predicted by speciation modelling are plotted against the measured free trace metal concentrations by the field DMT.

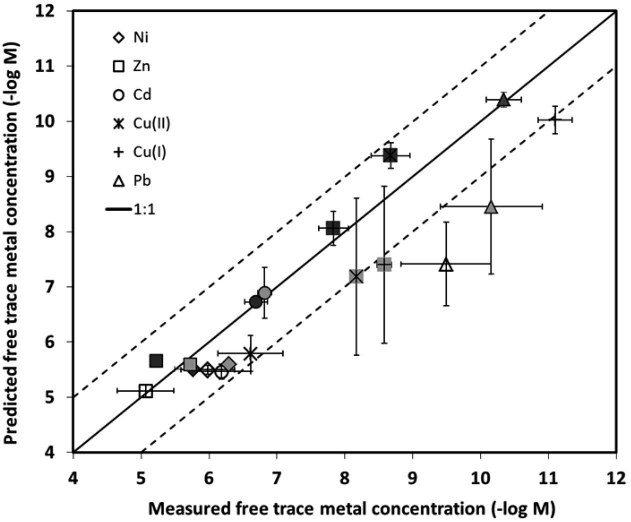

**Fig. 3.** The predicted free trace metal concentrations with ORCHESTRA in the water layer and the soil solution of the upper and bottom soil layers of the columns are plotted against the measured free trace metal concentrations with the field DMT at day 6 of the field DMT experiment. Each value represents the average ± standard deviation (based on $-^{10}\log$ M transformed values) of the two replicate soil columns. The solid line represents the 1:1 line and the dotted lines represent the ±1 $^{10}\log$-unit interval, respectively (white filling of the symbols represents the data from the water layer, grey filling represents the data from the upper soil layer, and black filling represents the data from the bottom soil layer).

For the water layer, the predicted free concentrations of all trace metals, except Pb, are within one $^{10}\log$-unit from their measured values, as is evidenced by their low root-mean-square residuals (RMSR) (Table 3). These results are in line with those of previous studies where the field DMT was successfully applied to measure free trace metal concentrations in surface waters under similar aerobic conditions (Kalis et al., 2006; Vega and Weng, 2013). In our study, the free Pb concentrations measured with the field DMT were much lower than those predicted by speciation modelling. This may be due to the lack of specific NICA-Donnan parameters for the PPHA used in the acceptor solution of the field DMT cell (Kalis et al., 2006, 2007). Alternatively, Fe-(hydr)oxide colloids present in the water layer of the soil column (Kretzschmar et al., 1999; Regelink et al., 2011, 2013) may play a role in the disagreement between predicted and measured free Pb concentrations, because particularly Pb can bind strongly to such colloids (Regelink et al., 2011). This process is not incorporated in our speciation modelling approach, which, therefore, may lead to an overestimation of the predicted free Pb concentrations in the overlying water layer.

**Table 3**

Root-mean-square residual (RMSR) between the predicted and measured free trace metal concentrations ($-^{10}$log M transformed concentrations) in the water layer and soil solution of the upper and bottom soil layers of the two replicate soil columns at day 6 of the field DMT experiment.

| | Ni | Zn | Cd | Cu(I) | Cu (II) | Pb |
|---|---|---|---|---|---|---|
| Water layer | 0.53 | 0.22 | 0.75 | 1.08 | 0.83 | 2.08 |
| Upper soil layer | 0.71 | 0.13 | 0.41 | 1.50 | 1.36 | 2.20 |
| Bottom soil layer | 0.31 | 0.43 | 0.13 | 0.44 | 0.79 | 0.28 |

In the slightly anaerobic soil solution of the upper soil layer (Fig. 2), the predicted free concentrations of all trace metals, except Cu(I), shows the same pattern as for the measured free concentrations, i.e., a decrease of the free concentrations, as discussed above (see Section 4.3.2). In contrast, the free Cu(I) concentrations increased, because the upper soil layer is slightly anaerobic as compared to the aerobic water layer (Fig. 2). For Ni, Zn, and Cd, our speciation model adequately predicted their free concentrations, as supported by their low RMSR values (Table 3). For Cu(I), Cu(II), and Pb, there is quite some variation in the predicted free metal concentrations between the two replicate soil columns, which is reflected by their high RMSR values (Table 3). Nevertheless, the average predicted values of free Cu(I) and Cu(II) correspond reasonably well with the results from the field DMT measurements. The predicted free Pb concentrations are much higher than the measured free ion concentrations, but this is consistent with the findings for the overlying water layer, as discussed above.

In the bottom soil layer, with more strongly anaerobic conditions as compared to the upper soil layer (Fig. 2), there is a noticeable difference between trace metals exhibiting a high affinity to form complexes with DOM (i.e., Cu(II) and Pb) on one hand and trace metals with a lower affinity to form complexes with DOM (i.e., Ni, Zn, Cd, and Cu(I)) on the other hand. For Ni, Zn, Cd, and Cu(I), the measured free concentrations remain reasonably constant as compared to those in the upper soil layer and our speciation model adequately predicted their free concentrations, as evidenced by their low RMSR values (Table 3). For Cu(II) and Pb, the average predicted free concentrations decrease by about two $^{10}$log-units compared to those in the upper soil layer, while the measured free concentrations decrease by only about 0.5 and 0.2 $^{10}$log-units, respectively (Table 2). For Cu(II), the difference between the average measured and predicted free concentrations is still within one $^{10}$log-unit, which becomes clear from its relatively low RMSR value (Table 3). For Pb, the overestimation of the free concentrations as observed before for the water layer and the upper soil layer now seems to be counteracted by a decrease in the predicted free concentrations for the bottom soil layer.

In our modelling approach, we did not account for any change in the reactivity of the DOM towards trace metal complexation under anaerobic conditions. A lower reactivity of the DOM was assumed to be responsible for the lower total dissolved Cu and Pb concentrations in the soil solution of the bottom soil layer, as discussed above (see Section 4.3.2). Both the magnitude of this decrease in total dissolved Cu and Pb concentrations, in parallel with a DOM increase of about a factor of 1.5 at otherwise very similar conditions, and fitting of the DOM reactivity to obtain a similar deviation between the calculated and measured free Cu(II) and Pb concentrations in the upper and bottom soil layers, suggest an about ten times lower DOM reactivity in the anaerobic bottom soil layer relative to the upper soil layer. However, other uncertainties such as the affinity constant of Fe(II) binding to FA (i.e., stronger than assumed competition for DOM binding by the increasing Fe(II) concentration in the bottom soil layer) may play a role as well (Milne et al., 2003). In short, the speciation model used in our study adequately predicted the free trace metal concentrations in the aerobic water layer of the soil columns when compared to measured concentrations as obtained by the field DMT for most trace metals, except for Pb. For trace metals with a low affinity to form complexes with DOM, predictions of the free concentrations for the two anaerobic soil layers were in good agreement with the measured concentrations. The free concentrations of trace metals with a high affinity for complexation to DOM were poorly predicted under anaerobic conditions. Although the speciation modeling approach used here has been demonstrated to perform well under aerobic conditions in this and many previous studies (e.g., Weng et al., 2002; Kalis et al, 2006), it does not fully capture all the chemical processes occurring under anaerobic conditions. Therefore, to obtain better model predictions for trace metals with a high affinity for complexation with DOM, a better insight into the composition and reactivity of DOM released under anaerobic conditions is required.

## *4.4. Conclusions*

In this study, the applicability of the field DMT was tested in a carefully designed soil column experiment in which a field-contaminated paddy soil was flooded. According to this experiment, the field DMT can be a useful tool for the in-situ measurement of free trace metal concentrations in flooded paddy soils. The free concentrations of Ni, Zn, Cd, Cu(II), and Pb as measured with the field DMT were lower in the solution of the upper and bottom soil layers than in the overlying water layer, due to the increased pH in these layers under anaerobic conditions. Similarly, the total dissolved trace metal concentrations decreased from the overlying water layer to the two soil layers of the soil profile, which was attributed to a stronger binding of the trace metals to the soil solid phase at the elevated pH in these layers. The total dissolved concentrations of trace metals with a high affinity to bind to DOM (i.e., Cu(II) and Pb) decreased even further from the upper soil layer to the bottom soil layer. This observation was remarkable, because the DOM concentration in the soil solution in the bottom soil layer was higher than for the upper soil layer whereas the pH was nearly the same. Hence, Cu(II) and Pb seem to bind less strongly to the DOM released under anaerobic conditions. Therefore, the composition and reactivity of DOM under anaerobic conditions requires further investigation. In the aerobic water layer of the soil columns, the measured free trace metal concentrations were similar to those predicted by geochemical speciation modelling, except for Pb. This similarity was also obtained in the anaerobic soil layers for trace metals with a low affinity to form complexes with DOM. However, free concentrations of the strongly DOM-binding metals Cu and Pb were poorly predicted for these anaerobic conditions. Hence, the applied geochemical modeling approach, which is frequently being used and performs well under aerobic conditions, does not fully capture all chemical processes occurring under anaerobic conditions. Our findings suggest that a better insight into the composition and reactivity of DOM released under anaerobic conditions is required to obtain better model predictions for trace metals with a high affinity for complexation with DOM.

## References

Amery, F., Degryse, F., Degeling, W., Smolders, E., Merckx, R., 2007. The copper–mobilizing–potential of dissolved organic matter in soils varies 10–fold depending on soil incubation and extraction procedures. Environ Sci Technol 41, 2277–2281.

Batley, G.E., Apte, S.C., Stauber, J.L., 2004. Speciation and bioavailability of trace metals in water: Progress since 1982. Aust J Chem 57, 903–919.

Bell, P.F., Chaney, R.L., Angle, J.S., 1991. Free metal activity and total metal concentrations as indexes of micronutrient availability to barley [Hordeum vulgare (L.) 'Klages']. Plant Soil 130, 51–62.

Bonten, L.T.C., Groenenberg, J.E., Weng, L., van Riemsdijk, W.H., 2008. Use of speciation and complexation models to estimate heavy metal sorption in soils. Geoderma 146, 303–310.

Chito, D., Weng, L.P., Galceran, J., Companys, E., Puy, J., van Riemsdijk, W.H., van Leeuwen, H.P., 2012. Determination of free $Zn^{2+}$ concentration in synthetic and natural samples with AGNES (Absence of Gradients and Nernstian Equilibrium Stripping) and DMT (Donnan Membrane Technique). Sci Total Environ 421, 238–244.

de Livera, J., McLaughlin, M.J., Hettiarachchi, G.M., Kirby, J.K., Beak, D.G., 2011. Cadmium solubility in paddy soils: Effects of soil oxidation, metal sulfides and competitive ions. Sci Total Environ 409, 1489–1497.

Du Laing, G., Rinklebe, J., Vandecasteele, B., Meers, E., Tack, F.M.G., 2009. Trace metal behaviour in estuarine and riverine floodplain soils and sediments: A review. Sci Total Environ 407, 3972–3985.

Du Laing, G., Vanthuyne, D.R.J., Vandecasteele, B., Tack, F.M.G., Verloo, M.G., 2007. Influence of hydrological regime on pore water metal concentrations in a contaminated sediment–derived soil. Environ Pollut 147, 615–625.

Fulda, B., Voegelin, A., Kretzschmar, R., 2013a. Redox–controlled changes in cadmium solubility and solid–phase speciation in a paddy soil as affected by reducible sulfate and copper. Environ Sci Technol 47, 12775–12783.

Fulda, B., Voegelin, A., Maurer, F., Christl, I., Kretzschmar, R., 2013b. Copper redox transformation and complexation by reduced and oxidized soil humic acid. 1. X–ray absorption spectroscopy study. Environ Sci Technol 47, 10903–10911.

Gao, R., Temminghoff, E.J.M., van Leeuwen, H.P., van Valenberg, H.J.F., Eisner, M.D., van Boekel, M.A.J.S., 2009. Simultaneous determination of free calcium, magnesium, sodium and potassium ion concentrations in simulated milk ultrafiltrate and reconstituted skim milk using the Donnan Membrane Technique. Int Dairy J 19, 431–436.

Groenenberg, J.E., Koopmans, G.F., Comans, R.N.J., 2010. Uncertainty analysis of the nonideal competitive adsorption–donnan model: Effects of dissolved organic matter variability on predicted metal speciation in soil solution. Environ Sci Technol 44, 1340–1346.

Grybos, M., Davranche, M., Gruau, G., Petitjean, P., 2007. Is trace metal release in wetland soils controlled by organic matter mobility or Fe-oxyhydroxides reduction? J Colloid Interf Sci 314, 490–501.

Hanke, A., Sauerwein, M., Kaiser, K., Kalbitz, K., 2014. Does anoxic processing of dissolved organic matter affect organic–mineral interactions in paddy soils? Geoderma 228–229, 62–66.

Houba, V.J.G., Temminghoff, E.J.M., Gaikhorst, G.A., van Vark, W., 2000. Soil analysis procedures using 0.01 M calcium chloride as extraction reagent. Commun Soil Sci Plant Anal 31, 1299–1396.

Houba, V.J.G., van der Lee, J.J.G., Novozamsky, I., 1997. Soil and plant analysis. Part 1: soil analysis procedures. Wageningen University, Wageningen, The Netherlands.

Kaiser, K., Guggenberger, G., Haumaier, L., Zech, W., 1997. Dissolved organic matter sorption on subsoils and minerals studied by C–13–NMR and DRIFT spectroscopy. Eur J Soil Sci 48(2), 301–310.

Kalis, E.J.J., Weng, L.P., Dousma, F., Temminghoff, E.J.M., van Riemsdijk, W.H., 2006. Measuring free metal ion concentrations in situ in natural waters using the Donnan Membrane Technique. Environ Sci Technol 40, 955–961.

Kalis, E.J.J., Weng, L.P., Temminghoff, E.J.M., van Riemsdijk, W.H., 2007. Measuring free metal ion concentrations in multicomponent solutions using the Donnan Membrane Technique. Anal Chem 79, 1555–1563.

Khaokaew, S., Chaney, R.L., Landrot, G., Ginder–Vogel, M., Sparks, D.L., 2011. Speciation and release kinetics of cadmium in an alkaline paddy soil under various flooding periods and draining conditions. Environ Sci Technol 45, 4249–4255.

Kinniburgh, D.G., van Riemsdijk, W.H., Koopal, L.K., Borkovec, M., Benedetti, M.F., Avena, M.J., 1999. Ion binding to natural organic matter: competition, heterogeneity, stoichiometry and thermodynamic consistency. Colloid Surface A 151, 147–166.

Klitzke, S., Lang, F., 2007. Hydrophobicity of soil colloids and heavy metal mobilization: Effects of drying. J Environ Qual 36, 1187–1193.

Kögel–Knabner, I., Amelung, W., Cao, Z.H., Fiedler, S., Frenzel, P., Jahn, R., Kalbitz, K., Kolbl, A., Schloter, M., 2010. Biogeochemistry of paddy soils. Geoderma 157, 1–14.

Koopmans, G.F., Groenenberg, J.E., 2011. Effects of soil oven–drying on concentrations and speciation of trace metals and dissolved organic matter in soil solution extracts of sandy soils. Geoderma 161, 147–158.

Koopmans, G.F., Schenkeveld, W.D.C., Song, J., Luo, Y.M., Japenga, J., Temminghoff, E.J.M., 2008. Influence of EDDS on metal speciation in soil extracts: Measurement and mechanistic multicomponent modeling. Environ Sci Technol 42, 1123–1130.

Kretzschmar, R., Borkovec, M., Grolimund, D., Elimelech, M., 1999. Mobile subsurface colloids and their role in contaminant transport. Adv Agron 66, 121–193.

Laborte, A.G., de Bie, K., Smaling, E.M.A., Moya, P.F., Boling, A.A., van Ittersum, M.K., 2012. Rice yields and yield gaps in Southeast Asia: Past trends and future outlook. Eur J Agron 36, 9–20.

Lindsay, W.L., 1979. Chemical equilibria in soils. John Wiley & Sons, New York, pp. 449.

Mansfeldt, T., 2004. Redox potential of bulk soil and soil solution concentration of nitrate, manganese, iron, and sulfate in two Gleysols. J Plant Nutr Soil Sc 167, 7–16.

Maurer, F., Christl, I., Fulda, B., Voegelin, A., Kretzschmar, R., 2013. Copper redox transformation and complexation by reduced and oxidized soil humic acid. 2. Potentiometric titrations and dialysis cell experiments. Environ Sci Technol 47, 10912–10921.

Maurer, F., Christl, I., Hoffmann, M., Kretzschmar, R., 2012. Reduction and reoxidation of humic acid: Influence on speciation of cadmium and silver. Environ Sci Technol 46, 8808–8816.

McLaughlin, M.J., Parker, D.R., Clarke, J.M., 1999. Metals and micronutrients – food safety issues. Field Crop Res 60, 143–163.

Meeussen, J.C.L., 2003. ORCHESTRA: An object–oriented framework for implementing chemical equilibrium models. Environ Sci Technol 37, 1175–1182.

Meharg, A.A., Norton, G., Deacon, C., Williams, P., Adomako, E.E., Price, A., Zhu, Y.G., Li, G., Zhao, F.J., McGrath, S., Villada, A., Sommella, A., De Silva, P.M.C.S., Brammer, H., Dasgupta, T., Islam, M.R., 2013. Variation in rice cadmium related to human exposure. Environ Sci Technol 47(11), 5613–5618.

Milne, C.J., Kinniburgh, D.G., van Riemsdijk, W.H., Tipping, E., 2003. Generic NICA–Donnan model parameters for metal–ion binding by humic substances. Environ Sci Technol 37, 958–971.

Novozamsky, I., van Eck, R., Houba, V.J.G., van der Lee, J.J., 1986. Use of ICP–AES for determination of iron, aluminium and phosphorus in Tamm's soil extracts. Neth J Agric Sci 34, 185–191.

Osté, L.A., Temminghoff, E.J.M., Lexmond, T.M., van Riemsdijk, W.H., 2002. Measuring and modeling zinc and cadmium binding by humic acid. Anal Chem 74, 856–862.

Otto, M., Thomas, J.D.R., 1985. Model studies on multiple channel analysis of free magnesium, calcium, sodium, and potassium at physiological concentration levels with ion–selective electrodes. Anal Chem 57, 2647–2651.

Pan, Y.Y., Koopmans, G.F., Bonten, L.T.C., Song, J., Luo, Y.M., Temminghoff, E.J.M., Comans, R.N.J., 2014. Influence of pH on the redox chemistry of metal (hydr)oxides and organic matter in paddy soils. J Soil Sediment, 14, 1713–1726.

Parker, D.R., Fedler, J.F., Ahnstrom, Z.A.S., Resketo, M., 2001. Reevaluating the free–ion activity model of trace metal toxicity toward higher plants: Experimental evidence with copper and zinc. Environ Toxicol Chem 20, 899–906.

Parker, D.R., Pedler, J.F., 1997. Reevaluating the free–ion activity model of trace metal availability to higher plants. Plant Soil 196, 223–228.

Parthasarathy, N., Pelletier, M., Buffle, J., 1997. Hollow fiber based supported liquid membrane: A novel analytical system for trace metal analysis. Anal Chim Acta 350, 183–195.

Ponnamperuma, F.N., 1972. The chemistry of submerged soils. Adv Agron 24, 29–96.

Qian, J., Skyllberg, U., Frech, W., Bleam, W.F., Bloom, P.R., Petit, P.E., 2002. Bonding of methyl mercury to reduced sulfur groups in soil and stream organic matter as determined by X-ray absorption spectroscopy and binding affinity studies. Geochim Cosmochim Ac 66, 3873-3885.

Regelink, I.C., Weng, L.P., van Riemsdijk, W.H., 2011. The contribution of organic and mineral colloidal nanoparticles to element transport in a podzol soil. Appl Geochem 26, S241–S244.

Römkens, P.F.A.M., Guo, H.Y., Chu, C.L., Liu, T.S., Chiang, C.F., Koopmans, G.F., 2009a. Characterization of soil heavy metal pools in paddy fields in Taiwan: Chemical extraction and solid–solution partitioning. J Soil Sediment 9, 216–228.

Römkens, P.F.A.M., Guo, H.Y., Chu, C.L., Liu, T.S., Chiang, C.F., Koopmans, G.F., 2009b. Prediction of cadmium uptake by brown rice and derivation of soil–plant transfer models to improve soil protection guidelines. Environ Pollut 157, 2435–2444.

Schulz–Zunkel, C., Krueger, F., 2009. Trace metal dynamics in floodplain soils of the River Elbe: A review. J Environ Qual 38, 1349–1362.

Senn, D.B., Griscom, S.B., Lewis, C.G., Galvin, J.P., Chang, M.W., Shine, J.P., 2004. Equilibrium–based sampler for determining $Cu^{2+}$ concentrations in aquatic ecosystems. Environ Sci Technol 38, 3381–3386.

Sigg, L., Black, F., Buffle, J., Cao, J., Cleven, R., Davison, W., Galceran, J., Gunkel, P., Kalis, E., Kistler, D., Martin, M., Noel, S., Nur, Y., Odzak, N., Puy, J., van Riemsdijk, W., Temminghoff, E., Tercier-Waeber, M.L., Toepperwien, S., Town, R.M., Unsworth, E., Warnken, K.W., Weng, L.P., Xue, H.B., Zhang, H., 2006. Comparison of analytical techniques for dynamic trace metal speciation in natural freshwaters. Environ Sci Technol 40, 1934–1941.

Simmons, R.W., Pongsakul, P., Saiyasitpanich, D., Klinphoklap, S., 2005. Elevated levels of cadmium and zinc in paddy soils and elevated levels of cadmium in rice grain downstream of a zinc mineralized area in Thailand: Implications for public health. Environ Geochem Hlth 27, 501–511.

Smith, D.S., Bell, R.A., Kramer, J.R., 2002. Metal speciation in natural waters with emphasis on reduced sulfur groups as strong metal binding sites. Comp Biochem Phys C 133, 65-74.

Smolders, E., McLaughlin, M.J., 1996. Effect of Cl on Cd uptake by Swiss chard in nutrient solutions. Plant Soil 179, 57–64.

Tack, F.M.G., van Ranst, E., Lievens, C., Vandenberghe, R.E., 2006. Soil solution Cd, Cu and Zn concentrations as affected by short–time drying or wetting: The role of hydrous oxides of Fe and Mn. Geoderma 137, 83–89.

Temminghoff, E.J.M., Plette, A.C.C., van Eck, R., van Riemsdijk, W.H., 2000. Determination of the chemical speciation of trace metals in aqueous systems by the Wageningen Donnan Membrane Technique. Anal Chim Acta 417, 149–157.

Temminghoff, E.J.M., van der Zee, S.E.A.T.M., de Haan, F.A.M., 1997. Copper mobility in a copper–contaminated sandy soil as affected by pH and solid and dissolved organic matter. Environ Sci Technol 31, 1109–1115.

Tipping, E., 1998. Humic ion–binding model VI: An improved description of the interactions of protons and metal ions with humic substances. Aquat Geochem 4, 3–48.

Tsukahara, T., Ezaki, T., Moriguchi, J., Furuki, K., Shimbo, S., Matsuda–Inoguchi, N., Ikeda, M., 2003. Rice as the most influential source of cadmium intake among general Japanese population. Sci Total Environ 305, 41–51.

Unsworth, E.R., Warnken, K.W., Zhang, H., Davison, W., Black, F., Buffle, J., Cao, J., Cleven, R., Galceran, J., Gunkel, P., Kalis, E., Kistler, D., van Leeuwen, H.P., Martin, M., Noel, S., Nur, Y., Odzak, N., Puy, J., van Riemsdijk, W., Sigg, L., Temminghoff, E., Tercier–Waeber, M.L., Toepperwien, S., Town, R.M., Weng, L.P., Xue, H.B., 2006. Model predictions of metal speciation in freshwaters compared to measurements by in situ techniques. Environ Sci Technol 40, 1942–1949.

van der Stelt, B., Temminghoff, E.J.M., van Riemsdijk, W.H., 2005. Measurement of ion speciation in animal slurries using the Donnan Membrane Technique. Anal Chim Acta 552, 135–140.

Vega, F.A., Weng, L.P., 2013. Speciation of heavy metals in River Rhine. Water Res 47, 363–372.

Vink, J.P.M., Harmsen, J., Rijnaarts, H., 2010. Delayed immobilization of heavy metals in soils and sediments under reducing and anaerobic conditions; consequences for flooding and storage. J Soil Sediment 10, 1633–1645.

Weng, L.P., Temminghoff, E.J.M., Lofts, S., Tipping, E., van Riemsdijk, W.H., 2002. Complexation with dissolved organic matter and solubility control of heavy metals in a sandy soil. Environ Sci Technol 36, 4804–4810.

Weng, L.P., Temminghoff, E.J.M., van Riemsdijk, W.H., 2001. Contribution of individual sorhents to the control of heavy metal activity in sandy soil. Environ Sci Technol 35, 4436–4443.

Xue, H.B., Sunda, W.G., 1997. Comparison of [$Cu^{2+}$] measurements in lake water determined by ligand exchange and cathodic stripping voltammetry and by ion–selective electrode. Environ Sci Technol 31, 1902–1909.

Yu, K.W., Bohme, F., Rinklebe, J., Neue, H.U., DeLaune, R.D., 2007. Major biogeochemical processes in soils – A microcosm incubation from reducing to oxidizing conditions. Soil Sci Soc Am J 71, 1406–1417.

## Appendix

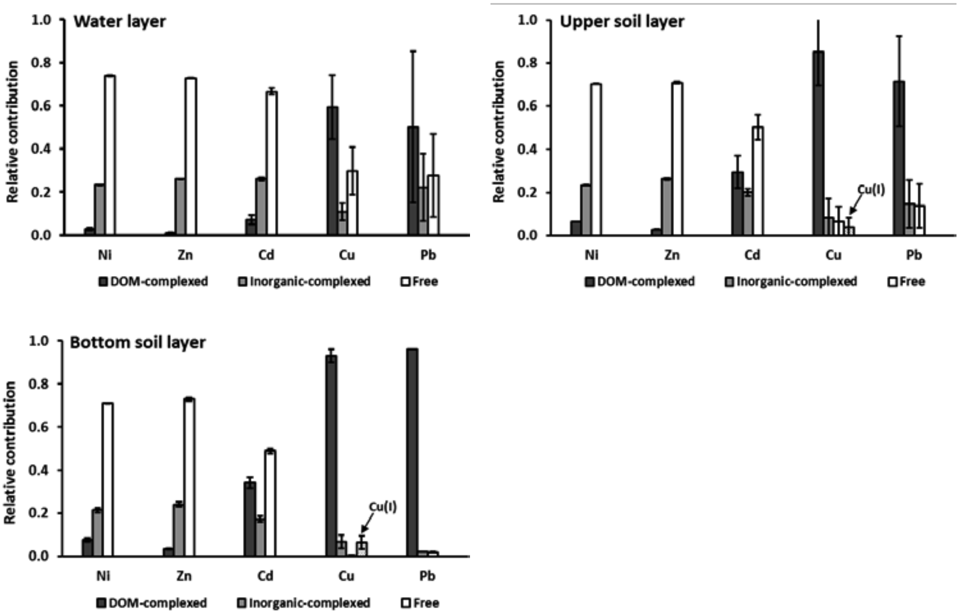

**Fig. A.1.** Calculated relative contribution of trace metal speciation in the water layer and the solution of the upper and bottom soil layers of the soil columns sampled at day 6 of the field DMT experiment. The average ± standard deviation of the two replicate soil columns is presented. The data of Cu represents the concentrations of the various Cu(II) forms relative to the total dissolved Cu concentrations, while the white dotted fourth bar represents the total dissolved Cu(I) concentrations relative to the total dissolved Cu concentrations as indicated by the arrow Cu(I). Cu(I) is predominantly present in the free form (results not shown).

# Chapter 5

# Temporal variability in trace metal solubility in a paddy soil not reflected in uptake by rice (Oryza sativa L.)

*Yunyu Pan, Gerwin F. Koopmans, Luc T.C. Bonten, Jing Song, Yongming Luo, Erwin J.M. Temminghoff, Rob N.J. Comans*

Under preparation, **2015**

## Abstract

Contamination of paddy soils with trace metals can increase their uptake by rice plants and their accumulation in rice grains, leading to concerns on human health risks. To minimize these risks, it is important to understand the processes controlling the uptake of trace metals by rice plants. However, the solubility of trace metals in soil solution in a paddy soil exposed to alternating flooding and drainage conditions, and how this sequence of processes is linked with metal uptake by rice plants over time, has received little attention. Therefore, the main objective of our study was to investigate the relationship between the solubility of trace metals and their uptake by two rice plant cultivars with either high or low Cd accumulation characteristics. We have investigated this relationship with a field-contaminated paddy soil in a pot experiment, in which the soil was subjected to two successive flooding and drainage cycles. Flooding led to a strong gradient in the redox potential (Eh) along the soil profile, and the pH and concentrations of Mn, Fe, and dissolved organic carbon increased with decreasing Eh, whereas drainage had the opposite effect. During flooding, the solubility of Cd, Zn, Cu, Ni, and Pb in all soil layers decreased markedly, which was explained by the formation trace metal sulfide precipitates under anaerobic conditions. Despite the low Cd solubility during flooding, the Cd content of the rice grains was found to exceed the food quality standards of P.R. China and the World Health Organization for both cultivars. For both rice plant cultivars, the trace metal contents in the different rice tissues (roots, stem, and leaves) increased at a constant rate or decreased after reaching a maximum value at later growth stages. As such, the uptake of trace metals by the rice plants over time did not reflect the high temporal variation in the solubility of the trace metals. The observed continuous metal uptake was explained by the presence of aerobic conditions near the root surface, that were maintained during the flooding periods, probably leading to a higher trace metal solubility in the rhizosphere than in the bulk soil. Consequently, the solubility of trace metals in the rhizosphere should be taken into account for further detailing the understanding of the effects of water management of paddy fields on the uptake of trace metals by rice plants.

*Keywords:* redox potential, trace metal, solubility, soil solution, paddy soil, uptake, rice tissues

## *5.1. Introduction*

Contamination of paddy soils with trace metals due to mining and smelting activities, application of fertilizers and sewage sludge, and wastewater irrigation has become a widespread problem (Kuo et al., 2006; Römkens et al., 2009a; Zeng et al., 2011; Fu and Wei, 2013). Trace metal contamination of paddy soils can lead to the accumulation of trace metals in rice grains (Römkens et al., 2009b; Zeng et al., 2011). Since rice is one of the most important staple food for human beings in South and Southeast Asia (Römkens et al., 2009a; Fu and Wei, 2013), consumption of rice with elevated trace metal levels is a serious threat to food security and human health (Römkens et al., 2009b; Laborte et al., 2012; Meharg et al., 2013). For typical rice-eating populations, the dietary intake of Cd via rice is the major exposure pathway for human beings to Cd (McLaughlin et al., 1999; Tsukahara et al., 2003; Meharg et al., 2013). For minimizing trace metal uptake by rice so as to safeguard food security and human health, it is important to understand the processes controlling the uptake of trace metals by rice plants.

The uptake of trace metals by rice plants depends on the bioavailability of trace metals in paddy soils (Simmons et al., 2008; Römkens et al., 2009b). For trace metals in paddy soils, three pools with a different bioavailability can be distinguished: the total, reactive, and directly available trace metal pools (Römkens et al., 2009a). The reactive pool represents trace metals adsorbed to reactive surfaces of soil organic matter (SOM), short-range ordered metal-(hydr)oxides, and clay, and it controls the trace metal concentrations in soil solution (Weng et al., 2001; Tipping et al., 2003). The size of this pool can be determined by the extraction of soil with 0.05 M EDTA, 0.1 M HCl, or 0.43 M $HNO_3$ (Römkens et al., 2009a). The directly available pool represents the free or total dissolved trace metal concentrations in soil solution which can be directly related to the uptake of trace metals by plants (Lofts et al., 2004; Peijnenburg et al., 2007). The size of this pool can be determined by either sampling of the soil solution with soil moisture samplers or lysimeters (Reynolds, 2004; Shen and Hoffland, 2007; Coutelot et al., 2014) or it can be mimicked by extraction of soil with weak salt extracts such as $CaCl_2$, $Ca(NO_3)_2$, or $NaNO_3$ (Houba et al., 2000; Peijnenburg et al., 2007). The size of the total pool is normally larger than the size of the reactive pool and the difference between these pools is interpreted to be nonreactive on a time scale relevant to the duration of a cropping season for rice (Römkens et al., 2009a). For paddy soils varying widely in soil properties such as pH and cation exchange capacity (CEC), regression-based log-log linear relationships have been used to link the directly available Cd pool as determined by 0.01 M $CaCl_2$ extraction of soil to the Cd content of rice grains (Simmons et al., 2008; Römkens et al., 2009b). In some studies, the Cd content of rice grains was linked to the reactive Cd pool based on the 0.43 M $HNO_3$ extraction of soil in combination with soil properties such as pH, SOM, and clay (Brus et al., 2009) or in combination with pH and CEC (Römkens et al., 2009b). These soil properties were included because they are known to affect the solid-solution partitioning of trace metals (Weng et al., 2001). However, most of the relationships in the aforementioned studies were determined for a specific growth stage of the rice plants, i.e., the rice grain filling stage. The solubility of trace metals in soil solution in a paddy soil exposed to alternating flooding and drainage conditions, and how this sequence of processes is linked with trace metal uptake by rice plants over time has, however, received very little attention.

Paddy soils usually undergo two flooding and draining cycles, which are known to lead to fluctuations in the redox potential (Eh) (Kögel-Knabner et al., 2010; Pan et al., 2014). Upon flooding, the Eh will decrease and the reduction of Mn- and Fe-(hydr)oxides will lead to their dissolution while organic matter will be released, resulting in elevated levels of $Mn^{2+}$ and $Fe^{2+}$ and dissolved organic matter (DOM) in soil solution (Tack et al., 2006; Grybos et al., 2007; Pan et al., 2014). Since SOM and metal-(hydr)oxides play an important role in the adsorption of trace metals in soils (Weng et al., 2001), a decrease in the reactive surfaces of these soil constituents can lead to an increase in the solubility of trace metals. The mobilization of trace metals might be even further amplified by the release of DOM after flooding (Pan et al., 2014), because trace metals including Cu and Pb can bind strongly to DOM (Amery et al., 2007; Koopmans and Groenenberg, 2011). On the other hand, the presence of $S^{2-}$ from the reduction of $SO_4^{2-}$ can precipitate trace metals in the form of poorly soluble minerals (de Livera et al., 2011; Khaokaew et al., 2011; Fulda et al., 2013). In addition to this, the pH of acidic soils can increase during flooding (Kögel-Knabner et al., 2010), which can enhance the adsorption of trace metals to the reactive surfaces of SOM and metal-(hydr)oxides (Weng et al., 2001). During drainage and subsequent oxidation of paddy soils, the (partial) reversal of the above mentioned reduction reactions can either immobilize trace metals via the precipitation of trace metals with freshly formed Mn (III/IV)- and Fe(III)-(hydr)oxides or mobilize trace metals via the dissolution of trace metal sulfide precipitates. The change of the pH back to its antecedent value will influence the adsorption of trace metals by SOM and metal-(hydr)oxides. These complex and dynamic effects of flooding and drainage on the Eh and redox chemistry of paddy soils are thus likely to have a large influence on the solubility of trace metals (Du Laing et al. 2009; Schulz-Zunkel and Krueger, 2009; Shaheen et al., 2014) and, subsequently, on the uptake of trace metals by rice plants over time including all growth stages of rice plants.

The main objective of our study is to investigate the relationship between the solubility of trace metals and their uptake by rice plants from a field-contaminated paddy soil over time in a pot experiment, in which the generally applied flooding and drainage cycles during rice growth are carefully simulated. Besides the bioavailability of trace metals in soils, trace metal uptake by rice also depends on rice plant-specific factors (Yu et al., 2006; Römkens et al., 2009b). For example, Indica and Japonica rice plant cultivars have been demonstrated to differ in their ability to translocate Cd from the roots into their shoots, with a higher ratio of Cd in rice grains to Cd in the roots for Indica than for Japonica (Römkens et al., 2009b). Therefore, we used two rice plant cultivars with high and low Cd accumulation characteristics (Hu et al., 2013) in our pot experiment. Rice undergoes three different growth phases: the vegetative phase (seedling and tillering stages), the reproductive phase (booting stage), and the ripening phase (grain filling stage and final harvest). In practice, flooded paddy soils are usually drained during the late tillering stage to control ineffective tillering and shortly before the harvest to enable faster rice ripening, to facilitate access to the paddy fields, and to ease harvesting (Kögel-Knabner et al., 2010). During our pot experiment, we used a similar water management of flooding and drainage of the paddy soil. The Eh was monitored continuously at five depths along the soil profile during the two successive flooding and drainage periods. Soil solution was sampled using soil moisture samplers during the major rice growth stages at the same depths to determine its chemical composition including pH and the concentrations of dissolved organic carbon (DOC) and total dissolved Mn, Fe and trace metals. Furthermore, the trace metal contents in different rice tissues including the roots, stem, leaves, husk, and grains were measured during the major rice growth stages. This experimental approach allowed us to link the solubility of trace metals with their uptake by rice plants over time.

## *5.2. Materials and methods*

### *5.2.1. Soil collection*

Soil with a clay loam texture was sampled from a paddy field (0-20 cm) nearby a former transformer and electronic waste stripping and recycling factory in Taizhou city, Zhejiang Province, P.R. China (Pan et al., 2014). This soil was severely contaminated with trace metals because of industrial activities in the proximity of the sampling site (Sun et al., 2013). The soil was air-dried, passed through a 2-mm sieve, and stored at room temperature before analyzing the soil characteristics and preparing the pot experiment.

### *5.2.2. Experimental setup of the pot experiment*

For the pot experiment, pots made of PVC material with a height of 35 cm and a diameter of 18 cm were used (Fig. 1). Quartz sand, pretreated and cleaned with 0.14 M $HNO_3$ and deionized water, was placed at the bottom of the pot in layer of 3 cm (Fig. 1). A piece of 1-mm nylon sieve material was put on top of the quartz sand. Each pot was filled with 4.5 kg of dried paddy soil. Before transferring the soil to each pot, it was thoroughly mixed with basal N, P, and K fertilizer including 1.8 g urea ($CO[NH_2]_2$), 1.58 g $KH_2PO_4$, and 0.46 g KCl. During mixing, the soil moisture content was adjusted to about 30% (w:w) to facilitate water penetration in the potted soil during the first flooding period. The thickness of the potted soil layer was 25 cm. In the pot experiment, two different rice cultivars were used (see Section 5.2.3.). The pot experiment was set up with 12 replicates for each of the two rice cultivars and had a total number of 24 pots. The pot experiment was carried out in a greenhouse. The temperature and light intensity in the greenhouse were regulated in accordance with the ambient weather conditions, because an optimal rice growth requires a high light intensity and temperature. The pot experiment was subjected to two successive flooding and drainage periods, which is in accordance with the water management of lowland paddy rice fields in practice, with one drainage period at the late tillering growth stage and one drainage period shortly before the harvest (Fig. 2). The first flooding period lasted for 58 days until the late tillering stage and was followed by a drainage period of 8 days aiming to control ineffective tillering. The second flooding period lasted for 46 days until the ripening stage and was followed by a drainage period of 16 days to enable faster rice ripening and to facilitate harvesting. For flooding of the pots, three liter deionized water was added to each pot in a step-wise manner so as to realize a final water layer on top of the soil layer of 5 cm (Fig. 1). The flooding procedure was completed within 3 hours for all 24 pots. From the 12 pots of each rice plant cultivar, three pots were randomly chosen to monitor the Eh and chemical composition of the soil solution. For Eh monitoring, a combined Eh-temperature glass fiber probe (Paleoterra Products, Amsterdam, The Netherlands) was inserted vertically in each of the six pots. The probes were tailor-made with five platinum Eh measurement points enabling us to monitor the Eh at 3 cm above the soil-water interface (+3 cm), at the interface (0 cm), and at depths of 5 (-5 cm), 10 (-10 cm), and 20 cm (-20 cm) below the interface (Fig. 1). The Ag-AgCl reference electrodes were positioned in the water layer. The Eh signal was automatically logged every 15 min. The Eh relative to the standard hydrogen electrode was calculated from the measured potential with a temperature-dependent correction for the potential of the Ag-AgCl reference electrode. The temperature was measured using the combined Eh-temperature probe by platinum electrodes at five positions within the soil columns: +3 cm, 0 cm, -5 cm, -10 cm, and -20 cm (Fig. 1). For collecting soil solution samples from the pots, five soil moisture samplers (SMS) (Rhizonsphere Research Products, Wageningen, The Netherlands) with a diameter of 2.5 mm, a mean pore size of 0.15 µm, and a porous section of 10 cm were placed horizontally at the same depths (+3 cm, 0 cm, -5 cm, -10 cm, and -20 cm) in the pot at which the Eh was measured. The connector of the SMS was made of silicone and it tightly sealed the holes of the pot preventing air penetration into the potted soil. During the pot experiment, soil solution was sampled at 11 occasions during the major rice growth stages (Fig. 2). During sampling, about 10 mL of soil solution were sampled with a vacuumed syringe. This syringe was connected to the female luer lock of the SMS, which was closed again immediately after sampling. The soil solution samples were split in two subsamples: one subsample was used to measure the concentrations of metals and sulfur after acidification by adding concentrated $HNO_3$ to a level of 1.2% (v:v) whereas the other subsample was used to measure the pH and DOC. The samples were stored in polypropylene tubes at 4°C until chemical analysis as further detailed in Section 5.2.4.2.

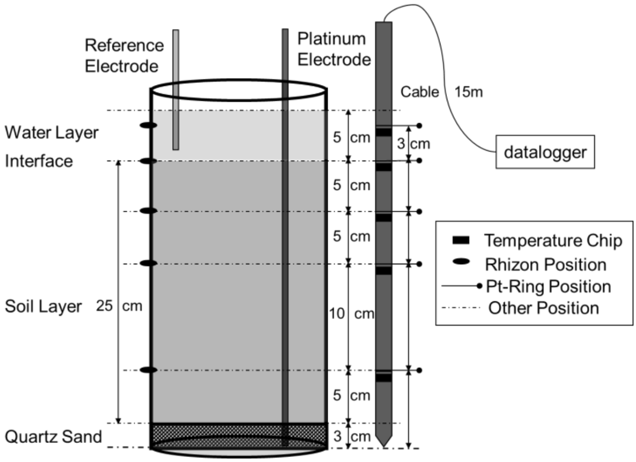

**Fig. 1.** Experimental setup of the pots for growing the two rice cultivars.

### *5.2.3. Rice plants management and harvest*

Two rice plant cultivars were used in our pot experiment: Zhongxiang No.1 (A16), which exhibits a low potential to accumulate Cd in brown rice, and Indonesia (A159) with a high potential for Cd accumulation in brown rice (Hu et al., 2013). The seeds of the two rice cultivars were provided by the China National Rice Research Institute, Hangzhou City, Zhejiang Province, P.R. China. The seeds of the two rice cultivars were disinfected with 10% $H_2O_2$ solution before use. After germination, germinated seeds were grown in an uncontaminated soil for 30 days before transplanting the seedlings to the pots. Four days after the setup of the pots, three clusters, with each cluster containing 6 seedlings, were transplanted to each pot. The clusters were evenly positioned over the soil surface of each pot. The transplantation of the seedlings from the uncontaminated soil to the pots was four days after the potted soil was flooded for the first time. During rice growth, an extra amount of 0.75 g urea was applied at the early-tillering stage (day 10) and another extra amount of 0.75 g urea was applied at the early grain filling stage (day 80). To maintain a water layer of 5 cm above the soil surface, we used deionized water to water the rice plants three times each day at 7 am, 2 pm, and 7 pm. Three pots for each rice cultivar were destructively harvested at the tillering stage (day 38), booting stage (day 72), filling stage (day 100), and ripening stage (day 128) (Fig. 2). The harvested rice plants were first thoroughly washed with tap water and then with deionized water to remove dust and adhering soil particles.

Furthermore, rice plants were separated into different plant tissues including root, stem, leaves, and grains. These tissues were wrapped in a clean paper envelope and oven-dried at 105ºC for 30 min and further dried at 80ºC to constant weight. The dried grains were then further separated into the husk and the brown rice. All the rice tissues were milled into powder by a stainless steel grinding machine for measuring the trace metal contents (see Section 5.2.4.3).

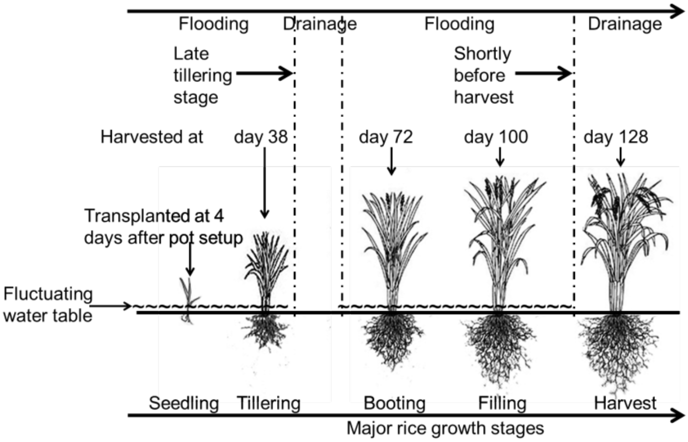

**Fig. 2.** Harvesting times of the rice plants during the major rice growth stages and alternating flooding and drainage periods in the pot experiment

*5.2.4. Chemical analysis*

*5.2.4.1 Soil analysis*

The pH was measured in a settling 1:10 (w:v) suspension of soil in 0.01 M $CaCl_2$ (Houba et al., 2000), the CEC was measured using 1 M $NH_4OAc$ buffered at pH 7.0 (USDA, 1996), SOM by loss-on-ignition (550°C), and clay by the sieve and pipette method (Houba et al., 1997). Dissolved organic carbon and sulfur were measured in the same $CaCl_2$ extract as used for the measurement of pH after filtration through a 0.45-µm filter (Schleicher & Schuell 602H). Dissolved organic carbon was measured by a TOC analyzer (Multi C/N 3000). Sulfur was measured by inductively coupled plasma-atomic emission spectrometry (ICP-AES; IRIS Intrepid II) and ion chromatography (DIONEX, ICS-2100) (Dick and Tabatabai, 1979). Since the results of both analytical techniques were very similar (results not shown), we interpreted sulfur measured in the $CaCl_2$

extract by ICP-AES as $SO_4^{2-}$ (Pan et al., 2014). Short-range ordered Al-, Fe-, and Mn-(hydr)oxides were determined by using the acid ammonium oxalate extraction method (Novozamsky et al., 1986). Concentrations of Al, Fe, and Mn in these extracts (i.e., Al-ox, Fe-ox, and Mn-ox) were measured by ICP-AES. The size of the reactive trace metal pools was determined by the extraction of soil with 0.43 M $HNO_3$ whereas the size of the total trace metal pools was determined by soil digestion with Aqua Regia (Houba et al., 1997). The Cd, Cu, Ni, Pb, Zn, Fe, Mn, and S concentrations in the 0.43 M $HNO_3$ extracts and the Aqua Regia digests were measured by ICP-AES. When these trace metal concentrations were below the detection limit of the ICP-AES, they were measured again but this time by an inductively coupled plasma-mass spectrometer (ICP-MS; Thermo Electron X7). All these soil properties were determined in triplicate and their average±standard deviation is presented in Table 1.

#### *5.2.4.2. Soil solution analysis*

The pH of the soil solution samples was measured directly after sampling with a combined glass electrode and DOC was measured by the TOC analyzer. In the acidified subsamples, Fe, Mn, and S were measured by ICP-AES and Cd, Cu, Ni, Pb, and Zn were measured by ICP-MS.

#### *5.2.4.3. Plant analysis*

For analyzing the trace metal contents in the different rice tissues, 0.5 g of milled rice plant tissue material was digested by using a mixture of 5 ml $HNO_3$ and 3 ml $HClO_4$ (Huang and Sculte, 1985). All chemicals used were of analytical grade. For quality control, a certified reference material (GBW07603, Institute of Geophysical and Geochemical Exploration in Langfang, Hebei Province, P.R. China was included and digested accordingly. The concentrations of Cu, Zn, Pb, Cd, and Ni in the digests were measured by ICP-MS.

## ***5.3. Results and discussion***

### *5.3.1. Physical-chemical soil properties*

Selected physical-chemical properties of the paddy soil used in our pot experiment are summarized in Table 1. The total Cd, Cu, Ni, and Zn contents exceed the Chinese environmental quality standard for soils (GB 15618-1995; Grade II for soil pH<6.5) about 23 (Cd), 9 (Cu), and 1.1 (Ni) times, respectively. Hence, this paddy soil is especially heavily contaminated with Cd and Cu. This soil is acidic in nature and the size of the reactive trace metal pools relative to the total pools increases in the order Ni (21%) < Zn (26%) < Cu (54%) < Pb (65%) < Cd (81%). These results are very similar to those of Römkens et al. (2009a) for paddy soils from Taiwan which are mostly slightly acidic and have a SOM content ranging from 3 to 9%. In this paddy soil, Cd is highly reactive whereas Zn and Ni are mostly present in chemically inert forms and are rather immobile. Hence, most of the total Cd pool can exchange with the soil solution and can become available with time for plant uptake. The available S-$SO_4^{2-}$ content in our paddy soil (Table 1) was in the upper range of the available S-$SO_4^{2-}$ contents (0.06 to 6.6 mmol kg$^{-1}$) reported for other paddy soils in different regions (Lefroy et al., 1992; Fulda et al., 2013). Under anaerobic conditions, trace metals present in our paddy soil might precipitate with sulfide to form sulfide minerals (Weber et al., 2009; Fulda et al., 2013; Hofacker et al., 2013).

**Table 1**

Selected physical and chemical properties of the paddy soil used in the pot experiment. All soil properties were determined in triplicate and the average±standard deviation is presented.

| Soil property | Unit | Value | Standard[g] |
|---|---|---|---|
| Clay (< 2 µm)[a] | % | 19.7±0.1 | - |
| SOM[b] | % | 9.8±0.1 | - |
| pH[c] | | 5.2±0.1 | - |
| DOC[c] | mg C L$^{-1}$ | 150±5 | |
| S-$SO_4^{2-}$[c] | mmol kg$^{-1}$ | 4.2±0.1 | |
| CEC | cmol[+] kg$^{-1}$ | 11.5±0.3 | - |
| Al-ox[d] | mmol kg$^{-1}$ | 38±1 | - |
| Fe-ox[d] | mmol kg$^{-1}$ | 95±1 | - |

| | | | |
|---|---|---|---|
| Mn-ox[d] | mmol kg$^{-1}$ | 1.7±0.1 | - |
| Reactive Cu[e] | μmol kg$^{-1}$ | 3965±31 | - |
| Total Cu[f] | μmol kg$^{-1}$ | 7380±79 | 787 |
| Reactive Cd[e] | μmol kg$^{-1}$ | 50.1±0.2 | - |
| Total Cd[f] | μmol kg$^{-1}$ | 62.0±0.5 | 2.7 |
| Reactive Pb[e] | μmol kg$^{-1}$ | 145±5 | - |
| Total Pb[f] | μmol kg$^{-1}$ | 222±10 | 1207 |
| Reactive Zn[e] | μmol kg$^{-1}$ | 596±31 | - |
| Total Zn[f] | μmol kg$^{-1}$ | 2309±76 | 3059 |
| Reactive Ni[e] | μmol kg$^{-1}$ | 164±5 | - |
| Total Ni[f] | μmol kg$^{-1}$ | 767±17 | 682 |

[a] Clay by the sieve and pipette method (Houba et al., 1997);

[b] Soil organic matter (SOM) by loss on ignition (550 °C) (Houba et al., 1997);

[c] 1:10 (w:v) 0.01 M $CaCl_2$ extraction (Houba et al., 2000);

[d] Extraction with acid ammonium oxalate (Novozamsky et al., 1986);

[e] 1:10 (w:v) 0.43 M $HNO_3$ (Houba et al., 1997);

[f] Aqua Regia (Houba et al., 1997);

[g] Grade II (pH<6.5) of the Chinese environmental quality standard for soils (GB 15618-1995).

### *5.3.2. Effect of alternating flooding and drainage on Eh, pH, and Mn, Fe, S, and DOC concentrations*

The Eh, pH, and Mn, Fe, S, and DOC concentrations in the overlying water layer and the soil solution of the soil layers at different depths during the two successive flooding and drainage periods for rice plant cultivar A159 are presented in Fig. 3. Since the results of rice plant cultivar A16 are very similar to those of cultivar A159, the results of the former cultivar are presented in the Appendix (Fig. A.1). The Eh showed a strong contrast between the water layer and the soil solution at a depth of -5, -10, and -20 cm: aerobic conditions were maintained in the water layer with an Eh of around 500 mV throughout the entire pot experiment, whereas anaerobic conditions with an Eh as low as about -300 mV were present in the three lower soil layers during the first flooding period. The Eh at the interface between the soil surface and the overlying water layer decreased during the first 20 days to a level of -200 mV but then it increased to a level of about 550 mV. During the first drainage period, the Eh rapidly reached a level of 400 mV in all soil layers, due to re-aeration and oxidation of the potted soil. During the entire second flooding period, the redox conditions remained aerobic in the water layer and at the interface. In the two lower soil layers, the Eh decreased to a level of about -200 mV. The Eh at a depth of -5 cm was higher than the Eh in the two lower soil layers but it showed a high temporal variation. Most rice plant roots in the potted soil were visually present at a depth of -5 cm. Therefore, the high temporal variation in Eh, which had a diurnal pattern, might be ascribed to internal aeration of the rice plants during the daily photosynthesis period, leading to downward transport of $O_2$ from the shoots to the submerged roots and leakage of $O_2$ to the local surrounding soil environment (Colmer et al., 2003; Mongon et al., 2014). During the second drainage period, aerobic conditions prevailed in all soil layers except for the bottom layer at a depth of -20 cm, which remained slightly anaerobic.

Based on the measured Eh range for our paddy soil, redox reactions including denitrification and reduction of Mn(III/IV) to Mn(II), Fe(III) to Fe(II), and $SO_4^{2-}$ to $S^{2-}$ can occur (Fig. 3 and Fig. A.1). Hence, reductive dissolution of Mn- and Fe-(hydr)oxides during flooding can explain the clearly elevated Mn and Fe concentrations in soil solution in the three lower soil layers as compared to those in the water layer. Precipitation of Mn and Fe in the form of Mn (III/IV)- and Fe(III)-(hydr)oxides can explain the lower concentrations of these metals during drainage and subsequent oxidation of our paddy soil (Schulz-Zunkel and Krueger, 2009; Shaheen et al., 2014). Since reduction of $SO_4^{2-}$ to $S^{2-}$ can be expected to occur resulting from the low Eh encountered during flooding in the three lower soil layers, the gradually decreasing sulfur concentration in soil solution over time (Fig. 3) are likely caused by the formation of poorly-soluble sulfide minerals during flooding periods (Murase and Kimura, 1997; Du Laing et al., 2009; Schulz-Zunkel and Krueger, 2009). Since the above-mentioned redox reactions including denitrification, reductive dissolution of Mn- and Fe-(hydr)oxides, and $SO_4^{-2}$ reduction consume protons, the pH increased from acidic to an almost neutral level in all soil layers during both flooding periods, whereas the pH in the water layer remained relatively constant (Fig. 3 and Fig. A.1). During both drainage periods, the pH in all soil layers decreased again. The DOC concentrations in the three lower anaerobic soil layers during flooding were clearly elevated compared to the aerobic overlying water layer, which can be attributed to reductive dissolution of Mn- and Fe-(hydr)oxides and the elevated pH, both leading to the release of adsorbed DOM

(Kaiser et al., 1997; Pan et al., 2014). In addition to these explanations, the release of fermentation products might have contributed to the elevated DOC concentrations in

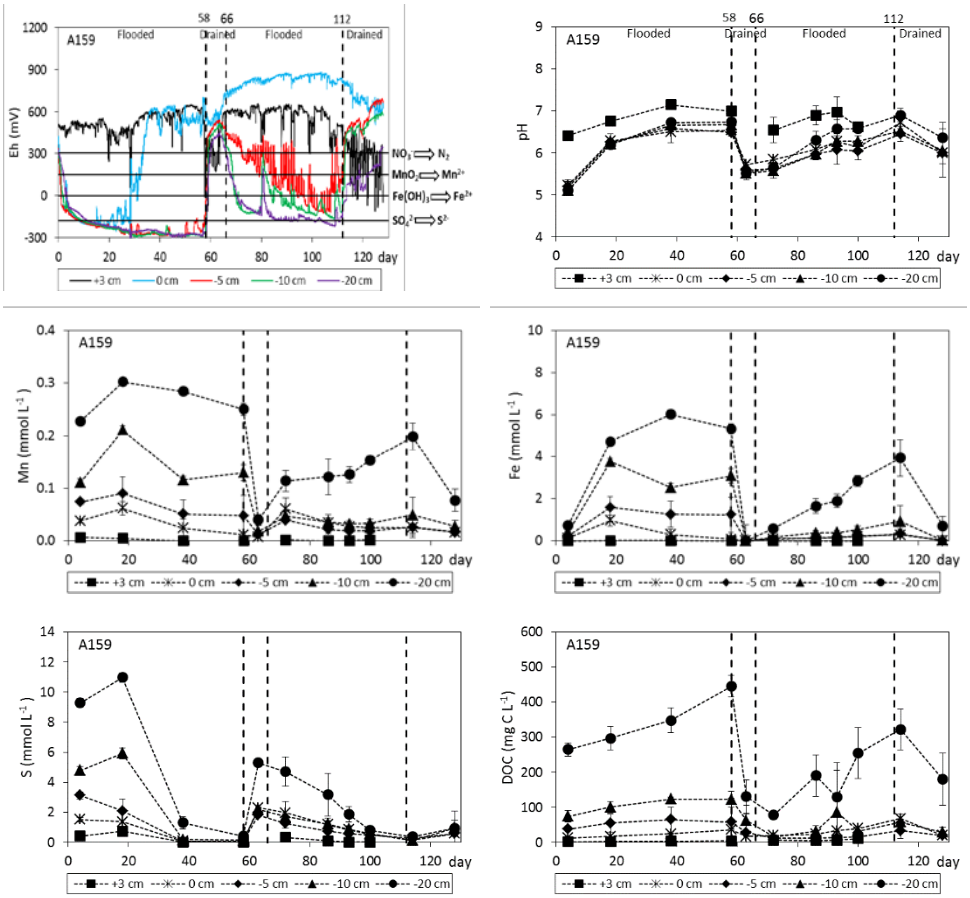

Fig. 3. The Eh, pH, and Mn, Fe, S, and DOC concentration in the soil solution as a function of time in the pot experiment with rice plant cultivar A159 (+3 cm refers to 3 cm above the interface, 0 cm equals the interface between the soil surface and the water layer, and -5, -10 cm, -20 cm refer to 5, 10, and 20 cm below the interface, respectively).

these layers because mineralization of organic matter can be incomplete under anaerobic conditions (Vink et al., 2010). The DOC concentrations decreased in all soil layers during both drainage periods.

### *5.3.3. Effect of alternating flooding and drainage on the solubility of Cu, Cd, Pb, Zn, and Ni*

In Fig. 4, the trace metal concentrations in the overlying water layer and soil solution of the soil layers at different depths are presented for the rice plant cultivar A159. The results for the rice plant cultivar A16 are very similar to those of cultivar A159 and are, therefore, presented in the Appendix (Fig. A.2). The solubility of all trace metals except Pb at the initial sampling occasion (day 4) clearly increased with depth. These initial differences between the trace metal concentrations cannot be explained by differences in pH, because the pH in the soil layers was very similar (Fig. 3 and Fig. A.1). The vertical gradient at the initial sampling occasion is possibly due to vertical displacement of trace metals via downward transport during the saturation of the potted soil by adding deionized water at the top of the soil surface. After the initial sampling occasion, the solubility of Cu, Cd, Pb, Zn, and Ni in the soil layers decreased markedly during the first flooding period, which might be due to the development of strongly anaerobic conditions (Fig. 3 and Fig. A.1). The low Eh probably allowed for the reduction of $SO_4^{2-}$ to $S^{2-}$ and the precipitation of Cu, Cd, Pb, Zn, and Ni in the form of sulfide minerals, which exhibit a low solubility (Weber et al., 2009; de Livera et al., 2011; Fulda et al., 2013). When assuming a stoichiometry of 2:1 for Cu:S and a stoichiometry of 1:1 for Cd, Pb, Zn, and Ni sulfides (Allison et al., 1991), there would be enough sulfur in this paddy soil to precipitate all five trace metals in the form of sulfide minerals when all available S-$SO_4^{2-}$ is reduced to $S^{2-}$ (Table 1). However, Cu sulfide minerals formed in anaerobic soil or sediment systems have been demonstrated to vary in stoichiometry, represented as $Cu_xS$ with x varying between 1 and 2 and with CuS and $Cu_2S$ as end members (Morse and Luther, 1999; Weber et al., 2009). When the stoichiometry of Cu sulfide formed in our paddy soil would approach 1:1, the sulfur content would be insufficient to precipitate all trace metals in the form of sulfide minerals (Table 1). Since Ni is the least stable sulfide mineral of the five trace metals considered here according to the thermodynamical “sulfide ladder” (Weber et al., 2009), the formation of NiS might be less likely when the sulfur content would limit precipitation of trace metals in the form of sulfide minerals. Instead, the solubility of Ni in the anaerobic soil layers might be governed by adsorption to SOM (Weng et al., 2001). The increase in pH during flooding (Fig. 3 and Fig. A.1), which results in an increased binding of trace metals to organic matter, can also explain the observed decrease in the solubility of Ni. During the first drainage period of our paddy soil, the trace metal concentrations increased in all soil layers. This increase might be attributed to the oxidation of sulfide minerals, due to re-aeration of the soil layers and the development of aerobic conditions (Fig. 3 and Fig. A.1). For Ni, the decrease in pH during the first drainage period (Fig. 3 and Fig. A.1) might play a role, leading to Ni desorption from SOM. During the second flooding period, the trace metal concentrations in the soil layers decreased again, but were generally higher in the two upper layers than in the three lower soil layers. This difference can be explained by the development of anaerobic conditions in the three lower layers (Fig. 3 and Fig. A.1) allowing for the formation of trace metal sulfide minerals in these layers. However, the Ni concentrations in the strongly anaerobic bottom soil layer were higher than those in the other less anaerobic soil layers, while the Eh in the bottom soil layer was low enough to sustain reduction of $SO_4^{2-}$ to $S^{2-}$ (Fig. 3 and Fig. A.1). Apparently, the solubility of Ni in this paddy soil was not controlled by Ni sulfides but rather by binding of Ni to organic matter in the form of DOM and SOM, as discussed above. The DOC concentrations in the bottom soil layer were higher than those in the other soil layers (Fig. 3 and Fig. A.1), which can explain the higher total dissolved Ni concentrations in the bottom soil layer (Pan et al., 2014). The solubility of the trace metals increased again in all soil layers during the second drainage period. In the latter period, aerobic conditions were present in most layers upon re-aeration of the soil columns (Fig. 3 and Fig. A.1). Consequently, the oxidation of sulfide minerals might increase the solubility of all trace metals except Ni. For Ni, the decrease in pH during the second drainage period (Fig. 3 and Fig. A.1) and subsequent desorption from SOM can explain its elevated solubility.

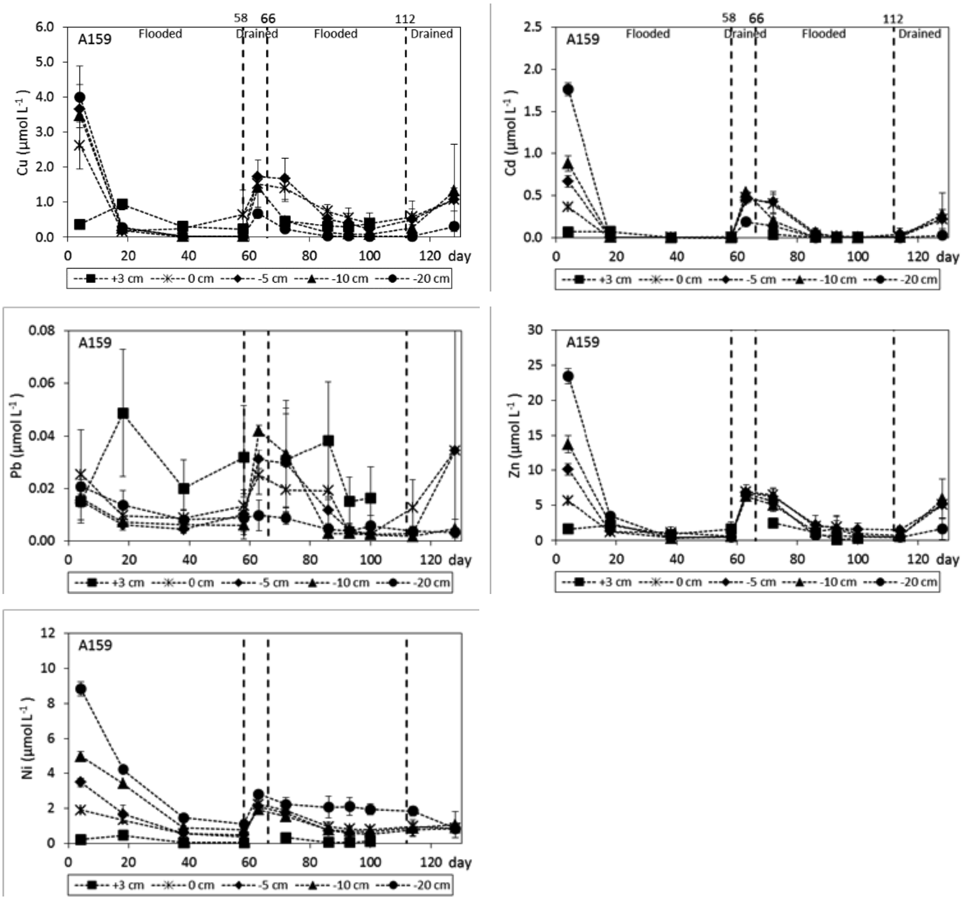

**Fig. 4.** Total dissolved concentrations of Cu, Cd, Pb, Zn, and Ni in the soil solution as a function of time in the pot experiment with rice plant cultivar A159 (+3 cm refers to 3 cm above the interface, 0 cm equals the interface between the soil surface and the water layer, and -5, -10 cm, -20 cm refer to 5, 10, and 20 cm below the interface, respectively).

### *5.3.4. Uptake of trace metals by different rice plant tissues during the major growth stages*

The trace metal contents of the different rice plant tissues and the accumulation of trace metals in the roots and above-ground biomass of rice plant cultivar A159 during the major rice growth stages are presented in Fig. 5. Also, the biomass of the roots and the above-ground plant tissues is included in this figure. The same data for rice plant cultivar A16 is presented in the Appendix (Fig. A.3). At the final harvest, the total amount of Cd accumulated within the roots and above-ground plant tissues of rice plant cultivar A159 relative to the total Cd pool in the paddy soil was clearly higher (4.6%) than for Zn (1.6%), Cu (0.3%), Ni (0.4%), and Pb (1.1%). Similar results were obtained for rice plant cultivar A16, although the difference in accumulation between Cd on the one hand and Zn, Cu, Ni, and Pb on the other hand was less prominent than for cultivar A159. These results agree very well with the size of the reactive trace metal pools relative to their total pools in the paddy soil, which indicated that Cd in this soil was largely present in reactive forms whereas the reactive fraction of the other trace metals was much lower, as previously discussed in Section 5.3.1. The biomass of the rice plant roots and above-ground plant tissues including the leaves and stem increased at a reasonably constant rate with time for both cultivars. For the last two harvests, the biomass of the husks and rice grains was included in the biomass of the above-ground plant tissues and contributed by about 50% to the total above-ground biomass at these harvests. The rates at which the trace metals were taken up by the roots and translocated from the roots into the above-ground biomass for rice plant cultivar A159 seemed to increase over the first drainage period when we expressed the data as absolute amounts of trace metals accumulated within these plant parts, while the uptake and translocation rates leveled off during the second drainage period. The increase in the root uptake rate of trace metals and their rate of translocation over the first drainage period was absent when we normalized the data for the biomass of the roots and above-ground plant tissues. Apparently, the water management of our pot experiment, which simulates that of lowland paddy rice fields in practice, did not affect the efficiency of trace metal uptake and translocation for the two rice plant cultivars.

Large differences are present in the translocation of Cd, Zn, Cu, Ni, and Pb from the rice plant roots into the above-ground plant tissues for both cultivars. For the final harvest, the ratios between the Cd and Zn contents in the stem, leaves, husk, and rice grains of rice plant cultivar A159 on the one hand and those in the roots on the other are much higher than those for Cu and Pb (Table 2 and Table A.1). These results reflect a higher translocation of Cd and Zn from the roots into the above-ground plant tissues than for Cu and Pb. The ratios for Ni are higher than for Cu and Pb but lower than for Cd and Zn (Table 2 and Table A.1), meaning Ni has an intermediate translocation behavior. Hence, root uptake and translocation of Cu and Pb into the above-ground plant tissues was strongly regulated whereas Cd and Zn translocation was more efficient. However, we measured the total trace metal contents of the rice plant roots and did not distinguish between trace metals adsorbed to the root surface and trace metals internalized within the roots, as has been done by Kalis et al. (2007) and Duffner et al. (2013) for grass and wheat, respectively. Consequently, it is not possible to be conclusive on whether exclusion of Cu from the above-ground plant biomass was due to a mechanism regulating root uptake or an internal mechanism controlling the transfer of Cu internalized within roots into the above-ground tissues.

**Table 2**

Ratios between trace metal contents in the above-ground rice plant tissues and roots for rice plant cultivar A159 at the final harvest (day 128).

| Ratios | Cd | Zn | Cu | Ni | Pb |
|---|---|---|---|---|---|
| Stem:root | 0.96±0.15 | 1.34±0.15 | 0.11±0.02 | 0.27±0.04 | 0.06±0.02 |
| Leave:root | 1.09±0.09 | 1.18±0.08 | 0.13±0.02 | 0.35±0.02 | 0.32±0.04 |
| Husk:root | 0.35±0.07 | 0.35±0.07 | 0.02±0.004 | 0.08±0.02 | 0.005±0.001 |
| Grain:root | 0.31±0.05 | 0.75±0.06 | 0.04±0.001 | 0.36±0.007 | 0.01±0.002 |

The Cd content in the rice grains of rice plant cultivar A159 at the final harvest was 3.6 mg kg$^{-1}$ and exceeds by far the food quality standards of the P.R. China (i.e., 0.2 mg Cd kg$^{-1}$) and the World Health Organization (WHO) (i.e., 0.4 mg Cd kg$^{-1}$) (Fig. 5). Although rice plant cultivar A16 is known to have a relatively low potential to accumulate Cd in rice grains (Hu et al., 2013), the Cd content still reached 2.5 mg kg$^{-1}$ and exceeds the Chinese and WHO standards (Fig. A.3). So despite the low solubility of Cd in soil solution during both flooding periods (Fig. 4 and Fig. A.2), still significant uptake and accumulation of Cd within the rice grains of both rice plant cultivars occurred. Therefore, human exposure to Cd resulting from the consumption of rice cropped in this specific contaminated paddy field might be unavoidable by specifically using the rice plant cultivar A16 with a low potential to accumulate Cd. Also, flooding as applied in our pot experiment does not prevent the two rice plant cultivars tested here from taking up Cd from soil solution by their roots and accumulating Cd in their grains to levels far above the Chinese and WHO food quality standards. In our study, the rice grains were not polished before chemical analysis and as a consequence, the Cd content was determined here in brown rice whereas most people eat polished white rice.

However, this is not expected to affect our results, because Masironi et al. (1977) and Kokot and Phoung (1999) found very similar Cd contents in unpolished and polished rice grains. Furthermore, milling of brown rice grains does not significantly reduce Cd levels in the grain (Moriyama et al., 2003).

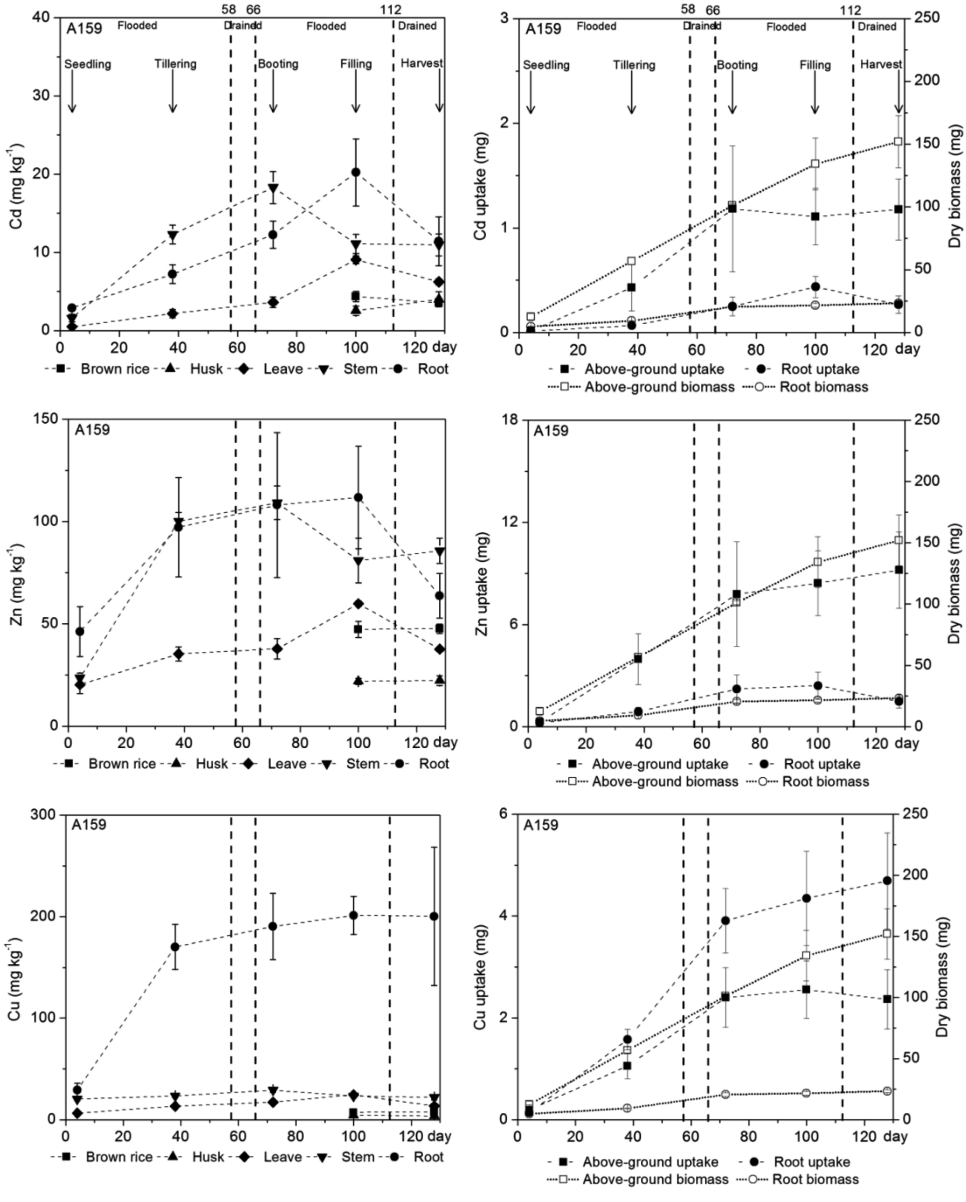

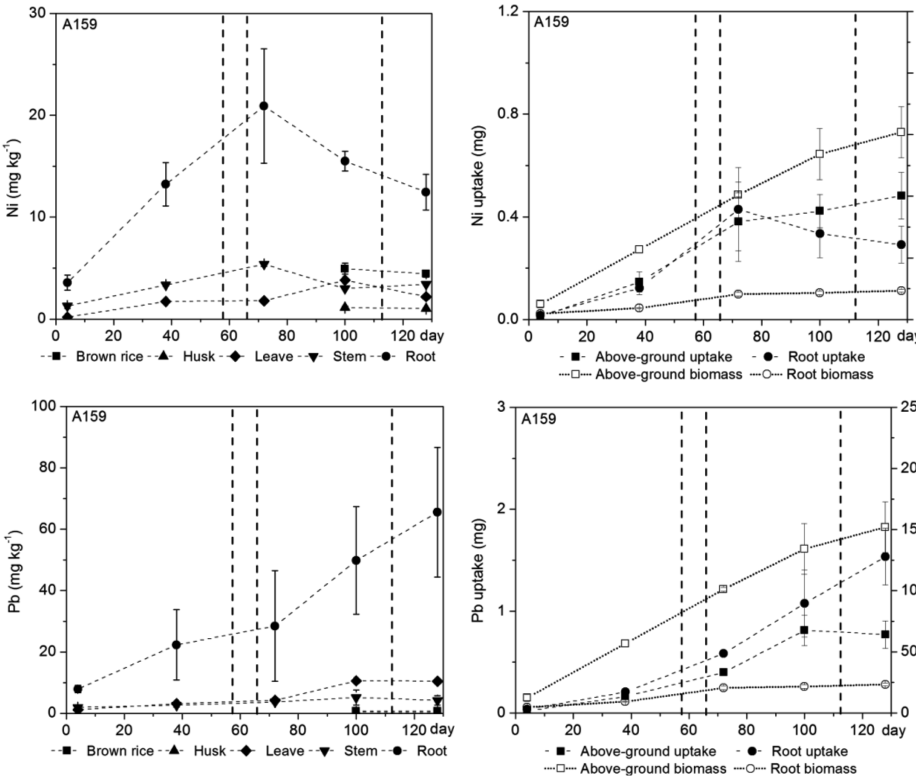

**Fig. 5.** Trace metal contents of the different rice plant tissues (left) and the biomass of the roots and the above-ground plant tissues including brown rice, husk, leave and stem and the accumulation of trace metals in the roots and above-ground biomass (right) of rice cultivar A159 during the major rice growth stages. Brown rice and husks were only harvested during the last two harvests.

We expected to find a clear impact of water management of the paddy soil in the pot experiment on the uptake of trace metals by the rice plants over time, with trace metal contents in the various rice plant tissues increasing during both drainage periods when the solubility of trace metals showed a large increase (Fig. 4 and Fig. A.2), as has been found in previous studies (Chaney et al., 1996; Kashem and Singh, 2001; Simmons et al., 2008). Instead, the trace metal contents of the rice plant roots and the above-ground plant tissues seemed to increase at a reasonably constant rate over the entire course of the pot experiment or decreased after reaching a maximum value at later growth stages. As such, our experimental results did not show a relation between the high temporal variation in the solubility of trace metals and their uptake by the rice plants over time. In our pot experiment, the dissolved trace metal concentrations were measured in soil solution sampled by SMS, which were installed within the bulk soil whereas plant uptake of trace metals is known to occur predominantly from the rhizosphere (Shuman and Wang, 1997). During the second flooding period, the Eh at a depth of 5 cm below the soil surface had a high temporal variation (Fig. 3 and Fig. A.1), which can be explained by leakage of $O_2$ from the rice plant roots (see Section 5.3.2.). This $O_2$ leakage apparently maintained aerobic conditions in the rhizosphere, since precipitation of $Fe^{3+}$ in the form of Fe-(hydr)oxides was observed as a thin red layer on the root surface of both rice plant cultivars harvested from the pot experiment. This phenomenon is called iron plague formation and is ubiquitous for wetland plants such as rice (Weis and Weis, 2004; Liu et al., 2006). Iron plague formation was not limited to the second flooding period when a diurnal pattern in Eh at a depth of 5 cm below the soil surface was noticeable in the bulk soil solution, but occurred also during the first flooding period when such a pattern was not detected and apparently limited to the environment close to the roots (Fig. 6). The presence of iron plague extended over the entire root length of about 5 to 15 cm for both rice plant cultivars. Although the role of iron plague itself on root uptake and translocation of Cd into shoots of rice plants has been suggested to be insignificant (Liu et al., 2008), the presence of iron plague on the root surface of both rice plant cultivars in our pot experiments can only be explained from aerobic conditions prevailing in the proximity of the roots. The solubility of trace metals in this local aerobic soil environment surrounding the rice plant roots is likely to be higher than in the anaerobic bulk soil where trace metal solubility was controlled by sulfides. This maintained aerobic environment near the roots might have facilitated a continuous uptake of trace metals by the rice plants at a constant rate and is apparently not necessarily related to the solubility of trace metals in the bulk soil. Consequently, the solubility of trace metals in the rhizosphere should be taken into account to deepen the understanding of the effects of water management of paddy fields on the uptake of trace metals by rice plants.

**Fig. 6.** Photographs taken from the rice plants harvested at the rice tillering stage (day 38) showing iron plague formation on the root surface of rice plant cultivar A159.

### *5.4. Conclusion*

Two successive flooding-draining cycles of a field-contaminated paddy soil greatly affected the solubility of trace metals at different depths along the soil profile. During flooding, the solubility of Cd, Zn, Cu, Ni, and Pb in all soil layers decreased markedly, which was explained by the formation trace metal sulfide precipitates under anaerobic conditions. Despite the low Cd solubility during flooding, the Cd content of the rice grains exceeds by far the food quality standards of P.R. China and the WHO for both cultivars. For both rice plant cultivars, the trace metal contents in the different rice tissues (roots, stem, and leaves) increased at a constant rate or decreased after reaching a maximum value at later growth stages. As such, the uptake of trace metals by the rice plants over time did not show a relation with the high temporal variation in the solubility of trace metals. The lack of such a relationship was explained by the presence of aerobic conditions near the root surface, probably leading to a higher trace metal solubility in the rhizosphere than in the bulk soil and a continuous uptake of trace metals over time. Consequently, the solubility of trace metals in the rhizosphere should be taken into account when quantifying the effects of water management on the uptake of trace metals by rice plants. In order to facilitate rice production on trace metal contaminated paddy soils, either selection and breeding of rice cultivars that further minimize Cd accumulation or in-situ immobilization of trace metals by using stabilizing amendments should be investigated as a measure to mitigate human health risks from trace metal contamination.

## References

Allison, J.D., Brown, D.S., Novo-Gradac, K.J., 1991. MINTEQA2/PRODEFA2, A geochemical assessment model for environmental systems: version 3.0 user's manual. US EPA, Athens, GA. EPA/600/3–91/021.

Amery, F., Degryse, F., Degeling, W., Smolders, E., Merckx, R., 2007. The copper-mobilizing-potential of dissolved organic matter in soils varies 10-fold depending on soil incubation and extraction procedures. Environ Sci Technol 41, 2277–2281.

Chaney, R.L, J.A. Ryan,Y.M. Li, R.M. Welch, P.G. Reeves, S.L. Brown, Green, C.E., 1996. Phyto-availability and bio-availability in risk assessment for cadmium in agricultural environments. In: Sources of Cadmium in the Environment, OECD, Paris, France, pp. 49–78.

Colmer, T.D., 2003. Aerenchyma and an inducible barrier to radial oxygen loss facilitate root aeration in upland, paddy and deep-water rice (Oryza sativa L.). Annals of Botany 91, 301–309.

Coutelot, F., Sappin-Didier, V., Keller, C., Atteia, O., 2014. Comparison of soil solution sampling techniques to assess metal fluxes from contaminated soil to groundwater. Environ Monit Assess 186, 8929–8941.

Cui, Y., Zhang, X., Zhu, Y., 2008. Does copper reduce Cd uptake by different rice genotypes? Journal of Environmental Sciences 20, 332–338.

de Livera, J., McLaughlin, M.J., Hettiarachchi, G.M., Kirby, J.K., Beak, D.G., 2011. Cadmium solubility in paddy soils: Effects of soil oxidation, metal sulfides and competitive ions. Sci Total Environ 409, 1489–1497.

Dick, W.A., Tabatabai, M.A., 1979. Ion chromatographic determination of sulfate and nitrate in soils. Soil Sci Soc Am J 43, 899–904.

Du Laing, G., Rinklebe, J., Vandecasteele, B., Meers, E., Tack, F.M.G., 2009. Trace metal behaviour in estuarine and riverine floodplain soils and sediments: A review. Sci Total Environ 407, 3972–3985.

Duffner, A., Hoffland, E., Weng, L.P., van der Zee, S.E.A.T.M., 2013. Predicting zinc bioavailability to wheat improves by integrating pH dependent nonlinear root surface adsorption. Plant Soil 373, 919–930.

Fu, S., Wei, C.Y., 2013. Multivariate and spatial analysis of heavy metal sources and variations in a large old antimony mine, China. J Soil Sediment 13, 106–116.

Fulda, B., Voegelin, A., Kretzschmar, R., 2013. Redox-controlled changes in cadmium solubility and solid-phase speciation in a paddy soil as affected by reducible sulfate and copper. Environ Sci Technol 47, 12775–12783.

Grybos, M., Davranche, M., Gruau, G., Petitjean, P., 2007. Is trace metal release in wetland soils controlled by organic matter mobility or Fe-oxyhydroxides reduction? J Colloid Interf Sci 314, 490–501.

Harrison, S.J., Lepp, N.W., Phipps, D.A., 1979. Uptake of copper by excised roots .2. Copper desorption from the free space. Z Pflanzenphysiol 94, 27–34.

Hofacker, A.F., Voegelin, A., Kaegi, R., Weber, F.A., Kretzschmar, R., 2013. Temperature-dependent formation of metallic copper and metal sulfide nanoparticles during flooding of a contaminated soil. Geochim Cosmochim Ac 103, 316–332.

Houba, V.J.G., Temminghoff, E.J.M., Gaikhorst, G.A., van Vark, W., 2000. Soil analysis procedures using 0.01 M calcium chloride as extraction reagent. Commun Soil Sci Plant Anal 31, 1299–1396.

Houba, V.J.G., van der Lee, J.J.G., Novozamsky, I., 1997. Soil and plant analysis. Part 1: soil analysis procedures. Wageningen University, Wageningen, The Netherlands.

Hu, P.J., Li, Z., Yuan, C., Ouyang, Y.N., Zhou, L.Q., Huang, J.X., Huang, Y.J., Luo, Y.M., Christie, P., Wu, L.H., 2013. Effect of water management on cadmium and arsenic accumulation by rice (Oryza sativa L.) with different metal accumulation capacities. J Soil Sediment 13, 916–924.

Huang, C.Y.L., Schulte, E.E., 1985. Digestion of plant-tissue for analysis by ICP Emission-Spectroscopy. Commun Soil Sci Plan 16, 943–958.

Kalis, E.J.J., Temminghoff, E.J.M., Visser, A., van Riemsdijk, W.H., 2007. Metal uptake by Lolium perenne in contaminated soils using a four-step approach. Environ Toxicol Chem 26, 335–345.

Kaiser, K., Guggenberger, G., Haumaier, L., Zech, W., 1997. Dissolved organic matter sorption on subsoils and minerals studied by C-13-NMR and DRIFT spectroscopy. Eur J Soil Sci 48, 301–310.

Kashem, M.A., Singh, B.R., 2001. Metal availability in contaminated soils: II. Uptake of Cd, Ni and Zn in rice plants grown under flooded culture with organic matter addition. Nutr Cycl Agroecosys 61, 257–266.

Khaokaew, S., Chaney, R.L., Landrot, G., Ginder-Vogel, M., Sparks, D.L., 2011. Speciation and release kinetics of cadmium in an alkaline paddy soil under various flooding periods and draining conditions. Environ Sci Technol 45, 4249–4255.

Kögel-Knabner, I., Amelung, W., Cao, Z.H., Fiedler, S., Frenzel, P., Jahn, R., Kalbitz, K., Kolbl, A., Schloter, M., 2010. Biogeochemistry of paddy soils. Geoderma 157, 1–14.

Kokot, S., Phuong, T.D., 1999. Elemental content of Vietnamese rice - Part 2. Multivariate data analysis. Analyst 124, 561–569.

Koopmans, G.F., Groenenberg, J.E., 2011. Effects of soil oven-drying on concentrations and speciation of trace metals and dissolved organic matter in soil solution extracts of sandy soils. Geoderma 161, 147–158.

Kukier, U., Chaney, R.L., 2002. Growing rice grain with controlled cadmium concentrations. J Plant Nutr 25, 1793–1820.

Kuo, S., Lai, M.S., Lin, C.W., 2006. Influence of solution acidity and $CaCl_2$ concentration on the removal of heavy metals from metal-contaminated rice soils. Environ Pollut 144, 918–925.

Laborte, A.G., de Bie, K., Smaling, E.M.A., Moya, P.F., Boling, A.A., Van Ittersum, M.K., 2012. Rice yields and yield gaps in Southeast Asia: Past trends and future outlook. Eur J Agron 36, 9–20.

Lefroy, R.D.B., Mamaril, C.P., Blair, G.J., Gonzales, P. J., 1992. Sulphur cycling in rice wetlands. In sulphur cycling on the continents: wetlands, terrestrial ecosystems and associated water bodies. John Wiley & Sons Ltd:Chicherster, pp. 279−300.

Liu, J.G., Qian, M., Cai, G.L., Yang, J.C., Zhu, Q.S., 2007. Uptake and translocation of Cd in different rice cultivars and the relation with Cd accumulation in rice grain. J Hazard Mater 143, 443−447.

Liu, W.J., Zhu, Y.G., Hu, Y., Williams, P.N., Gault, A.G., Meharg, A.A., Charnock, J.M., Smith, F.A., 2006. Arsenic sequestration in iron plaque, its accumulation and speciation in mature rice plants (Oryza sativa L.). Environ Sci Technol 40, 5730−5736.

Lofts, S., Spurgeon, D.J., Svendsen, C., Tipping, E., 2004. Deriving soil critical limits for Cu, Zn, Cd, and pH: A method based on free ion concentrations. Environ Sci Technol 38, 3623–3631.

Masironi, R., Koirtyohann, S.R., Pierce, J.O., 1977. Zinc, cadmium, copper and chromium in polished and unpolished rice. Sci Total Environ 7, 27–43.

McLaughlin, M.J., Singh, B.R., 1999. Cadmium in soils and plants. Dordrecht, The Netherlands, Kluwer Academic Publishing, pp. 13–21.

McLaughlin, M.J., Parker, D.R., Clarke, J.M., 1999. Metals and micronutrients - food safety issues. Field Crop Res 60, 143–163.

Meharg, A.A., Norton, G., Deacon, C., Williams, P., Adomako, E.E., Price, A., Zhu, Y.G., Li, G., Zhao, F.J., McGrath, S., Villada, A., Sommella, A., De Silva, P.M.C.S., Brammer, H., Dasgupta, T., Islam, M.R., 2013. Variation in rice cadmium related to human exposure. Environ Sci Technol 47, 5613–5618.

Mongon, J., Konnerup, D., Colmer, T.D., Rerkasem, B., 2014. Responses of rice to $Fe^{2+}$ in aerated and stagnant conditions: growth, root porosity and radial oxygen loss barrier. Funct Plant Biol 41, 922–929.

Moriyama, T., Shindoh, K., Taguchi, Y., Watanabe, H., Yasui, A., Joh, T., 2003. Changes in the cadmium content of rice during the milling process. J Food Hyg Soc Jpn 44, 145–149.

Murase, J., Kimura, M., 1997. Anaerobic reoxidation of $Mn^{2+}$, $Fe^{2+}$, $S^0$ and $S^{2-}$ in submerged paddy soils. Biol Fert Soils 25, 302–306.

Novozamsky, I., van Eck, R., Houba, V.J.G., van der Lee, J.J., 1986. Use of ICP-AES for determination of iron, aluminium and phosphorus in Tamm’s soil extracts. Neth J Agric Sci 34, 185–191.

Pan, Y.Y., Koopmans, G.F., Bonten, L.T.C., Song, J., Luo, Y.M., Temminghoff, E.J.M., Comans, R.N.J., 2014. Influence of pH on the redox chemistry of metal (hydr)oxides and organic matter in paddy soils. J Soil Sediment 14, 1713–1726.

Peijnenburg, W.J.G.M., Zablotskaja, M., Vijver, M.G., 2007. Monitoring metals in terrestrial environments within a bioavailability framework and a focus on soil extraction. Ecotox Environ Safe 67, 163–179.

Reynolds, B., Stevens, P.A., Hughes, S., Brittain, S.A., 2004. Comparison of field techniques for sampling soil solution in an upland peatland. Soil Use Manage 20, 454–456.

Römkens, P.F., Guo, H.Y., Chu, C.L., Liu, T.S., Chiang, C.F., Koopmans, G.F., 2009a. Characterization of soil heavy metal pools in paddy fields in Taiwan: chemical extraction and solid-solution partitioning. J Soil Sediment 9, 216–228.

Römkens, P.F.A.M., Guo, H.Y., Chu, C.L., Liu, T.S., Chiang, C.F., Koopmans, G.F., 2009b. Prediction of cadmium uptake by brown rice and derivation of soil-plant transfer models to improve soil protection guidelines. Environ Pollut 157, 2435–2444.

Schulz-Zunkel, C., Krueger, F., 2009. Trace metal dynamics in floodplain soils of the River Elbe: A review. J Environ Qual 38, 1349–1362.

Shaheen, S.M., Rinklebe, J., Rupp, H., Meissner, R., 2014. Lysimeter trials to assess the impact of different flood-dry-cycles on the dynamics of pore water concentrations of As, Cr, Mo and V in a contaminated floodplain soil. Geoderma 228–229, 5–13.

Shen, J.B., Hoffland, E., 2007. In situ sampling of small volumes of soil solution using modified micro-suction cups. Plant Soil 292, 161–169.

Shuman, L.M., Wang, J., 1997. Effect of rice variety on zinc, cadmium, iron, and manganese content in rhizosphere and non-rhizosphere soil fractions. Commun Soil Sci Plan 28, 23–36.

Simmons, R.W., Noble, A.D., Pongsakul, P., Sukreeyapongse, O., Chinabut, N., 2008. Analysis of field-moist Cd contaminated paddy soils during rice grain fill allows reliable prediction of grain Cd levels. Plant Soil 302, 125–137.

Song, J., Zhao, F.J., Luo, Y.M., McGrath, S.P., Zhang, H., 2004. Copper uptake by Elsholtzia splendens and Silene vulgaris and assessment of copper phytoavailability in contaminated soils. Environ Pollut 128, 307–315.

Sun, M.M., Luo, Y.M., Teng, Y., Jia, Z.J., Li, Z.G., Deng, S.P., 2013. Remediation of polycyclic aromatic hydrocarbon and metal-contaminated soil by successive methyl-beta-cyclodextrin-enhanced soil washing-microbial augmentation: a laboratory evaluation. Environ Sci Pollut R 20, 976–986.

Tack, F.M.G., van Ranst, E., Lievens, C., Vandenberghe, R.E., 2006. Soil solution Cd, Cu and Zn concentrations as affected by short-time drying or wetting: The role of hydrous oxides of Fe and Mn. Geoderma 137, 83–89.

Tipping, E., Rieuwerts, J., Pan, G., Ashmore, M.R., Lofts, S., Hill, M.T.R., Farago, M.E., Thornton, I., 2003. The solid-solution partitioning of heavy metals (Cu, Zn, Cd, Pb) in upland soils of England and Wales. Environ Pollut 125, 213–225.

Tsukahara, T., Ezaki, T., Moriguchi, J., Furuki, K., Shimbo, S., Matsuda-Inoguchi, N., Ikeda, M., 2003. Rice as the most influential source of cadmium intake among general Japanese population. Sci Total Environ 305, 41–51.

Uraguchi, S., Mori, S., Kuramata, M., Kawasaki, A., Arao, T., Ishikawa, S., 2009. Root-to-shoot Cd translocation via the xylem is the major process determining shoot and grain cadmium accumulation in rice. J Exp Bot 60, 2677–2688.

USDA, 1996. Soil survey laboratory methods manual. Soil survey investigations, Report No. 42. USDA, Washington, DC.

Vink, J.P.M., Harmsen, J., Rijnaarts, H., 2010. Delayed immobilization of heavy metals in soils and sediments under reducing and anaerobic conditions; consequences for flooding and storage. J Soil Sediment 10, 1633–1645.

Wang, K.R., Gong, H.Q., 1996. Compared study on the cadmium absorption and distribution of two genotypes rice (in Chinese, with English abstract). Agro-environ Prot 15, 145.

Weber, F.A., Voegelin, A., Kretzschmar, R., 2009. Multi-metal contaminant dynamics in temporarily flooded soil under sulfate limitation. Geochim Cosmochim Ac 73, 5513–5527.

Weng, L.P., Temminghoff, E.J.M., van Riemsdijk, W.H., 2001. Contribution of individual sorbents to the control of heavy metal activity in sandy soil. Environ Sci Technol 35, 4436–4443.

Weis, J.S., Weis, P., 2004. Metal uptake, transport and release by wetland plants: implications for phytoremediation and restoration. Environ Int 30, 685–700.

Williams, P.N., Zhang, H., Davison, W., Zhao, S.Z., Lu, Y., Dong, F., Zhang, L., Pan, Q., 2012. Evaluation of in situ DGT measurements for predicting the concentration of Cd in Chinese field-cultivated rice: Impact of soil Cd:Zn ratios. Environ Sci Technol 46, 8009–8016.

Yu, H., Wang, J.L., Fang, W., Yuan, J.G., Yang, Z.Y., 2006. Cadmium accumulation in different rice cultivars and screening for pollution-safe cultivars of rice. Sci Total Environ 370, 302–309.

Zeng, F.R., Ali, S., Zhang, H.T., Ouyang, Y.B., Qiu, B.Y., Wu, F.B., Zhang, G.P., 2011. The influence of pH and organic matter content in paddy soil on heavy metal availability and their uptake by rice plants. Environ Pollut 159, 84–91.

## Appendix

**Table A.1.**

Ratios between trace metal contents in the above-ground rice plant tissues and roots for rice plant cultivar A159 at the final harvest (day 128).

| Ratios | Cd | Zn | Cu | Ni | Pb |
|---|---|---|---|---|---|
| Stem:root | 0.99±0.26 | 1.28±0.15 | 0.12±0.04 | 0.16±0.04 | 0.03±0.01 |
| Leave:root | 0.72±0.10 | 1.17±0.12 | 0.17±0.02 | 0.46±0.11 | 0.19±0.08 |
| Husk:root | 0.20±0.04 | 0.33±0.07 | 0.03±0.01 | 0.08±0.02 | 0.01±0.002 |
| Grain:root | 0.27±0.06 | 0.52±0.09 | 0.05±0.01 | 0.24±0.08 | 0.003±0.001 |

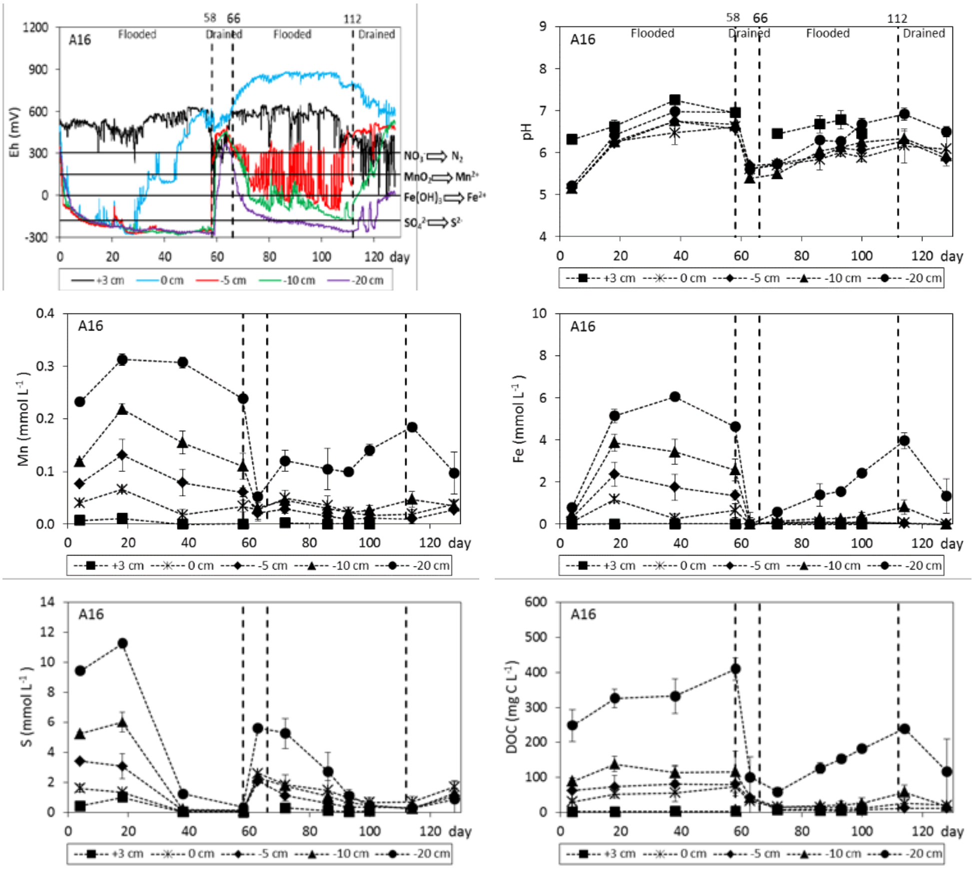

**Fig. A.1.** The Eh, pH, and Mn, Fe, S, and DOC concentration in the soil solution as a function of time in the pot experiment with rice plant cultivar A16 (+3 cm refers to 3 cm above the interface, 0 cm equal the interface between the soil surface and the water layer, and -5, -10 cm, -20 cm below the interface, respectively).

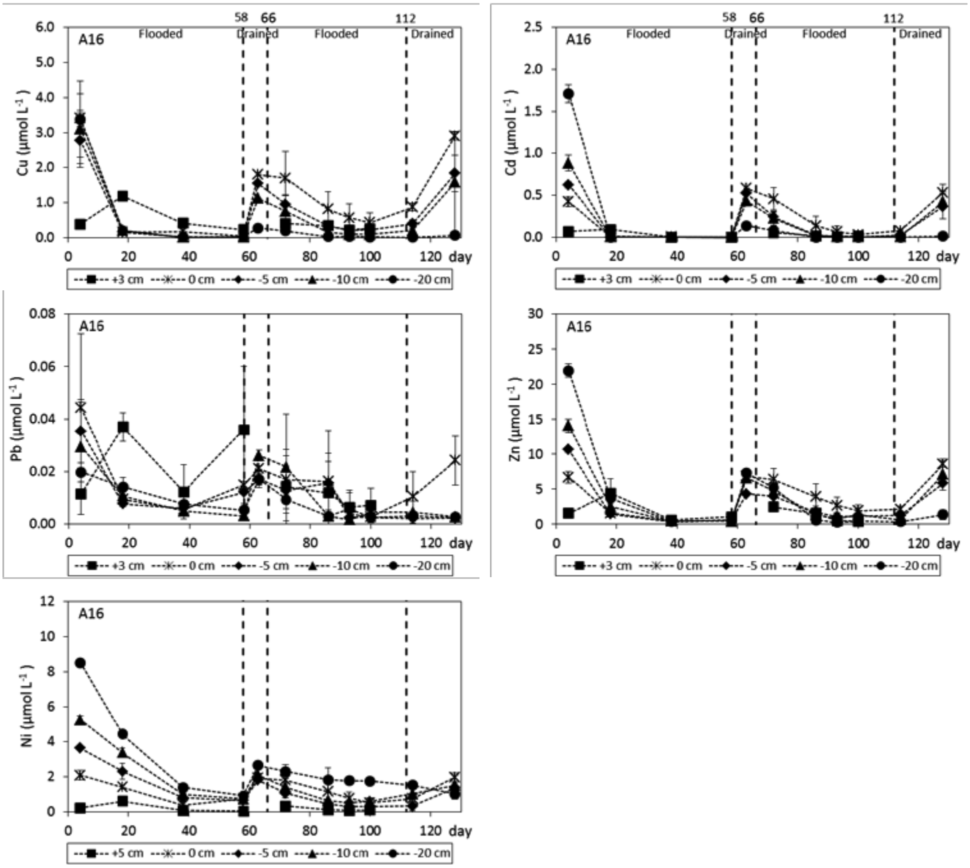

**Fig. A.2.** Total dissolved concentrations of Cu, Cd, Pb, Zn, and Ni in the soil solution as a function of time in the TZ soil with growing A16 (+3 cm refers to 3 cm above the interface, 0 cm equal the interface between the soil surface and the water layer, and -5, -10 cm, -20 cm below the interface, respectively).

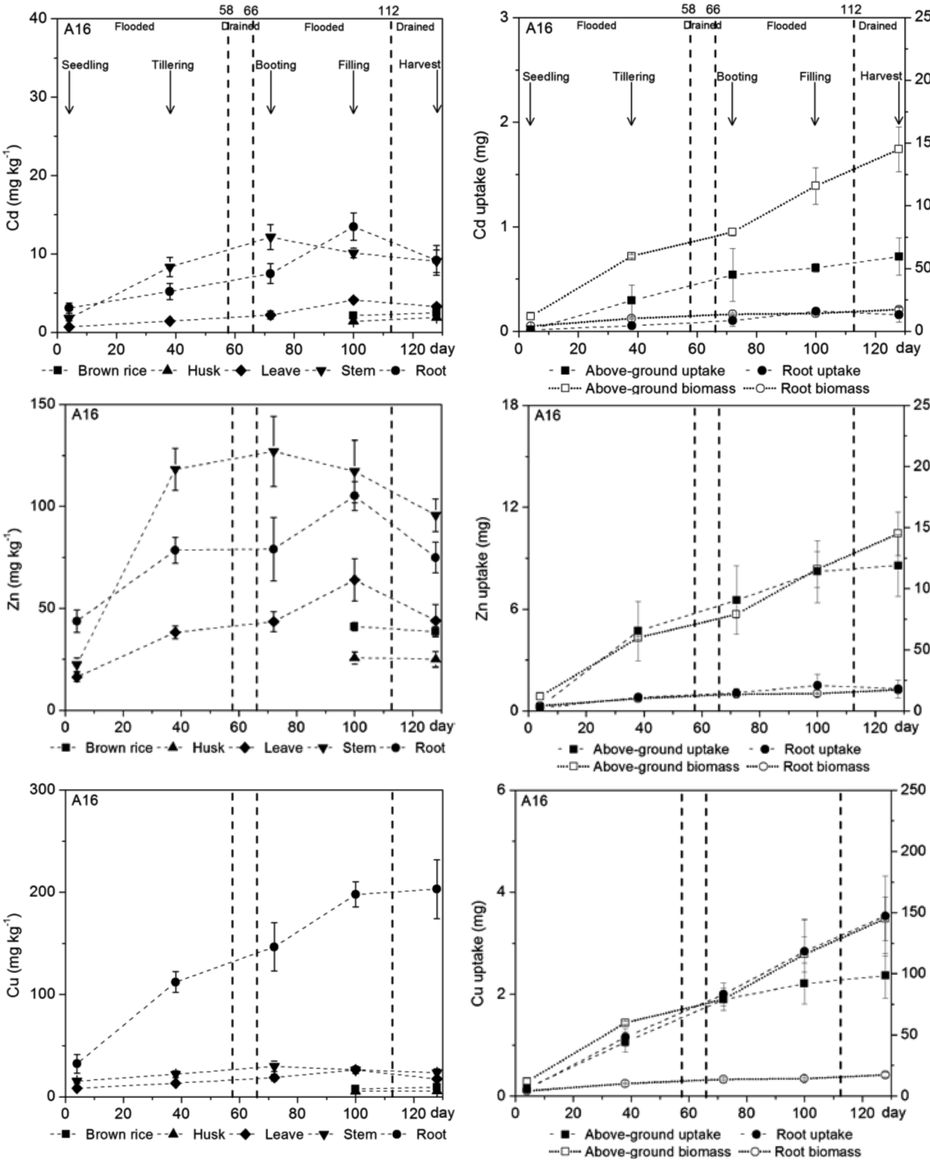
A16
58
66
112
Flooded
Drained
Flooded
Drained
Seedling
Tillering
Booting
Filling
Harvest
Cd (mg kg-1)
Cd uptake (mg)
Dry biomass (mg)
Zn (mg kg-1)
Zn uptake (mg)
Cu (mg kg-1)
Cu uptake (mg)
day
Brown rice
Husk
Leave
Stem
Root
Above-ground uptake
Root uptake
Above-ground biomass
Root biomass

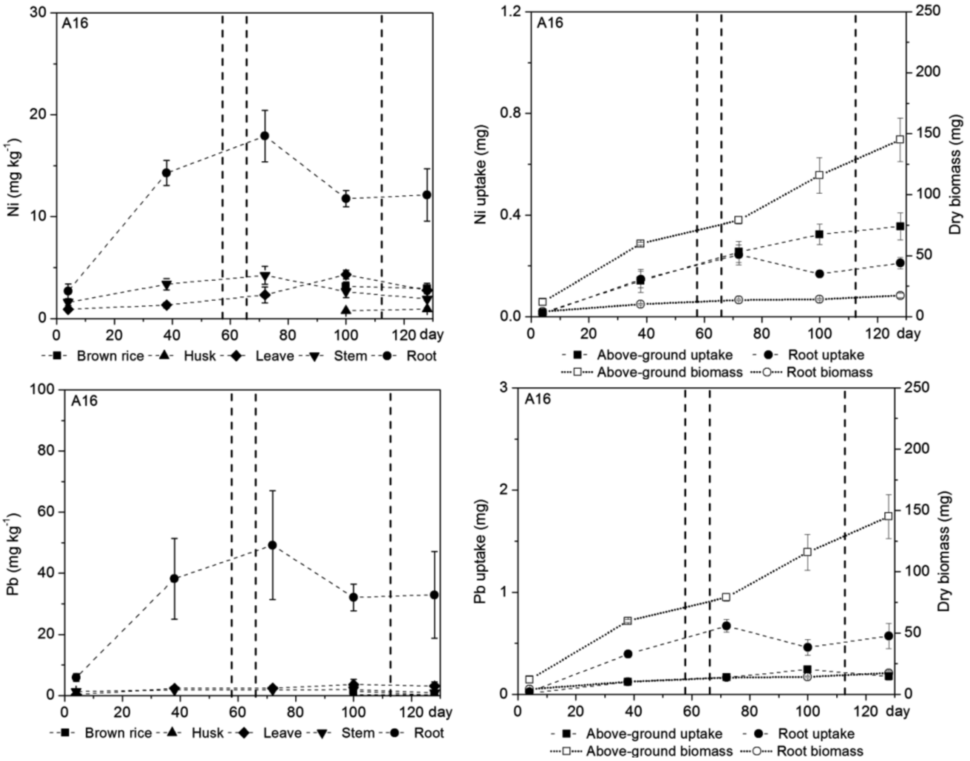

**Fig. A.3.** Total contents of trace metals (left) and uptake rate of trace metals (right) in different rice tissues of the rice cultivar A16 during major rice growth stages.

# Chapter 6

# General discussion

*Yunyu Pan*

## *6.1. Introduction*

The uptake of trace metals by rice (*Oryza sativa* L.) depends on the bioavailability of trace metals in lowland paddy soils (Simmons et al., 2008; Römkens et al., 2009a) and also on specific factors of rice plants, i.e., different cultivars differing in their ability to transfer trace metals from root to shoot (Yu et al., 2006; Römkens et al., 2009b). The bioavailability of trace metals in lowland paddy soils is largely determined by the solubility of trace metals. During cultivation of lowland rice, solubility of trace metals in lowland paddy soils is influenced greatly by the alternating flooding and drainage periods (i.e., at late tillering stage and pre-harvest of rice), resulting in continuous fluctuations of redox potential (Eh) and consequently non-equilibrium or re-equilibration of trace metals' partitioning between soil solution (i.e., free metal concentrations, DOC-complexed, and inorganic-complexed forms) and the solid phase (i.e., complexation by clay, soil organic matter (SOM), and metal-(hydr)oxides). Particularly for these reactive surfaces, they are important parameters in determining the speciation and bioavailability of trace metals in paddy soils. As for the uptake of trace metals by rice plants, the uptake and translocation of trace metals were regulated by different rice cultivars and genotypes, by different rice tissues particularly the root retention and root to shoot translocation (Liu et al., 2007; Uraguchi et al., 2009), by different rice growth stages particularly the rice filling stage coinciding with the drainage period for pre-harvest (Chaney et al., 1996; Kashem and Singh, 2001; Simmons et al., 2005, 2008). Therefore, the overall objective of this Ph.D. thesis was to study the speciation of trace metals with regard to their bioavailability in lowland paddy soils and subsequently the uptake of trace metals by rice plants.

To understand the speciation of trace metals in lowland paddy soils, I chose two typical contaminated paddy soils (Chapter 2 and 3) and more importantly, Cd content of rice grain is much higher than that of food criteria (0.2 mg kg$^{-1}$, P.R. China; 0.4 mg kg$^{-1}$, WHO) in these soil sampling areas (Brus et al., 2009; Sun et al., 2013). Further, I simulated the traditional water management for rice paddy fields and drained the paddy soils reflecting the two stages of rice growth: the late tillering stage in order to control ineffective tillering and shortly before the harvest to enable faster rice ripening and easier harvesting (Chapter 2, 3, and 5). Therefore, paddy soils undergo at least two successive flooding and drainage periods resulting in continuous Eh fluctuations. To monitor the Eh fluctuations, I employed an in-situ Eh measurement device to study the Eh dynamics (Chapter 2-5). Then, I used the Eh dynamics to explain the change of pH, SOM, and metal-(hydr)oxides, and the solubility of trace metals in the two paddy soils exposed to alternating flooding and drainage periods (chapter 2, 3, and 5). My results provide the insights to understand the pH effect on the magnitude of the redox chemistry of metal-(hydr)oxides and organic matter, and the effects of changes in Eh and redox chemistry of these reactive surfaces on the solubility of trace metals in contaminated paddy soil systems exposed to alternating flooding and drainage conditions. Among these different metal forms between soil solution and the solid phase, the free trace metal ions in soil solution are usually considered to be the most bioavailable species for plant uptake (Bell et al., 1991; Smolders and McLaughlin, 1996; Parker and Pedler, 1997). To further understand the free trace metal concentrations in soil solution, we employed the modified field Donnan Membrane Technique (DMT) (van der Stelt et al., 2005) to measure free trace metal concentrations in situ at different depths in a flooded paddy soil (Chapter 4). This successful application of field DMT provides a potential tool to measure free trace metal concentrations in flooded soil and sediment systems in situ. To study metal speciation, a multi-surface modeling approach similar to that of Bonten et al. (2008) and Dijkstra et al. (2009) was used to investigate the metal speciation in soil solution (Chapter 4) and the partitioning of the metals between the solution and the solid phase (Chapter 2 and 3) under both aerobic and anaerobic conditions. The application of the multi-surface modeling approach under anaerobic conditions provides the insight of trace metals' distribution in a widened environmental context and raises more interesting topics with regard to future model development, i.e., incorporating features or processes that are currently insufficiently accommodated in the model to provide adequate predictions of metal speciation under anaerobic conditions. To understand the uptake of trace metals by rice plants, we chose two rice cultivars of high and low Cd accumulation in brown rice (Hu et al., 2013) growing in an acidic paddy soil (Chapter 5). We further linked the soil solution concentrations of trace metals with their uptake by rice plants during major rice growth stages over time (Chapter 5).

In this last chapter, I will discuss the major findings and their implications and I will give suggestions for future research. Firstly, I will discuss the influence of pH on redox chemistry of metal-(hydr)oxides and organic matter in paddy soils. Secondly, I will discuss the solubility of trace metals in the same two paddy soils exposed to alternating flooding and drainage periods. Thirdly, I will discuss the potential application of field DMT in the flooded paddy soil. Fourthly, I will discuss the constraints of multi-surface modeling approach when applying it under anaerobic conditions. Finally, I will discuss the relationship between the soil solution concentrations of trace metals in the lowland paddy soil and their uptake by rice during major rice growth stages over time.

## *6.2. The role of pH in redox chemistry in lowland paddy soils*

Rice is usually cropped in lowland paddy soils. During cultivation of lowland rice, paddy soils undergo at least two successive flooding and drainage periods (Chapter 2). These flooding and drainage periods can considerably affect the redox chemistry of paddy soils by either reduction (i.e., $NO_3^-$ to $NO_2^-$, $Mn^{+3/+4}$ to $Mn^{+2}$, $Fe^{+3}$ to $Fe^{+2}$, and $SO_4^{2-}$ to $S^{2-}$) or oxidation (i.e., organic matter oxidized and DOM release) processes. In either reduction or oxidation processes, soil and soil solution chemistry change markedly, especially with regard to metal-(hydr)oxides and organic matter. The magnitude of the redox processes is determined by soil properties, especially pH. However, the current knowledge is still limited with regard to the effects of pH on the redox chemistry of metal-(hydr)oxides and organic matter in soil systems with alternating flooding and drainage conditions.

In Chapter 2, I have clearly shown the influence of pH on the redox chemistry of metal-(hydr)oxides and organic matter in two lowland paddy soils. During the two successive flooding-draining cycles, vertical gradients in the Eh decreasing with depth developed at different layers during flooding periods but increased rapidly to an Eh level of 400 mV in all layers during drainage periods in both paddy soils. Correspondingly, the pH of the acidic soil increased with decreasing Eh and vice versa, whereas the pH of the alkaline soil was buffered by $CaCO_3$. The decrease in Eh upon flooding associated with the pH difference between two soils led to a different response in the solubility of Mn- and Fe-(hydr)oxides between the acidic soil and the alkaline soil. In the acidic soil, Mn and Fe solubility increased during flooding due to reductive dissolution of their (hydr)oxides and decreased during drainage because of re-oxidation. In the alkaline soil, Mn and Fe solubility did not increase during flooding, because Mn(II) and Fe(II) immediately precipitated as $MnCO_3$, $FeCO_3$, and/or FeS. By comparing the measured concentrations of Mn and Fe with their predicted concentrations, the kinetically-limited reductive dissolution of Mn- and Fe-(hydr)oxides was revealed in the acidic soil. In the alkaline soil, such kinetically-limited reduction processes were not observed because the higher pH results in the likely formation of $MnCO_3$ and $Fe(II)CO_3$ and a lower solubility of Fe-(hydr)oxides maintaining the Mn and Fe solubility at low level. After flooding, DOC was mobilized in both soils. In the acidic paddy soil, a high correlation between DOC and dissolved Fe concentrations was found, which can be attributed to the decrease in the reactive surface area of Fe (III)-(hydr)oxides due to reductive dissolution and subsequently the increase in DOC concentrations as mobilized from the adsorbed SOM on the Fe (III)-(hydr)oxides. However, such correlation was not found in the alkaline paddy soil, which can be attributed to the precipitation of dissolved Fe (II) as $FeCO_3$ or FeS after reduction of Fe (III)-(hydr)oxides. In addition to DOC mobilization by reductive dissolution of Fe (III)-(hydr)oxides, release of fermentation products might also have contributed to the elevated DOC concentrations because mineralization is incomplete under anaerobic conditions (Vink et al. 2010).

These results suggest that the pH largely determines the magnitude of the redox processes with regard to the metal-(hydr)oxides and organic matter. Particularly in the acidic soil, the revealed kinetically-limited dissolution of metal-(hydr)oxides provides an in-depth understanding of metal-(hydr)oxides' dissolution under anaerobic conditions by comparing the measurements with the predictions. Nevertheless, multi-surface modeling only provides an indication for the solubility of metal-(hydr)oxides. Further studies should use mineralogical techniques to identify the real formed minerals controlling Mn and Fe solubility before and after flooding and subsequently the release of DOC associated to such minerals. Moreover, the present modeling approach assumes chemical equilibrium. A more dynamic modeling approach should be developed with consideration of the mineralization rate of SOM and the dissolution rate of metal-(hydr)oxides under changing redox conditions. An in-depth understanding of the dissolution of metal-(hydr)oxides and release of DOM under anaerobic conditions will increase the understanding of trace metal solubility in lowland paddy soils exposed to alternating flooding and drainage conditions.

### *6.3. The role of SOM and metal sulfides in determining solubility of trace metals in lowland paddy soils*

The solubility of trace metals in paddy soils exposed to alternating flooding and drainage conditions determines their bioavailability and uptake by rice plants. Flooding and drainage of paddy soils will influence the Eh and redox chemistry of paddy soils (Chapter 2), but current knowledge on how the changes in Eh and redox chemistry will affect the solubility of trace metals in contaminated paddy soils is still limited.

In Chapter 3, I have studied the solubility of trace metals in the same two paddy soils exposed to alternating flooding and drainage periods. To understand the solubility-controlling processes of trace metals, I firstly performed two types of model calculations: one including the formation of metal sulfides and cuprite and one without these minerals to reveal the trace metal distribution between the solution and solid phase under both anaerobic and aerobic conditions, respectively. Comparison between measurements and predictions of total dissolved trace metal concentrations by the multi-surface modeling approach clearly showed the importance of including sulfide minerals in our model calculations when predicting the solubility of trace metals under anaerobic conditions. In addition, the modeling results suggest SOM is the dominant reactive surface in the binding of trace metals under aerobic conditions whereas sulfide minerals largely control the solubility of trace metals under anaerobic conditions. These modeling results provided the in-depth understanding and interpretation of trace metals' distribution and solubility in lowland paddy soils exposed to alternating flooding and drainage conditions.

Indeed, during two successive flooding-draining cycles of the two paddy soils, the dynamics in Eh and pH and the change in the reactive surface of SOM and the minerals of sulfide precipitates greatly affected the solubility of trace metals for both soils. The solubility of trace metals was generally much lower in the alkaline soil than in the acidic soil due to the higher pH level and the presence of $CaCO_3$ in the alkaline soil. Under aerobic conditions, the higher pH of the alkaline soil leads to a stronger complexation of trace metals by reactive surfaces within the soil solid phase than in the acidic soil. Under anaerobic conditions, the solubility of most trace metals in both soils is controlled by sulfide precipitates, but the higher pH of the alkaline soil leads to lower trace metal concentrations in soil solution at equilibrium. When we drained the soil columns, the oxidation of sulfide precipitates can increase the trace metals in soil solution of the acidic soil, whereas the high pH conditions might maintain trace metal concentrations at low level in the soil solution of the alkaline soil

The combination of modeling and experimental approaches is evidenced as an effective method to identify the solubility-controlling processes. In this case, the solubility of trace metals under anaerobic conditions was adequately explained by modeling output. Our results also provide new thoughts for the present ecological risk assessment and the derivation of risk-based standards to protect the endangered species. Apparently, in flooded soil or sediment systems, Eh is a very crucial parameter determining the solubility and bioavailability of trace metals under anaerobic conditions. Besides Eh, sulfate content is another important parameter determining the capacity of flooded soils or sediments for sequestering trace metals into sulfide precipitates. Therefore, it is recommended to incorporate these parameters in deriving risk-based standards to reflect the flooding conditions and ecological risks.

## *6.4. Field DMT- a useful tool to measure free trace metal concentrations in flooded soil systems in situ*

The distribution of trace metals between soil solution and solid phase has been discussed in Chapter 3. In soil solution, total dissolved trace metal concentrations can be considered as the directly available pool of trace metals related to the uptake of metals by soil organisms and plants (Römkens et al., 2009a). Among the species of dissolved trace metals in soil solution, the free trace metal concentrations are usually considered as the most bioavailable species for plant uptake (Bell et al., 1991; Smolders and McLaughlin, 1996; Parker and Pedler, 1997). To measure free trace metal concentrations in solution systems, several analytical techniques have been briefly summarized in Chapter 4. These techniques, however, have not been applied in flooded soil systems. Among these techniques, the DMT has shown unique advantages, which do not perturb the equilibrium between free trace metal ions and other forms of trace metals in solution and allows for measuring the free ion concentrations of multiple elements at the same time (Temminghoff et al., 2000). Particularly the field DMT could be potentially applied in flooded paddy soils in situ without perturbing the Eh and maintaining anaerobic conditions as described in Chapter 2 and 3. Nevertheless, before the field DMT can be used in paddy fields, this analytical technique first needs to be tested since it has not been used previously to measure free trace metal concentrations in-situ in flooded soils.

In Chapter 4, I tested this field DMT technique in a carefully designed soil column experiment in which a field-contaminated paddy soil was flooded. During the course of flooding the column, the Eh gradients were developed from the aerobic water layer to the anaerobic bottom soil layer, leading to the reductive dissolution of Mn- and Fe-(hydr)oxides, and the increase of pH and DOC concentrations in soil layers, particularly the bottom soil layer. The free concentrations of Ni, Zn, Cd, Cu(II), and Pb as measured with the field DMT were lower in the solution of the upper and bottom soil layers than in the overlying water layer, due to the increased pH in these layers under anaerobic conditions. Similarly, the total dissolved trace metal concentrations decreased from the overlying water layer to the two soil layers of the soil profile, which was attributed to a stronger binding of the trace metals to the soil solid phase at the elevated pH in these layers. The total dissolved concentrations of trace metals with a high affinity to bind to DOM (i.e., Cu(II) and Pb) decreased even further from the upper soil layer to the bottom soil layer, whereas the DOM concentrations was higher in the bottom soil layer than in the upper soil layer, in which the pH was nearly the same. This further decrease in the total dissolved Cu and Pb concentrations while their free concentrations remain the same might be due to the decrease in the reactivity of DOM in the soil solution under anaerobic conditions relative to the DOM reactivity in the less anaerobic upper soil layer. This is in agreement with the findings of Hanke et al. (2014), who found a decrease in the affinity of DOM to bind to short-range ordered Fe-(hydr)oxides under anaerobic conditions. They attributed these findings to compositional changes in the DOM due to anaerobic processes. In parallel with a possible decrease in the reactivity of the DOM, reduction of humic acids present within SOM in the bottom soil layer, which was more strongly reduced than the upper soil layer, might have led to compositional changes including the formation of reduced sulfur-containing ligands (Qian et al., 2002). Trace metals have a higher affinity to bind to reduced sulfur-containing ligands of humic acids than to oxygen-containing ligands such as carboxylic groups (Smith et al., 2002; Maurer et al., 2012). Consequently, reduction of humic acids present within SOM and formation of such reactive functional groups in the bottom soil layer might have contributed to the lower total dissolved Cu and Pb concentrations in this layer. Therefore, the composition and reactivity of DOM and SOM under anaerobic conditions requires further investigation.

In Chapter 4, I also used the field DMT measurements to validate the multi-surface modeling approach in widened environmental conditions including the anaerobic soil solution systems. In general, the multi-surface modeling used in our study adequately predicted the free trace metal concentrations in the aerobic water layer of the soil columns when compared to measured concentrations as obtained by the field DMT for most trace metals, except for Pb. For trace metals with a low affinity to form complexes with DOM, predictions of the free concentrations for the two anaerobic soil layers were in good agreement with the measured concentrations. However, the free concentrations of trace metals with a high affinity for complexation to DOM were poorly predicted under anaerobic conditions. Although the speciation modeling approach used here has been demonstrated to perform well under aerobic conditions in this and many previous studies (e.g., Weng et al., 2002; Kalis et al, 2006), it does not fully capture all the chemical processes occurring under anaerobic conditions.

According to this experiment in Chapter 4, the field DMT has been proved to be a useful tool for the in-situ measurement of free trace metal concentrations in flooded paddy soils. Potentially, this technique can be also applied in wetlands and sediments. Since free trace metal concentrations are the most bioavailable species for organism and plant uptake, the measured free metal concentrations, other than the normally used total metal concentrations, can be incorporated in the biotic ligand model (BLM) that are being used for the purpose in developing more risk-based water quality criteria and in performance of aquatic risk assessments for metals (Santore et al., 2001; Paquin et al., 2002; Reiley, 2007). More recently, the measured free metal concentrations by combining with the BLM can be used in tiered risk assessments under the European Water Framework Directive (Comber et al., 2008). For ongoing developments with regard to the protection of soil ecosystems, DMT can be also used in soils similar to the study in this Ph.D. thesis with combination of BLM to derive risk-based standards and perform risk assessments for metals in soils.

### *6.5. Constraints of multi-surface modeling approach under anaerobic conditions*

Geochemical speciation modeling can be a useful tool to investigate the underlying mechanisms of trace metal speciation in soil solution and the solid phase. In Chapter 2, 3, and 4, we used the multi-surface modeling approach to provide the insight of metal speciation under both the aerobic and anaerobic conditions and major modeling results have been reported in these corresponding chapters.

Generally, the multi-surface modeling approach has performed well under aerobic conditions, whereas the constraints with regard to the application of this approach under anaerobic conditions have been found. For soil solution speciation modeling, I found that the free concentrations of trace metals with a high affinity for complexation to DOM were poorly predicted under anaerobic conditions (Chapter 4). The proper reason can be attributed to the decreased reactivity and the compositional changes of DOM under anaerobic conditions as discussed previously. Therefore, a better insight into the composition and reactivity of DOM released under anaerobic conditions is required to obtain better model predictions for trace metals with a high affinity for complexation with DOM.

For partitioning modeling of trace metals between soil solution and the solid phase, several constraints might hamper the application of multi-surface modeling under anaerobic conditions. In Chapter 2, I found that chemical processes such as precipitation and dissolution of Fe-(hydr)oxides under alternating flooding and drainage conditions can be kinetically-limited, which might restrict the applicability of multi-surface modeling for such systems due to their chemical equilibrium nature. In Chapter 2 and 4, I found that the reactive surfaces of adsorbents including SOM and Fe-(hydr)oxides can decrease upon flooding while compositional changes can take place within the SOM and DOM including the formation of reduced sulfur-containing ligands (Qian et al., 2002) which influence the reactivity of these surfaces for binding trace metals. In Chapter 3, I found that formation of minerals such as metal sulfides in flooded soils or sediments can take place under anaerobic conditions (Morse and Luther, 1999; Weber et al., 2009). Since there is still little experimental evidence on the chemical identity of such (particularly Cu) sulfides formed under anaerobic conditions (Weber et al., 2009), it is difficult to include this process in multi-surface modeling approach. It is also worth pointing out that multi-surface modeling only provides an indication but not conclusive evidence. For confirmation of this indication, however, mineralogical techniques such as x-ray diffraction, electron induced x-ray emission spectroscopy, and x-ray absorption near edge structure spectroscopy can be used (Shenker and Bloom, 2005). Particularly due to the complexity of Cu sulfides under anaerobic conditions (Morse and Luther, 1999; Weber et al., 2009), the presence and chemical identity of Cu sulfide minerals formed during flooding and their solubility products should be quantified so as to allow their incorporation in multi-surface modeling approach to enable better model predictions of trace metal solubility under anaerobic conditions (Chapter 3). In summary, my results suggest that under anaerobic conditions, due to the change of composition and reactivity of DOM and SOM, and the formation of sulfide minerals, a detailed investigation with regard to the DOM, the SOM and sulfide minerals by combining the mineralogical techniques and modeling approach is required for understanding the solubility of trace metals exposed to alternating flooding and drainage.

### *6.6. Relationship between solution concentrations of trace metals and their uptake by rice plants*

Uptake of trace metals by rice plants depends on the bioavailability of trace metals in the paddy soils (Chapter 3, 4, and 5) and also depends on rice plant-specific factors (Chapter 5). The uptake of trace metals in rice grains is controlled by two pathways: uptake by the roots and translocation from roots to shoots and then to the rice grains (Liu et al., 2007; Uraguchi et al., 2009). Uptake of trace metals by rice also differs in different rice growth stages. Particularly, the rice grain filling stage has been frequently studied because this stage coincides with the second drainage period, which might increase the concentrations of trace metals in soil solution due to the dissolution of metal sulfides and potentially might increase the uptake of trace metals by rice grains (Chaney et al., 1996; Kashem and Singh, 2001; Simmons et al., 2005, 2008). Nevertheless, the solubility of trace metals in soil solution in a paddy soil exposed to alternating flooding and drainage conditions and how this sequence of processes is linked with the trace metal uptake by rice plants over time has received much less attention.

In Chapter 5, I studied the relationship between the solubility of trace metals and their uptake by rice plants from a field-contaminated paddy soil over time in a pot experiment. In this study, Cd content in brown rice exceeded the food quality standards of P.R. China (i.e., 0.2 mg kg$^{-1}$) and the WHO (i.e., 0.4 mg kg$^{-1}$) in both high (A159) and low (A16) Cd accumulation rice cultivars due to the heavy Cd contamination in soil and the high translocation of Cd from root to shoot and finally to the brown rice for both cultivars. So despite the low solubility of Cd in soil solution during both flooding periods due to the decrease of Eh and the formation of sulfide precipitates, still significant uptake and accumulation of Cd within the rice grains of both rice plant cultivars occurred. Therefore, human exposure to Cd resulting from the consumption of rice cropped in this specific contaminated paddy field might be unavoidable by specifically using the rice plant cultivar A16 with a low potential to accumulate Cd. Similar to Cd, Zn also shows high translocation rate from root to the above-ground plant tissues. On the contrary, Cu and Pb show much lower translocation rate from root to the above-ground plant tissues and are mostly retained by the root. The translocation rate of Ni are higher than for Cu and Pb but lower than for Cd and Zn, meaning Ni has an intermediate translocation behavior. Hence, root uptake and translocation of Cu and Pb into the above-ground plant tissues was strongly regulated whereas Cd and Zn translocation was more efficient.

During two successive flooding and drainage periods, the experimental results did not show a relation between trace metals' solubility and their uptake by rice tissues. The reason might be due to the fact that rice root area is a mimicked aerobic environment evidenced by the red and thin layered Fe-(hydr)oxides on the root surface. Similar to the aerobic processes during the drainage periods, Cd activities are higher in rhizosphere than in the bulk soil controlled by the sulfide minerals. Continued aerobic conditions in the rhizosphere during flooding and drainage periods might have facilitated a continuous uptake of trace metals by the rice plants at a constant rate and this is not necessarily related to the solubility of trace metals within the bulk soil. Consequently, the solubility of trace metals in the rhizosphere should be taken into account to further detail the understanding of the effects of water management of paddy fields on the uptake of trace metals by rice plants.

Our results show potential human health risks due to the high contamination level of the soil and high translocation rate of Cd from root to shoot and finally to the grains.

Therefore, selection and breeding of rice cultivars to minimize Cd accumulation is prioritizing task to reduce risks in food security and human health. Our results also suggest that for safe rice production on Cd contaminated paddy soils, soil remediation is necessary. However, remediation techniques should be cost-effective for such agricultural soil. In-situ immobilization of trace metals is a cost-effective technique by using stabilizing amendments such as lime and phosphorus rock and other Ca-Mg-P minerals (Liang et al., 2014; Zhou et al., 2014). This technique can significantly reduce the Cd content in rice grains, and meanwhile improve the Ca, Mg, and P nutrition. The alternative measure for controlling Cd contamination in paddy soils can be achieved via the change of land use and crops. For example, growing energy crops such as sugarcane and corn instead of rice can make use of the land efficiently and meanwhile produce bio-energy. For local agricultural government sector, it would be feasible to advice the farmers to use amendments in contaminated paddy soils. However, for heavily contaminated paddy soils, it would be wise to change land use or crops to reduce human health risks from trace metal contamination and meanwhile ensure farmers' living standards.

### *6.7. Future perspectives*

This Ph.D. thesis used the combined experimental and modeling approach to study the speciation of trace metals in paddy soils exposed to alternating flooding and drainage periods, and further linked the speciation of trace metals to the uptake by rice plants. However, the modeling approach used in this Ph.D. thesis assumes chemical equilibrium, which might not be able to reflect the non-equilibrium or re-equilibration of trace metals between soil solution and the solid phase under alternating flooding and drainage conditions. Therefore, a more dynamic modeling approach with incorporating mineralization rate of SOM and dissolution rate of metal-(hydr)oxides under changing redox conditions should be developed in future. Furthermore, to validate chemical processes under anaerobic conditions identified by multi-surface modeling, mineralogical techniques should be employed to investigate the composition and reactivity of DOM and SOM, and the formation of sulfide minerals for understanding the solubility of trace metals exposed to alternating flooding and drainage. In this Ph.D.

thesis, Eh and sulfate content showed the great importance in determining the speciation and bioavailability of trace metals in flooded paddy soils. Therefore, incorporation of these two parameters in derivation of risk-based standards would be more representative for the flooding conditions and ecological risks. In this Ph.D. thesis, the successful application of the field DMT in flooded paddy soil could be potentially extended to wetlands, sediments, freshwater, and seawater. More importantly, the free metal concentrations measured by field DMT can be incorporated in the BLM for improvement or implementation of present human health and ecological risk assessments. In this Ph.D. thesis, I suggest further investigation of processes controlling metal solubility and uptake by rice plants in the rhizosphere because of the mimicked aerobic environment in rice root area. The observed high Cd translocation rate from root to shoot requires countermeasures to minimize Cd risks. Therefore, selection and breeding of rice cultivars to minimize Cd accumulation is a prioritizing task, and in-situ immobilization of trace metals by using stabilizing amendments is a cost-effective soil remediation technique, and alternatively the change of land use and crops would be also feasible to reduce human health risks from trace metal contamination while ensuring farmers' living standards. In summary, this study will be useful in understanding of trace metal solubility in flooded soil and sediment systems, development of multi-surface modeling, derivation of risk-based standards, and production of safe rice on contaminated paddy soils.

## References

Bell, P.F., Chaney, R.L., Angle, J.S., 1991. Free metal activity and total metal concentrations as indexes of micronutrient availability to barley [Hordeum vulgare (L.) 'Klages']. Plant Soil 130, 51–62.

Brus, D.J., Li, Z.B., Song, J., Koopmans, G.F., Temminghoff, E.J.M., Yin, X.B., Yao, C.X., Zhang, H.B., Luo, Y.M., Japenga, J., 2009. Predictions of spatially averaged cadmium contents in rice grains in the Fuyang Valley, P.R. China. J Environ Qual 38, 1126–1136.

Bonten, L.T.C., Groenenberg, J.E., Weng, L., van Riemsdijk, W.H., 2008. Use of speciation and complexation models to estimate heavy metal sorption in soils. Geoderma 146, 303–310.

Chaney, R.L, J.A. Ryan,Y.M. Li, R.M. Welch, P.G. Reeves, S.L. Brown, Green, C.E., 1996. Phyto-availability and bio-availability in risk assessment for cadmium in agricultural environments. In: Sources of Cadmium in the Environment, OECD, Paris, France, pp. 49–78.

Comber, S.D.W., Merrington, G., Sturdy, L., Delbeke, K., van Assche, F., 2008. Copper and zinc water quality standards under the EU Water Framework Directive: The use of a tiered approach to estimate the levels of failure. Sci Total Environ 403, 12-22.

Dijkstra, J.J., Meeussen, J.C.L., Comans, R.N.J., 2009. Evaluation of a generic multisurface sorption model for inorganic soil contaminants. Environ Sci Technol 43, 6196–6201.

Hanke, A., Sauervvein, M., Kaiser, K., Kalbitz, K., 2014. Does anoxic processing of dissolved organic matter affect organic-mineral interactions in paddy soils? Geoderma 228, 62–66.

Kalis, E.J.J., Weng, L.P., Dousma, F., Temminghoff, E.J.M., van Riemsdijk, W.H., 2006. Measuring free metal ion concentrations in situ in natural waters using the Donnan Membrane Technique. Environ Sci Technol 40, 955–961.

Kashem, M.A., Singh, B.R., 2001. Metal availability in contaminated soils: I. Effects of flooding and organic matter on changes in Eh, pH and solubility of Cd, Ni and Zn. Nutr Cycl Agroecosys 61, 247–255.

Liang, X.F., Han, J., Xu, Y.M., Sun, Y.B., Wang, L., Tan, X., 2014. In situ field-scale remediation of Cd polluted paddy soil using sepiolite and palygorskite. Geoderma 235, 9-18.

Liu, J.G., Qian, M., Cai, G.L., Yang, J.C., Zhu, Q.S., 2007. Uptake and translocation of Cd in different rice cultivars and the relation with Cd accumulation in rice grain. J Hazard Mater 143, 443–447.

Maurer, F., Christl, I., Hoffmann, M., Kretzschmar, R., 2012. Reduction and reoxidation of humic acid: Influence on speciation of cadmium and silver. Environ Sci Technol 46, 8808–8816.

Morse, J.W., Luther, G.W., 1999. Chemical influences on trace metal-sulfide interactions in anoxic sediments. Geochim Cosmochim Ac 63, 3373–3378.

Paquin, P.R., Gorsuch, J.W., Apte, S., Batley, G.E., Bowles, K.C., Campbell, P.G.C., Delos, C.G., Di Toro, D.M., Dwyer, R.L., Galvez, F., Gensemer, R.W., Goss, G.G., Hogstrand, C., Janssen, C.R., McGeer, J.C., Naddy, R.B., Playle, R.C., Santore, R.C., Schneider, U., Stubblefield, W.A., Wood, C.M., Wu, K.B., 2002.

The biotic ligand model: a historical overview. Comp Biochem Phys C 133, 3-35.

Parker, D.R., Pedler, J.F., 1997. Reevaluating the free-ion activity model of trace metal availability to higher plants. Plant Soil 196, 223–228.

Qian, J., Skyllberg, U., Frech, W., Bleam, W.F., Bloom, P.R., Petit, P.E., 2002. Bonding of methyl mercury to reduced sulfur groups in soil and stream organic matter as determined by X-ray absorption spectroscopy and binding affinity studies. Geochim Cosmochim Ac 66, 3873–3885.

Reiley, M.C., 2007. Science, polic, and trends of metals risk assessment at EPA: How understanding metals bioavailability has changed metals risk assessment at US EPA. Aquat Toxicol 84, 292-298.

Römkens, P.F., Guo, H.Y., Chu, C.L., Liu, T.S., Chiang, C.F., Koopmans, G.F., 2009a. Characterization of soil heavy metal pools in paddy fields in Taiwan: Chemical extraction and solid-solution partitioning. J Soil Sediment 9, 216–228.

Römkens, P.F.A.M., Guo, H.Y., Chu, C.L., Liu, T.S., Chiang, C.F., Koopmans, G.F., 2009b. Prediction of cadmium uptake by brown rice and derivation of soil-plant transfer models to improve soil protection guidelines. Environ Pollut 157, 2435–2444.

Santore, R.C., Di Toro, D.M., Paquin, P.R., Allen, H.E., Meyer, J.S., 2001. Biotic ligand model of the acute toxicity of metals. 2. Application to acute copper toxicity in freshwater fish and Daphnia. Environ Toxicol Chem 20, 2397-2402.

Shenker, M., Bloom, P.R., 2005. Comments on "Amounts, forms, and solubility of pbosphorus in soils receiving manure". Soil Sci Soc Am J 69, 1353–1354.

Simmons, R.W., Noble, A.D., Pongsakul, P., Sukreeyapongse, O., Chinabut, N., 2008. Analysis of field-moist Cd contaminated paddy soils during rice grain fill allows reliable prediction of grain Cd levels. Plant Soil 302, 125–137.

Simmons, R.W., Pongsakul, P., Saiyasitpanich, D., Klinphoklap, S., 2005. Elevated levels of cadmium and zinc in paddy soils and elevated levels of cadmium in rice grain downstream of a zinc mineralized area in Thailand: Implications for public health. Environ Geochem Hlth 27, 501–511.

Smith, D.S., Bell, R.A., Kramer, J.R., 2002. Metal speciation in natural waters with emphasis on reduced sulfur groups as strong metal binding sites. Comp Biochem Phys C 133, 65–74.

Smolders, E., McLaughlin, M.J., 1996. Effect of Cl on Cd uptake by Swiss chard in nutrient solutions. Plant Soil 179, 57–64.

Sun, M.M., Luo, Y.M., Teng, Y., Jia, Z.J., Li, Z.G., Deng, S.P., 2013. Remediation of polycyclic aromatic hydrocarbon and metal-contaminated soil by successive methyl-beta-cyclodextrin-enhanced soil washing-microbial augmentation: a laboratory evaluation. Environ Sci Pollut R 20, 976–986.

Temminghoff, E.J.M., Plette, A.C.C., Van Eck, R., Van Riemsdijk, W.H., 2000. Determination of the chemical speciation of trace metals in aqueous systems by the Wageningen Donnan Membrane Technique. Anal Chim Acta 417, 149–157.

Uraguchi, S., Mori, S., Kuramata, M., Kawasaki, A., Arao, T., Ishikawa, S., 2009. Root-to-shoot Cd translocation via the xylem is the major process determining shoot and grain cadmium accumulation in rice. J Exp Bot 60, 2677–2688.

van der Stelt, B., Temminghoff, E.J.M., van Riemsdijk, W.H., 2005. Measurement of ion speciation in animal slurries using the Donnan Membrane Technique. Anal Chim Acta 552, 135–140.

Vink, J.P.M., Harmsen, J., Rijnaarts, H., 2010. Delayed immobilization of heavy metals in soils and sediments under reducing and anaerobic conditions; consequences for flooding and storage. J Soil Sediment 10, 1633–1645.

Weber, F.A., Voegelin, A., Kretzschmar, R., 2009. Multi-metal contaminant dynamics in temporarily flooded soil under sulfate limitation. Geochim Cosmochim Ac 73, 5513–5527.

Weng, L.P., Temminghoff, E.J.M., Lofts, S., Tipping, E., Van Riemsdijk, W.H., 2002. Complexation with dissolved organic matter and solubility control of heavy metals in a sandy soil. Environ Sci Technol 36, 4804–4810.

Yu, H., Wang, J.L., Fang, W., Yuan, J.G., Yang, Z.Y., 2006. Cadmium accumulation in different rice cultivars and screening for pollution-safe cultivars of rice. Sci Total Environ 370, 302–309.

Zhou, X., Zhou, H., Zeng, M., Hu, M., Yang, W.T., Liu, L., Liao, B.H., 2014. Effects of combined amendment (limestone + sepiolite) on heavy metal accumulation in brown rice. Acta Pedologica Sinica 51, 555–563. (in Chinese with English abstract)

# Summary

Rice (*Oryza sativa* L.) is the most staple food in South and Southeast Asia and plays a very important role in food security. However, with fast urbanization and industrialization and economic growth in these parts of the world, the production and quality of rice has become an increasing concern, because contamination of paddy soils with trace metals in industrialized areas can lead to yield reduction of rice, a decline in the nutritional quality of the rice, and accumulation of trace metal contents in rice grains. The consumption of rice with high levels of trace metals can lead to unacceptable human health risks. For example, the Cd content of rice grains cropped in paddy fields across the western plains of Taiwan has been demonstrated to frequently exceed the food quality standard of the World Health Organization (WHO), even at low levels of Cd contamination. For populations with a rice-based diet, dietary intake of Cd with rice is the major Cd exposure pathway for human beings, leading to chronic Cd poisoning with the kidneys being particularly susceptible to damage. This illustrates the need for a thorough understanding of the processes determining the uptake of trace metals by rice plants. The uptake of trace metals by rice plants is largely determined by the bioavailability of trace metals in paddy soils and by rice plant-specific factors. The bioavailability of trace metals in paddy soils is determined by complex (competition) interactions between trace metals and major cations and reactive surfaces of soil constituents like soil organic matter (SOM), clay, and Fe-, Al-, and Mn-(hydr)oxides. These interactions are, in turn, affected by environmental conditions like pH and redox potential (Eh). For all of these interactions and environmental conditions, little is known about the effects of Eh on the bioavailability of trace metals. For rice, this is particularly important, because rice is mostly grown in paddy fields where alternating flooding and draining of the fields lead to a continuously fluctuating Eh, which will affect the solubility of trace metals. The trace metal concentrations in soil solution can be directly related to uptake of trace metals by rice plants. To predict the solubility of trace metals in paddy soils, different surface complexation models can be combined into a so-called multi-surface modeling approach. This approach allows for the calculation of trace metal complexation by different reactive surfaces in soils, including SOM and dissolved

organic matter, metal-(hydr)oxides, and clay, and their precipitation as minerals. For aerobic conditions, the multi-surface modeling approach is known to adequately predict the solubility of most trace metals. For anaerobic conditions, however, this is unclear because many of the chemical reactions involved in redox processes are relatively slow, leading to non-equilibrium conditions in paddy soils. Consequently, it needs to be examined whether commonly used multi-surface models, which assume thermodynamic equilibrium, can be directly applied to such anaerobic conditions. Since the dynamic effects of flooding and drainage on the Eh and redox chemistry of paddy soils will have a large influence on the solubility of trace metals, trace metal uptake by rice plants might not be constant over time but might vary with different growth stages. For example, rice has a critical grain filling stage, and the Eh and the resulting bioavailability of trace metals during this stage might greatly determine the levels of trace metals in the rice grains. In short, it is important to quantify the solubility of trace metals in paddy soils exposed to flooding and drainage and to examine the applicability of the multi-surface modeling approach to predict trace metal solubility under anaerobic conditions. Also, the relationship between the solubility of trace metals in paddy soils exposed to alternating flooding and drainage conditions and how this sequence of processes is linked with metal uptake by rice plants over time needs to be investigated.

In Chapter 2, I investigated how flooding and draining cycles affected the redox chemistry of metal-(hydr)oxides and organic matter in paddy soils and how the pH influenced these processes. Also, I examined to what extent the multi-surface modeling approach could be used to predict the solubility of Mn and Fe during flooding and draining cycles in paddy soils. I performed a carefully-designed column experiment with two paddy soils with similar soil properties but contrasting pH. The Eh and the chemical composition of the soil solution were monitored at four depths along the soil profile during two successive flooding and drainage cycles. Flooding led to strong Eh gradients in the columns of both soils. In the acidic soil, the pH increased with decreasing Eh and vice versa, whereas the pH in the alkaline soil was buffered by $CaCO_3$. In the acidic soil, Mn and Fe solubility increased during flooding due to reductive dissolution of their (hydr)oxides and decreased during drainage because of re-oxidation. In the alkaline soil, Mn and Fe solubility did not increase during flooding due to Mn(II) and Fe(II) precipitation as $MnCO_3$, $FeCO_3$, and/or FeS. During flooding, the concentrations of dissolved organic carbon (DOC) increased in both soils, probably because of reductive dissolution of Fe-(hydr)oxides and the observed increase in the pH in the acidic soil. Comparison between measurements and multi-surface model predictions revealed that reductive dissolution of Mn- and Fe-(hydr)oxides was kinetically-limited in the acidic soil. Therefore, such rate-limiting reactions should be parameterized when applying multi-surface models to systems with changing redox conditions so as to enable more accurate predictions of the Mn and Fe solubility.

In Chapter 3, I quantified how two flooding and drainage events affected the solubility of trace metals in the same two field-contaminated paddy soils and column experiment as described in Chapter 2. Also, I tested to what extent a multi-surface modeling approach could be used to predict the solubility of trace metals under changing redox conditions. The dynamics in Eh and pH and the change in the DOC concentrations greatly affected the solubility of trace metals for both soils during two successive flooding and drainage cycles. Under aerobic conditions, the higher pH of the alkaline soil led to a stronger complexation of trace metals by reactive surfaces within the soil solid phase than in the acidic soil. Under anaerobic conditions, the solubility of most trace metals in both soils was controlled by sulfide precipitates, but the higher pH of the alkaline soil led to lower trace metal concentrations in soil solution at equilibrium. Comparison between measurements and predictions of total dissolved trace metal concentrations by multi-surface models clearly showed the importance of including sulfide minerals in our model calculations when predicting the solubility of trace metals under anaerobic conditions. However, the presence and chemical identity of Cu sulfide minerals formed during flooding and their solubility products should be quantified so as to allow their incorporation in multi-surface models and to enable better model predictions of trace metal solubility under anaerobic conditions.

In Chapter 4, I tested the potential of the field Donnan Membrane Technique (DMT) in a column experiment to measure the free trace metal concentrations in-situ in the soil solution of a flooded paddy soil under anaerobic conditions. The acidic paddy soil used in this chapter was the same one as used in Chapters 2 and 3. Also, I compared the field DMT measurements of free trace metal concentrations with predicted free trace metal concentrations as obtained by speciation modeling. In this modeling approach, the

Objects Representing CHEmical Speciation and TRAnsport (ORCHESTRA) framework was used, which includes the NICA-Donnan model. It is important to validate such a modeling approach under a wide range of geochemical conditions, because the performance of this approach under varying redox conditions has received little attention. Flooding led a strong Eh gradient along the soil profile and the pH and concentrations of Mn, Fe, and DOC increased with decreasing Eh. Under anaerobic conditions, the total dissolved trace metal concentrations decreased from the overlying water layer to the soil layers, which might be ascribed to the elevated pH outweighing the effect of the increased DOC concentrations. Also, free trace metal concentrations were lower in the soil solution of the upper and bottom soil layers than in the overlying water layer, largely due to the increased pH under anaerobic conditions. The DMT measurements and model predictions of the free trace metal concentrations were similar in the aerobic water layer, except for Pb. In both anaerobic soil layers, however, free $Cu^{2+}$ and $Pb^{2+}$ were poorly predicted. Therefore, the speciation modeling approach tested here, which is frequently being used and performs well under aerobic conditions, does not fully capture all the chemical processes occurring under anaerobic conditions. Overall, the field DMT proved to be a useful tool for the in-situ measurement of free trace metal concentrations in flooded paddy soils.

In Chapter 5, I investigated the relationship between the solubility of trace metals and their uptake by rice plants from a field-contaminated paddy soil over time in a pot experiment. Two rice plant cultivars were used with either high or low Cd accumulation characteristics. During the pot experiment, I used a water management of two successive flooding and drainage cycles of the paddy soil, similar as in Chapters 2 and 3. Also, the acidic paddy soil used here was the same one as Chapters 2, 3, and 4. The Eh was monitored continuously at five depths along the soil profile during the two successive flooding and drainage periods. Soil solution samples were taken during the major rice growth stages at the same depths to determine their chemical composition, such as the pH and the concentrations of DOC and total dissolved Mn and Fe and trace metals. Furthermore, the trace metal contents in different rice tissues including the roots, stem, leaves, husk, and brown rice were measured during the major rice growth stages. Flooding led to a strong gradient in the Eh along the soil column, and the pH and concentrations of Mn, Fe, and DOC increased with decreasing Eh, whereas drainage had the opposite effect. During flooding, the solubility of Cd, Zn, Cu, Ni, and Pb in all soil layers decreased markedly, which was explained by the formation of trace metal sulfide precipitates under anaerobic conditions. Despite the low Cd solubility during flooding, the Cd content of the rice grains exceeds the food quality standards of P.R. China and the WHO for both cultivars. For both rice plant cultivars, the trace metal contents in the different rice tissues (roots, stem, and leaves) increased at a constant rate or decreased after reaching a maximum value at later growth stages. As such, the uptake of trace metals by the rice plants over time did not reflect the high temporal variation in the solubility of the trace metals. The observed continuous metal uptake was explained by the presence of aerobic conditions near the root surface, that were maintained during the flooding periods, probably leading to a higher trace metal solubility in the rhizosphere than in the bulk soil. Consequently, the solubility of trace metals in the rhizosphere should be taken into account for further detailing the understanding of the effects of water management of paddy fields on the uptake of trace metals by rice plants. For rice production on trace metal contaminated paddy soils, either selection and breeding of rice cultivars that further minimize Cd accumulation or the potential of in-situ immobilization of trace metals by using stabilizing amendments should be investigated as a measure to mitigate human health risks from trace metal contamination.

In my Ph.D. thesis, I used a combination of experimental research and mechanistic modeling to investigate the solubility of trace metals in paddy soils exposed to alternating flooding and drainage and to link trace metal solubility to the uptake by rice plants over time. Under alternating flooding and drainage periods, the pH greatly affected the redox chemistry of metal-(hydr)oxides and organic matter in paddy soils (Chapter 2). In turn, the dynamics of Eh, pH, concentrations of Mn, Fe, and DOC had a large impact on the solubility of trace metals in paddy soils exposed to two successive flooding and drainage cycles (Chapter 3). Also, redox chemistry had a great influence on the free trace metal concentrations as these concentrations were lower in the soil solution of the upper and bottom soil layers than in the overlying water layer, largely due to the decreased Eh and increased pH under anaerobic conditions during flooding (Chapter 4). The applied multi-surface modeling approach, which works well under aerobic conditions, does not fully capture all the chemical processes occurring under anaerobic conditions (Chapters 2, 3, and 4). No significant relationship was found

between the solubility of trace metals and their uptake by different rice tissues of two different rice cultivars over time. Importantly, translocation of Cd from the roots into the above-ground biomass was high in both rice plant cultivars and the Cd contents in the rice grains exceeded the Chinese and WHO food quality standards (Chapter 5). The results of these individual chapters are integrated and discussed within a wider context in Chapter 6. In conclusion, the results of the research described in my Ph.D. thesis contribute to the understanding of how redox chemistry affects the solubility of trace metals in flooded soil and sediment systems and provide a tool for the measurement of the free trace metal concentrations in flooded soil and sediment systems in situ in the form of the field DMT. Also, my PhD thesis points to the necessity of further implementing the chemical identity of trace metal minerals formed during flooding by using mineralogical techniques so as to enable better model predictions of the solubility of trace metals. Lastly, my PhD thesis provides new ideas for the derivation of risk-based standards for trace metals by considering Eh and the sulfate content in similar flooded systems and it gives suggestions how to safeguard the production and quality of rice cropped on paddy soils contaminated with trace metals.

# Samenvatting

Rijst (*Oryza sativa* L.) is het belangrijkste voedselgewas voor de bevolking van Zuid- en Zuidoost-Azië en speelt een zeer belangrijke rol in de voedselzekerheid. Door de snelle verstedelijking, industrialisatie en economische groei in deze delen van de wereld neemt de bezorgheid over de productie en de kwaliteit van rijst toe. Dit wordt met name veroorzaakt door bodemverontreiniging van natte rijstvelden met zware metalen in geïndustrialiseerde gebieden. Dit kan namelijk leiden tot een lagere rijstoogst, een afname van de voedingswaarde van de rijst en ophoping van zware metalen in de rijstkorrels. De consumptie van rijst met hoge gehalten aan zware metalen kan leiden tot onaanvaardbare gezondheidsrisico's voor mensen. Zelfs bij lage Cd-gehalten van natte rijstteeltgronden in het westelijke deel van Taiwan overschrijdt het Cd-gehalte in rijstkorrels in veel gevallen de norm van de Wereldgezondheidsraad (WHO) voor Cd in rijst. De inname van Cd met rijst is de belangrijkste blootstellingsroute voor de mens aan Cd. Een te hoge Cd-inname door mensen kan leiden tot chronische Cd-vergiftiging, waarbij vooral de nieren bijzonder gevoelig zijn voor schade. Er is dus een grondig inzicht nodig in de processen die de opname van zware metalen door rijstplanten bepalen. De opname van zware metalen door rijstplanten wordt deels bepaald door de biologische beschikbaarheid van zware metalen in de bodem van rijstvelden en deels door specifieke eigenschappen van de rijstplanten. De biologische beschikbaarheid van zware metalen in de bodem van rijstvelden wordt bepaald door complexe interacties tussen zware metaalionen, andere macro-kationen en reactieve oppervlakken van bodembestanddelen, zoals organische stof, klei, en Fe-, Al-, en Mn-(hydr)oxiden. Deze interacties worden op hun beurt beïnvloed door milieufactoren zoals de zuurgraad en redoxcondities. Er is echter nog weinig bekend over de effecten van redoxcondities op de biologische beschikbaarheid van zware metalen in de bodem. Deze kennis is belangrijk omdat het waterpeil van natte rijstvelden tijdens de teelt van rijst sterk varieert, door het rijstveld wisselend onder water te zetten en te draineren. Dit leidt tot sterke fluctuaties in de redoxtoestand, die de oplosbaarheid van zware metalen in sterke mate kunnen beïnvloeden. De concentraties van zware metalen in het bodemvocht zijn direct gerelateerd aan de opname van zware metalen door rijstplanten. Door het combineren van verschillende “surface complexation” modellen in een zogenaamde “multi-surface” model kan de oplosbaarheid van zware metalen in rijstteeltgronden worden voorspeld. Met deze aanpak kan een voorspelling worden gemaakt van de binding van zware metalen aan verschillende reactieve oppervlakken in de bodem, zoals organische stof en opgeloste organische stof in het bodemvocht, metaal-(hydr)oxiden en klei, en het neerslaan van zware metalen in de vorm van mineralen. Onder aerobe (zuurstofrijke) omstandigheden geeft deze aanpak met het “multi-surface” model een zeer goede voorspelling van de oplosbaarheid van de meeste zware metalen. Voor anaerobe (zuurstofloze) omstandigheden is echter onduidelijk of deze aanpak afdoende werkt, omdat veel van de chemische redoxprocessen die de oplosbaarheid van zware metalen beïnvloeden relatief traag zijn. Hierdoor zal er waarschijnlijk geen sprake zijn van chemisch evenwicht onder anaerobe omstandigheden, terwijl de aanpak met het “multi-surface” model is gebaseerd op de aanname van thermodynamisch evenwicht. Het is dus belangrijk om de toepasbaarheid van “multi-surface” modellen voor anaerobe omstandigheden vast te stellen. De opname van zware metalen door rijstplanten zal waarschijnlijk niet constant zijn tijdens het groeiseizoen van de rijst maar zal varieren tijdens de verschillende groeistadia van de rijst. Deze verwachting is gebaseerd op het sterk wisselende waterpeil van natte rijstvelden tijdens de verschillende groeistadia van de rijstplanten, wat weer leidt tot sterke fluctuaties in de redoxtoestand en de redoxchemie en de oplosbaarheid van zware metalen. Rijstplanten hebben bijvoorbeeld een laatste groeistadium waarbij de rijstkorrels afrijpen; de redoxtoestand en de biologische beschikbaarheid van zware metalen tijdens dit stadium bepalen mogelijk de mate van ophoping van zware metalen in de rijstkorrels. Kortom, het is belangrijk om de oplosbaarheid van zware metalen in de bodem met een wisselend waterpeil experimenteel te kwantificeren en om de toepasbaarheid van de aanpak met een “multi-surface” model onder anaerobe omstandigheden vast te stellen. Daarnaast dient de wijze waarop de effecten van het wisselende waterpeil op de oplosbaarheid van zware metalen zijn gerelateerd aan de opname van zware metalen door rijstplanten tijdens de rijstteelt te worden gekwantificeerd.

In hoofdstuk 2 heb ik gekeken naar de effecten van nat-droog cycli van rijstteeltgronden op de redoxchemie van Fe- en Mn-(hydr)oxiden en bodemorganisch stof en heb ik onderzocht hoe de pH deze redox-processen beïnvloedt. Daarnaast heb ik onderzocht in in hoeverre een “multi-surface” aanpak met chemische evenwichtsmodellen gebruikt kan worden om de oplosbaarheid van Fe en Mn te voorspellen tijdens de nat-droog cycli. Hiervoor heb ik een zorgvuldig ontworpen kolomproef uitgevoerd met twee verschillende rijstteeltgronden. De twee gronden hadden vergelijkbare bodemeigenschappen, maar één grond was relatief zuur terwijl de andere grond kalkrijk was. Tijdens de kolomproef zijn de veranderingen van de redoxpotentiaal (Eh) en de samenstelling van het bodemvocht gedurende twee opeenvolgende nat-droog cycli op vier verschillende dieptes gevolgd. Het onder water zetten van de kolommen leidde tot een duidelijke Eh gradient voor beide grondmonsters. In de relatief zure grond steeg de pH met afnemende Eh en nam af met een toenemende Eh, terwijl in de kalkrijke grond de pH werd gebufferd door het in de grond aanwezige kalk ($CaCO_3$). In de relatief zure grond namen tijdens de natte periode de concentraties van Mn en Fe in het bodemvocht toe als gevolg van reductie van Mn- en Fe-(hydr)oxiden. Na drainage van de grondkolommen trad het omgekeerde effect op. In de kalkrijke grond namen de concentraties Mn en Fe niet toe na het onder water zetten van de grondkolommen, omdat het gereduceerde Mn en Fe onmiddellijk neersloeg in de vorm van $MnCO_3$, $FeCO_3$ en FeS. In beide gronden nam de concentratie opgelost organische koolstof (DOC) in het bodemvocht sterk toe tijdens de natte periode. Dit werd waarschijnlijk veroorzaakt door het vrijkomen van DOC bij de reductie van Mn- en Fe-hydroxiden. Daarnaast speelde in de relatief zure grond de stijging van de pH een rol bij het vrijkomen van DOC. Uit de vergelijking van de metingen en modelresultaten blijkt dat de reductie van Mn- en Fe-(hydr)oxiden een relatief traag proces is. Dit betekent dat dergelijke trage processen geparameteriseerd moeten worden om de “multi-surface” aanpak met chemische evenwichtsmodellen te kunnen gebruiken voor bodemsystemen met sterk wisselende redoxcondities. Alleen dan kunnen de concentraties van Mn en Fe goed voorspeld worden.

In hoofdstuk 3 heb ik onderzocht hoe nat-droog cycli de oplosbaarheid van zware metalen beïnvloeden. Hiervoor heb ik dezelfde kolomproef gebruikt als in hoofdstuk 2. In hoofdstuk 3 heb ik vastgesteld in hoeverre de “multi-surface” aanpak met verschillende chemische evenwichtsmodellen gebruikt kan worden om de oplosbaarheid van zware metalen te voorspellen onder sterk wisselende redoxomstandigheden. De gemeten veranderingen in de redoxcondities, pH en DOC-concentraties tijdens twee opeenvolgende nat-droog cycli hadden een grote invloed op de concentraties van zware metalen in het bodemvocht. Onder aerobe omstandigheden werden zware metalen veel sterker gebonden in de kalkrijke grond dan in de relatief zure grond als gevolg van de hogere pH in de kalkrijke grond. Na het onder water zetten van de grondkolommen en het ontstaan van anaerobe omstandigheden namen de zware metaalconcentraties in het bodemvocht van beide gronden sterk af, door de vorming van slecht-oplosbare sulfide precipitaten; door de hogere pH waren de concentraties van zware metalen in het bodemvocht de kalkrijke grond lager dan in de relatief zure grond. Uit de vergelijking van de metingen en modelresultaten blijkt dat de vorming van slecht oplosbare sulfides een belangrijk proces is. Dit proces moet dus worden meegenomen in de modelberekeningen om de zware metaalconcentraties in het bodemvocht onder anaerobe omstandigheden goed te kunnen voorspellen. Koper kan echter verschillende soorten sulfides vormen. Hierdoor is het noodzakelijk om de chemische vorm van het neergeslagen kopersulfide te bepalen om uiteindelijk zowel de concentratie van Cu als de concentraties van de andere zware metalen in het bodemvocht onder anaerobe omstandigheden goed te kunnen voorspellen.

In hoofdstuk 4 heb ik in een kolomproef getest of de veld-Donnan membraantechniek (DMT) kan worden gebruikt om in-situ onder anaerobe omstandigheden de vrije concentraties van zware metalen in het bodemvocht van natte rijstvelden te meten. De in dit hoofdstuk gebruikte relatief zure rijstteeltgrond is dezelfde grond als die eerder werd gebruikt in hoofdstukken 2 en 3. Daarnaast hebt ik de veld-DMT metingen van de vrije zware metaalconcentraties vergeleken met de vrije concentraties die ik heb voorspeld met behulp van speciatie-modellering. In mijn modelaanpak heb ik gebruik gemaakt van het computerprogramma ORCHESTRA waarin het NICA-Donanmodel is opgenomen. Evenals in de experimenten die beschreven zijn in hoofdstuk 2 en 3 leidde het onder water zetten van de grondkolommen tot een sterke gradiënt van de Eh in de grondkolommen. De pH en de concentraties van Mn, Fe en DOC namen toe toe met een afname van de Eh. Onder anaerobe omstandigheden waren de totale opgeloste concentraties van zware metalen in het bodemvocht van de onderste en bovenste bodemlagen lager dan die in de waterlaag bovenop de grondkolommen; deze lagere concentraties waren het gevolg van de hogere pH in beide bodemlagen en dit effect was blijkbaar belangrijker dan het effect van de hogere DOC concentraties. Bovendien waren de vrije zware metaalconcentraties in het bodemvocht van de onderste en bovenste bodemlagen lager dan in de waterlaag bovenop de grondkolommen, waarschijnlijk door de toename van de pH in deze bodemlagen onder anaerobe omstandigheden. De resultaten van de DMT-metingen en modelvoorspellingen van de vrije zware metalenconcentraties in de aerobe waterlaag kwamen goed overeen, behalve voor Pb. In beide anaerobe bodemlagen werden de vrije concentraties van Cu en Pb in het bodemvocht slecht voorspeld. Blijkbaar bevat het chemische speciatie-model, wat vaak wordt toegepast en goede voorspellingen geeft onder aerobe omstandigheden, niet alle relevante chemische processen die bijdragen aan het bepalen van de oplosbaarheid van zware metalen onder anaerobe omstandigheden. De veld-DMT blijkt een nuttig instrument te zijn voor het in-situ meten van de vrije concentraties van een aantal zware metalen in natte rijstvelden.

In hoofdstuk 5 heb ik in een potproef de relatie onderzocht tussen de oplosbaarheid van zware metalen in een rijstteeltgrond en de opname van zware metalen door rijstplanten tijdens een volledige gewascyclus. In deze potproef heb ik twee rijst-cultivars gebruikt: een cultivar met een relatief laag vermogen om Cd te accumuleren in de rijstkorrels en een cultivar met een relatief hoge mate van Cd-accumulatie. Tijdens het experiment is de grond in de potten onderworpen aan twee opeenvolgende nat-droog cycli, vergelijkbaar met het waterbeheer in de praktijk (en in hoofdstukken 2 en 3). De relatief zure rijstteeltgrond die in deze potproef werd gebruikt is dezelfde grond als die eerder werd gebruikt in hoofdstukken 2, 3 en 4. De Eh werd continu gemeten op vijf verschillende dieptes in de grondkolom gedurende de twee nat-droog cycli. Tijdens de verschillende groestadia van de rijstplanten werden op dezelfde vijf dieptes monsters genomen van het bodemvocht. Deze monsters werden gebruikt om chemische samenstelling van het bodemvocht te bepalen zoals de pH en de concentraties van DOC en totaal opgelost Mn en Fe en zware metalen. Daarnaast werden tijdens de belangrijkste groeistadia van de rijstplanten de gehalten van zware metalen in verschillende plantenweefsels bepaald, waaronder de wortels, stengel, blad, rijstkaf en ongeslepen rijst. Het onder water zetten van de grond in de potten leidde tot een sterke gradiënt van de Eh in de grondkolom. De pH en concentraties van Mn, Fe en DOC namen toe met afnemende Eh terwijl drainage het tegenovergestelde effect had op deze parameters. Tijdens het onder water zetten van de grond in de potten nam de oplosbaarheid van Cd, Zn, Cu, Ni en Pb in alle bodemlagen aanzienlijk af. Dit kan verklaard worden door de vorming van neerslagen van zware metalen met sulfide onder anaerobe omstandigheden. Het Cd-gehalte van de rijstkorrels van beide cultivars was hoger dan de normen van de Volksrepubliek China en de WHO voor Cd in rijst, ondanks de relatief lage oplosbaarheid van Cd in de onder water staande potten. De opname van de zware metalen van de verschillende plantenweefsels (wortels, stam en bladeren) van beide cultivars was constant in de tijd of nam af in de latere groeistadia na eerder een maximum te hebben bereikt. Deze trend in de opname van zware metalen door de rijstplanten komt niet overeen met de hoge temporele dynamiek in de concentraties van zware metalen in het bodemvocht tijdens de potproef. Dit kan worden verklaard door de aanwezigheid van aërobe omstandigheden vlakbij het worteloppervlak (de rhizosfeer), zelfs toen de grond in de potten onder water stond: hierdoor was tijdens de twee natte perioden de oplosbaarheid van zware metalen in de rhizosfeer waarschijnlijk hoger dan in de bulkgrond. Het is dus belangrijk om de oplosbaarheid van zware metalen in de rhizosfeer van rijstplanten mee te nemen tijdens toekomstig onderzoek om de effecten van het sterk wisselende waterpeil van rijstvelden op de opname van zware metalen door rijstplanten beter te leren begrijpen. Het verdient aanbeveling om maatregelen, zoals selectie en veredeling van rijstrassen met een relatief lage mate van ophoping van Cd in de rijstkorrels of in-situ immobilisatie van zware metalen in de bodem met behulp van immobiliserende stoffen die aan de bodem toegevoegd kunnen worden, verder te onderzoeken om zo de menselijke gezondheidsrisico’s te verminderen, die verbonden zijn aan het consumeren van rijst geteeld op met zware metalen verontreinigde rijstvelden.

In mijn proefschrift heb ik een combinatie van experimenteel onderzoek en mechanistische modellering gebruikt om de oplosbaarheid van zware metalen in de bodem van rijstvelden met een dynamisch waterbeheer te kwantificeren en beter te leren begrijpen. Bovendien heb ik getracht om de oplosbaarheid van zware metalen te koppelen aan de opname van zware metalen door rijstplanten tijdens een volledige gewascyclus. Bij nat-droog cycli van rijstteeltgronden beïnvloedde de pH in sterke mate de redoxchemie van metaal-(hydr)oxiden en organische stof (hoofdstuk 2). De veranderingen van de redoxtoestand, pH en de concentraties van Mn, Fe en DOC tijdens twee opeenvolgende nat-droog cycli hadden een groot effect op de oplosbaarheid van zware metalen in rijstteeltgronden (hoofdstuk 3). De redoxchemie had bovendien een grote invloed op de vrije concentraties van zware metalen, want de vrije zware metaalconcentraties in het bodemvocht van de onderste en bovenste bodemlagen waren lager dan in de waterlaag bovenop de grondkolom. Deze afname van de vrije zware metaalconcentrations werd toegeschreven aan de lagere Eh en de hogere pH van beide bodemlagen onder anaerobe omstandigheden (hoofdstuk 4). De aanpak met het “multi-surface” model, wat goed werkt onder aerobe omstandigheden, bevat waarschijnlijk niet alle relevante chemische processen die van belang zijn bij het bepalen van de oplosbaarheid van zware metalen onder anaerobe omstandigheden (hoofdstukken 2, 3 en 4). De zware metaalconcentraties in het bodemvocht tijdens de potproef waren niet direct gerelateerd aan de opname van zware metalen door de twee rijstcultivars. De mate van translocatie van Cd van de wortels naar de bovengrondse biomassa was hoog voor beide cultivars en het Cd-gehalte van de rijstkorrels overschreed de normen van de Volksrepubliek China en de WHO (hoofdstuk 5). De resultaten van deze individuele hoofdstukken zijn geïntegreerd en bediscussieerd en in een bredere context geplaatst in hoofdstuk 6. De resultaten van het in mijn proefschrift beschreven onderzoek dragen bij aan een beter begrip van hoe redoxchemie de oplosbaarheid van zware metalen in gronden en sedimenten met een wisselend waterpeil beïnvloedt. In mijn proefschrift wordt een instrument aangedragen in de vorm van de veld-DMT voor het in-situ onder anaerobe omstandigheden meten van de vrije zware metaalconcentraties in onder water staande gronden en sedimenten. Bovendien wijst mijn proefschrift op de noodzaak om de chemische identiteit van neerslagen van zware metalen die zijn gevormd onder anaerobe omstandigheden te achterhalen met behulp van mineralogische technieken, om zo een verbetering van modelvoorspellingen van de oplosbaarheid van zware metalen mogelijk te maken. Tot slot, mijn proefschrift draagt nieuwe ideeën aan voor de afleiding van risico-gebaseerde normstelling voor zware metalen in systemen met een sterk wisselend waterpeil, door rekening te houden met de Eh en het sulfaatgehalte en er worden suggesties gegeven over hoe de productie en kwaliteit van rijst geteeld op met zware metalen verontreinigde natte rijstvelden gewaarborgd kan worden.

# 摘要

水稻（*Oryza sativa* L.）是南亚和东南亚人群最重要的主食，在食物安全领域起着极其重要的作用。然而，随着快速城市化和工业化进程，水稻产量和质量日益引起人们的关注。重金属污染水稻土会导致重金属在水稻籽粒中富集。消费重金属污染稻米则会导致不可接受的健康风险。以稻米为主食的人群而言，口腔摄入途径已成为人群镉暴露的最主要途径。举例而言，种植于台湾西部平原的水稻籽粒镉含量经常超过世界卫生组织食品质量标准，即使在镉污染水平较低情况下水稻籽粒镉污染也可能出现。这就有必要对决定水稻吸收重金属的途径进行深入研究。水稻吸收重金属很大程度上取决于稻田土壤中重金属的生物有效性，同时也取决于水稻的植物特性。水稻土中重金属的生物有效性取决于重金属和土壤组分有效表面如土壤有机质、粘土矿物和金属（氢）氧化物之间的交互作用。反过来，这些交互作用又受到环境条件如pH和氧化还原电位（Eh）的影响。对于这些交互作用和环境条件，Eh对重金属的生物有效性的影响还所知甚少。这对于水稻特别重要，因为水稻主要种植于稻田土壤上。稻田交替淹水和排水会导致持续的Eh动态变化，从而影响重金属的溶解度。土壤溶液重金属浓度可以与水稻吸收重金属直接关联。在模型预测稻田土壤重金属溶解度时，不同的表面络合模型可以嵌入多表面模型方法中。该方法可以计算重金属在土壤不同活性表面之间的分配。这些表面包括土壤有机质、可溶性有机质、金属（氢）氧化物、粘土矿物及矿物沉淀。该模型方法已证实在有氧条件下能充分预测大部分重金属的溶解度。然而，该模型方法在厌氧条件下的适用性还不明确，因为在此条件下大部分与氧化还原反应相关的化学过程都相对较慢，处于不平衡状态。因此，这就有必要对现有的以化学平衡为前提的多表面模型是否能够直接应用于厌氧条件进行验证。由于淹水和排水对水稻土Eh和氧化还原化学的动态效果会对重金属溶解度产生很大影响，水稻吸收重金属在不同的生长期可能吸收速率不

一致。举例而言，水稻生长有一个关键的灌浆期。在该生育期，Eh 变化和相应的重金属生物有效性可能很大程度上决定了水稻籽粒中的重金属浓度。总之，量化淹水和排水条件下稻田土壤重金属的溶解度以及验证多表面模型在厌氧条件下预测重金属的适用性就十分重要。同样地，在淹水和排水条件下稻田土壤重金属溶解度和水稻吸收重金属之间的关系需要进一步调查研究。上述反映了本论文的第一章内容。

论文第二章详细探讨了交替淹水和排水条件下 pH 对稻田土壤金属（氢）氧化物和有机质氧化还原化学的影响。同时，验证了多表面模型在交替淹水排水条件下预测锰和铁溶解度的能力。实验在一个仔细设计的土柱实验中进行，使用了土壤性质基本相同但 pH 迥异的两种水稻土。在两个连续淹水排水周期，Eh 和土壤溶液的化学成分在土柱剖面四个层次进行连续监测。淹水导致两种土壤 Eh 沿土柱剖面形成垂直梯度。在酸性土壤中，pH 随着 Eh 的下降而升高，反之亦然。然而，在碱性土壤中，pH 主要由碳酸钙缓冲。在酸性土壤中，锰和铁的溶解度随着淹水还原溶解而升高，但随着排水氧化而降低。在碱性土壤中，锰和铁的溶解度并未随淹水而升高，这可能是因为还原的二价锰和铁沉淀为 $MnCO_3$，$FeCO_3$ 和（或）FeS。在淹水期间，两种水稻土可溶性有机碳的浓度随着淹水而上升。这与铁（氢）氧化物的还原溶解以及酸性土壤 pH 上升相关。通过比较实测值和模型预测值表明，锰和铁（氢）氧化物的还原溶解是动力学受限的反应。因此，对于氧化还原条件动态变化的研究体系，这些动力学受限的反应过程应在模型中加以完善，以提高预测锰和铁溶解度的精确性。

第三章详细探讨了淹水和排水周期对土柱实验（第二章）两种污染水稻土重金属溶解度的影响。同样地，验证了多表面模型在氧化还原动态变化条件下预测重金属溶解度的能力。两次连续淹水和排水期间，重金属溶解度受到 Eh、pH 和可溶性有机碳动态变化的很大影响。在有氧条件下，相对于酸性土壤，碱性土壤更高的 pH 条件导致重金属在土壤固相活性表面更强的结合。在厌氧条件下，两种水稻土大部分重金属的溶解度主要受金属硫化物控制，但碱性

土壤更高的 pH 条件导致土壤溶液平衡状态时更低的重金属浓度。通过比较研究测定值和模型预测值表明，金属硫化物对厌氧条件下模型预测重金属溶解度非常重要。然而，在淹水条件下形成的铜硫化物的化学特性和相应溶度积应加以确定，以提高多表面模型在厌氧条件下预测重金属的精确性。

第四章测试了原位道南膜（DMT）技术在土柱淹水稻田土壤溶液中测定自由态重金属的能力。该实验使用的酸性水稻土和在第二、三章中使用的水稻土一致。同样的，比较研究了原位 DMT 测定值和模型预测值。模型预测采用了 ORCHESTRA 模型平台，该平台包括了 NICA-Donnan 模型。由于该模型方法在厌氧条件下的相关研究还很少，验证该模型方法在此条件下的运用就非常重要。淹水导致 Eh 沿土柱形成垂直梯度。土壤溶液 pH、锰、铁和可溶性有机碳浓度随着 Eh 下降而上升。在厌氧条件下，土壤溶液重金属浓度从土柱水层向土层逐步下降。这可能是由于 pH 上升的效应超过了可溶性有机碳浓度上升的效应。同样地，自由态重金属浓度也从土柱水层向土层逐步下降。这同样可以用淹水导致 pH 值上升解释。在水层，除铅外，自由态重金属浓度原位 DMT 实测值与模型预测值相近。在厌氧两土层，自由态铜和铅离子的预测值较差。因此。多表面模型在有氧条件下预测能力较好，但还不能反映厌氧条件下所有的化学过程。总体而言，已证实原位 DMT 技术是淹水稻田土壤原位测定自由态重金属的有用工具。

第五章详细探讨了盆栽污染水稻土重金属溶解度和水稻在其主要生长期吸收重金属的相关关系。高、低镉积累两种水稻品种用于本实验。在盆栽实验期间，类似于第二、三章土柱实验，连续两次淹水排水周期运用于盆栽水分管理。盆栽土壤与第二至四章中使用的酸性土壤一致。在连续两次淹水排水期间，Eh 在土壤剖面五个层次连续原位监测。土壤溶液 pH 和化学组分，如可溶性有机碳、锰、铁和重金属浓度，也在相应五个层次连续监测。此外，在不同生长期水稻不同组织包括根、茎、叶、稻壳和糙米的重金属含量也得以确定。淹水导致 Eh 沿土柱形成垂直梯度，pH、锰、铁和可溶性有机碳的浓度随着淹水 Eh 下降而升高，但随着排水 Eh 上升而下降。淹水期间，Cd、Zn、

Cu、Ni 和 Pb 溶解度显著降低。这可以用厌氧条件下形成的金属硫化物解释。虽然淹水条件下 Cd 溶解度较低，但是两种水稻品种糙米中 Cd 含量均超过了中国和世界卫生组织食品质量标准。对于两种水稻品种而言，水稻不同组织（根，茎和叶）中的重金属含量以相对恒定的速率上升或在生长后期达到最大值后呈下降趋势。这样看来，水稻在不同生长期的重金属吸收并不能反映重金属溶解度随时间的变异。水稻持续吸收重金属的现象可以用淹水条件下根系表面维持的有氧状态解释，可能导致重金属在根圈的溶解度高于非根际土壤的溶解度。因此，根圈的重金属溶解度应进一步研究以阐明稻田水分管理对水稻吸收重金属的影响。

在本博士论文中，实验和模型相结合的方法用于调查交替淹水排水水稻土中重金属的溶解度变化，并将该变化与水稻在主要生长期吸收重金属相关联。在交替淹水和排水周期中，pH 对水稻土中金属（氢）氧化物和有机质的氧化还原化学产生了很大影响（第 2 章）。Eh、pH、溶解态锰、铁和可溶性有机碳浓度对两次连续淹水排水的水稻土重金属溶解度也产生了很大影响（第 3 章）。同样的，氧化还原化学对自由态重金属浓度也产生了很大影响。由于淹水后 Eh 下降和 pH 上升，上部和下部土层溶液中的自由态离子浓度低于水层中的浓度（第 4 章）。多表面模型在有氧条件下应用较好，却不能完全涵盖厌氧条件下的所有化学过程（第 2、3 和 4 章）。重金属的溶解度与两种水稻品种不同组织吸收重金属随时间变化并未呈现显著相关关系。更为重要的是，镉从根部向地上部转运的能力在两种水稻品种中均较高且两种水稻品种糙米中的镉含量都超过了中国和世界卫生组织食品质量标准（第 5 章）。这些单一章节的研究结果在第 6 章中进行了整合和系统讨论。总而言之，本博士论文的研究成果有利于加深氧化还原化学对淹水土壤和沉积物系统重金属溶解度影响的认识，可以为淹水土壤和沉积物体系提供原位测定自由态重金属的 DMT 工具。同样地，本博士论文指出有必要进一步通过使用矿物光谱技术确定金属矿物的化学属性，以利于模型更好的预测重金属溶解度。最后，本博士论文可为基于风险的标准制定提供新思路，明确指出 Eh 和硫酸根含量

对于淹水体系重金属溶解度的重要性。本博士论文也为今后在重金属污染稻田土壤上生产符合食品质量标准的大米提供了建议。

# Affiliation of Co-authors

**Rob N.J. Comans, Gerwin F. Koopmans, Erwin J.M. Temminghoff**
Department of Soil Quality, Wageningen University and Research Center (WUR), P.O. Box 47, 6700 AA, Wageningen, The Netherlands;

**Yongming Luo**
Yantai Institute of Costal Zone Research, Chinese Academy of Sciences, Yantai, 264003, P.R. China

**Luc T.C. Bonten**
Alterra, WUR, P.O. Box 47, 6700 AA, Wageningen, The Netherlands

**Jing Song**
Key Laboratory of Soil Environment and Pollution Remediation, Institute of Soil Science, Chinese Academy of Sciences, Nanjing, 210008, P.R. China

# Acknowledgements

The journey of pursuing the Ph.D. is a great challenge. After more than four years of hard working in the lab, greenhouse, and field, as well as in front of the computer, mixed feelings are hard to express. Ph.D. journey is doomed to be a lonely journey, fighting against all difficulties in research itself, tiredness and sometimes frustration. But on the other hand, Ph.D. journey is also a meaningful journey, filled with learning, thinking, try and error, and a sense of achievement at the end. Finally, the thesis is ready in your hands. I thank everybody who gave me the impetus to face this challenge and helped me all the way.

I am very grateful to my two promotors Prof. Rob N.J. Comans and Prof. Yongming Luo for accepting me as a Ph.D. student and jointly supervising my study in the Netherlands and in China, respectively, giving me constructive suggestions and advices throughout these years and commenting on my thesis. Rob, your comments are always very helpful in strengthening the scientific significance and novelty of the papers. Yongming, your full trust and sustained support always give me strength and faith to pursue my Ph.D. studies.

I am also very grateful to my daily supervisors, Gerwin F. Koopmans, Luc T.C. Bonten, Jing Song, and Erwin J.M. Temminghoff. Gerwin, what I learned from you is prudence. You always tease yourself you are not an expert on anything. On the contrary, you have very serious attitude toward science and are always critical on my research work. You have indulged yourself in different research projects and gained rich multi-disciplinary knowledge in soil science. You are very strict when reviewing the articles as editors for scientific journals and even for a comma or space, you will delete it and leave no imperfection in the manuscript. You are also very good at tackling the rebuttal when the feedback of my manuscript is back from reviewers. The last not the least, you have rich experience in the scientific writing helping me a lot in the text change and language editing.

Luc, what I learned from you is efficiency. As a modeler, you are really thinking insight, but really doing so simple. From simple excel tricks to complicated modeling set-up, you always show your wisdom and simplicity to solve the problems. For example, you always remind me of using shift + tab and control + shift + tab to select the designated area; you always help me program easy calculation modes in excel to handle thousands of data for different analysis purposes; you always ask me to play with the model to find and solve the problems by myself. Your help makes data handling much easier for me and saves me quite a lot of time. You are also very straightforward and rigorous when you spot the weakness in my model application and manuscript writing. Your cautious attitude now always remind me of double checking any files before I send them to you.

Jing, what I learned from you is patience. I thank you very much for your unreserved support to my study abroad and research work in China. For the joint Ph.D. project, I have encountered many kinds of problems such as bureaucratic files for going abroad, rice seeds selection, greenhouse reservation for pot experiment, and soil transferring for field experiment etc. You kind help saved me a lot of time so that I can focus on the scientific details. I remembered the field experiment very well. You negotiated with the local farmer for the compensation with great patience and rented a big lorry to transport 26 tons of polluted soil over several hundred kilometers to China Rice Research Institute for my field experiment. You also helped me arrange the cement tank to contain the transferred soil for rice plantation. During rice growing season, you personally travelled long distance with us to set up the experiment, sample soil solution and harvest rice. You always back me up and show your solid support. Without your help, I cannot imagine how I can finish all my experimental work in China.

Erwin, what I learned from you is positive attitude. You suffered a lot from brain tumour these years. Amazingly, you have gone through the difficulties and recovered by steady progress. Your spirit encouraged me a lot during my Ph.D. study. I respect you very much and personally thanks a lot for your supervision in the first 2 years of my study. I remembered very well that Gerwin and I visit you regularly by bike to get to know your recent situations and listen to your advice on my research progress and scientific manuscripts. We knew you conquered your physical constraints, and always managed to finish the discussion. I highly appreciated that.

Besides my supervisors, there are many people I need to thank for their help. Prof. Willem H. van Riemsdijk, my former promotor in the Netherlands, is gratefully acknowledged for his contribution to the joint Ph.D. project. Liping Weng is gratefully acknowledged for her kindness in helping me solve the problems in life and work in Wageningen. Hans Meeussen is gratefully acknowledged for his advice in constructing the Eh-pH diagrams with the ORCHESTRA modelling framework. Gerlinde Vink and Peter Nobels are gratefully acknowledged for the lab column experiment and sample analysis. Meifen Bao, Yujuan Huang, Haibo Yu, Dong Zhang, Peng Wu, and Mingchao Lv are gratefully acknowledged for helping me with the pot and field experiments. Angela Straathof, Inge Regelink, Jinmeng Wang, Wei Qin, Xinxin Wang, Supriatin, Cristian Terrones Cano, Andreas Duffner, Mart Ros, Zhaohai Bai, Yong Hou, Qian Liu, Junqi Zhu, Fang Gou, Tian Zeng, Yang Yu, Lin Ma, Liansun Wu, Wengfeng Cong, Guohua Li, Chunxu Song, Junfei Gu, Mingtian Yao, and Zheng Huang are greatly thanked for your help and accompany in Wageningen.

In the end, I would like to thank everyone in my family for their love and support, and for believing in me. I would like to thank my wife, Wu Shanshan for her support, companionship and belief throughout my Ph.D. journey, especially taking care of our son, Pan Junhao. My little boy, I will accompany your growth when I come back to China. I also thank all my Chinese friends in Wageningen. Thanks for your help and accompany. Your friendship is special and an encouragement in all the raining and shining days.

Heel erg bedankt!

Yunyu Pan

# Curriculum vitae

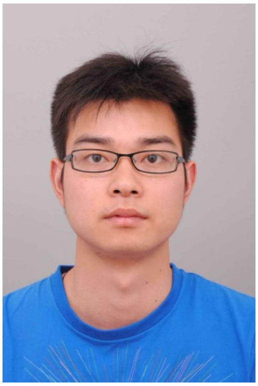

Yunyu Pan was born on July 18th, 1984 in the city of Liyang, Jiangsu Province, P.R. China. After finishing the high school, he studied the major of Agricultural Resource and Environment (Former Soil Chemistry and Plant Nutrition) in the college of Resources and Environmental Science in Nanjing Agricultural University (NAU) from 2003 to 2007. He successfully completed the Bachelor Degree with an internship sponsored by Student Research Training Program of NAU. He wrote the dissertation from the internship entitled as 'Water Moisture Affects the Dynamics of Microbial Carbon and Nitrogen in Agricutrual Soils'. After completion of Bachelor Degree, he was recommended by NAU to the Institute of Soil Science, Chinese Academy of Sciences (ISSCAS) for postgraduate study in Environment Science. He was grateful to be supervised by Prof. Yongming Luo and associate Prof. Jing Song. Both supervisors offered him a lot of opportunities to study and practice in multidisplinary subjects. During the master period, as project leader or backbone member, he undertook Encrop Project sponsored by Alterra, the Netherlands; ICA project sponsored by International Copper Association, the USA; MEP project, sponsored by the Ministry of Environment Protection, P.R. China; GEF/UNDP Dicofol Substitution Project and World Bank/CTF (Canadian POPs Trust Fund) Project. After carrying out these projects, he got meaningful experience in brownfields investigation and remediation, and human health risk assessment. Meanwhile, these valuable experience were utmost shown in the master dissertation entitled as 'Methodology Establishement of Human Health Risk Assessment and Remediation Technology Selection for Metallurgical Sites'.

After completion of Master Degree in July, 2010, he was luckily chosen as sandwich Ph.D. candidate funded by CAS-KNAW. From 2010 to 2014, he worked in both the Soil Quality group of Wageningen University in the Netherlands and in the ISSCAS in China. During the Ph.D. period, his interest focused on trace metal speciation in redox-active paddy soil and the mechanism of trace metal uptake by rice. The important results of his research during this period were presented in this thesis. After getting his PhD, he will still work on soil chemistry aspect and human health risk assessment aspect.

**List of Publications**

Pan, Y.Y., Koopmans, G.F., Bonten, L.T.C., Song, J., Luo, Y.M., Temminghoff, E.J.M., Comans, R.N.J., 2014. Influence of pH on the redox chemistry of metal (hydr)oxides and organic matter in paddy soils. Journal of Soils and Sediments 14, 1713–1726.

Pan, Y.Y., Koopmans, G.F., Bonten, L.T.C., Song, J., Luo, Y.M., Temminghoff, E.J.M., Comans, R.N.J., 2015. In-situ measurement of free trace metal concentrations in a flooded paddy soil using the Donnan Membrane Technique. Geoderma, 241–242, 59–67.

Pan, Y.Y., Bonten, L.T.C., Koopmans, G.F., Song, J., Luo, Y.M., Temminghoff, E.J.M., Comans, R.N.J., 2015. Solubility of trace metals in two contaminated paddy soils exposed to alternating flooding and drainage. Submitted to Geoderma.

Pan, Y.Y., Koopmans, G.F., Bonten, L.T.C., Song, J., Luo, Y.M., Temminghoff, E.J.M., Comans, R.N.J., 2015. Temporal variability in trace metal solubility in a paddy soil not reflected in uptake by rice (Oryza sativa L.). Under preparation.

## SENSE PhD Education Certificate

Netherlands Research School for the
Socio-Economic and Natural Sciences of the Environment

# DIPLOMA

***For specialised PhD training***

The Netherlands Research School for the
Socio-Economic and Natural Sciences of the Environment
(SENSE) declares that

***Yunyu Pan***

born on 18 July 1984 in Jiangsu, China

has successfully fulfilled all requirements of the
Educational Programme of SENSE.

Wageningen, 12 May 2015

the Chairman of the SENSE board
Prof. dr. Huub Rijnaarts

the SENSE Director of Education
Dr. Ad van Dommelen

*The SENSE Research School has been accredited by the Royal Netherlands Academy of Arts and Sciences (KNAW)*

KONINKLIJKE NEDERLANDSE
AKADEMIE VAN WETENSCHAPPEN

The SENSE Research School declares that **Mr Yunyu Pan** has successfully fulfilled all requirements of the Educational PhD Programme of SENSE with a work load of 53.2 EC, including the following activities:

**SENSE PhD Courses**

- Environmental Research in Context (2011)
- Research in Context Activity: ‘Visiting relevant academic groups for the improvement of PhD research and writing accessible news release about PhD research results’ (2011)
- Speciation and Bioavailability (2013)
- SENSE Summer Academy ‘Emerging Issues in Sustainable Energy and Water Systems’ (2013)

**Other PhD and Advanced MSc Courses**

- Soil and Plant Analysis and Data Handling, Wageningen University (2010)
- Chemical Processes in Soil, Water, Atmosphere, Wageningen University (2010)
- Advanced English for PhD candidate, Chinese Academy of Sciences (2011-2012)
- Dialectics of Nature and Scientific Socialism, Chinese Academy of Sciences (2011-2012)
- Limnology and Sedimentology, Chinese Academy of Sciences (2011-2012)
- Environmental Remediation Technology and Engineering, Chinese Academy of Sciences (2012-2013)
- High-Impact Writing Course, Wageningen University (2013)
- Scientific Publishing, Wageningen University (2013)
- Scientific Writing, Wageningen University (2013)
- Techniques for Writing and Presenting a Scientific Paper, Wageningen University (2013)
- Voice Matters and Presentation Skills Training, Wageningen University (2013)
- Workshop Presentation Skills, Wageningen University (2013)

**Management and Didactic Skills Training**

- Co-organisation of the 4th International Conference on Soil Pollution and Remediation and the 2nd International Workshop on Site Remediation (2012)

**Oral Presentations**

- Speciation of heavy metals in three paddy soils by DMT technique: A microcosm experiment with in-situ Eh monitoring. The 4th International Conference on Soil Pollution and Remediation, 23-26 September 2012, Yantai, P.R. China

SENSE Coordinator PhD Education

Dr. ing. Monique Gulickx

This research was conducted in a collaboration between Wageningen University and the Chinese Academy of Sciences (CAS).

This research was financially supported by the CAS-KNAW Joint PhD Training Programme (No. 5237829), the National Natural Science Foundation of China (No. 40971250), the Key Project of the National Natural Science Foundation of China (No. 41230858), and the Environmental Protection Public Welfare Project funded by the Chinese Ministry of Environmental Protection (No. 201409042-03). This research is also part of the strategic research program KBIV-“Sustainable spatial development of ecosystems, landscapes, seas and regions", which is funded by the Dutch Ministry of Economic Affairs.

The cover page was designed by Yunyu Pan.

Financial support from Wageningen University for printing this thesis is gratefully acknowledged.